SITE-SPECIFIC GLYCOSYLATION ANALYSIS OF IgG3 AND THE EFFECT OF GLYCOSYLATION ON THE STRUCTURE, PHYSICAL STABILITY AND Fc RECEPTOR INTERACTIONS OF IgG3 Fc

By

Ishan Shah
M.S., Pharmaceutical Chemistry, 2013, The University of Kansas, Lawrence, KS
M.S., Industrial Pharmacy, 2011, The University of Toledo, Toledo, OH
B.Pharm., Pharmacy, 2009, Sardar Patel University, VV Nagar, India

Submitted to the graduate degree program in Pharmaceutical Chemistry and the Graduate Faculty of the University of Kansas in partial fulfillment of the requirements for the degree of Doctor of Philosophy.

Chair: Thomas J. Tolbert, Ph.D.

David B. Volkin, Ph.D.

Christian Schöneich, Ph.D.

Michael Wang, Ph.D.

Eric Deeds, Ph.D.

Date Defended: 28 June 2017

The dissertation committee for Ishan Shah certifies that this is the approved version of the following dissertation:

SITE-SPECIFIC GLYCOSYLATION ANALYSIS OF IgG3 AND THE EFFECT OF GLYCOSYLATION ON THE STRUCTURE, PHYSICAL STABILITY AND Fc RECEPTOR INTERACTIONS OF IgG3 Fc

Chair: Thomas J. Tolbert, Ph.D.

Date Approved: 28 June 2017

Abstract

Therapeutic monoclonal antibodies based on the IgG class of antibodies are glycoproteins that contain glycosylation sites within their Fc region. Glycosylation is important for Fc-mediated effector functions such as Antibody Dependent Cellular Cytotoxicity (ADCC) and Complement Dependent Cytotoxicity (CDC). IgG has four subclasses: IgG1, IgG2, IgG3 and IgG4. All IgG subclasses contain a consensus glycosylation site in the C_H2 domain at N297, and glycosylation at that site is considered essential for optimal Fc function and stability. IgG3 is the only subclass that has an additional glycosylation site in the C_H3 domain at N392. This site has nearly gone unmentioned and was only recently shown to be partially glycosylated in serum IgG3; however, the biological role of N392 glycosylation remains uninvestigated in the literature. The primary focus of this dissertation work is to study the effect of N-glycosylation on Fc receptor interactions, structure and physical stability of IgG3.

LC-MS based glycopeptide mapping studies revealed that the N392 site is partially glycosylated in human serum IgG3 and the glycans at the N392 site showed significant differences compared to the N297 site in levels of core fucosylation, bisecting GlcNAc and mannosylation. The presence of glycosylation at the N392 site in the naturally occurring IgG3 establishes its biological relevance and makes a case for its characterization. For structural and biochemical characterization studies, the Fc fragment of IgG3 was expressed in a glycosylation-deficient strain of the yeast *Pichia pastoris*. Two variants of IgG3 Fc were produced, one with both sites glycosylated and another with only the N297 site glycosylated. These two forms were compared to investigate the effect of N392 glycosylation on the Fc receptor binding activity and physical stability of IgG3 Fc. Our results indicate that presence of the additional N392 glycan

does not affect the binding of IgG3 Fc with the FcγRIIIA and FcRn receptors but does affect the conformational stability and aggregation propensity of IgG3 Fc.

Additionally, crystal structures of both the IgG3 Fc variants were determined with a resolution of 1.8-2.0 Å and were compared with the published structures of Fc fragments from the other IgG subclasses. Structural analysis of key amino acid differences between IgG3 and other IgG subclasses provided insight into IgG3-specific properties, especially related to binding with protein A, protein G, and the FcRn receptor. The importance of N297 glycans for IgG3 Fc-FcγRIIIA interaction was also demonstrated from a structural perspective. The location and orientation of the N392 glycans in the IgG3 Fc structure provided a probable explanation for the observed effect of these glycans on Fc receptor binding activity and physical stability of IgG3 Fc.

Dedicated to:

My loving wife

Kinjal Amin

Acknowledgments

I would like to acknowledge and thank my advisor, Dr. Tom Tolbert for his support, guidance and advise throughout the course of this research project. I am grateful to him for the time he spent in the lab to get me acquainted with molecular biology and protein expression/purification techniques during my initial years in the lab. I have learnt a lot by interacting with him on topics not just related to my research project but also general aspects of glycobiology and immunology.

I want to thank Dr. David Volkin, Dr. Christian Schöneich, Dr. Teruna Siahaan, Dr. Michael Wang, and Dr. Eric Deeds for agreeing to serve on my dissertation committee. Their comments and suggestions have been very helpful in developing this dissertation project. I want to thank the Department of Pharmaceutical Chemistry for the Howard Rytting fellowship and for offering excellent coursework that I feel will be invaluable in my scientific career. I want to thank Dr. Heather Desaire and Jude Lakbub from KU Chemistry department for the opportunity to collaborate on IgG3 disulfide mapping project. I want to thank Dr. Scott Lovell from KU-COBRE Protein Structure lab for his help and guidance with the IgG3 Fc structural biology project. I thank Vishal Toprani (Dr. Volkin's lab) for helping me with protein biophysical analysis. I thank my lab members, Derek White, Solomon Okbagzhi, Khalid Al-Kinani and Kevin Hutchison for creating a conducive lab environment and their troubleshooting help with the instruments and experiments.

Finally, I would like to thank my parents, Sanjeev & Dipti, and my sister, Riya for their constant support and confidence in me that made me reach this far. I thank my uncle, aunt, cousin, grandparents, and in-laws for their encouragement. And lastly but most importantly, I would like to thank my wife, Kinjal Amin, without whom none of this would be possible. Her

unwavering support and constant encouragement, despite living 1500 miles away (that too coincidently in Lawrence, MA) was the sole reason I could accomplish this. I cannot thank her enough for the patience, sacrifice and endurance she has shown in the last six years to allow me to pursue my dreams. She often jokes that she deserves an honorary Ph.D for going through this valiant effort. I believe, she deserves a lot more…

Table of Content

Chapter 1 Introduction 1
1.1 Structure and function of immunoglobulins G (IgG) 2
1.2 Immunoglobulin isotypes and IgG isotype 4
1.3 IgG3 subclass 7
1.4 Fcγ receptors 10
1.5 Neonatal Fc receptor (FcRn) 11
1.6 Monoclonal antibody (mAb) therapeutics and antibody engineering 13
1.7 Protein glycosylation 15
1.8 Importance of glycosylation on IgG and glycoengineering 19
1.9 Production of homogenously glycosylated proteins in the yeast *Pichia pastoris* 21
1.10 References 24

Chapter 2 LC-MS based Site-Specific Glycosylation analysis of human serum IgG3 32
2.1 Introduction 33
2.2 Methods 36
2.2.1 Isolation of IgG3 from human serum 36
2.2.2 Deglycosylation of human serum IgG3 36
2.2.3 In-gel protease digestion 37
2.2.4 LC-MS analysis of N297 and N392 site glycosylation on human serum IgG3 37
2.3 Results 38
2.3.1 Isolation of IgG3 from human serum 38
2.3.2 Checking occupancy of the N392 glycosylation site in human serum IgG3 39
2.3.3 LC-MS based site-specific glycosylation analysis of human serum IgG3 41
2.4 Discussion 48
2.5 References 51

Chapter 3 Production and characterization of human IgG3 Fc expressed in glycosylation-deficient strains of the yeast *Pichia pastoris* and *in-vitro* glycan processing using an α-1,2 mannosidase 54
3.1 Introduction 55
3.2 Methods 59
3.2.1 Cloning of IgG3 Fc 59
3.2.2 Expression and purification of WT and mutant IgG3 Fc 60
3.2.3 Deglycosylation of IgG3 Fc 61
3.2.4 LC-MS analysis of IgG3 Fc 61
3.2.5 Preparation of IgG3 Fc glycovariants 62
3.2.6 *In-vitro* enzymatic modification of glycosylation 63
3.2.7 *In-vivo* enzymatic modification of glycosylation 64
3.3 Results 64
3.3.1 Expression and purification of WT IgG3 Fc and mutant IgG3 Fc 64
3.3.2 LC-MS analysis of the expressed WT and mutant IgG3 Fc 67
3.3.3 Producing IgG3 Fc glycovariants with site-specific glycosylation 71
3.3.4 In-vitro glycan processing of high mannose glycans on IgG3 Fc 73
3.4 Discussion 84
3.4.1 Production and characterization of IgG3 Fc expressed in yeast P pastoris 84

3.4.2 *In-vitro* glycan processing of high mannose glycosylation on IgG3 Fc 87
3.5 References 91

Chapter 4 Influence of N392 site glycosylation on Fc receptor interactions and physical stability of IgG3 Fc 96
4.1 Introduction 97
4.2 Methods 100
4.2.1 Expression and purification of FcγRIIIA 100
4.2.2 Cloning of FcRn receptor 100
4.2.3 Expression, purification and biotinylation of FcRn 103
4.2.4 Kinetic analysis of IgG3 Fc-FcγRIIIA binding 104
4.2.5 Kinetic analysis of IgG3 Fc-FcRn binding 104
4.2.6 Assessment of physical stability of IgG3 Fc glycovariants 105
4.3 Results 106
4.3.1 FcγRIIIA expression/purification/characterization 106
4.3.2 FcRn expression/purification/characterization 107
4.3.3 Sortase-mediated ligation of FcRn receptor 110
4.3.4 Binding interactions of IgG3 Fc glycovariants with FcγRIIIA 113
4.3.5 Binding interactions of IgG3 Fc glycovariants with FcRn 116
4.3.6 Effect of N392 glycosylation on physical stability of IgG3 Fc 117
4.4 Discussion 122
4.4.1 Binding interactions of IgG3 Fc glycovariants with Fc receptors 122
4.4.2 Effect of N392 glycosylation on physical stability of IgG3 Fc 125
4.5 References: 127

Chapter 5 Structural characterization of human IgG3 Fc 133
5.1 Introduction 134
5.2 Methods 135
5.2.1 Production and characterization of Man5-IgG3 Fc and tetraglycosylated IgG3 Fc 135
5.2.2 Crystallization and Data Collection 136
5.2.3 Structure Solution and Refinement 137
5.2.4 Binding analysis of IgG3 Fc glycoforms with FcγRIIIA 139
5.3 Results and Discussion 139
5.3.1 Characterization of Man5-IgG3 Fc and tetraglycosylated IgG3 Fc 139
5.3.2 Structural analysis of the two IgG3 Fc variants 140
5.3.3 Overall IgG3 Fc structure 141
5.3.4 C_H2 domain conformation 143
5.3.5 N-glycosylation 146
5.3.6 C_H2-C_H3 domain interface 150
5.3.7 IgG3-protein A and protein G interactions 154
5.3.8 IgG3-FcRn interactions 156
5.3.9 Crystal structure of tetraglycosylated IgG3 Fc 158
5.3.10 Influence of N392 glycans on Fc receptor binding and physical stability of IgG3 Fc 162
5.4 References 165

Chapter 6 Summary, Conclusions and Future directions 172
6.1 Summary 173

6.2 Conclusions 175
6.3 Future directions 176
6.4 References: 177

List of Figures

Figure 1.1: Structure of Immunoglobulin G (IgG). 3

Figure 1.2: Modes of antibody action engaged in removal or destruction of pathogen or killing of a tumor cell. 4

Figure 1.3: Schematic representation of structural variation with respect to inter- and intra-chain disulfide bonds in IgG subclasses 6

Figure 1.4: Amino acid differences in IgG3 allotypes (G3m) 8

Figure 1.5: Recycling of IgG by FcRn receptor 12

Figure 1.6: N-glycosylation biosynthesis pathway in humans and yeast 16

Figure 1.7: Types of N-glycan: high mannose, hybrid and complex 18

Figure 1.8: Structure of a fully-processed complex-type glycoform. The variable addition of Fucose, bGlcNAc, Galactose and Sialic acid (marked by brackets) results in different glycoform structures. 19

Figure 2.1: Isolation of IgG3 from gamma globulins 39

Figure 2.2: Coomassie-stained SDS-PAGE under reducing conditions of papain-digested IgG3 41

Figure 2.3: Western blot showing deglycosylated products of the serum IgG3 Fc and yeast-expressed WT IgG3 Fc 41

Figure 2.4: MS analysis of serum IgG3 glycopeptides from trypsin digest 43

Figure 2.5: MS analysis of serum IgG3 glycopeptides from Asp-N digest 44

Figure 2.6: MS/MS spectra for the N392-Man5 glycopeptide at (A) 20 eV and (B) 40 eV collision energy 47

Figure 2.7: MS/MS spectra for the N297-G1F glycopeptide at (A) 20 eV and (B) 40 eV collision energy 47

Figure 3.1: *In-vitro* enzymatic synthesis of Man5, hybrid and complex glycans from high mannose glycans 58

Figure 3.2: Coomassie-stained SDS-PAGE for IgG3 Fc purified from yeast 66

Figure 3.3: Coomassie stained SDS-PAGE showing deglycosylated products of the WT IgG3 Fc and IgG3 Fc-N392K under reducing conditions with and without denaturation..... 67

Figure 3.4: Intact protein mass spectra of IgG3 Fc-N392K expressed in different glycosylation-deficient strains of *P. pastoris* 69

Figure 3.5: Intact protein mass spectra of WT IgG3 Fc expressed in different glycosylation-deficient strains of *P. pastoris* (Table 3.1)..... 70

Figure 3.6: Site-specific characterization of glycosylation on WT IgG3 Fc expressed in the OCH1 KO *P. pastoris* 71

Figure 3.7: (A) Hydrophobic interaction chromatography (HIC) trace for WT IgG3 Fc and IgG3 Fc-N392K 72

Figure 3.8: Conversion of high mannose glycans ($GlcNAc_2Man_{8-12}$/Man8-Man12) to Man5 ($GlcNAc_2Man_5$) glycoform. 73

Figure 3.9: Structures of α-1,2 mannosidase resistant high mannose glycans 74

Figure 3.10: Conversion of glucosylated high-mannose glycans to the Man5 glycoform 76

Figure 3.11: Intact protein MS spectra of IgG3 Fc-N392K expressed in different glycosylation-deficient strains of *P. pastoris* 77

Figure 3.12: Intact protein MS spectra of WT IgG3 Fc under reducing condition (A) before and (B) after α-1,2 mannosidase digestion 77

Figure 3.13: Intact protein MS spectra of IgG3 Fc-N392K expressed in *P. pastoris* with *in-vivo* α-1,2 mannosidase 79

Figure 3.14: Intact protein MS spectra of IgG3 Fc-N392K expressed in *P. pastoris* with *in-vivo* α-1,2 mannosidase activity after *in-vitro* digestion 80

Figure 3.15: Fractionation of phenyl sepharose elution peak of IgG3 Fc-N392K expressed in *P. pastoris* with *in-vivo* α-1,2 mannosidase activity 81

Figure 3.16: Intact protein MS spectra of the pools collected from fractionated phenyl sepharose chromatography of IgG3 Fc-N392K expressed in *P. pastoris* with *in-vivo* α-1,2 mannosidase activity..... 81

Figure 3.17: Intact protein MS spectra of IgG3 Fc-N392K Fc expressed in *P. pastoris* with *in-vivo* α-1,2 mannosidase..... 83

Figure 3.18: Intact protein MS spectra after *in-vitro* digestion of IgG3 Fc-N392K Fc expressed in *P. pastoris* with *in-vivo* α-1,2 mannosidase..... 83

Figure 3.19: Reaction mechanism of PNGase F 85

Figure 4.1: Schematic representation of IgG3 Fc glycovariants and IgG1 Fc used for Fc receptor binding and physical stability assessment of IgG3 Fc 100

Figure 4.2: Cloning of FcRn into *P. pastoris* expression vector 103

Figure 4.3: Coomassie-stained SDS-PAGE of FcγRIIIA receptor purified from Ni^{2+}-NTA affinity (lane2) and phenyl sepharose (lane3) purification 107

Figure 4.4: Coomassie-stained SDS-PAGE analysis of FcRn-ST receptor..... 109

Figure 4.5: Intact protein mass spectra of FcRn-ST under reducing conditions 110

Figure 4.6: Intact protein mass spectra of FcRn-ST 110

Figure 4.7: Production of biotinylated FcRn using sortase-mediated ligation between FcRn-ST-His_6 and GGG-EDA-Biotin 112

Figure 4.8: Intact protein mass spectra of biotinylated FcRn prepared using sortase-mediated ligation under reducing conditions 113
Figure 4.9: Representative BioLayer Interferometry (BLI) binding curves for the interaction of FcγRIIIA with the IgG3 Fc glycovariants 115
Figure 4.10: Representative BioLayer Interferometry (BLI) binding curves for the interaction of FcRn with the IgG3 Fc glycovariants 117
Figure 4.11: Biophysical characterization of IgG3 Fc glycovariants: tetraglycosylated, triglycosylated, diglycosylated (N392K) and diglycosylated (N392Q) 120
Figure 4.12: Biophysical characterization of IgG3 Fc glycovariants: tetraglycosylated, triglycosylated, diglycosylated-N392K and diglycosylated-N392Q 120
Figure 4.13: Comparison of representative DSC thermograms of IgG3 Fc glycovariants: tetraglycosylated, triglycosylated, diglycosylated (N392K) and diglycosylated (N392Q) 121
Figure 5.1: Characterization of Man5-IgG3 Fc and tetraglycosylated IgG3 Fc 140
Figure 5.2: The IgG3 Fc structure 142
Figure 5.3: Sequence alignment of IgG1 (3AVE), IgG2 (4HAF), IgG3, and IgG4 (4C54) 142
Figure 5.4: The orientation of the C_H2 domain relative to the C_H3 domain 145
Figure 5.5: N-glycans in IgG3 Fc structure 147
Figure 5.6: Binding analysis of IgG3 Fc glycoforms-FcγRIIIA 149
Figure 5.7: C_H2-C_H3 interface of IgG3 Fc 152
Figure 5.8: Comparison of IgG3 Fc with other Fc structures 153
Figure 5.9: IgG3 Fc at Fc-protein A/G binding interface 156
Figure 5.10: IgG3 Fc at the Fc-FcRn binding interface 158
Figure 5.11: Crystal structure of the tetraglycosylated IgG3 Fc 160

Figure 5.12: Conformation of the in-silico modeled Man8 glycan at the N392 site and its orientation in the Fc structure and crystal packing 161

Figure 5.13: Effect of N392 glycans on the C_H3-C_H3 interface of IgG3 Fc 165

List of Tables

Table 1.1: Properties of IgG subclasses. 6

Table 2.1: Relative abundances of glycoforms present at the N297 and N392 sites in human serum IgG3 from the trypsin and Asp-N digests 45

Table 3.1: List of *P. pastoris* strains used for IgG3 Fc expression..... 58

Table 4.1: Kinetic parameters obtained for binding of FcγRIIIA with IgG3 Fc glycovariants.. 115

Table 4.2: Kinetic parameters obtained for binding of FcRn with IgG3 Fc glycovariants 117

Table 4.3: Summary of physical stability parameters obtained by biophysical techniques for characterizing the physical stability of IgG3 Fc glycovariants..... 121

Table 5.1: Crystallographic data and refinement statistics for Man5-IgG3 Fc and Tetraglycosylated IgG3 Fc..... 138

Table 5.2: Separation between C_H2 domain in IgG3 Fc and reported IgG Fc structures 145

Table 5.3: Kinetic parameters obtained for binding of FcγRIIIA with the IgG3 Fc glycoforms 149

Chapter 1 Introduction

1.1 Structure and function of immunoglobulins G (IgG)

Immunoglobulins G (IgG) are heterodimeric proteins consisting of two identical heavy (H) chains and two identical light chains (L) (Fig 1.1). Each light chain is bound to a heavy chain by an inter-chain disulfide bonds. The identical heavy chains are held together by disulfide bonds in the hinge region and strong, non-covalent interactions in the C_H3 domain. IgG structure can be functionally divided into two components: Fab (fragment antigen binding) and Fc (fragment crystallizable). The Fab imparts specificity to IgG by binding to unique epitopes on the surface of antigens. The Fc imparts biological activity to IgG that results in the removal or destruction of antigens with the help of immune effector cells. The Fab is structurally divided into a variable region consisting of the V_H and V_L domains and a constant region consisting of the C_L and C_H1 domains. The Fc is divided into C_H2 and C_H3 domains. The complementarity-determining region (CDR) in the variable domain of the Fab provides diversity to antibodies by enabling them to bind to an infinite number of different epitopes. Finer details of IgG structure can be found in the reviews by Schroeder et al.[1] and the Kuby Immunology textbook.[2]

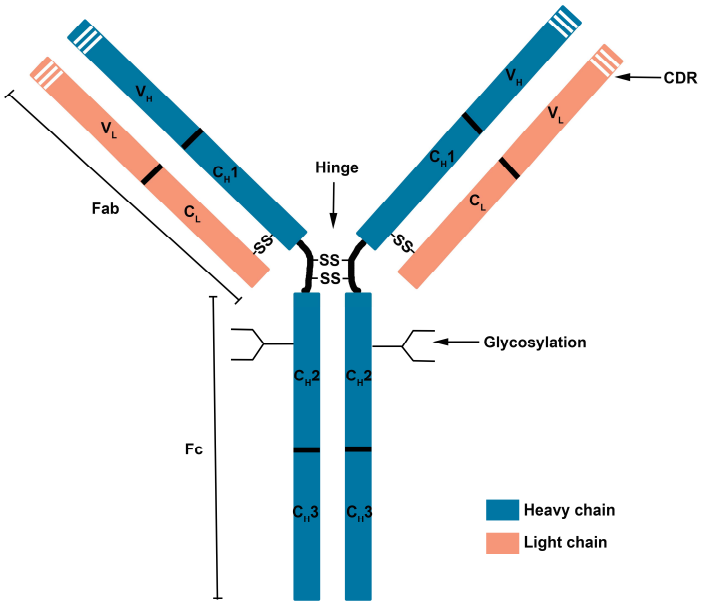

Figure 1.1: Structure of Immunoglobulin G (IgG).

Immunoglobulins/antibodies are mediators of the humoral immunity branch of the adaptive immune system. Upon exposure to antigen, naïve B cells are activated through a process that is generally initiated by helper T cells.[3] Activated B cells then differentiate into antibody-secreting plasma B cells and memory cells. The immune functions of IgG can be broadly classified into four pathways, as illustrated in Fig. 1.2.[3] These are (i) Neutralization: By binding to a pathogen or its toxins, an antibody can either prevent the pathogen's entry into cells, its replication or block its toxins from interacting with cell receptors. (ii) Antibody Dependent Cellular Phagocytosis (ADCP)/opsonization: IgG can coat the surface of pathogen and facilitate its uptake by phagocytic cells like macrophages. ADCP is mediated by binding of the Fc portion of pathogen-bound antibodies (immune complex) to the Fc receptors present on the surface of phagocytic cells. (iii) Complement activation: The Fc portion of IgG in an immune complex binds with the first complement protein C1q, which initiates a cascade of complement activity that ultimately results in the destruction of the pathogen by forming pores in its membrane. (iv)

Antibody Dependent Cellular Cytotoxicity (ADCC) is mediated by non-phagocytic cells like NK cells, basophils, and mast cells through binding of cell surface Fcγ receptors to the Fc region of IgG in an immune complex. Consequently, these activated cells release stored chemical mediators (perforins and granzymes) to lyse the target.

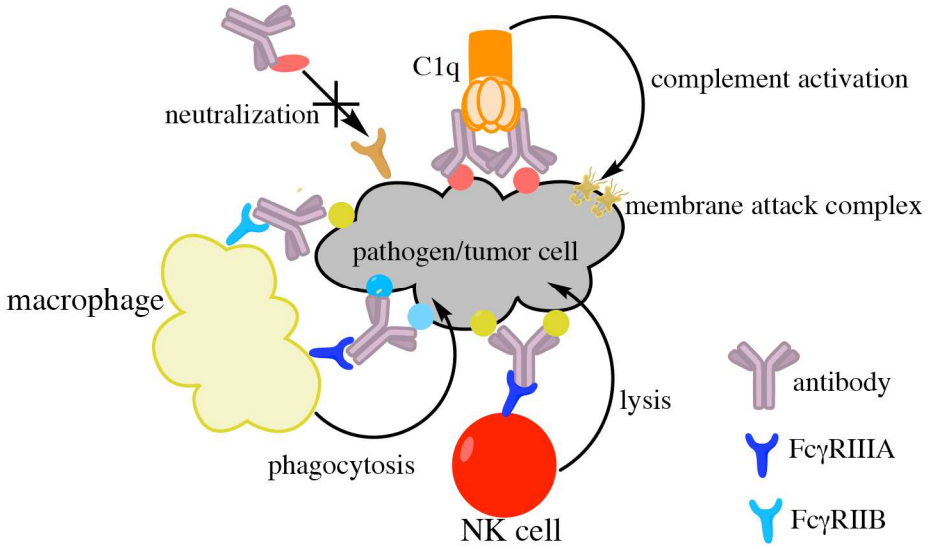

Figure 1.2: Modes of antibody action engaged in removal or destruction of pathogen or killing of a tumor cell.

1.2 Immunoglobulin isotypes and IgG isotype

There are five isotypes of immunoglobulins in humans: IgG, IgA, IgM, IgD, and IgE. The isotypes vary in their heavy chain domains and biological activities. IgM (5-10% of total serum immunoglobulin) is the first immunoglobulin to be expressed on a B-cell during its development and is present in a monomeric form on naïve B cells. An oligomeric (pentameric) form of IgM is secreted as part of the primary immune response that is initiated by opsonization of antigen and complement fixation.[1] IgD is also expressed on the surface of B cells, however its role in immunity is not fully understood. IgA (10-15% of total serum immunoglobulin) is

predominantly present in external secretions such as breast milk, saliva, and at mucosal surfaces of the gut, urogenital system and respiratory tract. It plays an important role in protection of mucosal surfaces from pathogens and their toxins.[4] IgE mediates hypersensitivity reactions from allergen exposure. Its activation leads to mast cell degranulation and an allergic response.

IgG is the most abundant isotype in serum consisting of 80% of serum immunoglobulins and is the most extensively studied isotype. IgG can elicit a pro- or anti-inflammatory response by variable binding to Fcγ receptors present on different immune cells. It is the only isotype that can cross the placenta and has the longest serum half-life among Ig isotypes.[2] The IgG isotype has four subclasses: IgG1, IgG2, IgG3 and IgG4, which are numbered in accordance to their serum levels. The IgG subclasses exhibit 90-95% homology in their heavy chain amino acid sequence.[5] In addition to amino acid differences, there are distinct structural differences among IgG subclasses with regards to the length of the hinge region and the position and location of the inter-chain (H-L) disulfide bonds (Fig 1.3). The subtle amino acid differences between the IgG subclasses are responsible for the observed differences in their Fcγ receptor interaction pattern and other IgG properties (Table 1.1). For example, IgG1 and IgG3 bind tightly to the majority of Fcγ receptors, whereas IgG2 and IgG4 bind weakly to most Fcγ receptors.[6] IgG3 is considered as the most efficient IgG subclass for eliciting complement activity followed by IgG1.[7] IgG2 is less efficient at activating complement and IgG4 does not activate complement at all. Preferential transport across the placental barrier occurs most readily for IgG1, followed by IgG4, IgG3 and IgG2.[8] The diversity in biological functions of IgG subclasses enables the immune system to choose a suitable IgG subclass for the intended immune response. Generally, IgG1 and IgG3 are associated with antibody-mediated pro-inflammatory responses, whereas IgG2 and IgG4 are associated with an immunomodulatory role. Moreover, the type of IgG subclass produced in

response to a natural infection also depends on the chemical nature of the antigen. For example, an IgG1 and IgG3 dominant response is observed for protein-based antigens, whereas polysaccharide based antigens trigger an IgG2 dominant response.[1]

Table 1.1: Properties of IgG subclasses.

	IgG1	**IgG2**	**IgG3**	**IgG4**
Molecular mass (kDa)[2]	146	146	170	146
Adult serum levels (mg/ml)[2]	5-12	2-6	0.5-1	0.2-1
Relative abundance (%)	60	32	4	4
Hinge[9]				
Amino acid residues	15	12	62	12
# of S-S	2	4	11	2
Allotypes[5]	4	1	13	0
Half-life (days)[10]	21	21	7	21
Binding to Fcγ receptors[6]				
FcγRI	+++	-	++++	++
FcγRIIAH131	+++	++	++++	++
FcγRIIAR131	+++	+	++++	++
FcγRIIB/C	+	-	++	+
FcγRIIIAF158	++	-	++++	-
FcγRIIIAV158	+++	+	++++	++
FcγRIIIB	++	-	++++	-
Binding to C1q[11]	+	+	+++	-
Binding to Protein A[12]	+	+	-	+
Binding to Protein G[12]	+	+	+	+

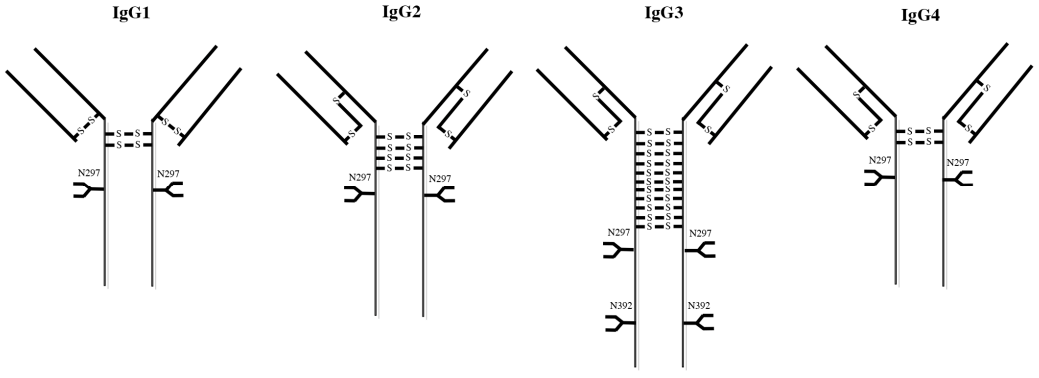

Figure 1.3: Schematic representation of structural variation with respect to inter- and intra-chain disulfide bonds in IgG subclasses

1.3 IgG3 subclass

IgG3 is the third most abundant IgG subclass consisting of 5-8% of total serum IgG and is a unique subclass for a variety of reasons.[5] It possesses the longest hinge region consisting of 11 disulfide bonds compared to the 2-4 disulfide bonds found in the other IgG subclasses. The IgG3 hinge is made of 62 amino acids, which includes 21 prolines and 11 cysteines, and adopts a rigid poly-proline helical structure.[13] In contrast, the hinge region in the other IgG subclasses consists of 12-15 amino acids and are encoded by a single exon for each subclass. In the case of IgG3, the longer hinge is due to extra copies (1-3) of a second homologous exon that is not present in the other IgG subclasses.[14] The actual hinge length of IgG3 varies among its allotypes depending upon the presence or absence of these multiple exons[5] (Fig 1.4). The long hinge is responsible for the higher MW (~170 kDa) of IgG3 relative to the other subclasses (~150 kDa).[15] It also provides a higher degree of flexibility between the Fab and the Fc region and also between the two Fab arms.[16-17] The long hinge is thought to provide additional flexibility for antigen binding, which is particularly important for sparsely distributed antigens.[16, 18] IgG3 shows extensive polymorphism with the largest number of known allotypes, 13, compared to 4, 1, and 0 allotypes known for the IgG1, IgG2, and IgG4 subclasses respectively.[19] Amino acid variations between IgG3 allotypes primarily reside in the hinge and the Fc region. The half-life of IgG3 is remarkably shorter (~7 days) than the other subclasses (~21 days).[10] This difference has been attributed to a single amino acid difference in the IgG3 Fc region (R435 in IgG3 versus H435 in the other IgG subclasses, although some IgG3 allotypes have H435 and display a longer half-life).[20] Another difference is that protein A, an Fc binding protein from *S. aureu*s commonly used for IgG purification, doesn't bind to IgG3, while it binds tightly to all the other IgG subclasses.[12] All the IgG subclasses have a single consensus N-glycosylation site at N297 in the

C_H2 domain of the Fc, while IgG3 is the only subclass that has an additional unique N-glycosylation site at N392 in the C_H3 domain. While the glycosylation at the N297 site in IgG3, like in case of IgG1, is known to be important for Fcγ receptor and C1q complement binding[21-23], the biological role of the N392 site glycosylation is not known, and its investigation is one of the research topics described in this dissertation work.

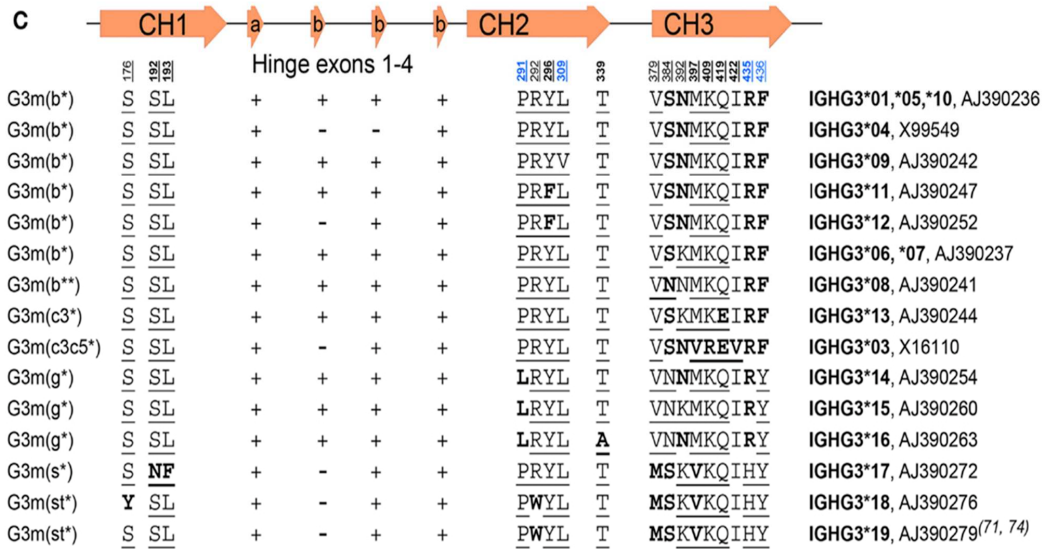

Figure 1.4: Amino acid differences in IgG3 allotypes (G3m). (+) and (-) indicate the presence and absence of the hinge exon. Amino acids in bold are unique to IgG3 or its allotype, and the underlined amino acids are present in other IgG subclasses (isoallotypes). The IMGT (in bold) numbers of IgG3 allotypes (IGHG3*) and the encoded protein accession numbers are shown on the right. This figure is reproduced from Vidarsson et al. *Frontiers in immunology* 2014, *5*, 520 under Creative Commons Attribution License.

IgG3 has potent pro-inflammatory properties since it is the most efficient IgG subclass for eliciting complement dependent cytotoxicity (CDC) and has an equivalent ADCC activity as IgG1.[5] IgG1 and IgG3 levels are generally increased in response to bacterial and viral pathogens with IgG3 appearing first during the initial phase of infection.[24] For example, IgG3 has been associated with immune protection in case of the malaria and chikungunya infections.[25] IgG1 and

IgG3 levels are also elevated in autoimmune conditions, an effect that is attributed to the strong effector functions of IgG3.[26] IgG3 deficiency is not known to be associated with any specific condition and is generally observed with concomitant deficiency of other IgG subclasses.[27-28] Recently, IgG3 has gained attention in the field of HIV vaccines. In the only successful HIV vaccine trial to date, the RV144 HIV trial, IgG3 was found as an immune correlate in vaccine protection. Subsequent analysis suggested a possible role of the Fc-mediated effector functions of IgG3 in the anti-viral activity.[29] Human IgG3 was found to be the dominant IgG subclass in cryoglobulins associated with myeloma.[30] In myeloma and autoimmune conditions, some IgG3 show a tendency to self-associate which causes them to precipitate at low temperatures.[31] The Fc region was shown to be important in this self-association property through Fc-Fc mediated interactions.[32-33] The molecular basis of cryoglobulin formation is still unclear, although certain unusual IgG structural characteristics or factors that affect protein solubility[34] are believed to be involved. At least in one case, the Fc fragment of a cryoglobulin IgG3, Jir protein from a myeloma patient was involved in IgG3 cryoglobulin formation.[33]

The majority of the therapeutic antibodies (mAbs) are based on the IgG1 subclass primarily due to its superior effector functions and high serum abundance. There are a few mAbs that are based on IgG2 and IgG4, and these are mostly used when effector functions are undesired or not required, for instance when only a blocking activity is desired. Currently, there are no marketed IgG3 based therapeutics, and multiple reasons can be suggested for this disfavor: (i) its shorter half-life, (ii) due to large number of allotypes, there exists a potential for anti-drug antibodies when therapeutic IgG3 is administered to an incompatible population group, (iii) IgG3 does not bind to protein A (used for affinity purification of the other IgG subclasses), which is the preferred and well-established method of antibody production in biotech industry,

(iv) manufacturing issues due to long hinge and its susceptibility to proteolysis (proteases like papain, pepsin, trypsin, and plasmin cleave within the hinge or close to the hinge region of antibodies. The IgG3 hinge, being more flexible and accessible is prone to proteolysis[35]) and (v) since IgG1-based therapeutics have been traditionally used successfully for pro-inflammatory applications, there is not a pressing need to develop IgG3 based therapeutics currently. Despite these factors, IgG3 can be an attractive choice for treating conditions that require a potent pro-inflammatory response (such as complement activation) owing to its strong effector functions. The shorter half-life of IgG3 may be beneficial in limiting the stimulation of immune system. Alternatively, IgG3 can be an ideal antibody candidate for diagnostic purpose owing to its relatively rapid clearance. IgG3 subclass may be useful to target sparsely distributed antigens on a target cell since it possesses more flexibility owing to the longer hinge region.

1.4 Fcγ receptors

Fc receptors are a family of cell surface receptors present on immune cells that bind to the Fc portion of IgG. Fc receptors play an important role in immune regulation by serving as a link between antibody-mediated responses and cellular effector functions. Specific Fc receptors exist for each Ig isotype: FcαR (IgA), FcδR (IgD), FcεR (IgE), FcμR (IgM), and FcγR (IgG). There are three classes of human Fcγ receptor: FcγRI, FcγRII, and FcγRIII and their respective subclasses: FcγRIA/B/C, FcγRIIA/B/C, and FcγRIIIA/B.[36] Functionally, Fcγ receptors can be classified as activating (FcγRI, FcγRIIA, FcγRIII) and inhibitory (FcγRIIB) receptors.[37] FcγR are transmembrane receptors (except FcγRIIIB), where the extracellular domain binds to IgG Fc and the cytosolic part or its associated signaling adaptor molecule (γ chain) contains distinct functional motifs for signal transduction. The activating motif is referred to as the immunoreceptor tyrosine-activating motif (ITAM), and the inhibitory motif is referred to as

immunoreceptor tyrosine-inhibitory motif (ITIM).[38] Generally, activation of an immune cell is not triggered by a monovalent FcγR (except FcγRIA) interaction, but requires cross-linking of FcγRs as found in an immune complex. Such a mechanism prevents constant stimulation of an immune response by monomeric IgG. Different immune cells show different patterns of FcγR expression and FcγRs engage with IgG subclasses with varied binding affinities.[36] The outcome of a FcγR-mediated immune response is determined by the type of IgG subclass, the class of FcγR and the nature of immune cell engaged in the response.

FcγRIIIA is a heavily glycosylated protein expressed on the surface of macrophages and monocytes. It is the sole Fcγ receptor present on the NK cells in most people. Two polymorphic variants of FcγRIIIA exist, the high affinity FcγRIIIA-V158 and low affinity FcγRIIIA-F158, which have marked differences in their IgG binding capacities. FcγRIIIA binds to the IgG subclasses with a rank order: IgG1=IgG3>>IgG4>IgG2. ADCC activity mediated by NK cells through binding with FcγRIIIA is considered important in the mechanism of action of many therapeutic monoclonal antibodies.[39] Recognizing the importance of FcγRIIIA in mAb therapeutics, there have been several Fc engineering efforts to increase FcγRIIIA affinity to confer increased potency to IgGs [see section 1.6, 1.8 (glycoengineering)].

1.5 Neonatal Fc receptor (FcRn)

FcRn is a heterodimer composed of a MHC-class-I-like heavy chain and β2 microglobulin (β2m).[40] The two well-known functions of FcRn are placental transfer of maternal IgG to fetuses (transcytosis) and the maintenance of long circulating half-lives of serum IgG and albumin (recycling). Although the precise site of recycling is not known, it is widely suggested to be in the vascular endothelium. The FcRn expressed in the placental syncytiotrophoblasts is responsible for transcytosis.[41] The receptor binds to the Fc portion of IgG at an acidic pH (<6.5)

but shows no binding at physiological pH (7.4). IgG and albumin are constantly pinocytosed by cells, where both the proteins bind to FcRn in the acidic environment of endosomes. The bound proteins are then recycled back to the cell surface and released at physiological pH (Fig. 1.5). This recycling mechanism rescues IgG and albumin from lysosomal degradation and thereby regulates its serum persistence. A similar pH dependent mechanism is involved in the FcRn-mediated directional transcytosis across placental epithelial barriers.[42] In recent studies, immune-related functions of FcRn have emerged that suggest its possible role in antigen presentation by professional APC cells and for conferring mucosal protection.[43] A good correlation between FcRn affinity and *in-vivo* half-life is known, and this led to Fc engineering strategies aimed at increasing serum half-lives of mAb therapeutics.[44] The involvement of the Fc in maintenance of IgG half-life has led to the development of a new class of biologic drugs, Fc-fusions, where biologically active peptides or proteins that otherwise clear rapidly are fused to the Fc region of IgG to increase their serum persistence.[45]

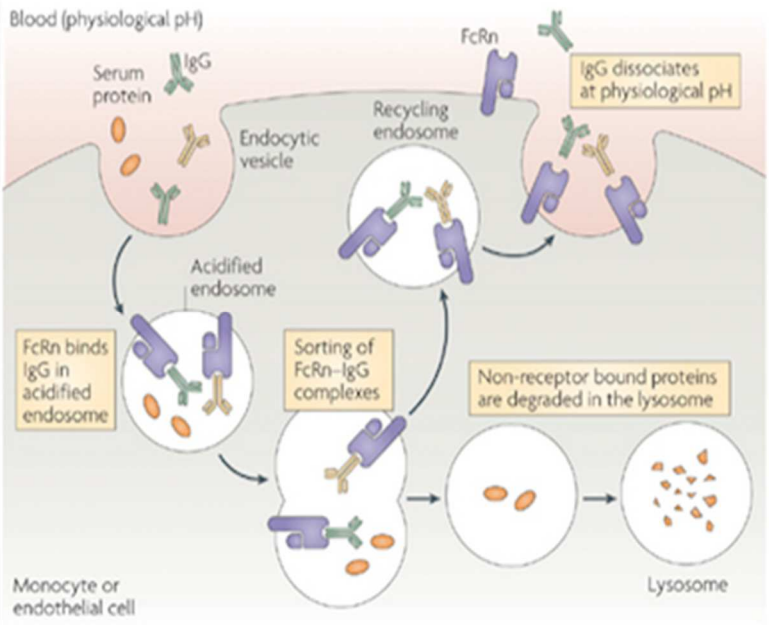

Figure 1.5: Recycling of IgG by FcRn receptor (Reprinted by permission from Macmillan Publishers Ltd: Nat Rev Immunol[42], copyright (2007).

1.6 Monoclonal antibody (mAb) therapeutics and antibody engineering

mAbs are antibodies that bind to a specific epitope on an antigen and are produced from a single B-cell clone. mAbs were first produced in 1975 from hybridoma cells, generated from the fusion of an immortalized myeloma cell and a B-cell clone from mouse.[46] A mouse B-cells was first used instead of human B-cells since the technology available at the time would have required injection of antigens into humans instead of mice to get the B-cells with the sacrifice of the subject. The first generation of therapeutic mAbs were murine mAbs, which were approved and used, though most have now been taken off the market because they induced a strong immune response due to their non-human amino acid sequence. This limitation was eliminated with the advent of chimerization and humanization technologies in mid 1980's.[47-48] Chimerization involves grafting of the variable regions from the Fab domain of a murine antibody onto the constant region of a human antibody. Humanization involves grafting of only the complementarity determining region (CDR) of the murine antibody on the human antibody. The further reduction in mouse-specific content in humanized therapeutic mAbs significantly reduced immunogenicity, and since then humanization technology has proved to be a successful antibody generation platform. In the last 15 years, fully human antibodies have been developed using phage display or the use of transgenic animals and are potentially better tolerated than the humanized antibodies.[49] Therapeutic mAbs have shown outstanding clinical outcomes compared to small molecule therapies, and have been successfully used in treating cancer, autoimmune diseases, inflammation and infections.

Since the Fc region of IgG is crucial for effector functions and half-life, there is an immense interest in Fc engineering approaches to improve the therapeutic efficacy and pharmacokinetic properties of antibody therapeutics. Engineering approaches mainly fall under

two categories: (i) protein engineering by replacing and/or deleting specific amino acids and (ii) alteration of N-linked glycans on the Fc (glycoengineering, discussed in section 1.8). Protein engineering using rational design or directed evolution has been successfully used to optimize the Fc amino acid sequence to improve FcγR binding and C1q binding and thereby modulate the strength and selectivity of effector functions.[50] The following are a few examples of engineered IgG with improved functions. First, a triple mutant Fc (S239D/I332E/A330L) and double mutant Fc (S239D/I332E) both showed higher affinity for the activating receptor FcγRIIIA over the inhibitory receptor FcγRIIB resulting in a significantly enhanced ADCC activity.[51] Second, removal of glycans from IgG results in loss of FcγR binding ability, and in another study, specific amino acids mutations were introduced to restore the FcγR binding ability of aglycosylated IgG.[52-53] This is a significant finding since aglycosylated IgG can be produced in *E.coli* with significantly lower production costs. Third, a Rituximab Fc variant with a double mutation (K326W/E333S) showed five-fold higher C1q binding and over two-fold higher CDC activity.[54] An another Rituximab variant based on an IgG1/IgG3 hybrid showed higher CDC than either IgG1 or IgG3. The hybrid contained the C_H1 domain from IgG1, and the C_H2 and C_H3 domains from IgG3 (with the exception of an IgG1-like C-terminal C_H3 domain to restore protein A binding capacity of the hybrid).[55] Fourth, multiple Fc variants with mutations that specifically increases affinity to FcRn at an acidic pH have been identified and have been shown to have longer half-life in animal models.[56-58] A well-known example of an engineered antibody with extended half-life is motavizumab (an IgG1 antibody) with the YTE mutation in the Fc region (M252Y, S254T, T256E). The mutant antibody resulted in a 10-fold increase in FcRn affinity at pH 6.0 and a 2 to 4 fold increase in serum half-life in humans compared to the native motavizumab.[59]

1.7 Protein glycosylation

Glycosylation is a post-translational modification (often considered as a co-translational modification in case of N-glycosylation) that covalently attaches oligosaccharides to the growing polypeptide chain. It is estimated that more than half of all proteins synthesized in the body are glycosylated. Based on the site of attachment, glycosylation can be classified as N-linked or O-linked. The Asn in a consensus sequence N-X-S/T (X is any amino acid but Pro) acts as an acceptor site for N-glycans, while any Ser or Thr in the protein sequence can be an acceptor site for O-glycosylation. Glycosylation, unlike protein synthesis is not a template driven process, but is dictated by glycosylation processing machinery consisting of sugar substrates, glycosyltransferases and glycosidases. N-glycosylation is the primary focus of this dissertation work and will be discussed in further details.

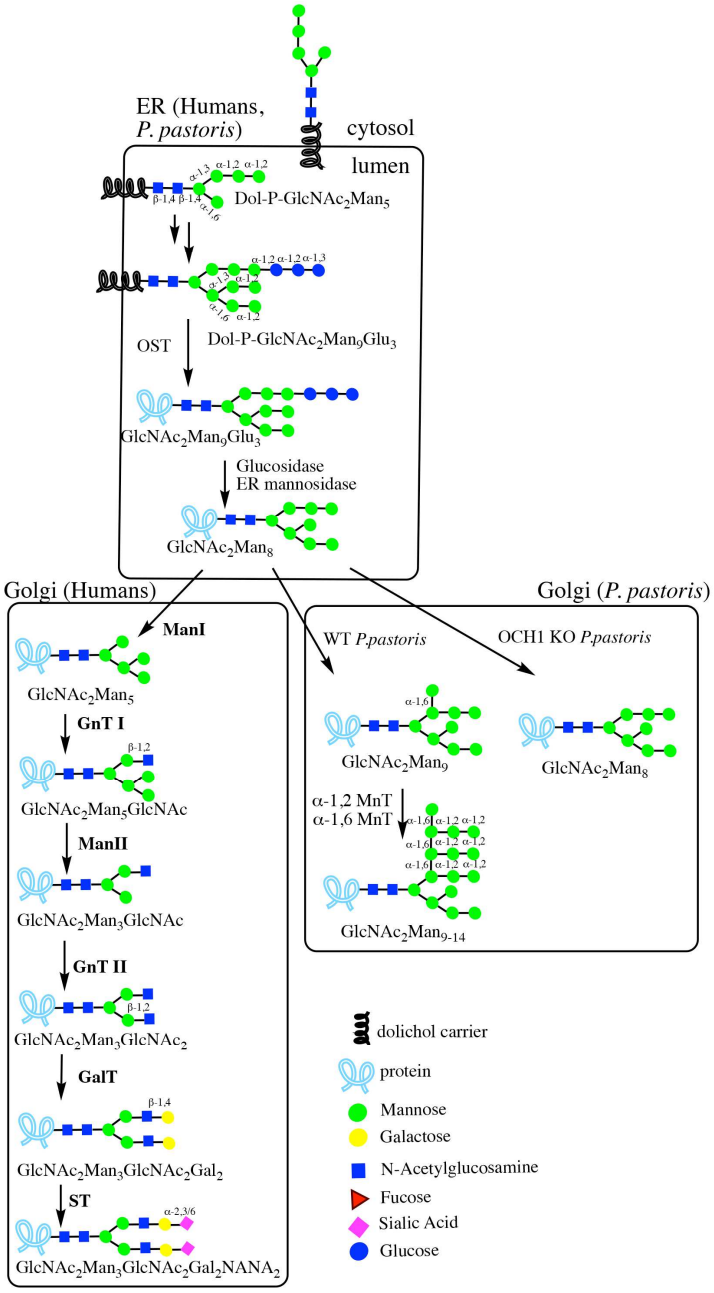

Figure 1.6: N-glycosylation biosynthesis pathway in humans and yeast. Enzyme abbreviations used in the figure are OST: Oligosaccharyltransferase, Man I/II: mannosidase, GnT: N-acetylglucosaminyl transferase, GalT: galactosyltransferase, ST: sialyltransferase, ManT: mannosyltransferase.

Human N-glycosylation biosynthesis is depicted in Fig.1.6 and is described below with limited details; more exhaustive information can be found elsewhere.[60] N-glycosylation begins

on the cytosolic face of the endoplasmic reticulum (ER) by transfer of N-acetylglucosamine (GlcNAc) from UDP-GlcNAc onto dolichol-P-phosphate (lipid carrier). The initial GlcNAc-P-dolichol is extended to $Man_5GlcNAc_2$-P-dolichol by addition of GlcNAc and Mannose sugars in glycosyltransferase reactions. This structure is then flipped across the ER membrane and into the luminal face of the ER. In the ER lumen, the structure is elongated to $Glu_3Man_9GlcNAc_2$-P-dolichol, which is then transferred from the dolichol carrier to the nitrogen atom of the Asn side chain with the help of a multi-subunit enzyme complex called oligosaccharyltransferase (OST). A glycosylation site on a protein may or may not be glycosylated, which generates copies of same protein with variable glycosylation site-occupancy, commonly referred as macroheterogeneity.

The $Glu_3Man_9GlcNAc_2$ structure on the protein is sequentially trimmed to $Man_9GlcNAc_2$ by action of glucosidase I and II. Glucose trimming is critical for correct protein folding and is a part of protein quality control in the ER. Incorrectly folded proteins can be re-glucosylated and allowed to fold correctly. Chaperons such as calnexin and calreticulin are lectins that recognize glucose and help in the protein folding process.[61] The $Man_9GlcNAc_2$ structure in a correctly folded protein is trimmed to a $Man_8GlcNAc_2$ structure by the removal of a terminal α-1,2 mannose by ER mannosidase. $Man_8GlcNAc_2$ exits the ER and enters the golgi apparatus, where further trimming of mannose by mannosidase enzymes result in the $Man_5GlcNAc_2$ structure in the *cis*-golgi. At this point in humans, three different classes of N-linked glycans can be synthesized from the $Man_5GlcNAc_2$ glycan: high mannose, hybrid and complex types of glycan that share the common trimannosyl core (Fig. 1.7). High mannose glycans consist of all the five mannoses present in the $Man_5GlcNAc_2$ structure and may have additional mannose residues. Complex glycans consist of the trimannosyl core with GlcNAc attached to the α-1,3 and α-1,6

branches of the trimannosyl core and may have additional branching. Hybrid glycans consist of mannose residues on the α-1,6 branch (like high mannose glycans) but contains GlcNAc on the α-1,3 branch (like complex glycans).

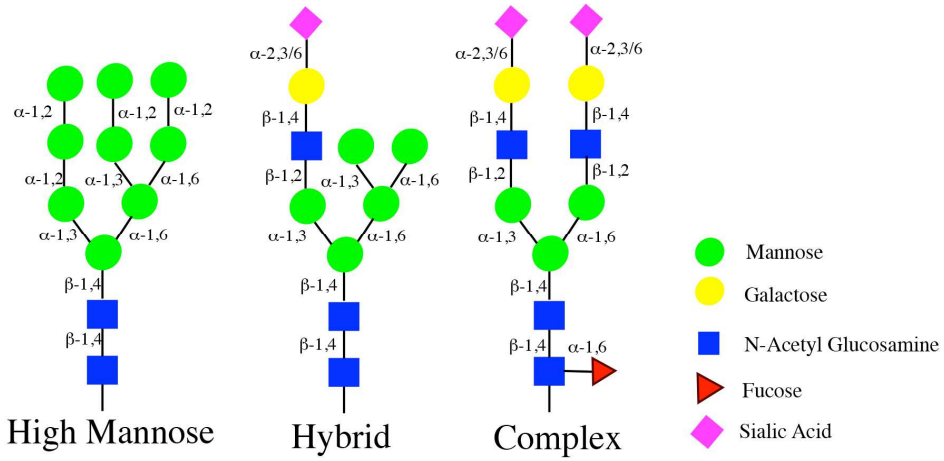

Figure 1.7: Types of N-glycan: high mannose, hybrid and complex

For the formation of complex glycans, the $Man_5GlcNAc_2$ structure undergoes a series of step-wise glycoprocessing steps in the *medial*-golgi. First, a GlcNAc is added on the α-1,3 branch of the $Man_5GlcNAc_2$ structure by N-acetyl glucosaminyl transferase I (GnTI) to produce hybrid glycan. This is then subjected to further mannose trimming by mannosidase II to cleave terminal α-1,3 and α-1,6 mannose residues to yield a $GlcNAc_1Man_3GlcNAc_2$ structure. This structure is then converted to a complex-type glycan by addition of GlcNAc on the α-1,6 arm by GnTII. The resulting structure $GlcNAc_2Man_3GlcNAc_2$ is referred to as the core heptasaccharide, a structural feature common to all the complex-type glycoforms.

The core heptasaccharide structure can be further modified by galactose, bisecting GlcNAc, N-acetylneuraminic acid (Neu5Ac/sialic acid) and fucose in the *trans*-golgi (Fig. 1.8). The multiple glycan modifying enzymes and sugar substrates are localized across different golgi compartments which make biosynthesis of an N-glycan a highly complex process. The variable

addition of sugars on the core heptasaccharide results in microhetergeneity, which is the presence of different glycan structures (glycoforms) at the same site in different copies of the same protein. Additional branching to the biantennary structure generates tri- and tetra-antennary glycans, which introduces additional heterogeneity. The factors that control glycosylation are not fully understood, but glycosylation is believed to be a highly-regulated process. Factors like competition between glycoprocessing enzymes, availability of active-sugar donors, site-accessibility, protein translocation rate, and golgi residence time contribute to this complex process.[62]

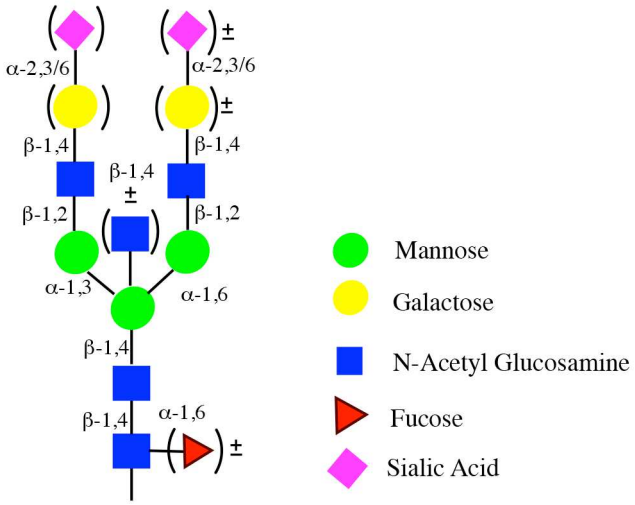

Figure 1.8: Structure of a fully-processed complex-type glycoform. The variable addition of Fucose, bGlcNAc, Galactose and Sialic acid (marked by brackets) results in different glycoform structures.

1.8 Importance of glycosylation on IgG and glycoengineering

All the human IgG subclasses have a conserved N-glycosylation site at N297 in the C_H2 domain of the Fc. The majority of glycans at the N297 site are complex biantennary type with core fucose and a varying number of galactose, bisecting GlcNAc (bGlcNAc) and sialic acid sugar residues.[63] There is also a minor presence of non-fucosylated complex biantennary glycans

with or without bisecting GlcNAc. High mannose and hybrid type glycans may also be present in trace amounts.[64] Microheterogeneity from N297 glycosylation can produce over 30 different glycoforms. Changes in the IgG glycosylation pattern have been associated with physiological (such as age, pregnancy) and pathological conditions (such as autoimmune conditions and others).[65] Altered glycoform distribution is well-characterized in autoimmune conditions, where elevated levels of agalactosylated glycoforms are found.[66] The pro-inflammatory nature of agalactosylated IgG is hypothesized to be reflective of an overall increased inflammatory state in an autoimmune condition. In a contrasting scenario, increased levels of galactosylation and sialylation (suggested to have an anti-inflammatory activity) are found in pregnancy, where an increase in inflammatory state would be undesirable.[67] With the success of antibody therapeutics, a significant amount of research work has focused on investigating the role of glycosylation on IgG effector functions.[68-70] The outcome of these efforts has led to the development of antibodies with specific glycosylation patterns through glycoengineering approach to modulate immune responses. The following paragraph discusses the influence of variable sugar residues in complex glycans on the immune-related function of IgG.

Core fucosylation is addition of α-1,6 linked fucose to the first GlcNAc of the core heptasaccharide by fucosyltransferase. It is widely accepted that the removal of fucose from the N297 glycan in IgG1 significantly increases IgG1 affinity for FcγRIIIA and consequently its ADCC activity.[71] This effect was also demonstrated for the other IgG subclasses but with different magnitudes of improvement.[72] The molecular basis behind such an effect has been attributed to the formation of favorable glycan (Fc)-glycan (FcγRIIIA) contacts upon removal of fucose.[73] Incidentally, more than 80% of the N297 glycans from serum IgG and IgG produced from CHO cells are fucosylated. Two approaches have been utilized to produce afucosylated

therapeutic antibodies that potentially have a higher *in-vivo* ADCC activity. The first approach involves deletion of the FUT8 gene in CHO cells that encodes for α-1,6 fucosyltransferase. The engineered CHO cell line was developed by Kyowa Hakko Kirin company and is presently used to produce mogamulizumab (currently approved in Japan, in clinical trial in US), the first marketed glycoengineered mAb. The second approach involves the overexpression of β-1,4 N-acetylglucosaminyl transferase III (GnTIII), which adds a bisecting GlcNAc on the trimannosyl core. As a result, further addition of fucose is inhibited in CHO cells. This engineered CHO cell line was developed by Roche-Glycart and is used to produce obinutuzumab (approved in US). Originally, IgG glycoforms with **bisecting GlcNAc** were thought to have higher FcγRIIIA binding and ADCC activity, but it was later shown that this effect was largely due to lack of fucose rather than presence of bisecting GlcNAc.[74] The evidence in literature for the role of galactose is conflicting. Some reports attribute higher ADCC activity to higher galactosylated forms of IgG, while others have suggested hypogalactosylated IgG to have more pro-inflammatory activity. The presence of α-2,6 **sialic acid** has been shown to impart anti-inflammatory activity to IgG. The suggested underlying mechanism behind such effect is attributed to upregulation of inhibitory FcγRIIB receptor upon binding of sialylated Fc to the SIGN-RI receptor in mice. These results are based on mouse models, and its applications in humans is currently contested.[75] Producing antibodies with specific glycosylation patterns (glycoengineering) to engage specific immune response can be more beneficial than protein engineering strategies, since changes to the natural antibody sequence can be potentially immunogenic.

1.9 Production of homogenously glycosylated proteins in the yeast *Pichia pastoris*

Glycosylated antibodies have been traditionally produced in mammalian expression

systems. Commonly used mammalian cells are Chinese Hamster Ovary (CHO) and mouse myeloma cells (NS0 or SP2.0). The majority of therapeutic mAbs are produced in CHO cells, and these cells are considered as a reliable platform for industrial-scale mAb production.[76] Antibodies expressed in mammalian cells possess human-like glycosylation for the most part. The types of sugars and their linkages produced in non-human cell lines are very similar to humans; however, some non-human sugars can be still found in small amounts. For example, the SP2.0 or NS0 cells can produce α-1,3 galactose and N-glycolylneuraminic acid (Neu5Gc) sugars on IgG that are not found in humans. Also, antibodies expressed in mammalian cells exhibit microheterogeneity (like the endogenous antibodies), which is not suitable for investigating glycoform-dependent antibody properties.[77] A few shortcomings of mammalian cell expression systems are high production cost, the requirement of complex growth media, slower growth, and a potential for viral contamination. To overcome these limitations, alternate expression systems using yeast, plant, and insect cells have been explored by researchers.

Yeast is an attractive expression host because of lower production cost, faster growth times, high protein titers, and the ability to perform eukaryotic post-translational modifications like protein folding, disulfide bond formation and glycosylation.[78] A major drawback of N-glycosylation in yeast is that it produces hypermannosylated glycans, which are not found in humans (and hence immunogenic) and are recognized by macrophage mannose receptors leading to rapid clearance.[79] The N-glycosylation biosynthesis pathway in yeast shares its initial steps (in the ER) with the human pathway (Fig. 1.6). The $Man_8GlcNAc_2$ structure synthesized in the yeast ER is similar to humans, but its further processing in the golgi is species dependent. In the yeast golgi, by action of an α-1,6 mannosyltransferase (encoded by OCH1 gene), α-1,6 mannose is added to the α-1,3 arm of the trimannosyl core. The resulting structure becomes a substrate for

other mannosyltransferases and ultimately generates a heterogeneous mixture of multi-branched hypermannosylated structures.[79] *Saccharomyces cerevisiae* (baker's yeast) and *Pichia pastoris* are the two commonly used yeast species for heterologous protein expression. *P. pastoris* is a preferred over *S. cerevisiae* due to lower levels of hypermannosylation and the absence of the α-1,3 mannose linkage (a non-human linkage).[78]

The last 15 years have witnessed significant advances in yeast N-glycosylation engineering to replace the native glycosylation pathway in the yeast with the human pathway. A breakthrough in yeast engineering efforts was achieved with the knock out of the OCH1 gene, first demonstrated in *S. cerervisiae* by the Jigami group[80] and later in *P. pastoris* by the Contreras[81] and Gerngross groups[82]. The OCH1 deletion in *P. pastoris* result in production of homogenous high mannose type of glycosylation consisting of mainly a $Man_8GlcNAc_2$ (Man8) structure. The Man8 structure was the starting point for introducing a human glycosylation pathway in yeast that produces fully-human, complex-type glycoforms, as shown by the Callewaert[83] and Gerngross groups[84]. The humanization of the *Pichia* glycosylation pathway involves (i) introduction of genes that encode for various glycosidases and glycosyltransferases that allow trimming of mannose sugars and the addition of new sugars to synthesize complex glycoforms. These enzymes are localized to specific golgi compartments by use of appropriate signal peptides. (ii) expression of UDG-galactose and UDP-GlcNAc transporters to transfer sugars into the golgi.[85] The glycosylation produced in the humanized *Pichia* was shown to be more homogenous than mammalian cell expressed IgG. Moreover, it provides a platform to produce antibodies with specific glycoforms as opposed to a mixture of glycoforms produced from mammalian cells.

1.10 References

1. Schroeder Jr, H. W.; Cavacini, L., Structure and function of immunoglobulins. *Journal of Allergy and Clinical Immunology* **2010,** *125* (2), S41-S52.

2. Kuby, J., *Immunology*. 3rd ed.; W.H. Freeman: New York, 1997; p xxiv, 664 p.

3. Murphy, K. M.; Travers, P.; Walport, M., Janeway's immunobiology (immunobiology: the immune system (Janeway)). *Garland Science* **2007,** *7*.

4. Brezski, R. J.; Georgiou, G., Immunoglobulin isotype knowledge and application to Fc engineering. *Current opinion in immunology* **2016,** *40*, 62-69.

5. Vidarsson, G.; Dekkers, G.; Rispens, T., IgG subclasses and allotypes: from structure to effector functions. *Frontiers in immunology* **2014,** *5*, 520.

6. Bruhns, P.; Iannascoli, B.; England, P.; Mancardi, D. A.; Fernandez, N.; Jorieux, S.; Daëron, M., Specificity and affinity of human Fcγ receptors and their polymorphic variants for human IgG subclasses. *Blood* **2009,** *113* (16), 3716-3725.

7. Tao, M.-H.; Smith, R.; Morrison, S., Structural features of human immunoglobulin G that determine isotype-specific differences in complement activation. *The Journal of experimental medicine* **1993,** *178* (2), 661-667.

8. Palmeira, P.; Quinello, C.; Silveira-Lessa, A. L.; Zago, C. A.; Carneiro-Sampaio, M., IgG placental transfer in healthy and pathological pregnancies. *Clinical and Developmental Immunology* **2011,** *2012*.

9. Liu, H.; May, K. In *Disulfide bond structures of IgG molecules: structural variations, chemical modifications and possible impacts to stability and biological function*, MAbs, Taylor & Francis: 2012; pp 17-23.

10. Morell, A.; Terry, W. D.; Waldmann, T. A., Metabolic properties of IgG subclasses in man. *Journal of Clinical Investigation* **1970,** *49* (4), 673.

11. Schumaker, V. N.; Calcott, M. A.; Spiegelberg, H. L.; Mueller-Eberhard, H. J., Ultracentrifuge studies of the binding of IgG of different subclasses to the Clq subunit of the first component of complement. *Biochemistry* **1976,** *15* (23), 5175-5181.

12. Loghem, E. v.; Frangione, B.; Recht, B.; Franklin, E., Staphylococcal protein A and human IgG subclasses and allotypes. *Scandinavian journal of immunology* **1982,** *15* (3), 275-278.

13. Michaelsen, T. E.; Frangione, B.; Franklin, E. C., Primary structure of the" hinge" region of human IgG3. Probable quadruplication of a 15-amino acid residue basic unit. *Journal of Biological Chemistry* **1977,** *252* (3), 883-889.

14. Huck, S.; Fort, P.; Crawford, D.; Lefranc, M.-P.; Lefranc, G., Sequence of a human immunoglobulin gamma 3 heavy chain constant region gene: comparison with the other human Cγ genes. *Nucleic acids research* **1986,** *14* (4), 1779-1789.

15. Saluk, P. H.; Clem, L. W., The unique molecular weight of the heavy chain from human IgG3. *The Journal of Immunology* **1971,** *107* (1), 298-301.

16. Roux, K. H.; Strelets, L.; Michaelsen, T. E., Flexibility of human IgG subclasses. *The Journal of Immunology* **1997,** *159* (7), 3372-3382.

17. Dangl, J. L.; Wensel, T. G.; Morrison, S. L.; Stryer, L.; Herzenberg, L. A.; Oi, V. T., Segmental flexibility and complement fixation of genetically engineered chimeric human, rabbit and mouse antibodies. *The EMBO journal* **1988,** *7* (7), 1989.

18. Giuntini, S.; Granoff, D.; Beernink, P.; Ihle, O.; Bratlie, D.; Michaelsen, T., Human IgG1, IgG3, and IgG3 Hinge-Truncated Mutants Show Different Protection Capabilities against Meningococci Depending on the Target Antigen and Epitope Specificity. *Clinical and Vaccine Immunology* **2016,** *23* (8), 698-706.

19. Jefferis, R.; Lefranc, M. P. In *Human immunoglobulin allotypes: possible implications for immunogenicity*, 2009; pp 332-338.

20. Stapleton, N. M.; Andersen, J. T.; Stemerding, A. M.; Bjarnarson, S. P.; Verheul, R. C.; Gerritsen, J.; Zhao, Y.; Kleijer, M.; Sandlie, I.; de Haas, M., Competition for FcRn-mediated transport gives rise to short half-life of human IgG3 and offers therapeutic potential. *Nature Communications* **2011,** *2*, 599.

21. Walker, M. R.; Lund, J.; Thompson, K. M.; Jefferis, R., Aglycosylation of human IgG1 and IgG3 monoclonal antibodies can eliminate recognition by human cells expressing Fc gamma RI and/or Fc gamma RII receptors. *Biochemical Journal* **1989,** *259* (2), 347.

22. Lund, J.; Toshiyuki, T.; Noriko, T.; Sarmay, G.; Yoji, A.; Jefferis, R., A protein structural change in aglycosylated IgG3 correlates with loss of huFcγR1 and huFcγR111 binding and/or activation. *Molecular immunology* **1990,** *27* (11), 1145-1153.

23. Jefferis, R.; Lund, J.; Goodall, M., Modulation of FcγR and human complement activation by IgG3-core oligosaccharide interactions. *Immunology Letters* **1997,** *1* (58), 67.

24. Ferrante, A.; Beard, L. J.; Feldman, R. G., IgG subclass distribution of antibodies to bacterial and viral antigens. *The Pediatric infectious disease journal* **1990,** *9* (8), 516-524.

25. Roussilhon, C.; Oeuvray, C.; Müller-Graf, C.; Tall, A.; Rogier, C.; Trape, J.-F.; Theisen, M.; Balde, A.; Pérignon, J.-L.; Druilhe, P., Long-term clinical protection from falciparum malaria is strongly associated with IgG3 antibodies to merozoite surface protein 3. *PLoS Med* **2007,** *4* (11), e320.

26. Zhang, H.; Li, P.; Wu, D.; Xu, D.; Hou, Y.; Wang, Q.; Li, M.; Li, Y.; Zeng, X.; Zhang, F., Serum IgG subclasses in autoimmune diseases. *Medicine* **2015,** *94* (2), e387.

27. Meyts, I.; Bossuyt, X.; Proesmans, M.; De, B., Isolated IgG3 deficiency in children: to treat or not to treat? Case presentation and review of the literature. *Pediatric allergy and immunology* **2006,** *17* (7), 544-550.

28. Buckley, R. H., Immunoglobulin G subclass deficiency: fact or fancy? *Current allergy and asthma reports* **2002,** *2* (5), 356-360.

29. Chung, A. W.; Ghebremichael, M.; Robinson, H.; Brown, E.; Choi, I.; Lane, S.; Dugast, A.-S.; Schoen, M. K.; Rolland, M.; Suscovich, T. J., Polyfunctional Fc-effector profiles mediated by IgG subclass selection distinguish RV144 and VAX003 vaccines. *Science translational medicine* **2014,** *6* (228), 228ra38-228ra38.

30. Grey, H. M.; Kohler, P. F.; Terry, W. D.; Franklin, E. C., Human monoclonal γG-cryoglobulins with anti—γ-globulin activity. *Journal of Clinical Investigation* **1968,** *47* (8), 1875.

31. Dammacco, F.; Sansonno, D.; Piccoli, C.; Tucci, F.; Racanelli, V., The cryoglobulins: an overview. *European journal of clinical investigation* **2003,** *31* (7), 628-638.

32. Capra, J.; Kunkel, H., Aggregation of γG3 proteins: relevance to the hyperviscosity syndrome. *Journal of Clinical Investigation* **1970,** *49* (3), 610.

33. NISHIMURA, Y.; NAKAMURA, H., Human monoclonal cryoimmunoglobulins. I. Molecular properties of IgG3k (Jir protein) and the cryo-coprecipitability of its molecular fragments by papain. *Journal of biochemistry* **1984,** *95* (1), 255-265.

34. Middaugh, C.; Lawson, E.; Litman, G.; Tisel, W.; Mood, D.; Rosenberg, A., Thermodynamic basis for the abnormal solubility of monoclonal cryoimmunoglobulins. *Journal of Biological Chemistry* **1980,** *255* (14), 6532-6534.

35. Ackerman, M.; Nimmerjahn, F., *Antibody Fc:: Linking Adaptive and Innate Immunity*. Academic Press: 2013.

36. Gessner, J.; Heiken, H.; Tamm, A.; Schmidt, R., The IgG Fc receptor family. *Annals of hematology* **1998,** *76* (6), 231-248.

37. Bournazos, S.; Ravetch, J. V., Fcγ receptor pathways during active and passive immunization. *Immunological reviews* **2015,** *268* (1), 88-103.

38. Nimmerjahn, F.; Ravetch, J. V., Fcγ receptors as regulators of immune responses. *Nature Reviews Immunology* **2008,** *8* (1), 34-47.

39. Moroi, R.; Endo, K.; Kinouchi, Y.; Shiga, H.; Kakuta, Y.; Kuroha, M.; Kanazawa, Y.; Shimodaira, Y.; Horiuchi, T.; Takahashi, S., FCGR3A-158 polymorphism influences the biological response to infliximab in Crohn's disease through affecting the ADCC activity. *Immunogenetics* **2013,** *65* (4), 265-271.

40. Firan, M.; Bawdon, R.; Radu, C.; Ober, R. J.; Eaken, D.; Antohe, F.; Ghetie, V.; Ward, E. S., The MHC class I-related receptor, FcRn, plays an essential role in the maternofetal transfer of γ-globulin in humans. *International immunology* **2001,** *13* (8), 993-1002.

41. Ghetie, V.; Ward, E. S., Multiple roles for the major histocompatibility complex class I–related receptor FcRn. *Annual review of immunology* **2000,** *18* (1), 739-766.

42. Roopenian, D. C.; Akilesh, S., FcRn: the neonatal Fc receptor comes of age. *Nature Reviews Immunology* **2007,** *7* (9), 715-725.

43. Baker, K.; Qiao, S.-W.; Kuo, T.; Kobayashi, K.; Yoshida, M.; Lencer, W. I.; Blumberg, R. S. In *Immune and non-immune functions of the (not so) neonatal Fc receptor, FcRn*, Seminars in immunopathology, Springer: 2009; pp 223-236.

44. Datta-Mannan, A.; Chow, C.-K.; Dickinson, C.; Driver, D.; Lu, J.; Witcher, D. R.; Wroblewski, V. J., FcRn affinity-pharmacokinetic relationship of five human IgG4 antibodies engineered for improved in vitro FcRn binding properties in cynomolgus monkeys. *Drug Metabolism and Disposition* **2012,** *40* (8), 1545-1555.

45. Rath, T.; Baker, K.; Dumont, J. A.; Peters, R. T.; Jiang, H.; Qiao, S.-W.; Lencer, W. I.; Pierce, G. F.; Blumberg, R. S., Fc-fusion proteins and FcRn: structural insights for longer-lasting and more effective therapeutics. *Critical reviews in biotechnology* **2015,** *35* (2), 235-254.

46. Köhler, G.; Milstein, C., Continuous cultures of fused cells secreting antibody of predefined specificity. *nature* **1975,** *256* (5517), 495-497.

47. Morrison, S. L.; Johnson, M. J.; Herzenberg, L. A.; Oi, V. T., Chimeric human antibody molecules: mouse antigen-binding domains with human constant region domains. *Proceedings of the National Academy of Sciences* **1984,** *81* (21), 6851-6855.

48. Jones, P. T.; Dear, P. H.; Foote, J.; Neuberger, M. S.; Winter, G., Replacing the complementarity-determining regions in a human antibody with those from a mouse. **1986**.

49. Carter, P., Improving the efficacy of antibody-based cancer therapies. *Nature Reviews Cancer* **2001,** *1* (2), 118-129.

50. Park, H. I.; Yoon, H. W.; Jung, S. T., The highly evolvable antibody Fc domain. *Trends in biotechnology* **2016,** *34* (11), 895-908.

51. Lazar, G. A.; Dang, W.; Karki, S.; Vafa, O.; Peng, J. S.; Hyun, L.; Chan, C.; Chung, H. S.; Eivazi, A.; Yoder, S. C., Engineered antibody Fc variants with enhanced effector function. *Proceedings of the National Academy of Sciences of the United States of America* **2006,** *103* (11), 4005-4010.

52. Jung, S. T.; Reddy, S. T.; Kang, T. H.; Borrok, M. J.; Sandlie, I.; Tucker, P. W.; Georgiou, G., Aglycosylated IgG variants expressed in bacteria that selectively bind FcγRI potentiate tumor cell killing by monocyte-dendritic cells. *Proceedings of the National Academy of Sciences* **2010,** *107* (2), 604-609.

53. Sazinsky, S. L.; Ott, R. G.; Silver, N. W.; Tidor, B.; Ravetch, J. V.; Wittrup, K. D., Aglycosylated immunoglobulin G1 variants productively engage activating Fc receptors. *Proceedings of the National Academy of Sciences* **2008,** *105* (51), 20167-20172.

54. Idusogie, E. E.; Wong, P. Y.; Presta, L. G.; Gazzano-Santoro, H.; Totpal, K.; Ultsch, M.; Mulkerrin, M. G., Engineered antibodies with increased activity to recruit complement. *The Journal of Immunology* **2001,** *166* (4), 2571-2575.

55. Natsume, A.; In, M.; Takamura, H.; Nakagawa, T.; Shimizu, Y.; Kitajima, K.; Wakitani, M.; Ohta, S.; Satoh, M.; Shitara, K., Engineered antibodies of IgG1/IgG3 mixed isotype with enhanced cytotoxic activities. *Cancer Research* **2008,** *68* (10), 3863-3872.

56. Yeung, Y. A.; Leabman, M. K.; Marvin, J. S.; Qiu, J.; Adams, C. W.; Lien, S.; Starovasnik, M. A.; Lowman, H. B., Engineering human IgG1 affinity to human neonatal Fc receptor: impact of affinity improvement on pharmacokinetics in primates. *The Journal of Immunology* **2009,** *182* (12), 7663-7671.

57. Borrok, M. J.; Wu, Y.; Beyaz, N.; Yu, X.-Q.; Oganesyan, V.; Dall'Acqua, W. F.; Tsui, P., pH-dependent binding engineering reveals an FcRn affinity threshold that governs IgG recycling. *Journal of Biological Chemistry* **2015,** *290* (7), 4282-4290.

58. Hinton, P. R.; Xiong, J. M.; Johlfs, M. G.; Tang, M. T.; Keller, S.; Tsurushita, N., An engineered human IgG1 antibody with longer serum half-life. *The Journal of Immunology* **2006,** *176* (1), 346-356.

59. Robbie, G. J.; Criste, R.; Dall'Acqua, W. F.; Jensen, K.; Patel, N. K.; Losonsky, G. A.; Griffin, M. P., A novel investigational Fc-modified humanized monoclonal antibody, motavizumab-YTE, has an extended half-life in healthy adults. *Antimicrobial agents and chemotherapy* **2013,** *57* (12), 6147-6153.

60. Brooks, S. A., Protein Glycosylation. *Encyclopedia of Industrial Biotechnology* **2010**.

61. Helenius, A.; Trombetta, E. S.; Hebert, D. N.; Simons, J. F., Calnexin, calreticulin and the folding of glycoproteins. *Trends in cell biology* **1997,** *7* (5), 193-200.

62. Spahn, P. N.; Lewis, N. E., Systems glycobiology for glycoengineering. *Current opinion in biotechnology* **2014,** *30*, 218-224.

63. Wuhrer, M.; Stam, J. C.; van de Geijn, F. E.; Koeleman, C. A.; Verrips, C. T.; Dolhain, R. J.; Hokke, C. H.; Deelder, A. M., Glycosylation profiling of immunoglobulin G (IgG) subclasses from human serum. *Proteomics* **2007,** *7* (22), 4070-4081.

64. Raju, T. S., Terminal sugars of Fc glycans influence antibody effector functions of IgGs. *Current opinion in immunology* **2008,** *20* (4), 471-478.

65. Parekh, R.; Roitt, I.; Isenberg, D.; Dwek, R.; Rademacher, T., Age-related galactosylation of the N-linked oligosaccharides of human serum IgG. *Journal of Experimental Medicine* **1988,** *167* (5), 1731-1736.

66. Rademacher, T. W.; Williams, P.; Dwek, R. A., Agalactosyl glycoforms of IgG autoantibodies are pathogenic. *Proceedings of the National Academy of Sciences* **1994,** *91* (13), 6123-6127.

67. van de Geijn, F. E.; Wuhrer, M.; Selman, M. H.; Willemsen, S. P.; de Man, Y. A.; Deelder, A. M.; Hazes, J. M.; Dolhain, R. J., Immunoglobulin G galactosylation and sialylation are associated with pregnancy-induced improvement of rheumatoid arthritis and the postpartum flare: results from a large prospective cohort study. *Arthritis research & therapy* **2009,** *11* (6), R193.

68. Lux, A.; Nimmerjahn, F., Impact of differential glycosylation on IgG activity. *Crossroads between Innate and Adaptive Immunity III* **2011**, 113-124.

69. Mimura, Y.; Church, S.; Ghirlando, R.; Ashton, P.; Dong, S.; Goodall, M.; Lund, J.; Jefferis, R., The influence of glycosylation on the thermal stability and effector function expression of human IgG1-Fc: properties of a series of truncated glycoforms. *Molecular immunology* **2000,** *37* (12), 697-706.

70. Krapp, S.; Mimura, Y.; Jefferis, R.; Huber, R.; Sondermann, P., Structural analysis of human IgG-Fc glycoforms reveals a correlation between glycosylation and structural integrity. *Journal of molecular biology* **2003,** *325* (5), 979-989.

71. Shields, R. L.; Lai, J.; Keck, R.; O'Connell, L. Y.; Hong, K.; Meng, Y. G.; Weikert, S. H.; Presta, L. G., Lack of fucose on human IgG1 N-linked oligosaccharide improves binding to human FcγRIII and antibody-dependent cellular toxicity. *Journal of Biological Chemistry* **2002,** *277* (30), 26733-26740.

72. Niwa, R.; Natsume, A.; Uehara, A.; Wakitani, M.; Iida, S.; Uchida, K.; Satoh, M.; Shitara, K., IgG subclass-independent improvement of antibody-dependent cellular cytotoxicity by fucose removal from Asn< sup> 297</sup>-linked oligosaccharides. *Journal of immunological methods* **2005,** *306* (1), 151-160.

73. Ferrara, C.; Grau, S.; Jäger, C.; Sondermann, P.; Brünker, P.; Waldhauer, I.; Hennig, M.; Ruf, A.; Rufer, A. C.; Stihle, M., Unique carbohydrate–carbohydrate interactions are required for high affinity binding between FcγRIII and antibodies lacking core fucose. *Proceedings of the National Academy of Sciences* **2011,** *108* (31), 12669-12674.

74. Shinkawa, T.; Nakamura, K.; Yamane, N.; Shoji-Hosaka, E.; Kanda, Y.; Sakurada, M.; Uchida, K.; Anazawa, H.; Satoh, M.; Yamasaki, M., The absence of fucose but not the presence of galactose or bisecting N-acetylglucosamine of human IgG1 complex-type oligosaccharides shows the critical role of enhancing antibody-dependent cellular cytotoxicity. *Journal of Biological Chemistry* **2003,** *278* (5), 3466-3473.

75. Tjon, A. S.; van Gent, R.; Geijtenbeek, T. B.; Kwekkeboom, J., Differences in anti-inflammatory actions of intravenous immunoglobulin between mice and men: more than meets the eye. *Frontiers in immunology* **2015,** *6*, 197.

76. Frenzel, A.; Hust, M.; Schirrmann, T., Expression of recombinant antibodies. *Frontiers in immunology* **2013,** *4*, 217.

77. Butler, M.; Spearman, M., The choice of mammalian cell host and possibilities for glycosylation engineering. *Current opinion in biotechnology* **2014,** *30*, 107-112.

78. Cereghino, G. P. L.; Cereghino, J. L.; Ilgen, C.; Cregg, J. M., Production of recombinant proteins in fermenter cultures of the yeast< i> Pichia pastoris</i>. *Current Opinion in Biotechnology* **2002,** *13* (4), 329-332.

79. Bretthauer, R. K.; Castellino, F. J., Glycosylation of Pichia pastoris‐derived proteins. *Biotechnology and applied biochemistry* **1999,** *30* (3), 193-200.

80. Nakayama, K.-i.; Nagasu, T.; Shimma, Y.-I.; Kuromitsu, J.-R.; Jigami, Y., OCH1 encodes a novel membrane bound mannosyltransferase: outer chain elongation of asparagine-linked oligosaccharides. *The EMBO Journal* **1992,** *11* (7), 2511.

81. Vervecken, W.; Kaigorodov, V.; Callewaert, N.; Geysens, S.; De Vusser, K.; Contreras, R., In vivo synthesis of mammalian-like, hybrid-type N-glycans in Pichia pastoris. *Applied and environmental microbiology* **2004,** *70* (5), 2639-2646.

82. Choi, B.-K.; Bobrowicz, P.; Davidson, R. C.; Hamilton, S. R.; Kung, D. H.; Li, H.; Miele, R. G.; Nett, J. H.; Wildt, S.; Gerngross, T. U., Use of combinatorial genetic libraries to humanize N-linked glycosylation in the yeast Pichia pastoris. *Proceedings of the National Academy of Sciences* **2003,** *100* (9), 5022-5027.

83. Laukens, B.; De Wachter, C.; Callewaert, N., Engineering the Pichia pastoris N-glycosylation pathway using the GlycoSwitch technology. *Glyco-Engineering: Methods and Protocols* **2015**, 103-122.

84. Li, H.; Sethuraman, N.; Stadheim, T. A.; Zha, D.; Prinz, B.; Ballew, N.; Bobrowicz, P.; Choi, B.-K.; Cook, W. J.; Cukan, M., Optimization of humanized IgGs in glycoengineered Pichia pastoris. *Nature biotechnology* **2006,** *24* (2), 210-215.

85. Beck, A.; Cochet, O.; Wurch, T., GlycoFi's technology to control the glycosylation of recombinant therapeutic proteins. *Expert opinion on drug discovery* **2010,** *5* (1), 95-111.

Chapter 2 LC-MS based Site-Specific Glycosylation analysis of human serum IgG3

2.1 Introduction

Protein glycosylation is a post-translational modification that adds glycans to specific amino acid residues on proteins. It is well accepted that glycans play an important role in the cellular recognition and signaling functions of glycoproteins. Glycosylation exhibits a high degree of heterogeneity, which can be classified as macro- and micro-heterogeneity. Macroheterogeneity is generated by the variable occupancy of glycans at a glycosylation site. For a protein with multiple glycosylation sites, macroheterogeneity results in a mixture of fully, partially and non-glycosylated forms of the same protein. Microheterogeneity is generated from different glycoforms present at the same glycosylation site, which results in a heterogeneous mixture of the same protein but with different glycoforms.

The immunoglobulin G (IgG) class of antibodies are glycoproteins, and their glycosylation analysis is a subject of immense interest since the glycans are linked to the biological functions of IgGs.[1] All the four human IgG subclasses have a conserved N-glycosylation site at N297 in the C_H2 domain of the Fc region. For all of the IgG subclasses, the type of glycosylation found on the N297 site is mostly complex-biantennary type of glycan, which is predominantly fucosylated and bears a variable number of sialic acid, galactose and bisecting GlcNAc residues.[2] Glycosylation at the N297 site is essential for Fc-mediated effector functions such as binding to Fcγ receptors and C1q complement protein.[3] Apart from the N297 site, N-glycosylation can also be found in the variable regions of the Fab domains of about 15-25% of endogenous IgG.[4] There are no conserved N-glycosylation sites in the Fab domain but sites are generated as a result of somatic hypermutation. Glycosylation analysis of Fab domain glycans showed

higher levels of bisecting GlcNAc and sialylation and lower levels of fucosylation compared to the N297 site glycans from the Fc domain.[5]

There is an additional unique glycosylation site at N392 in the C_H3 domain of IgG3. This site has nearly gone unmentioned and remains under-investigated in the literature. Only recently, the N392 site has been shown to be partially glycosylated in human serum IgG3 by Stavenhagen et al.[6] and the work described in this chapter. The Asn at the 392 position is not conserved across all the IgG3 allotypes as some IgG3 allotypes and all the other IgG subclasses contain a Lys at that position. The Asn/Lys392 difference in the 13 IgG3 allotypes is not a serologically-determined allotypic marker but is considered as a polymorphism that is present on 10 out of the 17 DNA sequence correlates of the IgG3 alleles that are known so far.[7-8] The IgG3 sequence with Asn at position 392 is commonly accepted as the primary IgG3 sequence in the literature.

Protein glycosylation is commonly characterized by mass spectrometry with a prior chromatographic separation (LC-MS).[9-10] There are three approaches to characterize protein glycosylation: intact glycoprotein MS, glycan-based and glycopeptide-based MS analyses.[11] The first approach involves molecular weight (MW) determination of intact glycoprotein, based on which the MW (and hence composition) of glycan can be deduced if the protein MW (i.e. its amino acid sequence) is known. The glycan-based approach involves release of glycans, either chemically or enzymatically, and their subsequent analysis. One drawback of this approach is that the information about the site of glycan attachment is lost, which is particularly important for glycoproteins with multiple glycosylation sites. For the glycopeptide-based approach, a glycoprotein is subjected to proteolysis to yield a mixture of peptides and glycopeptides, which can then be

chromatographically separated and detected by mass spectrometry. The advantage of this approach is that site-specific analysis of glycosylation is possible since the glycans remain attached to the peptides. Since MS analysis only provides the mass of glycopeptides, MS/MS analysis is often required for unambiguous glycopeptide assignment, particularly in the case of isobaric glycopeptides that differ in glycan composition or peptide sequence.[12] For MS/MS analysis, a glycopeptide is selected and fragmented to provide detailed structural information. MS/MS with Collisional Induced Dissociation (CID) and Electron Transfer Dissociation (ETD) are often used together to provide complete and complementary glycopeptide structure information.[13-14] CID provides glycan-specific information, whereas ETD provides peptide sequence information. Recently, an energy resolved CID fragmentation technique (application of differential collisional energy during MS/MS acquisition) has been developed that provides limited peptide sequence information in addition to the glycan-related information in a single MS/MS run.[15-16]

In this chapter, the IgG3 subclass was isolated from a mixture of IgG subclasses obtained from human serum to investigate its glycosylation profile. LC-MS analysis revealed full glycosylation occupancy at the N297 site but only partial occupancy at the N392 site. Interestingly, the glycoform repertoire at the two sites showed significant differences in the levels of fucosylation and bisecting GlcNAc. The presence of glycosylation at the N392 site in endogenous human IgG3 suggests that this site is biologically relevant and thus makes a case for studying its influence on the structure, stability and biological functions of IgG3.

2.2 Methods

2.2.1 Isolation of IgG3 from human serum

Gamma globulin from human serum (Sigma Aldrich, St. Louis, MO) was used as a source of human IgG3. IgG3 was purified from the mixture of IgG subclasses present in human gamma globulins using protein A and G affinity chromatographies, as per our previous work.[17] Briefly, 100 mg of gamma globulin was passed over a protein A column to capture IgG1, IgG2, and IgG4 while IgG3 remained in the flow through. The captured IgG's were then eluted, and the IgG3-containing flow through was passed one more time over the protein A column to capture any residual IgG1, 2, and 4 remaining in the flow through. The IgG3-containing flow through from the second protein A column pass was then passed over a protein G column to capture IgG3. The column was washed extensively, and IgG3 was eluted at pH 2.7 and immediately neutralized. IgG present at each step of the purification was checked by SDS-PAGE. The presence of IgG3 at the final step was confirmed by western blot using an anti-hIgG3 antibody-alkaline phosphatase conjugate (ThermoFisher, Waltham, MA).

2.2.2 Deglycosylation of human serum IgG3

Human serum IgG3 was treated with immobilized papain (Agarose resin, ThermoScientific) to digest IgG3 into Fab and Fc fragments. IgG3 was incubated with papain (E:S=1:80) in 20 mM sodium phosphate buffer, pH 7.0, 10 mM cysteine for 7 hours at 37°C with shaking. The resulting Fc fragment was compared to a recombinantly IgG3 Fc fragment for the deglycosylation experiment. Deglycosylation was carried out using the PNGase F enzyme under non-denaturing and denaturing conditions (refer to chapter 3, section 3.2.3). The deglycosylated protein was detected by western blot using

an anti-human IgG Fc-alkaline phosphatase primary antibody.

2.2.3 In-gel protease digestion

The heavy and light chains of serum isolated IgG3 was separated using SDS-PAGE under reducing conditions. The band corresponding to the heavy chain was excised, and used for in-gel protease digestion using protocol of Shevchenko et al.[18] with some modifications. Briefly, the excised band was cut into smaller pieces, transferred to a microcentrifuge tube, and incubated with a washing solution of 0.2 M ammonium bicarbonate in 50% acetonitrile at 37°C for 45 min to completely remove the coomassie blue stain. The wash solution was discarded, and the gel pieces were allowed to air dry. The gel pieces were then incubated with 10 mM DTT in 100 mM ammonium bicarbonate with enough buffer to completely cover the gel pieces at 56°C for 30 min. The tube was brought to room temperature, and the DTT solution was discarded. The gel pieces were incubated with 55 mM iodoacetamide in 100 mM ammonium bicarbonate at room temperature for 20 min in the dark. Finally, the gel pieces were shrunk with neat acetonitrile for 20 min. Acetonitrile was removed, and the gel pieces were air dried. The gel pieces were treated with trypsin (1:50 ratio) and Asp-N (1:100 ratio) in 10 mM ammonium bicarbonate buffer at 37°C overnight. The gel pieces were then centrifuged, and the supernatant was used for mass spectrometry analysis.

2.2.4 LC-MS analysis of N297 and N392 site glycosylation on human serum IgG3

IgG3-digest samples were applied to a reverse phase (RP) column (C8, 4.6x150mm, 300°A, Agilent, Santa Clara, CA) using a HPLC system (Agilent 1200). The column was equilibrated using 95% mobile phase A (water with 0.1% formic acid) and 5% mobile phase B (acetonitrile with 0.1% formic acid) at 40°C at a flow-rate of 0.5

ml/min. A gradient elution to 45% B in 40 min and to 80% B in 10 min followed by an isocratic elution at 80% B for 3 min was employed. The HPLC was coupled online to an ESI-q-TOF mass spectrometer (Agilent 6520). The source parameters were as follows: drying gas of 11 L/min, capillary temperature of 350°C, and a voltage of 3.5 kV. The MS data was acquired using MassHunter acquisition software B.03 (Agilent) in a range of 300-3000 m/z at the rate of 1 spectra/sec. For MS/MS, energy-resolved collision-induced dissociation (CID) was used for fragmentation of the selected glycopeptide precursor ion with collision energies of 40 eV and 20 eV. The data was analyzed using MassHunter qualitative analysis software B.03 (Agilent). For relative quantification of glycoforms, the peak intensity (of the most intense peak in the isotopic cluster) from the most abundant charge state of the glycopeptide/peptide was calculated.

2.3 Results

2.3.1 Isolation of IgG3 from human serum

Human gamma globulin was used as a source of serum IgG consisting of the IgG1-4 subclasses purified from pooled human plasma. Protein G binds to all IgG subclasses, whereas protein A binds to all but IgG3. This selective binding property of protein A was used to purify IgG3 from the gamma globulin mixture of IgG subclasses. The IgG subclasses present at each step of purification were checked by SDS-PAGE (Fig. 2.1A). The IgG mixture was loaded onto a protein A column to capture IgG1, 2, and 4 while IgG3 remained in the flow through (first pass). The protein A-bound IgG's were then eluted and the first-pass flow through was loaded again onto the protein A column to capture any remaining IgG1, 2, and 4. The second-pass flow through from the protein A column contained IgG3 with no notable presence of the other IgG subclasses, based on

SDS-PAGE. As an additional purification step for the collected IgG3, the flow through was passed over a protein G column. The column was washed extensively to remove any other contaminating serum proteins (that may be originally present in the gamma globulin starting material). IgG3 was eluted from the column, and its presence was confirmed by western blot using an anti-hIgG3 antibody (Fig. 2.1B).

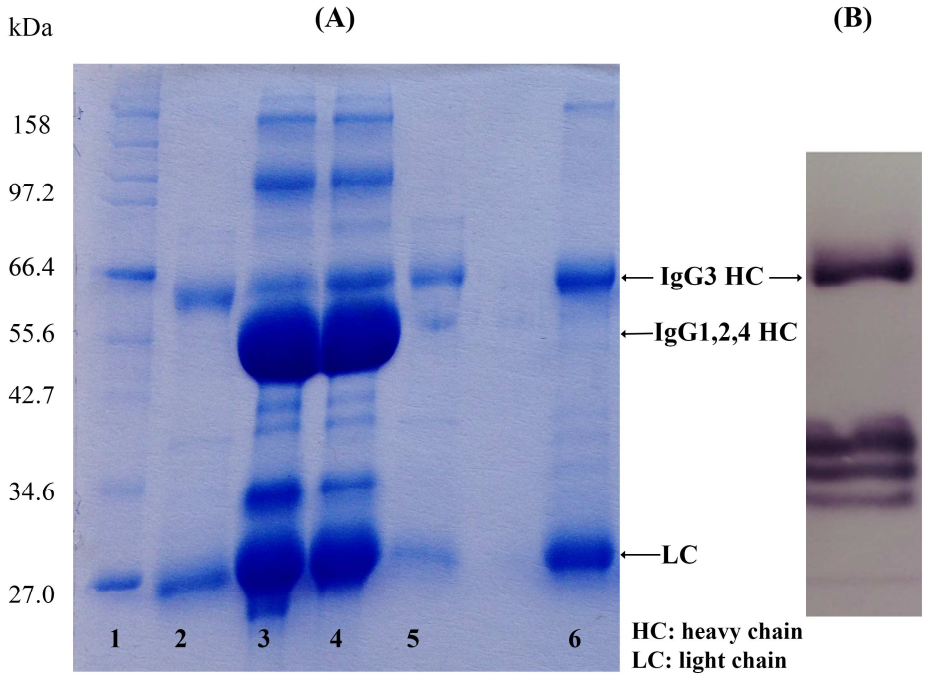

Figure 2.1: Isolation of IgG3 from gamma globulins. (A) SDS-PAGE (under reducing conditions) showing IgGs at each step of purification. Lanes 1: MW marker, 2: first-pass protein A flow through, 3,4: elution from protein A, 5: second-pass protein A flow through, 6: elution from protein G. The higher MW of IgG3 heavy chain is due to its long hinge. (B) western blot of isolated IgG3 using an anti-hIgG3-alkaline phosphatase antibody. The observed lower MW weights are likely from the heavy chain proteolysis.

2.3.2 Checking occupancy of the N392 glycosylation site in human serum IgG3

Human serum IgG3 was treated with the papain enzyme to convert full-length IgG3 to an Fc fragment (Fig. 2.2). The serum Fc fragment was compared with the yeast-expressed IgG3 Fc fragment in a deglycosylation experiment to check for the occupancy

of the N392 site glycosylation in the serum sample. The results for deglycosylation of yeast-expressed WT IgG3 Fc (both N297 and N392 glycosylated) are described in detail in chapter 3, section 3.3.1. It was shown that glycans at the N392 site were cleaved by the PNGase F enzyme only under denaturing conditions but remained attached to protein under native deglycosylation conditions. This conclusion was drawn from the persistence of monoglycosylated band (in SDS-PAGE analysis) in the PNGase F treated yeast-expressed Fc sample under non-denaturing conditions and its subsequent disappearance under denaturing conditions (Fig. 3.3). The serum Fc sample showed similar gel shifts as the yeast-expressed Fc, thereby indicating that the N392 site was also glycosylated in the serum sample (Fig. 2.3). A western blot was used for detection because extra bands in the serum Fc sample (likely from the light chain or proteolysis of the heavy chain) interfered with the observation of the coomassie-stained gel bands. Moreover, it was evident that the level of N392 glycosylation site occupancy in the serum sample was significantly lower than the yeast-expressed sample, as judged from the intensity of the monoglycosylated band.

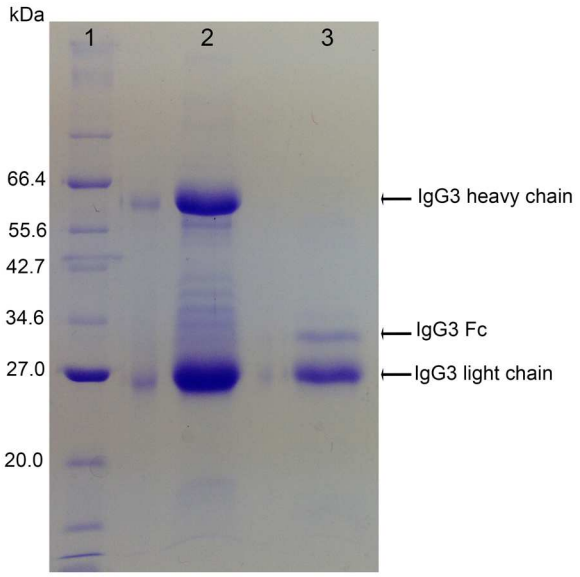

Figure 2.2: Coomassie-stained SDS-PAGE under reducing conditions of papain-digested IgG3. Lane (1) protein MW marker (2) IgG3 isolated from human serum (3) papain-digested IgG3

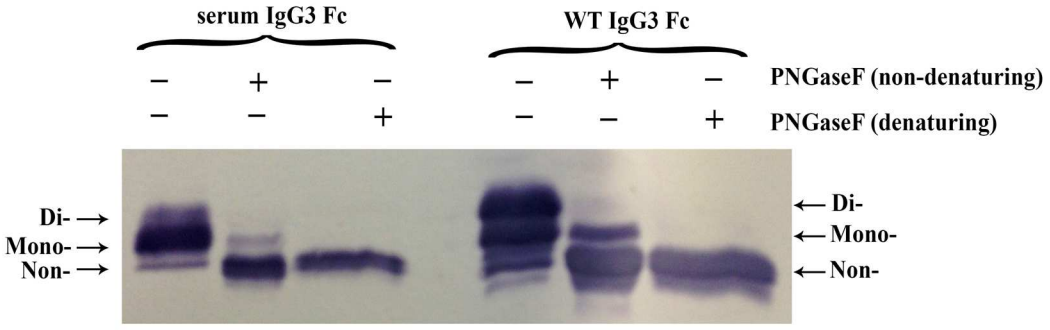

Figure 2.3: Western blot showing deglycosylated products of the serum IgG3 Fc and yeast-expressed WT IgG3 Fc following deglycosylation under reducing conditions with and without denaturation. An anti-hIgG Fc antibody-alkaline phosphatase conjugate was used to visualize the blot.

2.3.3 LC-MS based site-specific glycosylation analysis of human serum IgG3

The heavy chain band of serum IgG3 was excised from the SDS-PAGE gel and subjected to in-gel protease digestion to identify glycoforms at the N297 and N392 sites

using mass spectrometry. An in-gel digestion was performed to limit the peptide pool to contain only peptides of interest as the presence of any non-relevant peptides (from the light chains or other serum contaminant proteins) may suppress the ionization of the glycopeptides, especially those that are present at low levels. Two proteases, Asp-N and trypsin were used to produce peptides of varying lengths. Trypsin digest produces 9 and 39 amino acid peptides at the N297 and N392 sites respectively. Asp-N digest produces 32 and 23 amino acid peptides at the N297 and N392 sites respectively. Generating glycopeptides of varying sizes helped to confirm glycopeptide mapping results obtained from either of the digests. The digests were subjected to C8-LC-ESI-qTOF MS, and the glycoforms at the two sites were characterized. Both of the sites showed the presence of complex, biantennary glycans with an additional high-mannose glycan ($GlcNAc_2Man_5$ or Man5 glycoform) present only at the N392 site. No non-glycosylated N297 peptide was detected, whereas a prominent peak for the non-glycosylated N392 peptide was observed. The two sites showed a different repertoire of complex glycoforms with major differences in the levels of fucosylation and bisecting GlcNAc. The m/z spectra for the glycopeptides from the trypsin and Asp-N digests are shown in Figures 2.4 and 2.5, respectively. Table 2.1 shows the relative percentage of each glycoform at both the sites in the total N-glycan pool. A majority of glycans at the N297 site were core fucosylated (89.7% for the trypsin peptide, 90.1% for the Asp-N peptide), but no fucosylated glycans were detected at the N392 site. A majority of the N392 glycans contained a bisecting GlcNAc (75.5% from the trypsin peptide, 71.8% from the Asp-N peptide), while only 16-17% of the N297 glycans contained bisecting GlcNAc. The N392 site showed higher levels of sialylation (~30%) than the N297 site (~21-24%). Interestingly, 11% of the

N392 glycans were of high mannose type (the Man5 glycoform). The glycosylation site occupancy at the N392 site was determined to be 9-10% based on the sum of intensities of all the N392 glycopeptides relative to the intensity of the N392 non-glycosylated peptide. Our results are in good agreement with the recently reported study on IgG3 glycosylation characterization by Stavenhagen et al.[6]

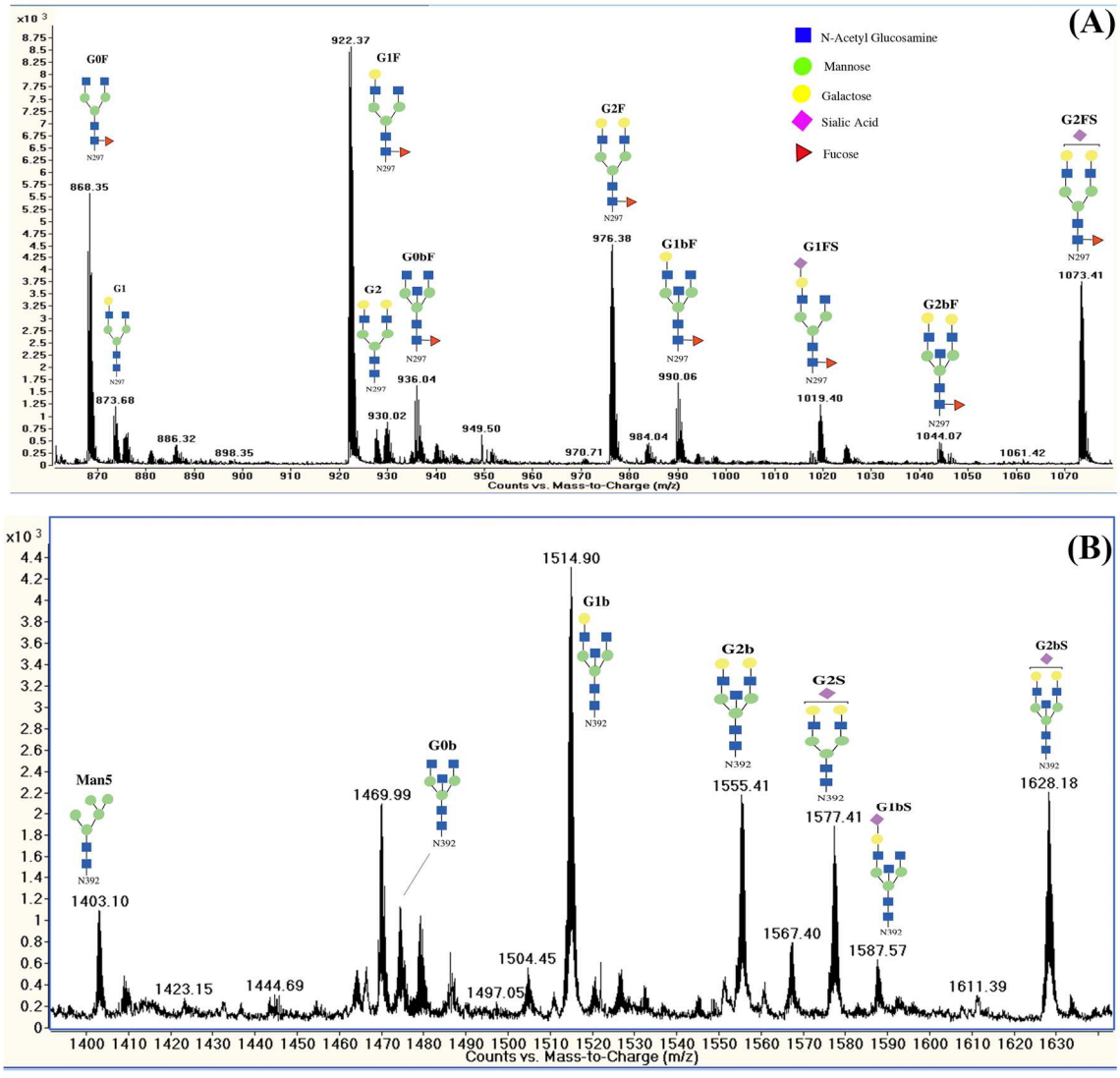

Figure 2.4: MS analysis of serum IgG3 glycopeptides from trypsin digest for (A) the N297 site (EEQFNSTFR) (B) the N392 site (GFYPSDIAVEWESSGQPENNYNPPMLDSDGSFFLYSK). The charge states for the N297 and N392 glycopeptide peaks are +3 and +4, respectively.

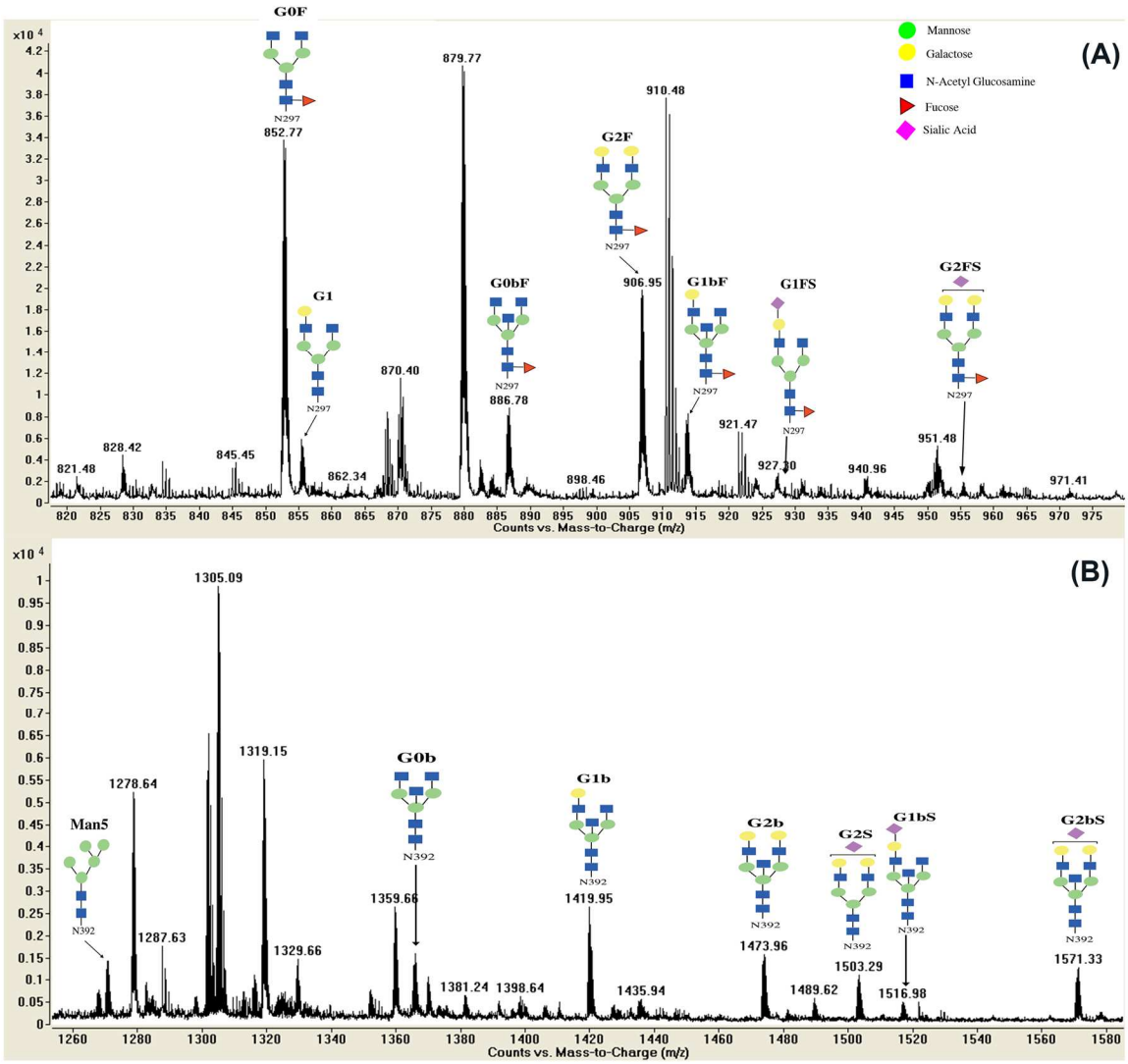

Figure 2.5: MS analysis of serum IgG3 glycopeptides from Asp-N digest for (A) the N297 site (DGVEVHNAKTKPREEQFNSTFRVVSVLTVLHQ) (B) the N392 site (DIAVEWESSGQPENNYNPPML). The charge states for the N297 and N392 glycopeptide peak are +6 and +3, respectively.

Table 2.1: Relative abundances of glycoforms present at the N297 and N392 sites in human serum IgG3 from the trypsin and Asp-N digests. The peak height of the most abundant peak in the isotopic distribution was used to calculate the percentage.

Glycoform	**% of N297 site**	**% of N297 site**	**% of N392 site**	**% of N392 site**
	(trypsin)	(Asp-N)	(trypsin)	(Asp-N)
G1F	20.1	19.6		
G0F	18.9	19.1		
G2F	15.8	15.7		
G2SF	13.7	15.8		
G0bF	7.3	5.6		
G1SF	6.1	7.2		
G1bF	5.9	5.6		
G1	5.9	1.8		0.4
G2bF	1.9	1.5		
G0	1.8	2.4		
G2S	1.3	1.3	1.2	1.2
G1b	0.7	1.7	2.7	2.2
G2b	0.8	2.8	1.7	1.7
G2bS			1.5	1.3
G0b			1.4	1.4
Man5			1.2	1.0
G1bS			0.4	0.3
Total	100.0	100.0	10.2	9.6

To further confirm and validate our MS results for glycopeptide assignment, a MS/MS experiment was performed on selected glycopeptides from the N297 and N392 sites using energy-resolved CID fragmentation. Generally, CID with low collisional energy results in preferential cleavage at glycosidic bonds in a glycopeptide, while higher energy collision results in limited peptide backbone fragmentation with almost complete loss of glycan.[15] The G1F and Man5 glycopeptides from the N297 and N392 sites

respectively were selected for fragmentation at 20 eV and 40 eV. The MS/MS spectra of the N392-Man5 glycopeptide at 20 eV collisional energy was dominated by product ions formed by fragmentation at glycosidic bonds with an intact peptide backbone (Fig. 2.6). The observed product ions confirmed the glycan composition and sequence of Man5 glycoform. A small number of product ions from peptide backbone fragmentation were also detected in the spectra with a prominent peak for $y15^{2+}$ ion generated by C-terminal cleavage after two Pro residues. At a collisional energy of 40 eV, the spectra exclusively contained product ions resulting from only peptide backbone fragmentation. The MS/MS spectra for the N297-G1F glycopeptide showed a similar fragmentation pattern. The lower collisional energy spectra yielded product ions from which the composition of G1F glycoform can be confirmed. The product ions from peptide backbone fragmentation at higher collisional energy were found in very low abundances (Fig. 2.7). Both the MS/MS spectra showed characteristic sugar oxonium ions (Hex: m/z 203, Hex-GlcNAc: m/z 366, Hex2- GlcNAc: m/z 528), which are a good indicator for presence of glycans in the selected precursor ion.

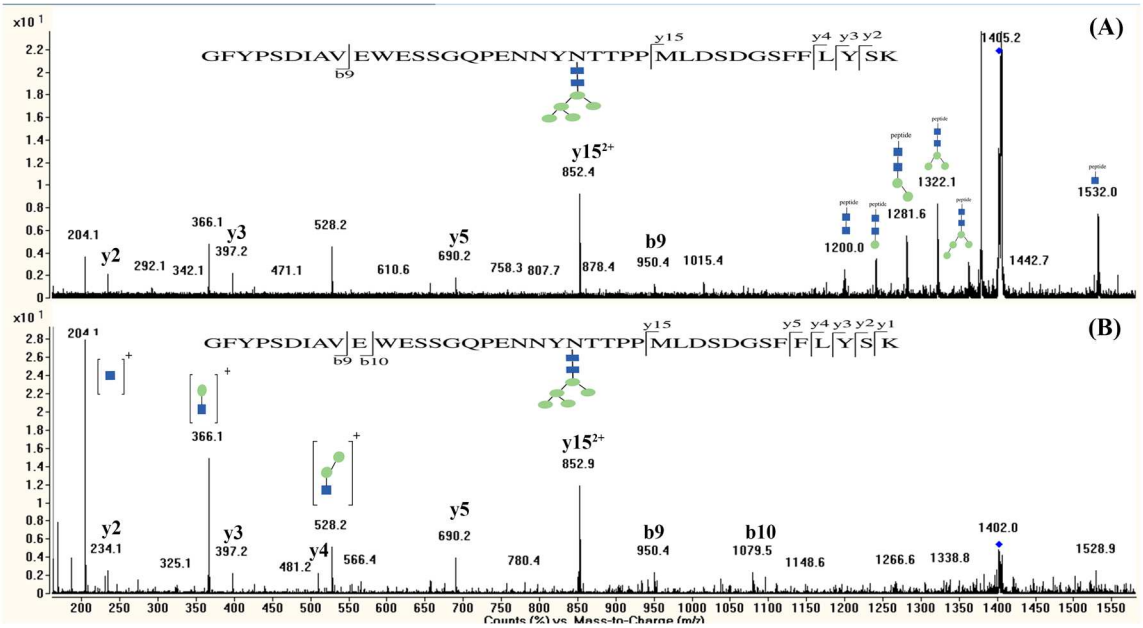

Figure 2.6: MS/MS spectra for the N392-Man5 glycopeptide at (A) 20 eV and (B) 40 eV collision energy. A precursor ion with m/z of 1402.34, z=4 was selected for CID fragmentation.

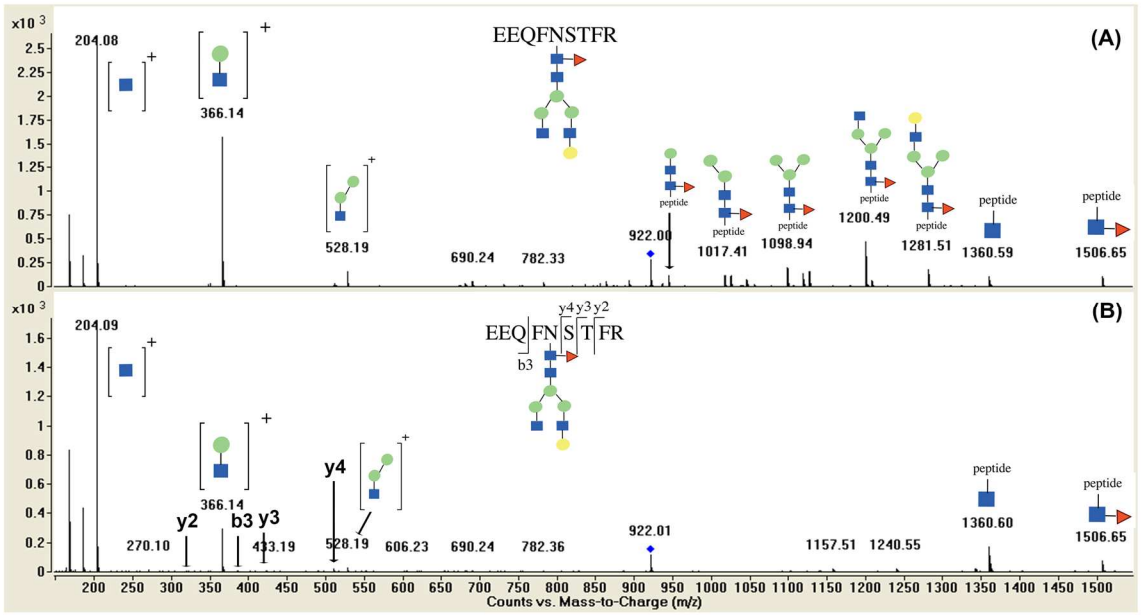

Figure 2.7: MS/MS spectra for the N297-G1F glycopeptide at (A) 20 eV and (B) 40 eV collision energy. A precursor ion with m/z of 922.03, z=3 was selected for CID fragmentation.

2.4 Discussion

IgG3 accounts for 5-8% of total serum IgG with serum levels of 0.5-1 mg/ml in adult humans.[19] IgG3 is generally purified from plasma samples using a two step affinity purification procedure employing protein A and G chromatographies.[2, 20] Theoretically, using only protein A (which doesn't bind to IgG3) should be sufficient to purify IgG3 from the human gamma globulins, but an additional protein G purification step (binds to IgG3) improves the quality of the isolated IgG3. An affinity chromatography step specific for IgG3 is particularly useful since human gamma globulin is prepared from plasma fractionation and can potentially have contamination from other co-purified serum proteins.

The inability of the N392 glycans to be cleaved with the PNGase F enzyme under native conditions was clearly demonstrated in the yeast-expressed IgG3 Fc. This property served as a simple identification test to check for the presence of the N392 glycans in the serum IgG3 sample. Based on these results, it can be concluded that the N392 glycans in the yeast-expressed Fc exist in a similar environment as the naturally occurring N392 glycans, and therefore yeast can be used as a suitable expression host for producing IgG3. Moreover, this distinct property of N392 glycans can be readily used to check the glycosylation occupancy at the N392 site for IgG3 expressed in different glycoprotein expression hosts such as mammalian and plant cells.

LC-MS analysis of the N297 and N392 site glycopeptides showed the presence of complex biantennary glycans, with additional high mannose glycans only at the N392 site. Complex and high mannose glycans are fully and partially processed forms respectively of the human glycan processing pathway in the golgi. The two sites showed

differences in the glycan repertoire (Table 2.1), where a major difference was seen in the levels of fucosylation and bisecting GlcNAc accompanied by a minor difference in the sialylation level. These results clearly indicate that the two sites show differences in the extent of glycan processing. The protein structure near to N-glycan sites can affect site occupancy, glycan type and glycan processing.[21] The fucosylation/bisecting GlcNAc difference can be explained on the basis of two factors. First, a glycan modified with bisecting GlcNAc is a poor substrate for α-1,6 fucosyltranferase (an enzyme that adds fucose to the first GlcNAc).[22] Second, lower levels of fucosylation are observed for shielded glycosylation sites than accessible ones.[21] Glycosylation site accessibility differences between the N297 and N392 sites in IgG3, based on IgG3 Fc structural analysis are presented in chapter 5, section 5.3.9.

The glycosylation pattern found at the N392 site resembles closely the pattern of Fab glycosylation. Fab glycosylation has been shown to have higher levels of glycans with bisecting GlcNAc, galactose, sialic acid, and high mannose, but also to have low levels of core fucose.[5] The biological significance of Fab glycosylation is still unclear, but it is generally thought to affect antigen binding, half-life and stability of antibodies. The level and glycosylation pattern of Fab glycosylation was found to be sensitive to physiological and pathological conditions like pregnancy and auto-immune conditions respectively, indicating a possible immunomodulatory role.[4] Based on this, the N392 glycans of IgG3 can be hypothesized to involved in an unknown physiological/pathological condition.

The N392 site glycosylation is only partially glycosylated with about 10% site-occupancy, whereas the N297 site was found to be completely glycosylated. Based on

this, if we assume that the formation of an Fc dimer is independent of N392 glycosylation site occupancy at one heavy chain of the Fc (and considering 100% occupancy at N297 site), it can be deduced that approximately 1% of endogenous IgG3 has all four sites glycosylated (tetraglycosylated) and about 18% (2*9%, considering N392 site is glycosylated on either of the heavy chains) of IgG3 has three sites glycosylated. There are mannose-binding receptors in mammalian tissues that clear glycoproteins with terminal mannose sugars.[23] Since the Man5 glycoform is detected at the N392 site, it may be possible that the actual N392 site-occupancy is higher when IgG3 is produced by B cells but low levels are detected in the circulating IgG3 due to faster clearance of IgG3 with the Man5 glycoform.

N-linked glycosylation is initiated in the ER when oligosaccharyl transferase (a large heteromeric membrane protein complex) adds a sugar precursor ($Glu_3Man_9GlcNAc_2$) to an Asn residue in the sequence Asn-Xaa-Ser/Thr (where X = any aa except proline). Amino acids around the sequence can affect this process by potentially altering the local conformation or by interfering with the enzyme active site.[24] A striking example is the presence of proline residue immediately following the N-linked glycosylation sequence, resulting in a severe impairment of glycosylation efficiency. A survey of glycosylation site-occupancy on a large dataset of glycoproteins showed that only 50% of glycoproteins with the N-X-T-P sequence are glycosylated.[25] It must be noted that some of these 50% glycosylated sequences may be actually partially glycosylated. In another report, glycosylation efficiency was estimated at the N-X-T-Y sequence by expressing a model glycoprotein with different amino acids at the Y position. Efficiency was around 10% for the Pro residue, whereas it was 81%-93% for all

the other residues.[24] The N392 site (N_{392}TTPPML) in IgG3 has two Pro residues following the glycosylation sequence, and that may contribute to its low site-occupancy. Thus, the differences in glycosylation occupancy and the type of glycans present at the N297 and N392 sites in IgG3 indicate a likely difference in the local protein structure around these sites. A higher level of site-occupancy at the N392 site was detected in the yeast-expressed IgG3 Fc fragment (chapter 3, section 3.3.1) compared to serum IgG3. This variation could be either due to differences in the oligosaccharyl transferase (OST) complex between yeast and human, size of the expressed protein (full-length IgG3 from serum vs. Fc fragment in yeast) or state of the cell producing glycoprotein (human B cells under physiological conditions for serum IgG3 vs. yeast cells under recombinant conditions).

2.5 References

1. Brooks, S. A.; Flickinger, M. C., Protein Glycosylation. In *Encyclopedia of Industrial Biotechnology*, John Wiley & Sons, Inc.: 2009.

2. Wuhrer, M.; Stam, J. C.; van de Geijn, F. E.; Koeleman, C. A.; Verrips, C. T.; Dolhain, R. J.; Hokke, C. H.; Deelder, A. M., Glycosylation profiling of immunoglobulin G (IgG) subclasses from human serum. *Proteomics* **2007,** *7* (22), 4070-4081.

3. Arnold, J. N.; Wormald, M. R.; Sim, R. B.; Rudd, P. M.; Dwek, R. A., The impact of glycosylation on the biological function and structure of human immunoglobulins. *Annu. Rev. Immunol.* **2007,** *25*, 21-50.

4. van de Bovenkamp, F. S.; Hafkenscheid, L.; Rispens, T.; Rombouts, Y., The Emerging Importance of IgG Fab Glycosylation in Immunity. *The Journal of Immunology* **2016,** *196* (4), 1435-1441.

5. Anumula, K. R., Quantitative glycan profiling of normal human plasma derived immunoglobulin and its fragments Fab and Fc. *Journal of immunological methods* **2012,** *382* (1), 167-176.

6. Stavenhagen, K.; Plomp, R.; Wuhrer, M., Site-Specific Protein N-and O-Glycosylation Analysis by a C18-Porous Graphitized Carbon–Liquid Chromatography-Electrospray Ionization Mass Spectrometry Approach Using Pronase Treated Glycopeptides. *Analytical chemistry* **2015,** *87* (23), 11691-11699.

7. Dard, P.; Lefranc, M.-P.; Osipova, L.; Sanchez-Mazas, A., DNA sequence variability of IGHG3 alleles associated to the main G3m haplotypes in human populations. *European Journal of Human Genetics* **2001,** *9* (10), 765-772.

8. Stapleton, N. M.; Andersen, J. T.; Stemerding, A. M.; Bjarnarson, S. P.; Verheul, R. C.; Gerritsen, J.; Zhao, Y.; Kleijer, M.; Sandlie, I.; de Haas, M., Competition for FcRn-mediated transport gives rise to short half-life of human IgG3 and offers therapeutic potential. *Nature Communications* **2011,** *2*, 599.

9. Wuhrer, M.; Deelder, A. M.; Hokke, C. H., Protein glycosylation analysis by liquid chromatography-mass spectrometry. *Journal of Chromatography B* **2005,** *825* (2), 124-133.

10. Morelle, W.; Canis, K.; Chirat, F.; Faid, V.; Michalski, J. C., The use of mass spectrometry for the proteomic analysis of glycosylation. *Proteomics* **2006,** *6* (14), 3993-4015.

11. Huhn, C.; Selman, M. H.; Ruhaak, L. R.; Deelder, A. M.; Wuhrer, M., IgG glycosylation analysis. *Proteomics* **2009,** *9* (4), 882-913.

12. Zhu, Z.; Desaire, H., Carbohydrates on proteins: site-specific glycosylation analysis by mass spectrometry. *Annual Review of Analytical Chemistry* **2015,** *8*, 463-483.

13. Mechref, Y., Use of CID/ETD mass spectrometry to analyze glycopeptides. *Current protocols in protein science* **2012**, 12.11. 1-12.11. 11.

14. Alley, W. R.; Mechref, Y.; Novotny, M. V., Characterization of glycopeptides by combining collision‐induced dissociation and electron‐transfer dissociation mass spectrometry data. *Rapid Communications in Mass Spectrometry* **2009,** *23* (1), 161-170.

15. Kolli, V.; Dodds, E. D., Energy-resolved collision-induced dissociation pathways of model N-linked glycopeptides: implications for capturing glycan connectivity and peptide sequence in a single experiment. *Analyst* **2014,** *139* (9), 2144-2153.

16. Vékey, K.; Ozohanics, O.; Tóth, E.; Jekő, A.; Révész, Á.; Krenyácz, J.; Drahos, L., Fragmentation characteristics of glycopeptides. *International Journal of Mass Spectrometry* **2013,** *345*, 71-79.

17. Lakbub, J. C.; Clark, D. F.; Shah, I. S.; Zhu, Z.; Su, X.; Go, E. P.; Tolbert, T. J.; Desaire, H., Disulfide bond characterization of endogenous IgG3 monoclonal antibodies using LC-MS: an investigation of IgG3 disulfide-mediated isoforms. *Analytical Methods* **2016,** *8* (31), 6046-6055.

18. Shevchenko, A.; Tomas, H.; Havli, J.; Olsen, J. V.; Mann, M., In-gel digestion for mass spectrometric characterization of proteins and proteomes. *Nature protocols* **2006,** *1* (6), 2856-2860.

19. Vidarsson, G.; Dekkers, G.; Rispens, T., IgG subclasses and allotypes: from structure to effector functions. *Frontiers in immunology* **2014,** *5*, 520.

20. Dechavanne, C.; Guillonneau, F.; Chiappetta, G.; Sago, L.; Lévy, P.; Salnot, V.; Guitard, E.; Ehrenmann, F.; Broussard, C.; Chafey, P., Mass spectrometry detection of G3m and IGHG3 alleles and follow-up of differential mother and neonate IgG3. *PLoS One* **2012,** *7* (9), e46097.

21. Thaysen-Andersen, M.; Packer, N. H., Site-specific glycoproteomics confirms that protein structure dictates formation of N-glycan type, core fucosylation and branching. *Glycobiology* **2012,** *22* (11), 1440-1452.

22. Schachter, H., Biosynthetic controls that determine the branching and microheterogeneity of protein-bound oligosaccharides. *Biochemistry and cell Biology* **1986,** *64* (3), 163-181.

23. Goetze, A. M.; Liu, Y. D.; Zhang, Z.; Shah, B.; Lee, E.; Bondarenko, P. V.; Flynn, G. C., High-mannose glycans on the Fc region of therapeutic IgG antibodies increase serum clearance in humans. *Glycobiology* **2011,** *21* (7), 949-959.

24. Mellquist, J.; Kasturi, L.; Spitalnik, S.; Shakin-Eshleman, S., The amino acid following an asn-X-Ser/Thr sequon is an important determinant of N-linked core glycosylation efficiency. *Biochemistry* **1998,** *37* (19), 6833-6837.

25. Gavel, Y.; von Heijne, G., Sequence differences between glycosylated and non-glycosylated Asn-X-Thr/Ser acceptor sites: implications for protein engineering. *Protein engineering* **1990,** *3* (5), 433-442.

Chapter 3 Production and characterization of human IgG3 Fc expressed in glycosylation-deficient strains of the yeast *Pichia pastoris* and *in-vitro* glycan processing using an α-1,2 mannosidase

3.1 Introduction

The biological activity of human IgG3 is equivalent to human IgG1, which is the most studied and therapeutically used IgG subclass. IgG3 mediates Antibody Dependent Cellular Cytotoxicity (ADCC) activity as efficiently as IgG1 and elicits the strongest Complement Dependent Cytotoxicity (CDC) among the IgG subclasses.[1-2] All IgG subclasses have a consensus N-glycosylation site at N297 in the C_H2 domain of the Fc region. The presence of glycosylation at the N297 site is critical for effector functions like ADCC and CDC.[3-4] There is an extensive body of work on IgG1 glycosylation and how it influences its effector functions.[5-7] However, the role of N297 glycosylation on the effector functions of IgG3 subclass is under represented in the literature. Interestingly, there is an additional N-glycosylation site at N392 in the C_H3 domain of the consensus sequence[8] of IgG3 that is not present in any other subclass. Whether the N392 site is glycosylated or not in the naturally occurring endogenous IgG3 was not known for a long time. Only recently, the Wuhrer group[9] and the Tolbert lab (Chapter 2) discovered partial glycosylation occupancy at the N392 site in human serum IgG3. This discovery makes the N392 site biologically relevant, but its role in IgG3 structure and function remains to be investigated. Given the importance of the N297 site glycosylation on IgG1 and the similarities in the effector functions of IgG1 and IgG3, it is of interest to evaluate the influence of N297 and N392 site glycosylation on the properties of IgG3. For carrying out such a study, it is necessary to produce IgG3 Fc with well-characterized glycosylation as a starting point.

In this chapter, heterologous expression of the IgG3 Fc fragment in the glycosylation-deficient yeast *Pichia pastoris* is described. Two versions of IgG3 Fc were produced, a WT and mutant IgG3 Fcs, where the N392 site was mutated to other amino acids. The expressed proteins were extensively characterized with respect to glycosylation at the N297 and N392 sites. Site-

specific glycosylated variants of IgG3 Fc were produced: one with both the sites glycosylated (tetraglycosylated/Fc dimer) and other with only the N297 site glycosylated (diglycosylated/Fc dimer). These IgG3 Fc glycovariants were used to study the influence of N392 glycosylation on IgG3 Fc-Fc receptor binding and physical stability assessment of IgG3 Fc (Chapter 4) and structure of IgG3 Fc (Chapter 5).

One of the advantages of using the glycosylation-deficient yeast *P. pastoris* to express antibody fragments is the relatively homogenous nature of its glycosylation. The yeast strain used in this study produces high mannose glycans comprising mainly of Man8-Man12 ($GlcNAc_2Man_{8-12}$) glycoforms. However, there are some of drawbacks as well which include lower glycosylation site-occupancy and modifications of high mannose glycans such as mannose phosphorylation, β-mannosylation and incomplete removal of capping glucose residues. The yeast expression conditions can influence the levels of glycosylation site-occupancy and modified high mannose glycans, as we have seen some variability in the glycosylation pattern for the protein expressed in spinner flask (less controlled fermentation conditions) vs. fermentor expression (more controlled). In contrast to yeast expression, mammalian cells such as CHO cells produce complex glycans (found in humans) that exhibit a high degree of micro-heterogeneity.[10] The micro-heterogeneity is not well-suited for studies that focus on characterizing the effect of a single, specific glycoform on antibody immune functions. The high mannose glycans produced in the yeast can be converted to the complex-type glycans using two approaches. The first approach involves introduction of a new set of genes in the yeast secretory pathway that replicates the human glycoprotein biosynthesis.[11-12] Whereas, the second approach involves producing high mannose glycans produced in yeast that are then modified through a

series of enzymatic *in-vitro* glycan processing steps that will ultimately generate complex-type glycans (Fig. 3.1).

The Tolbert lab has adopted the second approach to produce IgG Fc with specific glycoforms since this approach allows for greater control over glycan processing and does not involve extensive genetic manipulation of yeast. The first step in the *in-vitro* glycan processing is the conversion of the high mannose glycans (Man8-Man12) to the Man5 ($GlcNAc_2Man_5$) glycoform using an α-1,2 mannosidase enzyme. Complete conversion to the Man5 glycoform is necessary since the undigested high mannose glycans will compromise the homogeneity of the glycoform produced at each step in the enzymatic pathway. Other groups have shown that *P. pastoris* can produce low levels of modified high mannose glycans that are not a substrate for α-1,2 mannosidase. These modified glycans contains non-cleavable linkages (for α-1,2 mannosidase enzmye) such as mannose-phosphate-mannose, β-mannose or capping glucose residues.[13-16] Researchers have previously shown that some of these modifications can be reduced by knocking out specific genes in *P. pastoris*.[12, 17] Based on this information, the members of the Tolbert lab knocked out additional genes (in addition to OCH1 gene) involved in the yeast glycosylation pathway. These genes include PNO1 and BMT1-2, whose gene products are responsible for phophomannosylation and β-1,2 mannosylation of high mannose glycans, respectively.[18-19] The endomannosidase enzyme was used to convert glucosylated high mannose glycans to high mannose glycans.[20]

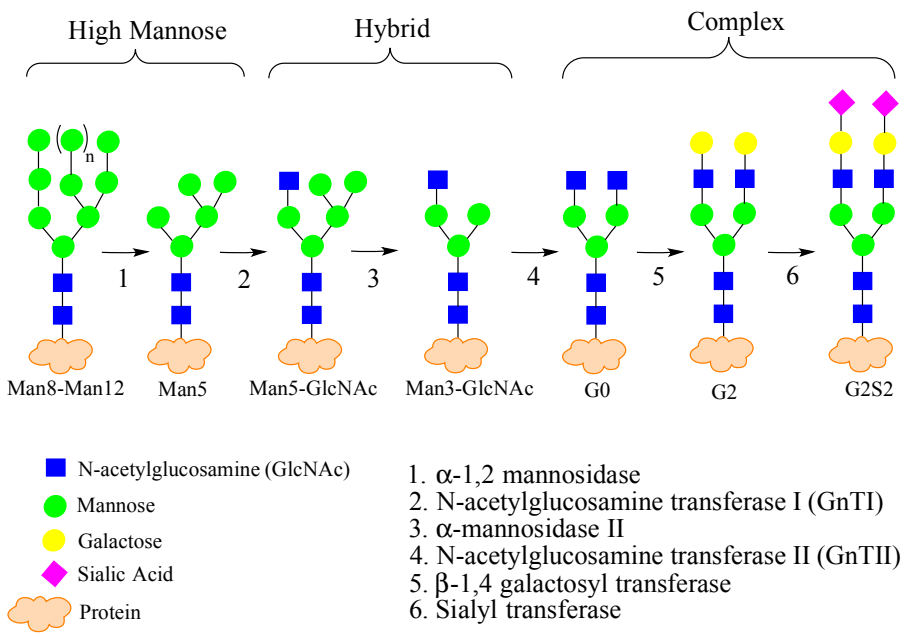

Figure 3.1: *In-vitro* enzymatic synthesis of Man5, hybrid and complex glycans from high mannose glycans. Man8-Man12 glycoforms are produced on glycoproteins expressed in the glycosylation-deficient (OCH1 KO) *P. pastoris*. The enzyme used at each step is indicated.

The work herein investigates the pattern of high mannose glycans produced on IgG3 Fc-N392K (chosen as a model system) expressed in different glycosylation-deficient strains of *P. pastoris* and its susceptibility to α-1,2 mannosidase digestion. These strains differ in the type of the glycosylation-related genes that are disrupted (Table 3.1). The α-1,2 mannosidase digestion efficiency was substantially improved upon deletion of the PNO1 and BMT genes. Additionally, a strategy to produce the Man5 glycoform *in-vivo* during protein expression was also carried out by introducing α-1,2 mannosidase activity to the yeast glycosylation pathway.

Table 3.1: List of *P. pastoris* strains used for IgG3 Fc expression

P. pastoris strain	Gene(s) deleted	Gene added
Single KO	OCH1	-
Double KO	OCH1, PNO1	STT3D
Quadruple KO	OCH1, PNO1, BMT1, BMT2	STT3D

3.2 Methods

3.2.1 Cloning of IgG3 Fc

The cDNA of the Fc region of hIgG3 (ATCC: MGC-45809, accession: BC033178) was used as a template for PCR amplification. The forward and reverse primers used were 5'-GGCCCGCTCGAGAAAAGAACATGCCCACGGTGCCCAGCA-3' and 5'-GGGCCCGCGGCGGCCGCTCATTTACCCGGAGACAGGGAGAG-3', respectively. The primers were designed such that the Fc has a truncated hinge with only two disulfide bonds (from exon1: ELKTPLGDTTHT$_{225}$CPRCP) instead of the natural hinge with 11 disulfide bonds (from additional exons 2,3 and 4). The designed construct codes from Thr$_{225}$ to Lys$_{447}$ according to EU numbering.[21] The amplified DNA and *Pichia pastoris* expression vector pPICZαA were treated with EcoRI and NotI and then ligated using T4 DNA ligase. This cloning procedure was performed by Mark Pawlicki, a former Tolbert group member. For IgG3 Fc mutants, IgG3 Fc with N392K and N392Q mutations were produced using the QuickChange II site-directed mutagenesis kit (Agilent). The forward and reverse mutagenesis primers for N392K mutant were 5'- GCAGCCGGAGAACAACTACAAAACCACGCCTCC-3' and 5'-GGAGGCGTGGTTTTGTAGTTGTTCTCCGGCTGC-3', respectively. The forward and reverse mutagenesis primers for N392Q mutant were 5'-CAGCCGGAGAACAACTACCAAACCACGCCTCCCA-3' and 5'-TGGGAGGCGTGGTTTGGTAGTTGTTCTCCGGCTG-3', respectively. The WT and mutant IgG3 Fc plasmids were transformed into Top10'F by electroporation and selected on low-salt LB plates with 25 μg/ml zeocin. The colonies were screened by PCR for the presence of the insert and positive colonies were sequenced to ensure that no mutation occurred. The confirmed plasmid was purified from the colony and linearized with SacI for transformation into a

glycosylation-deficient *P. pastoris* yeast strain with OCH1 deletion (SMD1168)[22]. Additionally, the constructs were also transformed into two additional yeast strains produced during the course of this research: one with OCH1 and PNO1 deletion (double KO) and the other with OCH1, PNO1, BMT1 and BMT2 deletion (quadruple KO). Additionally, the STT3D gene from Leishmania major was added to the double and quadruple KO strain to improve the glycosylation site-occupancy.[23] Transformants were selected on YPD pates with 100 μg/ml zeocin. Colonies were checked for protein expression on a small scale (2ml) and high expressing colonies were chosen for large-scale protein expression.

3.2.2 Expression and purification of WT and mutant IgG3 Fc

The frozen stocks of the yeast expressing WT and mutant IgG3 Fcs were used to inoculate starter cultures in 2 ml of YPD media with 100 μg/ml zeocin incubated at 25°C for 72 hours with shaking. These starter cultures were used to produce the different forms of IgG3 Fc using the following general procedure. A 2 ml culture was used to inoculate a 50 ml YPD/zeocin culture in a shake flask for 1 L spinner flask expression or into a 250 ml YPD/zeocin culture in a baffled shake flask for fermentor expression. For spinner flask expression, the 50 ml culture was incubated for 72 hours and used to inoculate a 1 L of buffered glycerol-complex media (BMGY) containing 0.00004% biotin and 0.004% histidine in an aerated spinner flask. After about 60 hours, protein expression was induced by the addition of methanol to a final concentration of 1% for three days. For the fermentor expression, the 250 ml culture was used to inoculate 7 L of fermentation basal salt media (BSM). The fermentation conditions and protein induction was carried out according to the method previously published by the Tolbert group.[24] At the end of fermentation, the supernatant was separated from cells by centrifugation and was clarified. The supernatant was passed over a protein G affinity chromatography column, pre-equilibrated with

20 mM potassium phosphate buffer pH 6.0. The column was extensively washed with 20 mM potassium phosphate buffer pH 6.0, 500 mM NaCl, and the protein was eluted using 100 mM glycine-HCl buffer pH 2.7. The protein was immediately neutralized using 1 M Tris-HCl pH 9.0 and dialyzed against 50 mM sodium phosphate buffer pH 7.0 for the next step. The purified WT and mutant IgG3 Fcs were analyzed by SDS-PAGE under reducing and non-reducing conditions.

3.2.3 Deglycosylation of IgG3 Fc

The WT and mutant IgG3 Fc were subjected to deglycosylation using the PNGase F enzyme under both non-denaturing and denaturing conditions. For the non-denaturing condition, the enzyme was directly added to the sample and incubated overnight at room temperature. For the denaturing condition, the sample was first denatured and reduced by adding 0.5% SDS and 40 mM DTT. The sample was then incubated at 95°C for 10 min followed by cooling at room temperature. To prevent the SDS from inactivating PNGase F, NP-40 was added to a final concentration of 1%. Finally, PNGase F was added and the sample was incubated overnight at room temperature. The deglycosylated samples were analyzed by SDS-PAGE.

3.2.4 LC-MS analysis of IgG3 Fc

Glycosylation analysis of IgG3 Fc was carried using intact protein and glycopeptide mapping mass spectrometry. For intact MS, the sample (0.2 mg/ml) was reduced using a final concentration of 10 mM DTT. The electrospray ionization spectra of the reduced sample were acquired on an Agilent 6520 QTOF. The instrument was operated in positive ion mode and spectra were acquired covering mass range from 300-3000 m/z with acquisition rate of 1 spectra/second. The samples (60 ul injections) were desalted on a reverse phase C4 column, 50mm, 4.6mm I.D. (Vydac 214MS, 300 A pore size, 5 um particle size) using Agilent 1200 series liquid chromatography system. The solvents used were A (99.9%H_2O, 0.08% formic acid,

0.02% TFA) and B (99.9% acetonitrile, 0.08% formic acid, 0.02% TFA). A gradient was developed from 5% B to 90% B in 7 min with a flow rate of 0.5 ml/min. Intact MW was determined by maximum-entropy deconvolution function using an Agilent MassHunter software (version B.03). The percentage of each glycoform in the total N-glycan pool was calculated using peak intensities. For the glycopeptide mapping, the sample (0.5 mg/ml) was denatured using 0.1% SDS-PAGE, reduced using 50 mM DTT with incubation at 60 °C for 45 min, and alkylated using 100 mM iodoacetamide solution with incubation in the dark at room temperature for 30 min. The protein was then precipitated by cold absolute ethanol (1:10 v/v protein:ethanol) and kept at -20°C for overnight. The protein pellet was recovered after centrifugation and was washed with neat acetonitrile. Finally, the pellet was air-dried and re-dissolved in 200 µl of 50 mM ammonium bicarbonate and 10 µg of trypsin (Promega, Madison, WI). The sample was incubated at 37°C for overnight, and the digest solution was used for glycopeptide analysis. IgG3 Fc-digest samples were applied to a RP column (C8, 4.6x150mm, 300°A, Agilent, Santa Clara, CA) coupled to Agilent 6520 ESI-QTOF. The column was equilibrated using 95% mobile phase A (water with 0.1% formic acid) and 5% mobile phase B (acetonitrile with 0.1% formic acid) at 40 °C at a flow-rate of 0.5 ml/min. A gradient elution to 45% B in 40 min and to 80% B in 10 min followed by an isocratic elution at 80% B for 3 min was employed. The ESI source parameters were as follows: drying gas of 11 L/min, capillary temperature of 350°C, and a voltage of 3.5 kV. The MS data was acquired using MassHunter acquisition software B.03 (Agilent) in a range of 300-3000 m/z at the rate of 1 spectra/sec. The data was analyzed using MassHunter qualitative analysis software B.03 (Agilent).

3.2.5 Preparation of IgG3 Fc glycovariants

IgG3 Fc glycovariants with site-specific glycosylation were purified from WT and mutant IgG3 Fc using hydrophobic interaction chromatography (HIC). A 75 ml column packed with phenyl sepharose high-performance (GE healthcare, UK) and AKTAmicro chromatographic system was used. The samples were dialyzed in Buffer A (50 mM sodium phosphate buffer, pH 7.0, 1 M ammonium sulfate), and the column was pre-equilibrated in the same buffer. Separation was conducted in three gradient segments: 0% to 35% buffer B (50 mM sodium phosphate buffer, pH 7.0) in 5 CV, 35% to 50% B in 15 CV and to 100% B in 5 CV. 8 ml fractions were collected and checked for purity and identity of the glycovariant present by SDS-PAGE. The fractions containing a single glycovariant were pooled and checked by SDS-PAGE and mass spectrometry.

3.2.6 In-vitro enzymatic modification of glycosylation

The high mannose glycosylation on WT and mutant IgG3 Fc was converted to the Man5 glycoform in an *in-vitro* enzymatic reaction using *B.t.* α-1,2 mannosidase (Bt 3990 from *B. thetaiotamicron*) with a 1:10 enzyme : protein ratio (w/w).[25] The Bt3990 expression plasmid was gifted by the Gilbert laboratory at the Newcastle University. The proteins were extensively dialyzed in 10 mM MES, 150 mM NaCl, 5 mM $CaCl_2$, pH 6.6 (reaction buffer) before starting the reaction. The reaction was incubated at room temperature for 72 hours. The progress of the reaction was monitored by intact protein MS. The percent conversion to the Man5 glycoform was calculated from the peak intensities obtained from the deconvoluted spectra. Separately, rat endomannosidase was used in combination with α-1,2 mannosidase under the same reaction conditions. The enzyme was produced in the Tolbert laboratory as follows: the gene (accession # NM_080785) encoding for the catalytic domain^{20}(Asp60-Ser463) of rat endomannosidase was synthesized by Genscript. The construct was subcloned into pET28a using restriction enzymes

EcoRI and NotI and placed downstream of the N-terminal His6 tag in the vector. The enzyme was expressed in *E.coli* Rosetta 2 and purified using Ni^{2+}-NTA affinity chromatography. The percentage conversion to Man5 glycoform was compared between digestion with α-1,2 mannosidase alone and in combination with endomannosidase to check for contribution of the endomannosidase in mannose trimming.

3.2.7 In-vivo enzymatic modification of glycosylation

For introducing α-1,2 mannosidase activity into the yeast secretory pathway, members of the Tolbert laboratory cloned a murine mannosidase IA[26] in the *P. pastoris* vector pPIC6αA with a N-terminal HDEL tag[27] for retention in the endoplasmic reticulum. The linearized pPIC6αA-mannosidase IA was transformed into the double KO (OCH1 and PNO1 KO) strain, and transformants were selected using blasticidin marker. The resulting strain with *in-vivo* α-1,2 mannosidase activity was used to express WT and mutant IgG3 Fc. The mannose trimming efficiency of the strain was evaluated by intact protein MS analysis to check the type of glycosylation produced by these strains.

3.3 Results

3.3.1 Expression and purification of WT IgG3 Fc and mutant IgG3 Fc

The glycosylation-deficient yeast strain with the OCH1 KO was used to express both the WT and mutant IgG3 Fc (N392K/Q) in a spinner flask or a fermentor. Additionally, the proteins were also expressed in the double and quadruple KO yeast strains (Table 3.1). The average yield per liter of expression for all the proteins was about 20 mg and 50 mg in spinner flask and fermentor, respectively. The Fc proteins were purified by protein G affinity chromatography and

analyzed by SDS-PAGE to assess the quality and the glycosylation state of the purified protein. Partial glycosylation site-occupancy was observed at both glycosylation sites, N297 and N392, irrespective of the yeast strain utilized, but an improvement in site-occupancy was observed in the double and quadruple KO strains due to introduction of the STT3D gene (data not shown). Since the Fc is a homodimer formed by disulfide bonds in the hinge, partial site-occupancy in the WT IgG3 Fc generated macro-heterogeneity that resulted in a mixture of the tetra-, tri-, di-, and mono-glycosylated Fc under non-reducing conditions. This mixture resulted in di-, mono-, and non-glycosylated monomers under reducing conditions (Fig. 3.2). Similarly, for both of the IgG3 Fc-N392K/Q mutants, macro-heterogeneity resulted in di-, mono-, and non-glycosylated Fc under non-reducing conditions and corresponding mono- and non-glycosylated monomers under reducing conditions (Fig. 3.2). The intensities of the di- and mono-glycosylated WT IgG3 Fc monomers appears to be approximately equal upon visual assessment. Based on this, if we assume that formation of Fc-dimer is independent of Fc monomer glycosylation, then it can be deduced that nearly 50% of the WT IgG3 Fc mixture is tri-glycosylated and each of the tetra- and di-glycosylated forms constitute about 25% of the mixture.

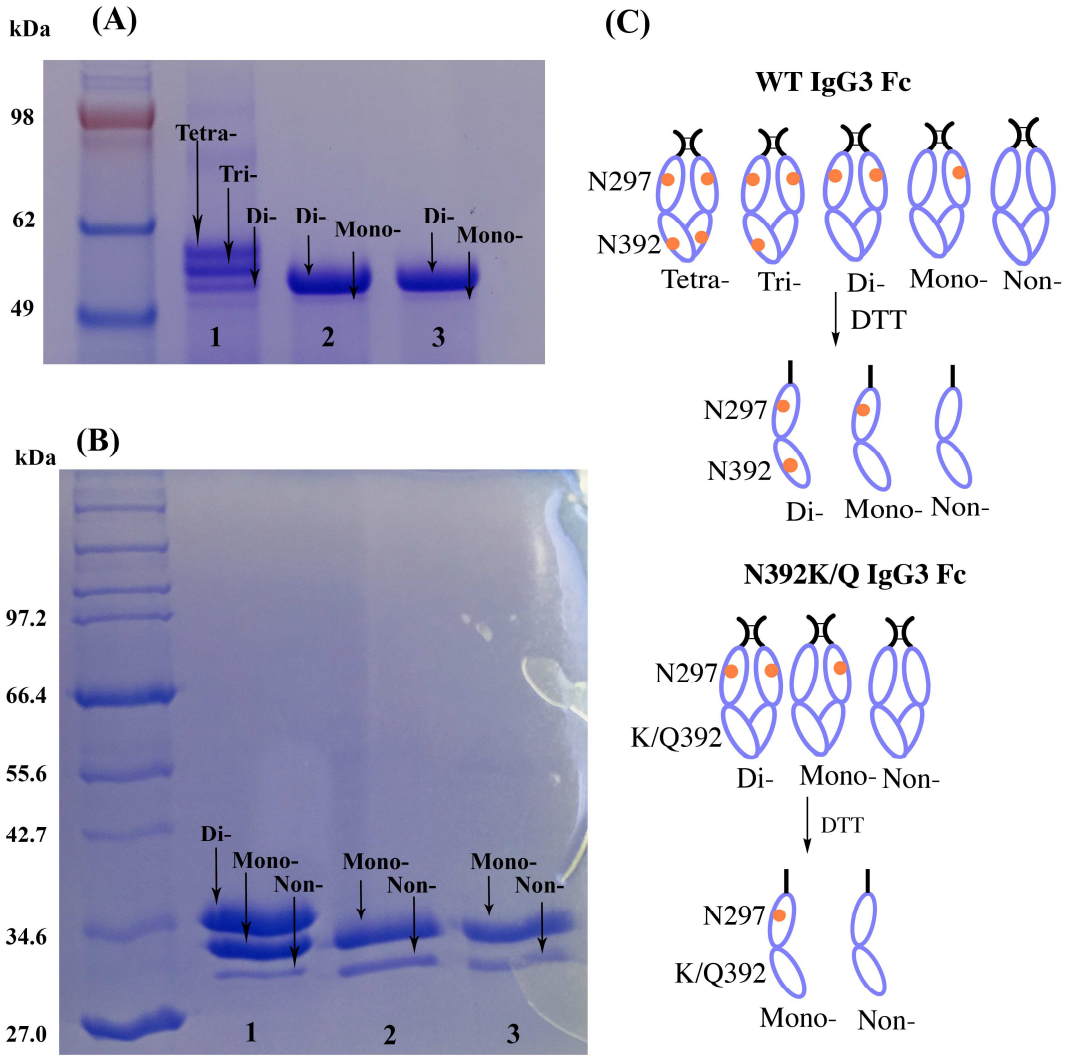

Figure 3.2: Coomassie-stained SDS-PAGE for IgG3 Fc purified from yeast under (A) non-reducing conditions and (B) reducing conditions. Lanes: (1) WT IgG3 Fc (2) IgG3 Fc-N392K (3) IgG3 Fc-N392Q (C) Schematic representation of glycovariants from the WT and mutant IgG3 Fc under reduced and non-reduced conditions.

To verify if the multiple bands seen on SDS-PAGE were due to glycosylation related macro-heterogeneity, the Fc protein was subjected to deglycosylation under non-denaturing and denaturing conditions using the PNGase F. The outcome of the deglycosylation experiment was assessed by SDS-PAGE. Deglycosylation under non-denaturing and reducing condition for IgG3 Fc-N392K resulted in the collapse of the mono-glycosylated band to the non-glycosylated band, suggesting that the N297 site glycans were labile to deglycosylation under the conditions used

(Fig. 3.3). Same treatment for the WT IgG3 Fc resulted in the loss of the di-glycosylated monomer band but persistence of the mono-glycosylated band, thereby implying that the N392 site glycans are resistant to deglycosylation under non-denaturing/native conditions. Deglycosylation of WT Fc IgG3 Fc under denaturating conditions resulted in loss of the mono-glycosylated band, which indicates that the N392 glycans are only cleaved if the protein is in an unfolded state (Fig. 3.3). This characteristic property was used to check if the N392 site was glycosylated in human serum IgG3 Fc, as described in chapter 2, section 2.3.2. Identical results for deglycosylation were observed for the WT IgG3 Fc and mutant IgG3 Fc expressed in the double and quadruple KO yeast strains.

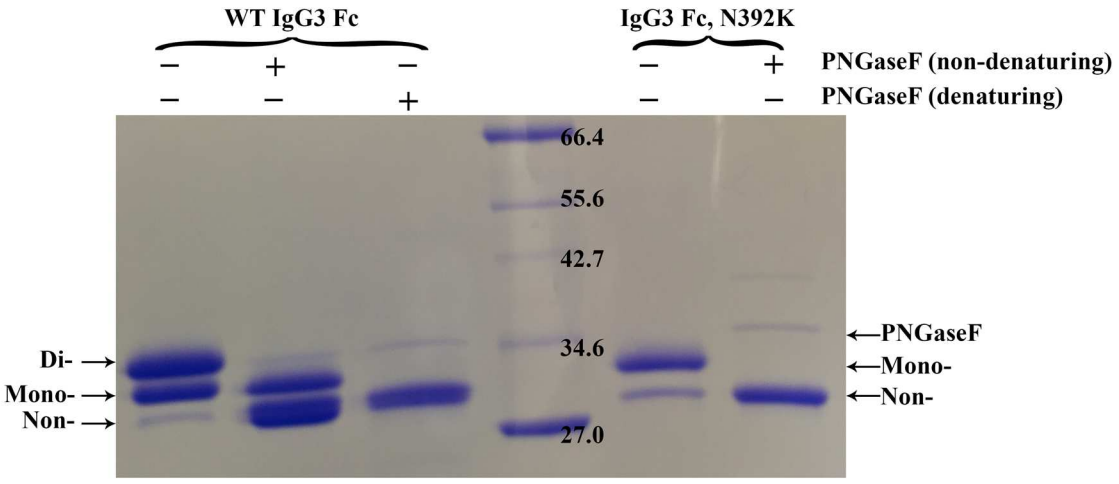

Figure 3.3: Coomassie stained SDS-PAGE showing deglycosylated products of the WT IgG3 Fc and IgG3 Fc-N392K under reducing conditions with and without denaturation.

3.3.2 LC-MS analysis of the expressed WT and mutant IgG3 Fc

The MW and glycosylation pattern of WT IgG3 Fc and IgG3 Fc-N392K expressed in different *P pastoris* yeast strains were determined by intact protein mass spectrometry. Incomplete site occupancy for the expressed protein was also evident in the MS spectrum as previously observed with SDS-PAGE. The IgG3 Fc-N392K expressed in the OCH1 KO strain

showed a peak corresponding to the non-glycosylated Fc and another set of peaks corresponding to high mannose glycoforms ($GlcNAc_2Man_{8-12}$ abbreviated as Man8-Man12) at the N297 site. Additional peaks with mass additions of 80 Da were also detected between the peaks corresponding to Man9-Man12 glycoforms (Fig. 3.4A). The +80 Da modification was determined to be present on the glycan and not the protein, since the MS spectrum for deglycosylated protein did not show this modification. The +80 Da peaks (expected average mass change for phosphorylation is +80 Da) may correspond to phosphorylated high mannose glycoforms (Man9P-Man11P), since it has been previously shown to occur on glycoproteins expressed in *P. pastoris*.[18] The total percentage of phosphomannosylated glycans was determined to be 7.5% in the total N297 glycan pool based on their peak intensities. The level of phosphomannosylation varied between 4 to 7.5% for different batches of IgG3 Fc-N392K Fc expressed in a spinner flask. Higher levels of up to 12% were detected in the fermentor-expressed protein. The WT IgG3 Fc expressed in same the *P. pastoris* strain showed a non-glycosylated Fc peak and two sets of peaks; the first set showing glycoforms present on one of the two glycosylation sites (monoglycosylated monomer) and a second set showing glycoforms present on both the glycosylation sites (diglycosylated monomer) (Fig. 3.5A). The +80 Da peaks were also detected in both sets of peaks, but it is not possible to ascertain if phosphomannosylation occurred at one of the two sites or at both the sites of WT IgG3 Fc, based on intact protein MS analysis. From intact protein MS analysis of both the proteins, it is evident that the predominant glycoform present in the distribution of high mannose glycoform is the Man8 glycoform at both the glycosylation sites.

Intact protein MS analysis of WT IgG3 Fc and IgG3 Fc-N392K expressed in the double OCH1 PNO1 KO strain showed a similar set of peaks as the OCH1 KO strain but with no

detectable levels of +80 Da peaks. This suggests that PNO1 disruption eliminated or reduced phosphomannosylation of high mannose glycans to a negligible level (Fig. 3.4-3.5B). Both the proteins expressed in the quadruple KO strain showed same set as peaks as seen in the double KO strain (Fig. 3.4-3.5C, Table 3.1). The BMT set of genes in *Pichia* adds β-1,2 linked mannose sugars in the high mannose glycans produced by *Pichia*.[19] The intact protein MS cannot distinguish between the α- and β-linked mannose and therefore no differences in the glycosylation pattern produced by the double and quadruple KO strain were observed by mass spectrometry.

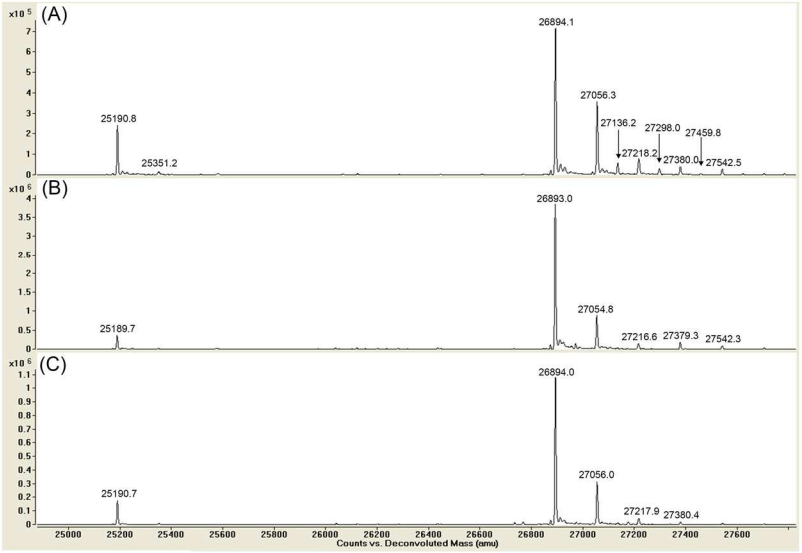

Glycoform	observed mass (Da)	calculated mass (Da)
NG	25190.8	25191.7
O-mannose	25351.2	25353.7
Man8	26894.1	26894.2
Man9	27056.3	27056.2
Man9P	27136.2	27136.2
Man10	27218.2	27218.2
Man10P	27298.0	27298.2
Man11	27380.0	27380.2
Man11P	27459.8	27460.2
Man12	27542.5	27542.2
NG	25189.7	25191.7
Man8	26893.0	26894.2
Man9	27054.8	27056.2
Man10	27216.6	27218.2
Man11	27379.3	27380.2
Man12	27542.3	27542.2
NG	25190.7	27191.7
Man8	26894.0	26894.2
Man9	27056.0	27056.2
Man10	27217.9	27218.2
Man11	27380.4	27380.2

*NG: non-glycosylated

Figure 3.4: Intact protein mass spectra of IgG3 Fc-N392K expressed in different glycosylation-deficient strains of *P. pastoris* (Table 3.1) under reducing conditions. A set of peaks corresponding to high mannose glycoforms present at the N297 site and the non-glycosylated protein are observed due to incomplete glycosylation site-occupancy. Accompanying table shows observed mass and calculated mass for the glycoforms detected in each spectra.

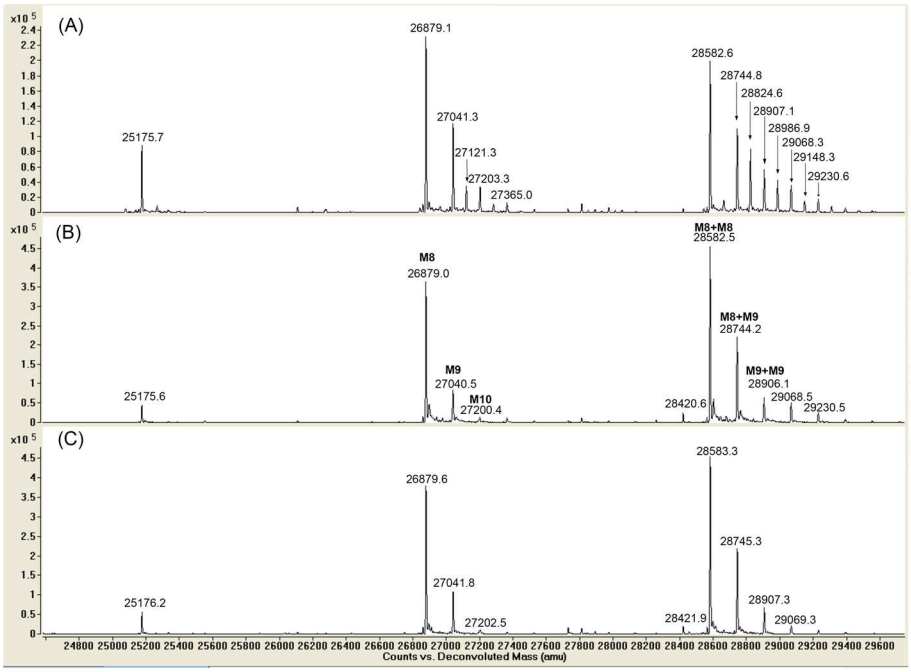

Figure 3.5: Intact protein mass spectra of WT IgG3 Fc expressed in different glycosylation-deficient strains of *P. pastoris* (Table 3.1) under reducing conditions. Two sets of peaks corresponding to high mannose glycans on one (monoglycosylated) or both (diglycosylated) glycosylation sites of WT IgG3 Fc along with a non-glycosylated protein peak are observed due to incomplete glycosylation site-occupancy. Accompanying table shows calculated mass for the WT IgG3 Fc glycoforms detected in the spectra. *NG: non-glycosylated

The glycosylation pattern at the two glycosylation sites in WT IgG3 Fc (expressed in the OCH1KO strain) was additionally characterized by (glyco)peptide mapping to identify glycoforms specific to the N297 and N392 sites. The distribution of high mannose glycoforms on the respective glycopeptides from both the sites was similar to that observed in intact protein MS analysis. Interestingly, the level of phosphomannosylation was found to be higher at the N392 site compared to the N297 site. A striking difference in the level of phosphomannosylated Man8

(Man8P) glycopeptide between the two sites was clearly visible in the spectra (Fig. 3.6).

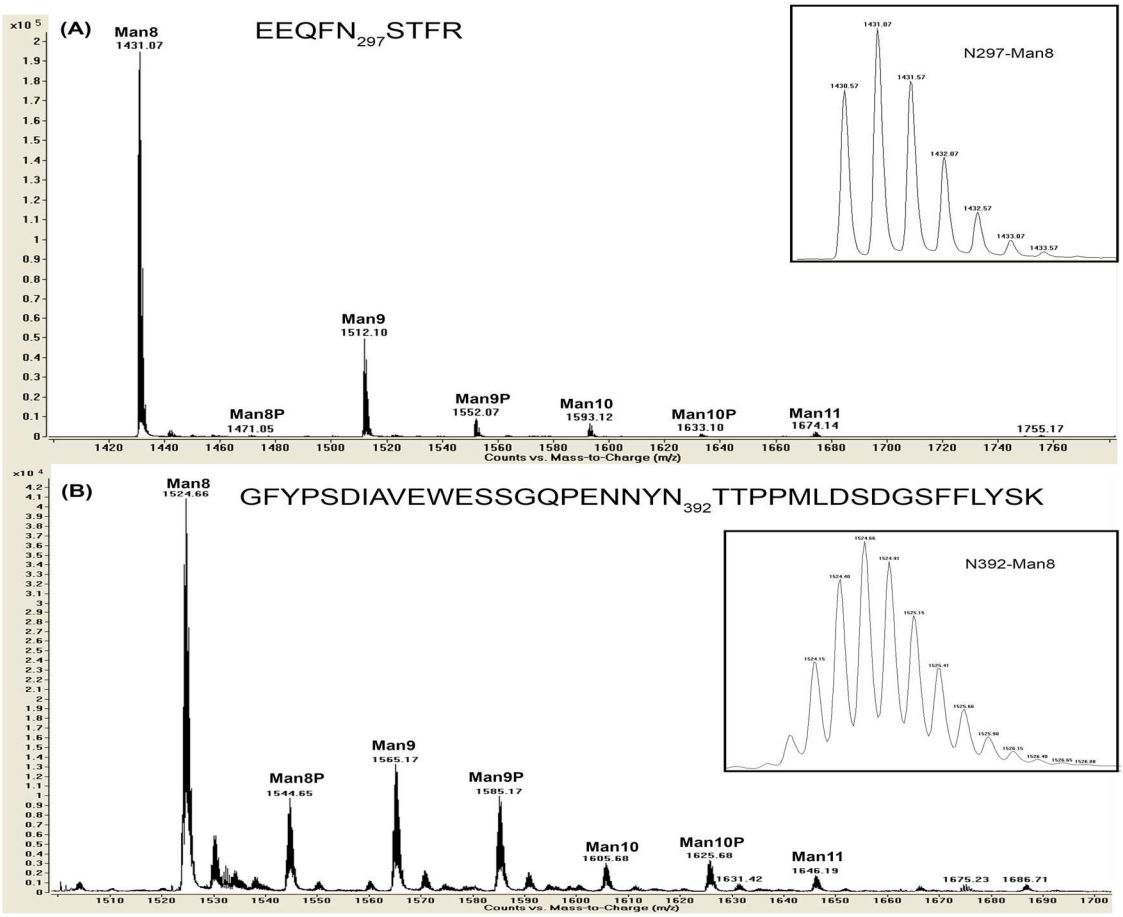

Figure 3.6: Site-specific characterization of glycosylation on WT IgG3 Fc expressed in the OCH1 KO *P. pastoris*. Peptide map showing high mannose glycans at the (A) N297 glycopeptide and (B) N392 glycopeptide. The insets show isotopic cluster of the glycopeptide with Man8 glycoform. Glycopeptides from the N297 and N392 sites bear +2 and +4 charge states, respectively.

3.3.3 Producing IgG3 Fc glycovariants with site-specific glycosylation

To study the influence of N392 site glycosylation, it is necessary to produce Fc with the N297 and N392 sites glycosylated (tetraglycosylated/Fc dimer) and compare it with Fc that only has the N297 site glycosylated (diglycosylated/Fc dimer). Glycovariants from the WT IgG3 Fc (tetra-, tri-, di-glycosylated forms) were separated by phenyl sepharose chromatography (HIC) with partial resolution (Fig. 3.7). Variants with higher site-occupancy were eluted before the lower site-occupied variants under HIC elution condition. Each fraction was checked by SDS-

PAGE to determine the fractions that contained only a single glycovariant. Fractions showing only tetra and tri-glcyosylated variants were pooled separately. Only a limited number of fractions with pure triglycosylated IgG3 Fc were recovered since it eluted between the tetra- and di-glycosylated forms without complete resolution. In a similar manner, the diglycosylated variant (with only N297 site glycosylated) from the IgG3 Fc-N392K/Q Fc was purified from the mixture of di-, mono- and non-glycosylated variants. These purified IgG3 Fc glycovariants will be used for Fc receptor binding studies and biophysical characterization (Chapter 4) and structural studies (Chapter 5).

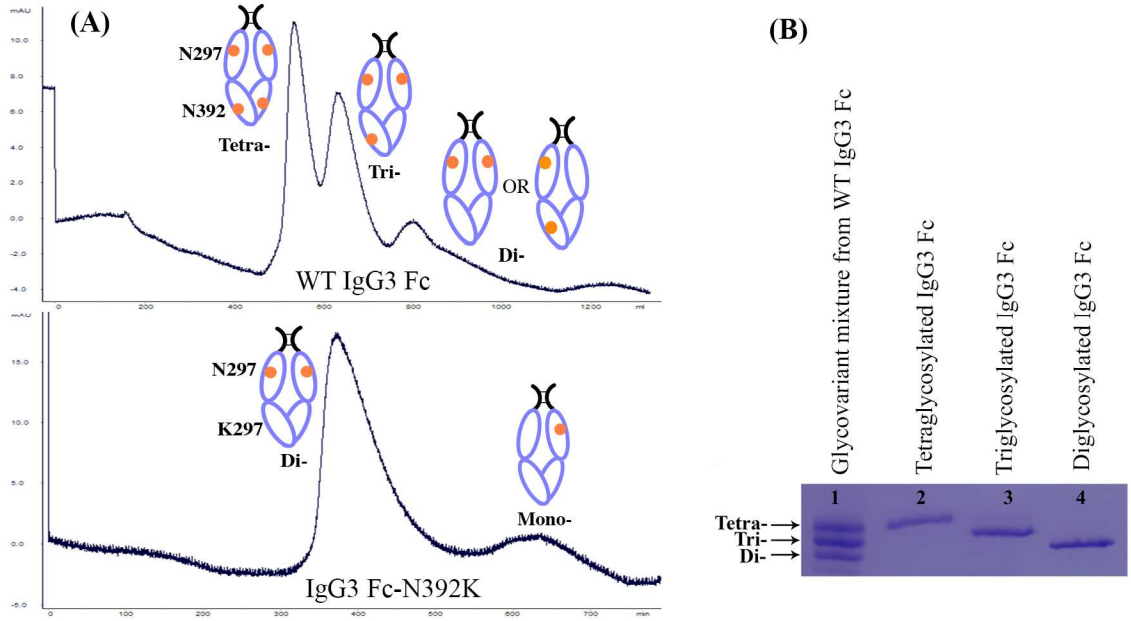

Figure 3.7: (A) Hydrophobic interaction chromatography (HIC) trace for WT IgG3 Fc and IgG3 Fc-N392K. Representative IgG3 Fc glycovariant associated with elution peaks is shown besides each peak. (B) SDS-PAGE (under non-reducing conditions) shows the homogeneity of the produced IgG3 Fc glycovariants. Lane (1) WT IgG3 Fc mixture (2) tetra- and (3) tri-glycosylated variant from WT IgG3 Fc (4) di-glycosylated variant from IgG3 Fc-N392K.

3.3.4 In-vitro glycan processing of high mannose glycans on IgG3 Fc

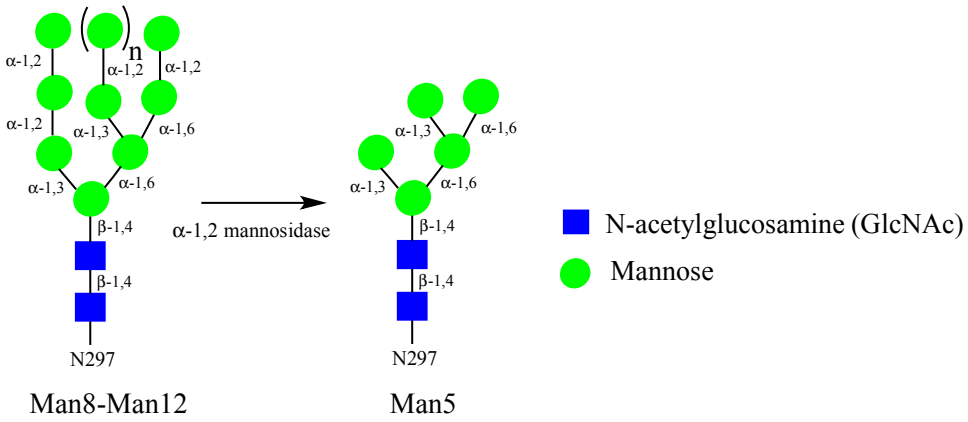

Figure 3.8: Conversion of high mannose glycans ($GlcNAc_2Man_{8-12}$/Man8-Man12) to Man5 ($GlcNAc_2Man_5$) glycoform.

High mannose glycans ($GlcNAc_2Man_{8-12}$/Man8-Man12) were found to be present at both the glycosylation sites in IgG3 Fc, irrespective of the yeast strain used. The conversion of high mannose glycans to complex type glycoforms through a series of *in-vitro* enzymatic glycoprocessing steps has been previously shown in the Tolbert lab (Fig. 3.1). The first step in this glycoprocessing scheme is conversion of the high mannose glycans to the Man5 glycoform by cleavage of α-1,2 linked mannoses (Fig. 3.8). Digestion of the IgG3 Fc-N392K expressed in the OCH1 KO strain with α-1,2 mannosidase yielded only 78% of Man5 glycoform in the total glycan pool (Fig. 3.11A). Among the undigested high mannose glycans, about 10% of the glycans were phosphomannosylated and the rest were presumably glycans that were resistant to α-1,2 mannosidase. High mannose glycans on glycoproteins expressed in *P. pastoris* that are resistant to α-1,2 mannosidase have been previously reported in the literature. These undigested glycans can be either phophomannosylated[28], have β-linked mannose instead of α-linked mannose[15] or have capping glucose(s) on the α-1,3 arm of the high mannose glycan[20] (Fig. 3.9).

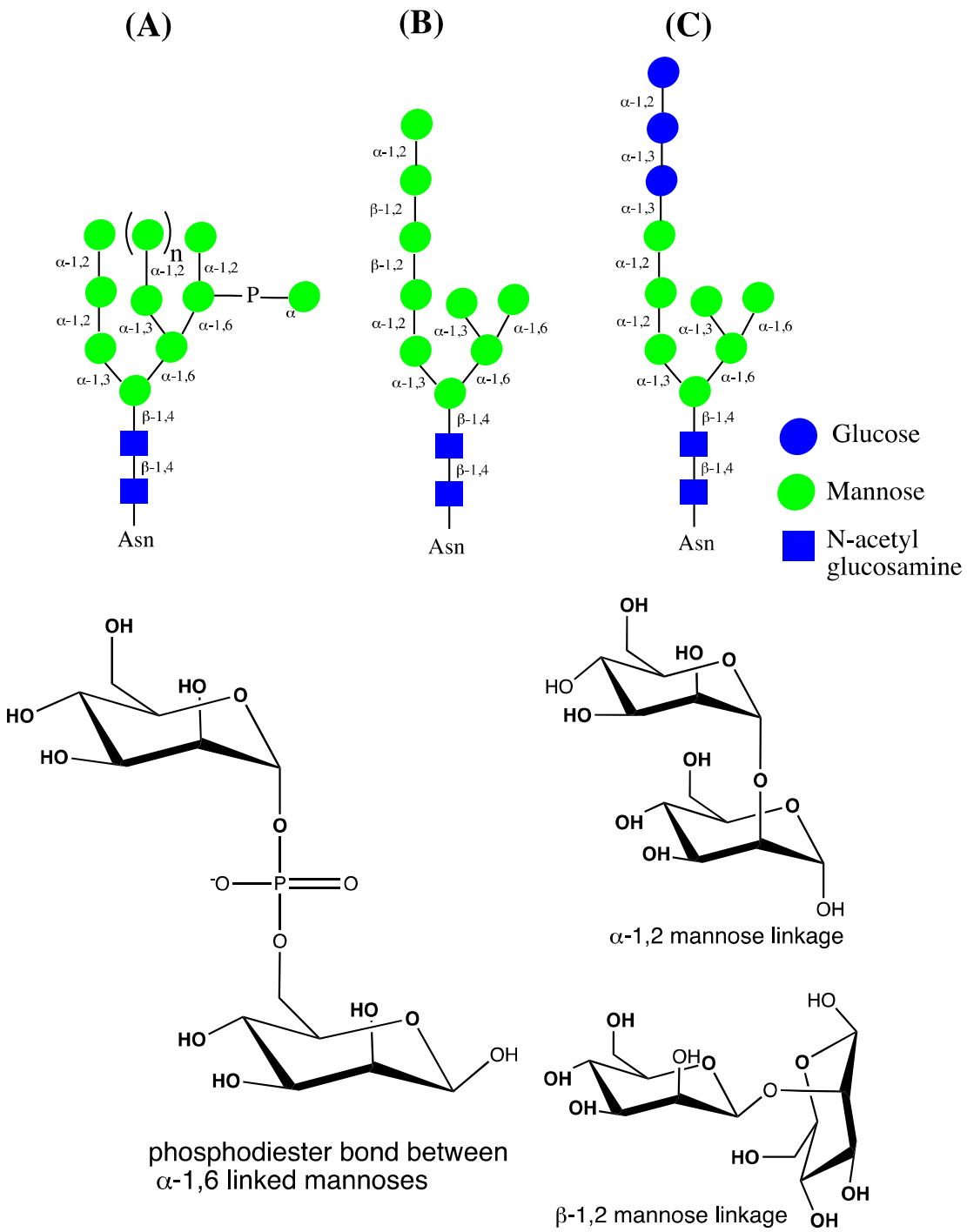

Figure 3.9: Structures of α-1,2 mannosidase resistant high mannose glycans (A) putative structure of a phosphomannosylated glycan (B) β-1,2 mannose present on α-1,3 arm of high mannose glycan (C) capping glucose on the α-1,3 arm of high mannose glycan structure. Chemical structures of phosphodiester bond between mannose residues and α- and β-linked mannoses are shown. Although the phosphate group shown here is between α-1,6 linked mannoses, it is not known for certain if phosphates are present in this linkage only.

In order to achieve a high level of conversion to the Man5 glycoform, it is necessary to eliminate these modified glycans. For this purpose, two additional yeast strains with an existing OCH1 KO background were generated: one with the disrupted PNO1 gene (double KO) and another with the disrupted PNO1, BMT1, BMT2 genes (quadruple KO). The PNO1 and BMT genes in *P. pastoris* are responsible for phosphomannosylation[18] and β-1,2 mannosylation of glycans[19], respectively. There are other genes such as MNN4B that are thought to be involved in mannose phosphorylation and have been deleted by other groups to reduce mannose phosphorylation.[29-30] To remove the capping glucose residues that may be present on high mannose glycans, the IgG3 Fc-N392K was treated with an endomannosidase enzyme, whose enzyme product is a substrate for the α-1,2 mannosidase (Fig. 3.10). As a result of these efforts, an improvement in the yield of Man5 glycoform was observed. The IgG3 Fc-N392K expressed in the double KO strain yielded 92% Man5 glycoform after digestion with α-1,2 mannosidase and endomannosidase (Fig. 3.11B). An increase of up to 2% for conversion to the Man5 glycoform was observed by using two enzymes versus using α-1,2 mannosidase alone. The IgG3 Fc-N392K expressed in the quadruple KO strain yielded 96% of the Man5 glycoform upon digestion with two enzymes (Fig. 3.11C). The percentage of the Man5 glycoform was determined after correcting for the contribution of a single O-mannose glycan (O-glycosylation) present on the protein, which shares its MW with an undigested Man6 glycoform. The percentage of a single O-mannose glycan on IgG3 Fc-N392K was estimated to be 3% and 4.5% for the protein expressed in the double and quadruple KO strains, respectively. Estimation of the O-mannose was based on the intact protein MS peak intensities after digestion of the protein with PNGase F, which only cleaves N-glycans but not O-glycans. These results indicate that a significant improvement in the conversion of the N297 high mannose glycans to the Man5

glycoform can be achieved by eliminating the modified high mannose glycans produced by *Pichia*.

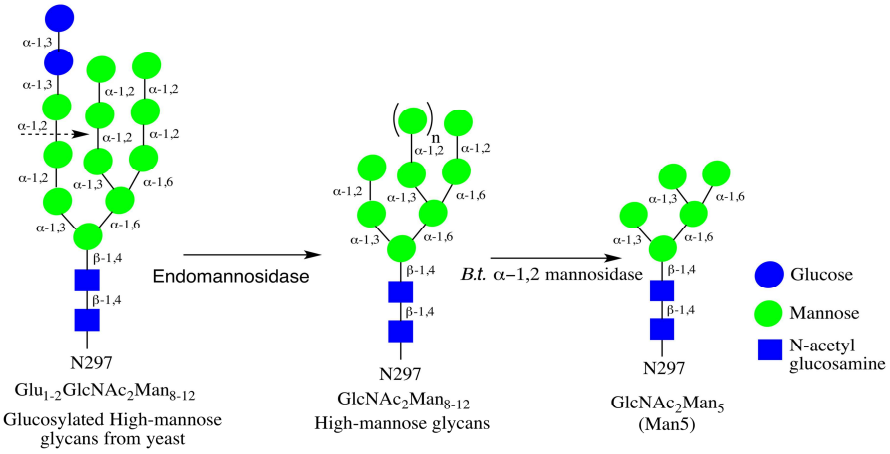

Figure 3.10: Conversion of glucosylated high-mannose glycans to the Man5 glycoform. Endomannosidase cleaves α-1,2 mannosidic bond between two mannoses, where one of the mannose is linked to glucose residue. An endoglycosidase (like endomannosidase) cleaves inside a glycan structure), whereas an exoglycosidase (like *B.t.* α-1,2 mannosidase) cleaves terminal monosaccharide, which in this case is blocked by additional glucose residues.

Digestion of WT IgG3 Fc with α-1,2 mannosidase resulted in an almost complete truncation to the Man5 glycoform at only one of the two sites, while incomplete truncation was observed at the other site (Fig. 3.12). Since it was previously determined that the N297 high mannose glycans in IgG3 Fc-N392K were converted to more than 95% of the Man5 glycoform, it can be implied that incomplete truncation occurred at the N392 site in the WT IgG3 Fc. As a result, a distribution of Man5-Man12 glycoforms at the N392 site was observed in the intact protein mass spectra (Fig. 3.12).

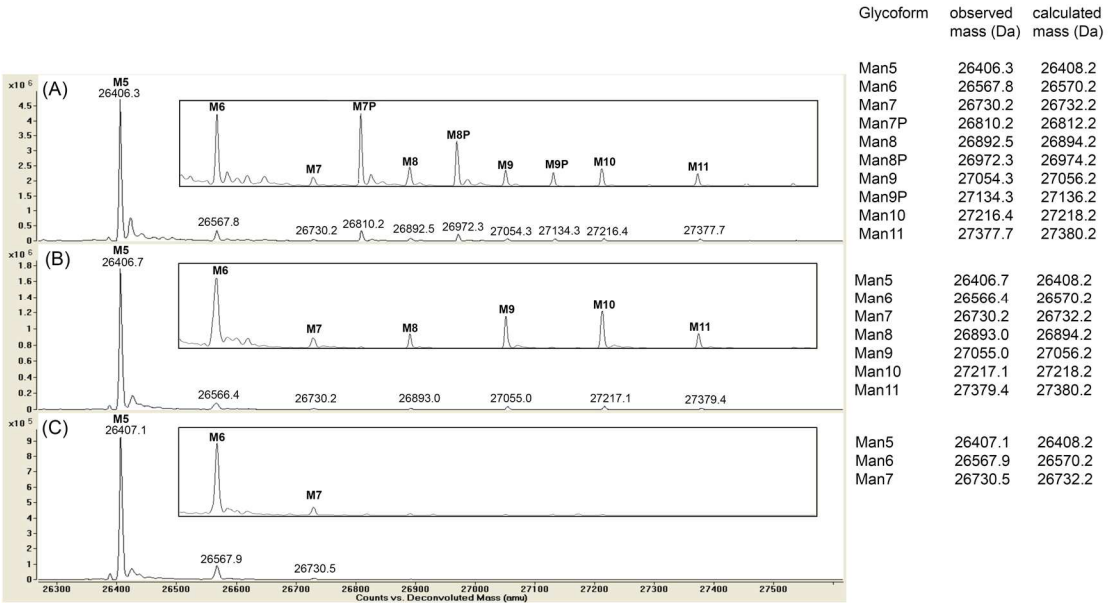

Glycoform	observed mass (Da)	calculated mass (Da)
Man5	26406.3	26408.2
Man6	26567.8	26570.2
Man7	26730.2	26732.2
Man7P	26810.2	26812.2
Man8	26892.5	26894.2
Man8P	26972.3	26974.2
Man9	27054.3	27056.2
Man9P	27134.3	27136.2
Man10	27216.4	27218.2
Man11	27377.7	27380.2
Man5	26406.7	26408.2
Man6	26566.4	26570.2
Man7	26730.2	26732.2
Man8	26893.0	26894.2
Man9	27055.0	27056.2
Man10	27217.1	27218.2
Man11	27379.4	27380.2
Man5	26407.1	26408.2
Man6	26567.9	26570.2
Man7	26730.5	26732.2

Figure 3.11: Intact protein MS spectra of IgG3 Fc-N392K expressed in different glycosylation-deficient strains of *P. pastoris* (Table 3.1) under reducing conditions after α-1,2 mannosidase and endomannosidase digestion. The insets show magnified spectra for the undigested Man6-Man11 glycoforms matched to the original spectra. Accompanying table shows observed and calculated mass for the IgG3 Fc-N392K high mannose glycans observed in each spectra.

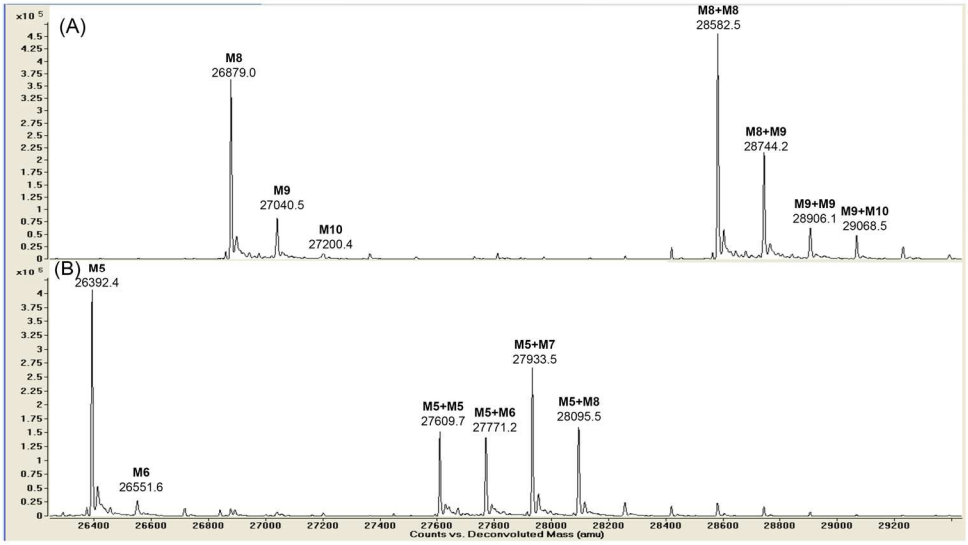

Glycoform	Calculated mass (Da)
Man8	26880.1
Man9	27042.1
Man10	27204.1
Man11	27366.1
Man8+Man8	28582.6
Man8+Man9	28744.6
Man9+Man9	28906.6
Man9+Man10	29068.6
Man10+Man10	29230.6
Man5	26394.1
Man6	26556.1
Man7	26718.1
Man5+Man5	27610.6
Man5+Man6	27772.6
Man5+Man7	27934.6
Man5+Man8	28096.6

Figure 3.12: Intact protein MS spectra of WT IgG3 Fc under reducing condition (A) before and (B) after α-1,2 mannosidase digestion. The set of peaks in (A) correspond to high mannose glycoforms on both sites of Fc (labeled with two glycoforms) and only one of the two sites of Fc (labeled with one glycoform). The peaks in (B) are labeled assuming complete truncation to Man5 glycoform at the N297 site and partial truncation at the N392 site based on results obtained

for IgG3 Fc-N392K (>95% truncation). Accompanying table shows calculated masses of the WT IgG3 Fc glycans detected in the spectra.

An attempt to produce the Man5 glycoform directly out of yeast in place of the high mannose glycans was carried by introducing α-1,2 mannosidase activity in the yeast glycosylation pathway. This was performed by localizing the gene that expresses murine α-1,2 mannosidase (mannosidase IA) in the yeast ER so that the high mannose glycans exiting the ER are trimmed by the enzyme and converted to Man5 glycoform.[27] The IgG3 Fc-N392K expressed in the double KO strain with this additional enzyme showed less than 50% of Man5 glycoform in the total N-glycan pool at the N297 site. This result indicated that the *in-vivo* mannosidase activity showed poor mannose trimming efficiency compared to the *in-vitro* digestion. It must be noted that enzyme used in the two conditions belonged to different species; a bacterial α-1,2 mannosidase (BT3990) for the *in-vitro* condition and a mammalian (murine) α-1,2 mannosidase for the *in-vivo* condition. Moreover, a striking difference in the level of Man5 glycoform was observed for IgG3 Fc-N392K expressed in a spinner flask (~17%) versus a fermentor expression (~44%) (Fig. 3.13). The WT IgG3 Fc expressed in the same strain (with an *in-vivo* α-1,2 mannosidase) also showed incomplete mannose trimming at both the glycosylation sites.

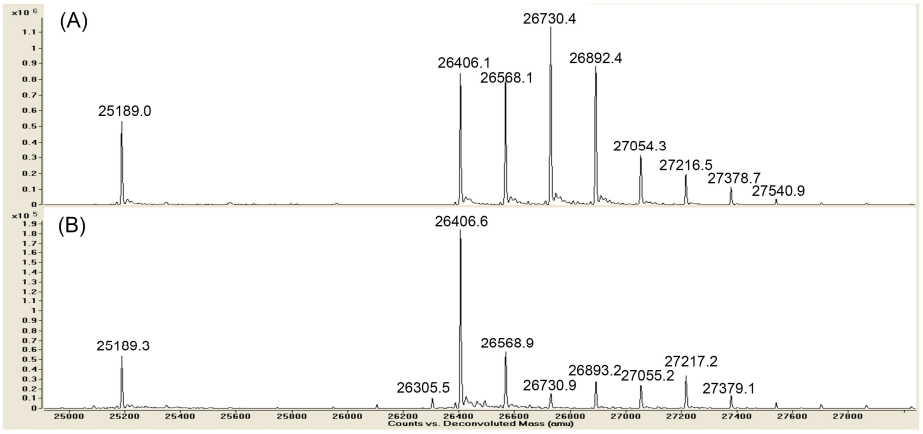

Glycoform	observed mass (Da)	calculated mass (Da)
NG	25189.0	25191.7
Man5	26406.1	26408.2
Man6	26568.1	26570.2
Man7	26730.4	26732.2
Man8	26892.4	26894.2
Man9	27054.3	27056.2
Man10	27216.5	27218.2
Man11	27378.7	27380.2
Man12	27540.9	27542.2

NG	25189.3	25191.7
Man5	26406.6	26408.2
Man6	26568.9	26570.2
Man7	26730.9	26732.2
Man8	26893.2	26894.2
Man9	27055.2	27056.2
Man10	27217.2	27218.2
Man11	27379.1	27380.2

Figure 3.13: Intact protein MS spectra of IgG3 Fc-N392K expressed in *P. pastoris* with *in-vivo* α-1,2 mannosidase activity in (A) spinner flask and (B) fermentor expression. The fermentor expressed protein showed a higher percentage of Man5 glycoform than the spinner flask expressed protein. Accompanying table shows observed and calculated mass for the IgG3 Fc-N392K glycans observed in each spectra. *NG: non-glycosylated

The high mannose glycans (Man5-Man15) present in the IgG3 Fc-N392K expressed in the strain with *in-vivo* α-1,2 mannosidase activity were subjected to *in-vitro* digestion with α-1,2 mannosidase alone and in combination with endomannosidase. An improvement in conversion to the Man5 glycoform was observed with two enzyme digestion (~76%) compared to digestion with α-1,2 mannosidase alone (~70 %) (Fig. 3.14). In comparison, a modest 1-2% increase in conversion to the Man5 glycoform was observed with two enzyme digestion for the same protein expressed in the strain without the *in-vivo* α-1,2 mannosidase. This result led us to believe that there was a larger fraction of glucosylated high mannose glycans (that are only digestible with endomannosidase) produced by the yeast which is modified with an *in-vivo* α-1,2 mannosidase. A visual comparison of the undigested glycans from the single versus double enzyme digest show that the level of undigested Man8 glycoform (although present at low level) was reduced in the case of the two enzyme digest (Fig. 3.14). Based on this, it could be proposed that the endomannosidase enzyme might be digesting the Man8 glycoform (that remained undigested

after digestion with α-1,2 mannosidase) and thereby result in an increased conversion to the Man5 glycoform.

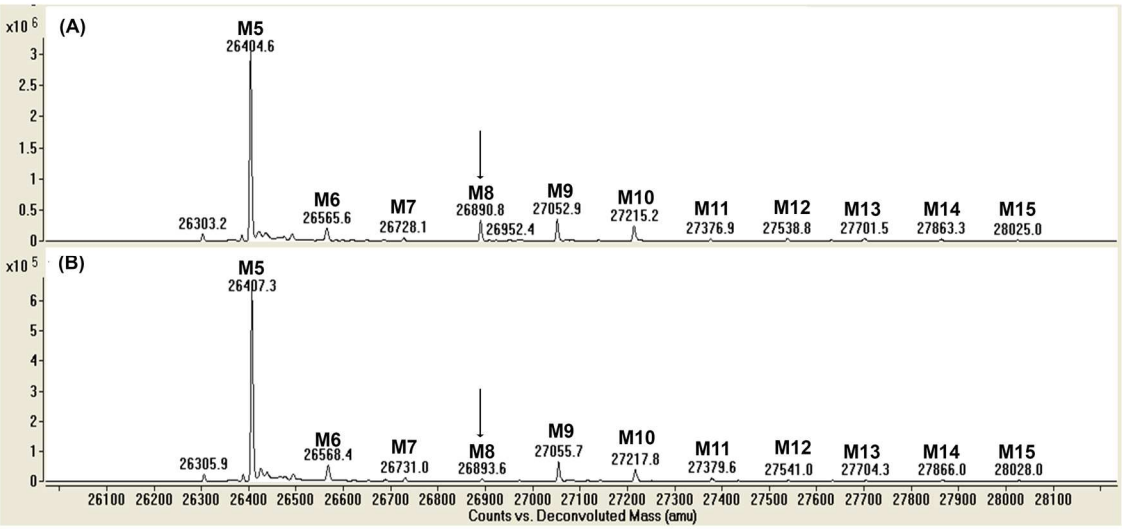

Figure 3.14: Intact protein MS spectra of IgG3 Fc-N392K expressed in *P. pastoris* with *in-vivo* α-1,2 mannosidase activity after *in-vitro* digestion with (A) only α-1,2 mannosidase (B) α-1,2 mannosidase and endomannosidase. Arrow points the difference in level of the undigested Man8 glycoform from the two digestion reactions.

To conclusively determine if endomannosidase is digesting the Man8 glycoform, it is preferable to have IgG3 Fc-N392K with higher levels of Man8 glycoform and use that to test endomannosidase activity. This was achieved by fractionating the phenyl sepharose chromatography elution peak for the diglycosylated IgG3 Fc-N392K, wherein the larger high mannose glycans (Man8-Man15) elute earlier than the smaller high mannose glycans (Man5-Man8) (Fig. 3.15). Fig 3.16 shows MS spectra for distribution of the high mannose glycans in the collected pools from the elution peak. It is clearly visible that pool 1 contained largest fraction of larger high mannose glycans (including Man8 glycoform) and therefore was an ideal substrate to check the substrate selectivity of endomannosidase.

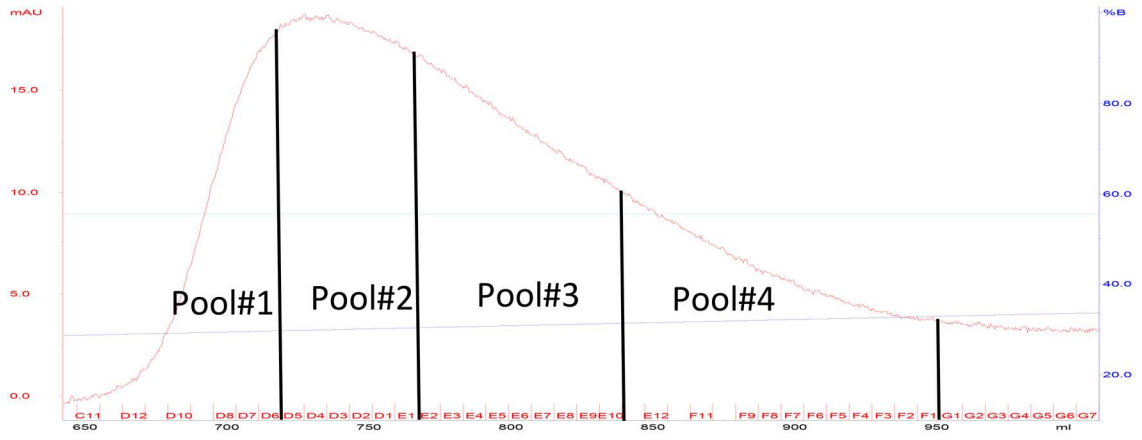

Figure 3.15: Fractionation of phenyl sepharose elution peak of IgG3 Fc-N392K expressed in *P. pastoris* with *in-vivo* α-1,2 mannosidase activity. The elution peak was fractionated into four pools as shown in the figure.

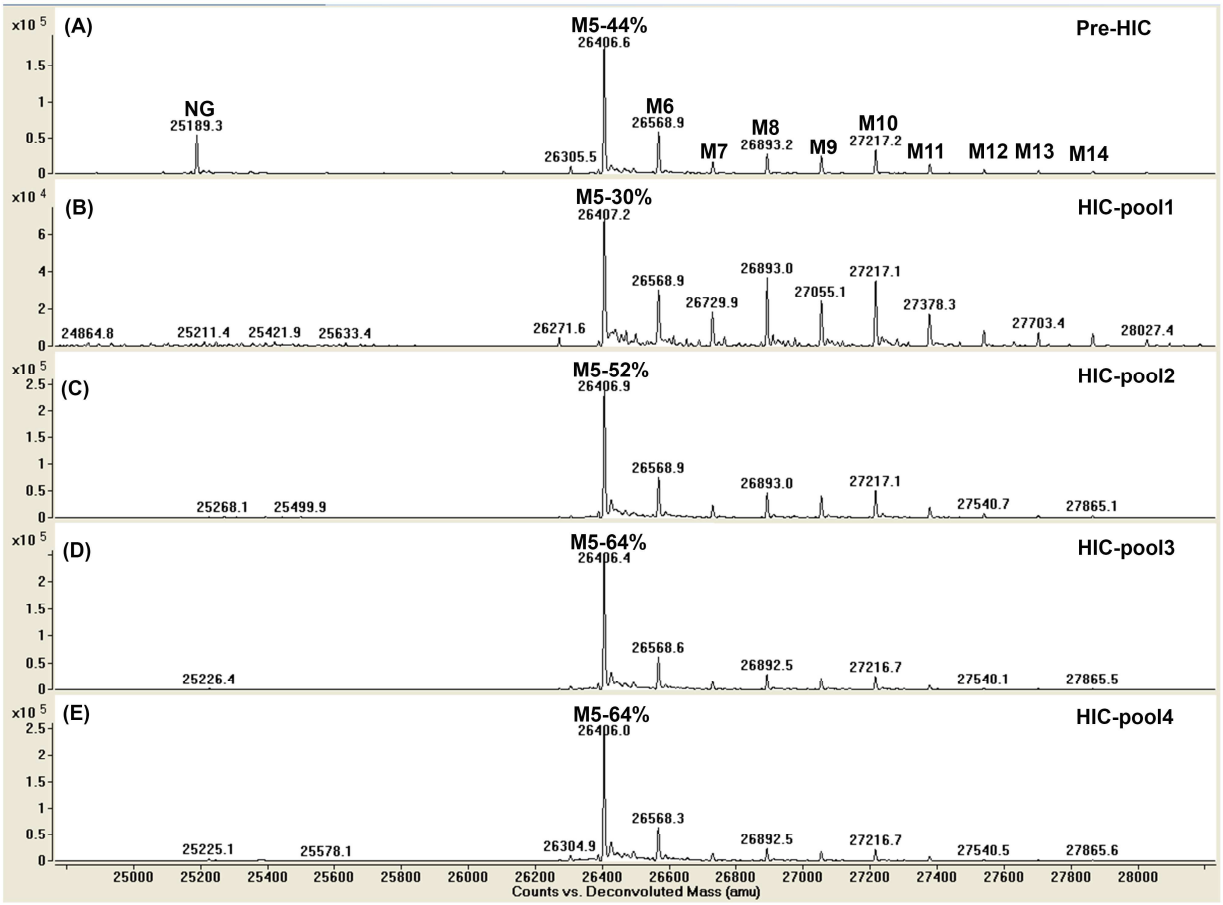

Figure 3.16: Intact protein MS spectra of the pools collected from fractionated phenyl sepharose chromatography of IgG3 Fc-N392K expressed in *P. pastoris* with *in-vivo* α-1,2 mannosidase activity. (A) distribution of glycans before separation; (B-E) distribution of glycans in the

collected pools (1-4) from the elution peak as shown in Fig. 3.15. Pool 1 shows highest level of larger mass high mannose glycans or lowest percentage of Man5 glycoform

Digestion of the protein collected from pool 1 with only endomannosidase produced a largest decrease in the level of Man8 glycoform with a concomitant increase in the level of Man6 glycoform (Fig. 3.17). In a separate experiment, the protein from pool 1 was digested with α-1,2 mannosidase with and without endomannosidase to evaluate the overall contribution of endomannosidase in mannose trimming. The level of undigested Man8 glycoform in the only α-1,2 mannosidase digestion reaction (~12%) was significantly reduced in the case of the digestion with both enzymes (~2%) (Fig. 3.18). The double enzyme digest increased the Man5 conversion by nearly 18%. Based on these results, it can be concluded that endomannosidase digests the Man8 glycoform to either the Man5 glycoform directly or to the Man6 glycoform, which can then be further digested by α-1,2 mannosidase to produce the Man5 glycoform. Consequently, if that interpretation is true, it can be implied that the composition of the Man8 glycoform is actually $Glu_{1-2}Man_{6-7}GlcNAc_2$ and not $Man_8GlcNAc_2$. From a yeast expression perspective, these results indicate that higher levels of glucosylated high mannose glycans are produced by the yeast that has been modified with an *in-vivo* α-1,2 mannosidase activity in the ER.

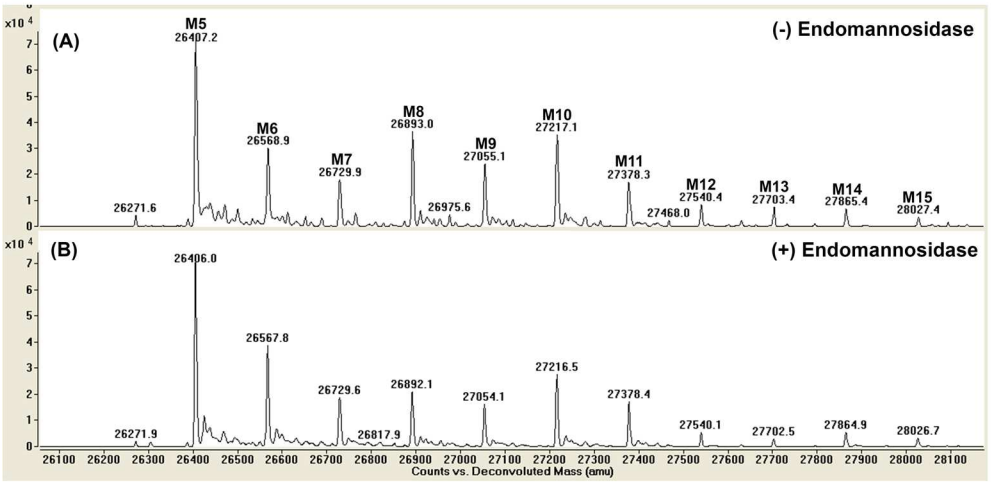

GF	(-) %	(+) %
M5	30.0	35.0
M6	11.2	16.0
M7	6.7	7.8
M8	13.6	8.7
M9	9.0	7.0
M10	13.0	11.5
M11	6.3	7.0
M12	3.0	2.3
M13	2.8	1.1
M14	2.5	2.2
M15	1.3	1.2

Figure 3.17: Intact protein MS spectra of IgG3 Fc-N392K Fc expressed in *P. pastoris* with *in-vivo* α-1,2 mannosidase. Spectra (A) before and (B) after *in-vitro* digestion with endomannosidase Accompanying table shows percentages for each glycoform (GF) calculated based on their relative peak intensities.

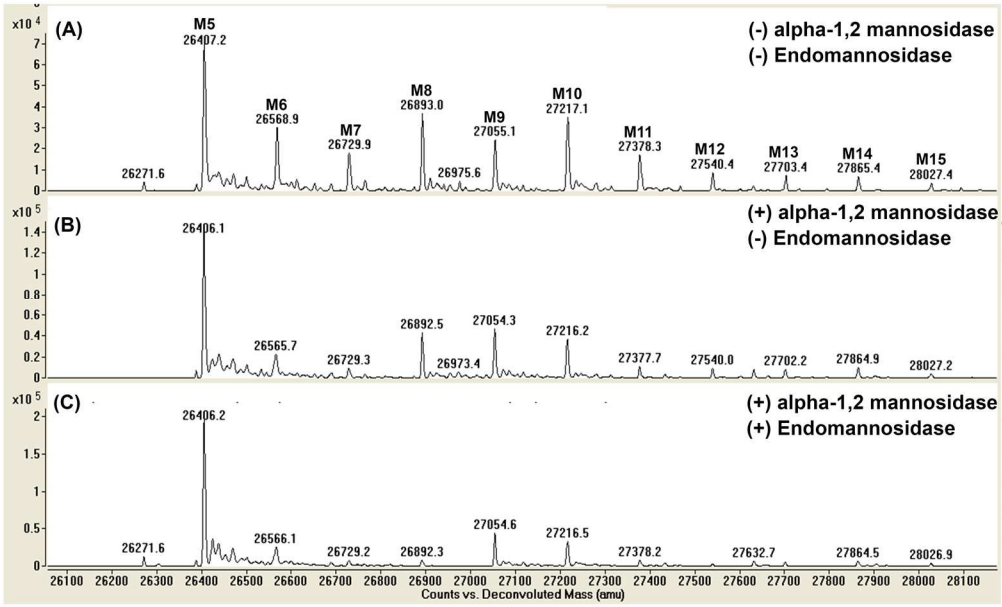

GF	(B) %	(C) %
M5	45.5	63.2
M6	6.1	6.6
M7	2.5	1.9
M8	11.6	2.0
M9	12.5	11.3
M10	10.0	8.5
M11	3.0	2.0
M12	2.5	0.7
M13	2.2	1.1
M14	2.7	1.7
M15	1.0	0.9

Figure 3.18: Intact protein MS spectra after *in-vitro* digestion of IgG3 Fc-N392K Fc expressed in *P. pastoris* with *in-vivo* α-1,2 mannosidase. Spectra (A) before digestion (B) after digestion with α-1,2 mannosidase (C) after digestion with α-1,2 mannosidase and endomannosidase. Accompanying table shows percentages for each glycoform in (B) and (C) calculated based on their relative peak intensities.

3.4 Discussion

3.4.1 Production and characterization of IgG3 Fc expressed in yeast P pastoris

There are several reports in literature that describe recombinant expression of IgG3 in mammalian cells, wherein glycosylation at the N297 site is characterized, but there is no mention of the N392 site or its glycosylation occupancy.[31-34] It is possible that these researchers failed to identify the second glycosylation site in the IgG3 sequence or didn't detect glycans at the N392 site owing to its partial site-occupancy. A rare closely related example is that of an IgG1/IgG3 hybrid antibody (with region around the N392 site from IgG3) showing about 10% glycosylation occupancy at the N392 site with presence of only Man6 glycoform.[35] Interestingly, no glycosylation was detected in the serum isolated IgG3 or the recombinantly expressed IgG3 antibody in the same study. We have expressed the WT and mutant IgG3 Fc (N392K/Q) in a glycosylation-deficient strain (OCH1 KO) of yeast *P pastoris*. The IgG3 Fc-N392K mutant was chosen since Lys is present at the 392 position in some of the natural allotypes of IgG3 as well as in the other IgG subclasses. The Gln in N392Q closely resembles Asn and is a good surrogate for IgG3 that is not glycosylated at the 392 position with a minimal change to the IgG3 Fc structure. Although partial glycosylation site-occupancy was observed at the N297 and N392 sites in IgG3 Fc, it is demonstrated for the first time that the N392 site in recombinantly expressed IgG3 was glycosylated. Our group[24] and other researchers[36] have previously reported partial site-occupancy at the N297 site in *Pichia* expressed IgG1 Fc. Thus, IgG3 Fc produced in yeast was suitable to conduct experiments that focus on glycosylation at the N297 site and more importantly at the N392 site.

Digestion of IgG3 Fc with PNGase F enzyme with and without prior protein denaturation revealed differences in the susceptibility for deglycosylation at the N297 and N392 sites. The

N297 site glycans were cleaved at a much faster rate than the N392 site glycans in the native state of the protein. The N392 site glycans were readily cleaved in the unfolded state. The N297 site the glycans in the IgG1, IgG2 and IgG4 subclasses are also cleaved without denaturation. This distinct property of the N392 site glycans serves as a simple identification test for checking its occupancy and possibly sheds light on its location in the protein structure. The PNGase F enzyme completely cleaves the glycan off the N-glycosylation site by cleaving between the first GlcNAc and Asn residue, acting close to the protein backbone (Fig. 3.19). The N392 site is located at the edge of C_H3-C_H3 dimerization interface and it might be inaccessible to the enzyme (more details in Chapter 5, section 5.3.9).

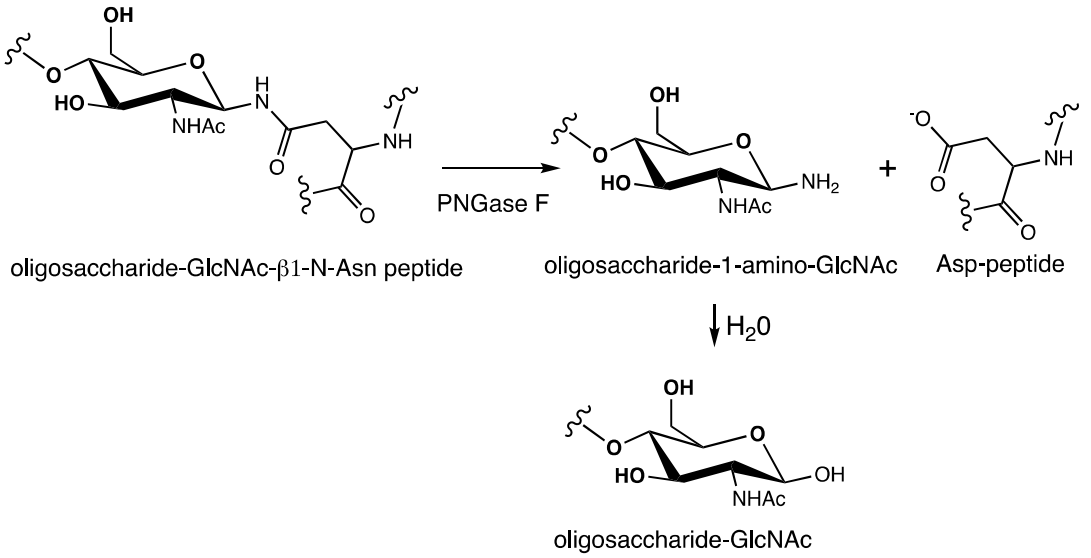

Figure 3.19: Reaction mechanism of PNGase F. The amide bond of β-aspartylglycosylamine is hydrolyzed to produce glycosylamine (which is further hydrolyzed) and Asp residue.

Due to the incomplete glycosylation site-occupancy, a mixture of glycovariants is produced from expression of WT IgG3 Fc (tetra-, tri-, di-, and mono-glycosylated) and IgG3 Fc-N392K/Q (di-, mono-, and non-glycosylated). To independently investigate the effect of each glycosylation site on protein properties, it is essential to separate these individual glycovariants. The IgG1 Fc glycovariants (resembling the IgG3 Fc-N392K/Q) were previously separated in the

Tolbert lab using phenyl sepharose chromatography (HIC).[24] Likewise, the tetra-, tri-, di-glycosylated IgG3 Fc from WT IgG3 Fc were partially separated using HIC. Only a limited quantity of the pure triglycosylated variant was recovered since it eluted between the other two variants. Moreover, since the amount of diglycosylated variant recovered from the WT IgG3 Fc chromatography was insufficient and the associated ambiguity (as to where the glycans are located), the diglycosylated variant was purified from HIC of IgG3 Fc-N392K/Q Fc. Thus, using HIC and site-directed mutagenesis, IgG3 Fc glycovariants with the both sites glycosylated (tetraglycosylated) and with only the N297 site glycosylated (diglycosylated) were produced.

Intact protein MS analysis of the WT and mutant IgG3 Fc showed micro-heterogeneity at both of the glycosylation sites. High mannose glycans with predominantly the Man8 glycoform along with low levels of Man9-Man12 glycoforms were detected at both the sites. Such distribution of glycan is commonly observed in glycoproteins expressed in the OCH1 disrupted *P. pastoris.*[37] The OCH1 gene in the WT *P. pastoris* is responsible for addition of α-1,6 mannose to the α-1,3 arm of high mannose glycoforms and formation of hypermannosylated glycans (Fig. 1.6). Glycopeptide mapping confirmed the presence of phosphomannosylation of glycans at both of the sites. Interestingly, a higher level of phosphorylated glycans was detected at the N392 site compared to the N297 site. This suggests that the phophomannosylation activity during glycoprotein biosynthesis in *P. pastoris* may be affected by the protein structure surrounding the glycosylation site. This is consistent with the results from site-specific glycosylation characterization of human serum IgG3, where glycoprocessing activity related to fucosylation and bisecting GlcNAc was distinctly different between the two sites (chapter 2, section 2.3.3).

3.4.2 In-vitro glycan processing of high mannose glycosylation on IgG3 Fc

The N-glycosylation biosynthesis pathway begins in the ER with the transfer of a preassembled oligosaccharide $Glu_3Man_9GlcNAc_2$ to the Asn of N-glycosylation site by the oligosaccharyltransferase (OST) complex (Fig. 1.6).[38] The $Glu_3Man_9GlcNAc_2$ is sequentially converted to $Man_8GlcNAc_2$ (Man8) by glucosidases and α-1,2 mannosidase in the ER. The resultant Man8 glycoform is processed by divergent pathways in the golgi of yeast and humans. In humans, Man8 is first converted to the Man5 glycoform, which undergoes further mannose trimming and ultimately matures into complex glycoforms through a series of glycan processing steps (Fig. 1.6).[39] In the OCH1 deleted strain of yeast *P. pastoris*, the Man8 glycoform transits to the golgi, where additional α-1,2 mannoses may be added to the initial Man8 structure by golgi α-1,2 mannosyltranferase.[37] As a result, the glycosylation produced by the OCH1KO strain is mainly comprised of the Man8-Man12 glycoforms. Our lab is interested in understanding the effect of glycosylation on antibody immune functions by changing the glycosylation on antibodies and assessing their impact. Under this approach, the high mannose glycosylation produced by the yeast will be converted to hybrid and complex type glycoforms using glycoprocessing enzymes (Fig.3.1). Such stepwise conversion of glycoforms will produce antibody fragments with a single specific glycoform, as opposed to a mixture of glycoforms, commonly seen with antibodies expressed in mammalian cell lines.

The first step in the *in-vitro* high mannose glycan processing is the conversion of the Man8-Man12 glycoforms to the Man5 glycoform using the α-1,2 mannosidase enzyme. Only 78% conversion to the Man5 glycoform (at the N297 site) was achieved for the IgG3 Fc expressed in the OCH1KO strain. Complete conversion to the Man5 glycoform is highly desirable since the undigested high mannose glycans (α-1,2 mannosidase resistant glycans)

compromise the homogeneity of the glycoforms produced at each step of glycoprocessing. The α-1,2 mannosidase resistant high mannose glycans on glycoproteins expressed in *P. pastoris* have been previously reported in the literature. Such glycans can be either be phosphorylated,[28] have a capping glucose sugar,[20] or contain β-linked mannose.[15] We have eliminated or reduced these modified high mannose glycans on the expressed glycoproteins by introducing additional gene disruptions in *P. pastoris* and using an endomannosidase enzyme to achieve a higher level of conversion to the Man5 glycoform.

Prior studies have reported phosphomannosylation of high mannose glycans in some glycoproteins expressed in *P. pastoris*.[13-14] The phosphate group was determined to be present in a phosphodiester linkage between two mannose units and hence resistant to alkaline phosphatases.[14] One of the genes responsible for phosphomannosylation activity in *P. pastoris* was identified as PNO1 (Phosphomanosylation of N-linked Oligosaccahrides).[18] The PNO1 gene was inactivated in the glycoengineered yeast strains developed by the Gengross[12 28] and Contreas[11] groups to produce antibodies with complex-type glycosylation. The Tolbert group has previously deleted the PNO1 gene in an IgG1 Fc expressing yeast strain, and the expressed protein in this strain showed no detectable levels of phosphomannosylation.[24] The level of phosphomannosylated high mannose glycans (estimated from intact protein MS) in the IgG3 Fc was between 4 to 12%, which is an impediment to the conversion of high mannose glycans to the Man5 glycoform since phosphomannosylated glycans are not a substrate for α-1,2 mannosidase. Disruption of the PNO1gene proved to be beneficial since a significant increase in the level of Man5 glycoform after α-1,2 mannosidase digestion was achieved.

Under normal N-glycosylation processing in the ER, the three glucose residues from the $Glc_3Man_9GlcNAc_2$ precursor are cleaved by glucosidases. An alternate deglucosylation pathway

was proposed to be present in the golgi by the action of endomannosidase enzyme, which cleaves α-1,2 mannosidic bond between two mannoses, where one of the mannose is linked to glucose. This pathway would process the glucosylated N-glycans that have escaped the ER glucosidase machinery and thereby generate a substrate for the golgi α-1,2 mannosidase for continued production of complex glycoforms.[40] It was previously reported that digestion of high mannose glycans produced in *P. pastoris* with endomannosidase resulted in trimming of high mannose glycans, thereby implying that glucosylated high mannose glycans can be produced by *P. pastoris*.[20] Based on this information, it was possible that some proportion of the α-1,2 mannosidase resistant high mannose glycans on the IgG3 Fc were glucosylated since glucosylated high mannose glycans are not a substrate for α-1,2 mannosidase. To check this, IgG3 Fc-N392K was digested with endomannosidase to produce deglucosylated glycans that can now be a substrate for α-1,2 mannosidase. A minor increase of 1-2% in conversion to the Man5 glycoform with additional use of endomannosidase suggests that *P. pastoris* can produce low levels of glucosylated high mannose glycans.

The other potential α-1,2 mannosidase resistant high mannose glycans produced in *Pichia* are high mannose glycans that have mannose sugars in a β-linkage instead of an α-linkage.[15] The β-l,2 mannosyltransferase activity in *P. pastoris* was determined to be under the influence of BMT (BMT1-3) genes.[19] It was shown that the disruption of three BMT genes (BMT 1-3) results in no detectable levels of β-linked mannose in the high mannose glycans.[17] Based on this information, the Tolbert lab initiated the deletions of the BMT genes. A quadruple KO strain with additional BMT1, BMT2 KO on an existing strain with OCH1 KO and PNO1 KO was generated. The conversion to the Man5 glycoform upon digestion of IgG3 Fc-N392K (expressed in quadruple KO starin) with α-1,2 mannosidase and endomannosidase improved by nearly 4%

compared to the strain without BMT deletions. We did not identify the nature of the mannose linkage in our expressed proteins, but an increase in the conversion to the Man5 glycoform does indicate that some proportion of the high mannose glycans produced by *P. pastoris* contain mannose residues in β-linkage.

Introduction of α-1,2 mannosidase activity in the *P. pastoris* glycosylation pathway was first demonstrated by the Contreras[11] and Gengross[12] groups while working on re-engineering the yeast glycosylation pathway. The Contreras group attached a tetrapeptide HDEL as an ER retention/retrieval tag to the C-terminus of α-1,2 mannosidase to localize the enzyme in the ER. They used a fungal α-1,2 mannosidase from *Trichoderma reesi* under the control of GAP promoter (constitutive expression), while the model glycoprotein was under AOX1 promoter (inducible expression).[27] Complete trimming of α-1,2 mannose was reported in this study. The Tolbert lab used HDEL ER retention signal fused to a mouse mannosidase enzyme (mannosidase IA) under the control of AOX1 promoter. Man1A was used since it was previously shown to be expressed in *P. pastoris* in an active form.[26] Only partial trimming of α-1,2 mannoses was observed for IgG3 Fc-N392K Fc expressed in yeast with *in-vivo* α-1,2 mannosidase activity suggesting a suboptimal enzyme activity. It is possible that the level of enzyme expression was insufficient for complete mannose trimming. The higher percentage of trimming for the fermentor-expressed protein is likely due to more consistent and controlled enzyme induction (by methanol addition rate) in the fermentor compared to the expression in a spinner flask. This disparity may suggest that the availability of the enzyme might be one of the limiting factor in mannose trimming. Further studies to produce Man5 *in-vivo* needs to be carried out by trying another retention signal and/or using α-1,2 mannosidase from a different species. More information about of these approaches can be found elsewhere.[41-42]

The partially truncated high mannose glycans of IgG3 Fc-N392K expressed in yeast with *in-vivo* mannosidase activity were further subjected to an *in-vitro* digestion with α-1,2 mannosidase and endomannosidase for complete truncation to the Man5 glycoform. From this finding, it was concluded that significantly higher levels of glucosylated high mannose glycans (~10%) were produced by the yeast modified with *in-vivo* mannosidase activity compared to the unmodified yeast (~1-2%). In the unmodified yeast, glucoses on high mannose glycans are trimmed by ER glucosidases during glycoprotein biosynthesis. In the modified yeast, an additional α-1,2 mannosidase activity is introduced in the ER that is not natural to the yeast. It may be possible that this may impair the ER glucosidase activity and cause the glucosylated glycans to end up in the golgi. To circumvent this issue, α-1,2 mannosidase from a different species (enzyme from rat species was used in our studies) can be tried or alternatively the α-1,2 mannosidase activity can be introduced in the early golgi compartment instead of the ER.

3.5 References

1. Vidarsson, G.; Dekkers, G.; Rispens, T., IgG subclasses and allotypes: from structure to effector functions. *Frontiers in immunology* **2014,** *5*, 520.

2. Irani, V.; Guy, A. J.; Andrew, D.; Beeson, J. G.; Ramsland, P. A.; Richards, J. S., Molecular properties of human IgG subclasses and their implications for designing therapeutic monoclonal antibodies against infectious diseases. *Molecular immunology* **2015,** *67* (2), 171-182.

3. Lux, A.; Nimmerjahn, F., Impact of differential glycosylation on IgG activity. *Crossroads between Innate and Adaptive Immunity III* **2011**, 113-124.

4. Arnold, J. N.; Wormald, M. R.; Sim, R. B.; Rudd, P. M.; Dwek, R. A., The impact of glycosylation on the biological function and structure of human immunoglobulins. *Annu. Rev. Immunol.* **2007,** *25*, 21-50.

5. Mimura, Y.; Church, S.; Ghirlando, R.; Ashton, P.; Dong, S.; Goodall, M.; Lund, J.; Jefferis, R., The influence of glycosylation on the thermal stability and effector function expression of human IgG1-Fc: properties of a series of truncated glycoforms. *Molecular immunology* **2000,** *37* (12), 697-706.

6. Kanda, Y.; Yamada, T.; Mori, K.; Okazaki, A.; Inoue, M.; Kitajima-Miyama, K.; Kuni-Kamochi, R.; Nakano, R.; Yano, K.; Kakita, S., Comparison of biological activity among nonfucosylated therapeutic IgG1 antibodies with three different N-linked Fc oligosaccharides: the high-mannose, hybrid, and complex types. *Glycobiology* **2007,** *17* (1), 104-118.

7. Subedi, G. P.; Barb, A. W., The structural role of antibody N-glycosylation in receptor interactions. *Structure* **2015,** *23* (9), 1573-1583.

8. Lefranc, M.-P.; Lefranc, G., Human Gm, Km, and Am allotypes and their molecular characterization: a remarkable demonstration of polymorphism. *Immunogenetics: Methods and Applications in Clinical Practice* **2012**, 635-680.

9. Stavenhagen, K.; Plomp, R.; Wuhrer, M., Site-Specific Protein N-and O-Glycosylation Analysis by a C18-Porous Graphitized Carbon–Liquid Chromatography-Electrospray Ionization Mass Spectrometry Approach Using Pronase Treated Glycopeptides. *Analytical chemistry* **2015,** *87* (23), 11691-11699.

10. Bondarenko, P. V.; Second, T. P.; Zabrouskov, V.; Makarov, A. A.; Zhang, Z., Mass measurement and top-down HPLC/MS analysis of intact monoclonal antibodies on a hybrid linear quadrupole ion trap–orbitrap mass spectrometer. *Journal of the American Society for Mass Spectrometry* **2009,** *20* (8), 1415-1424.

11. Jacobs, P. P.; Geysens, S.; Vervecken, W.; Contreras, R.; Callewaert, N., Engineering complex-type N-glycosylation in Pichia pastoris using GlycoSwitch technology. *Nature protocols* **2009,** *4* (1), 58-70.

12. Li, H.; Sethuraman, N.; Stadheim, T. A.; Zha, D.; Prinz, B.; Ballew, N.; Bobrowicz, P.; Choi, B.-K.; Cook, W. J.; Cukan, M., Optimization of humanized IgGs in glycoengineered Pichia pastoris. *Nature biotechnology* **2006,** *24* (2), 210-215.

13. Montesino, R.; Nimtz, M.; Quintero, O.; García, R.; Falcón, V.; Cremata, J. A., Characterization of the oligosaccharides assembled on the Pichia pastoris—expressed recombinant aspartic protease. *Glycobiology* **1999,** *9* (10), 1037-1043.

14. Miele, R. G.; Castellino, F. J.; Bretthauer, R. K., Characterization of the acidic oligosaccharides assembled on the Pichia pastoris‐expressed recombinant kringle 2 domain of human tissue‐type plasminogen activator. *Biotechnology and applied biochemistry* **1997,** *26* (2), 79-83.

15. Gomathinayagam, S.; Mitchell, T.; Zartler, E. R.; Heiss, C.; Azadi, P.; Zha, D.; Houston-Cummings, N. R.; Jiang, Y.; Li, F.; Giaccone, E., Structural elucidation of an α-1, 2-mannosidase resistant oligosaccharide produced in Pichia pastoris. *Glycobiology* **2011,** *21* (12), 1606-1615.

16. Stephen, H. Endomannosidases in the modification of glycoproteins in eukaryotes. US20120064568, 2012.

17. Hopkins, D.; Gomathinayagam, S.; Rittenhour, A. M.; Du, M.; Hoyt, E.; Karaveg, K.; Mitchell, T.; Nett, J. H.; Sharkey, N. J.; Stadheim, T. A., Elimination of β-mannose glycan structures in Pichia pastoris. *Glycobiology* **2011,** *21* (12), 1616-1626.

18. Miura, M.; Hirose, M.; Miwa, T.; Kuwae, S.; Ohi, H., Cloning and characterization in Pichia pastoris of PNO1 gene required for phosphomannosylation of N-linked oligosaccharides. *Gene* **2004,** *324*, 129-137.

19. Mille, C.; Bobrowicz, P.; Trinel, P.-A.; Li, H.; Maes, E.; Guerardel, Y.; Fradin, C.; Martínez-Esparza, M.; Davidson, R. C.; Janbon, G., Identification of a new family of genes involved in β-1, 2-mannosylation of glycans in Pichia pastoris and Candida albicans. *Journal of Biological Chemistry* **2008,** *283* (15), 9724-9736.

20. Hamilton, S. R.; Li, H.; Wischnewski, H.; Prasad, A.; Kerley-Hamilton, J. S.; Mitchell, T.; Walling, A. J.; Davidson, R. C.; Wildt, S.; Gerngross, T. U., Intact α-1, 2-endomannosidase is a typical type II membrane protein. *Glycobiology* **2005,** *15* (6), 615-624.

21. Kabat, E.; Wu, T.; Perry, H.; Gottesman, K.; Foeller, C., Sequences of proteins of immunological interest, NIH publication no. 91-3242. US Department of Health and Human Services. *Public Health Service, National Institutes of Health, Bethesda, MD* **1991**.

22. Xiao, J.; Chen, R.; Pawlicki, M. A.; Tolbert, T. J., Targeting a homogeneously glycosylated antibody Fc to bind cancer cells using a synthetic receptor ligand. *Journal of the American Chemical Society* **2009,** *131* (38), 13616-13618.

23. Choi, B.-K.; Warburton, S.; Lin, H.; Patel, R.; Boldogh, I.; Meehl, M.; d'Anjou, M.; Pon, L.; Stadheim, T. A.; Sethuraman, N., Improvement of N-glycan site occupancy of therapeutic glycoproteins produced in Pichia pastoris. *Applied microbiology and biotechnology* **2012,** *95* (3), 671-682.

24. Okbazghi, S. Z.; More, A. S.; White, D. R.; Duan, S.; Shah, I. S.; Joshi, S. B.; Middaugh, C. R.; Volkin, D. B.; Tolbert, T. J., Production, characterization, and biological evaluation of well-defined IgG1 Fc glycoforms as a model system for biosimilarity analysis. *Journal of pharmaceutical sciences* **2016,** *105* (2), 559-574.

25. Cuskin, F.; Lowe, E. C.; Temple, M. J.; Zhu, Y.; Cameron, E. A.; Pudlo, N. A.; Porter, N. T.; Urs, K.; Thompson, A. J.; Cartmell, A., Human gut Bacteroidetes can utilize yeast mannan through a selfish mechanism. *Nature* **2015,** *517* (7533), 165-169.

26. Lal, A.; Pang, P.; Kalelkar, S.; Romero, P. A.; Herscovics, A.; Moremen, K. W., Substrate specificities of recombinant murine Golgi α1, 2-mannosidases IA and IB and comparison with endoplasmic reticulum and Golgi processing α1, 2-mannosidases. *Glycobiology* **1998,** *8* (10), 981-995.

27. Vervecken, W.; Kaigorodov, V.; Callewaert, N.; Geysens, S.; De Vusser, K.; Contreras, R., In vivo synthesis of mammalian-like, hybrid-type N-glycans in Pichia pastoris. *Applied and environmental microbiology* **2004,** *70* (5), 2639-2646.

28. Bobrowicz, P.; Stadheim, T. A.; Wildt, S., Methods for eliminating mannosylphosphorylation of glycans in the production of glycoproteins. Google Patents: 2007.

29. Laukens, B.; Visscher, C. D.; Callewaert, N., Engineering yeast for producing human glycoproteins: where are we now? *Future microbiology* **2015,** *10* (1), 21-34.

30. Hamilton, S. R.; Davidson, R. C.; Sethuraman, N.; Nett, J. H.; Jiang, Y.; Rios, S.; Bobrowicz, P.; Stadheim, T. A.; Li, H.; Choi, B.-K., Humanization of yeast to produce complex terminally sialylated glycoproteins. *Science* **2006,** *313* (5792), 1441-1443.

31. Vestrheim, A.; Moen, A.; Egge‐Jacobsen, W.; Bratlie, D.; Michaelsen, T., Different glycosylation pattern of human IgG1 and IgG3 antibodies isolated from transiently as well as permanently transfected cell lines. *Scandinavian journal of immunology* **2013,** *77* (5), 419-428.

32. Jefferis, R.; Lund, J.; Goodall, M., Modulation of FcγR and human complement activation by IgG3-core oligosaccharide interactions. *Immunology letters* **1996,** *54* (2), 101-104.

33. Lund, J.; Takahashi, N.; Pound, J. D.; Goodall, M.; Jefferis, R., Multiple interactions of IgG with its core oligosaccharide can modulate recognition by complement and human Fc gamma receptor I and influence the synthesis of its oligosaccharide chains. *The Journal of Immunology* **1996,** *157* (11), 4963-4969.

34. Lund, J.; Toshiyuki, T.; Noriko, T.; Sarmay, G.; Yoji, A.; Jefferis, R., A protein structural change in aglycosylated IgG3 correlates with loss of huFcγR1 and huFcγR111 binding and/or activation. *Molecular immunology* **1990,** *27* (11), 1145-1153.

35. Rinpei Niwa, M. T. ANTIBODY VARIANTS COMPOSITION. 2012.

36. Ha, S.; Ou, Y.; Vlasak, J.; Li, Y.; Wang, S.; Vo, K.; Du, Y.; Mach, A.; Fang, Y.; Zhang, N., Isolation and characterization of IgG1 with asymmetrical Fc glycosylation. *Glycobiology* **2011,** *21* (8), 1087-1096.

37. Krainer, F. W.; Gmeiner, C.; Neutsch, L.; Windwarder, M.; Pletzenauer, R.; Herwig, C.; Altmann, F.; Glieder, A.; Spadiut, O., Knockout of an endogenous mannosyltransferase increases the homogeneity of glycoproteins produced in Pichia pastoris. *Scientific reports* **2013,** *3*.

38. Aebi, M., N-linked protein glycosylation in the ER. *Biochimica et Biophysica Acta (BBA)-Molecular Cell Research* **2013,** *1833* (11), 2430-2437.

39. Rich, J. R.; Withers, S. G., Emerging methods for the production of homogeneous human glycoproteins. *Nature chemical biology* **2008,** *5* (4), 206-215.

40. Hamilton, S., Endomannosidases in the modification of glycoproteins in eukaryotes. Google Patents: 2008.

41. Choi, B.-K.; Bobrowicz, P.; Davidson, R. C.; Hamilton, S. R.; Kung, D. H.; Li, H.; Miele, R. G.; Nett, J. H.; Wildt, S.; Gerngross, T. U., Use of combinatorial genetic libraries to humanize N-linked glycosylation in the yeast Pichia pastoris. *Proceedings of the National Academy of Sciences* **2003,** *100* (9), 5022-5027.

42. Contreras, R.; Callewaert, N. L.; Vervecken, W.; Kaigorodov, V., Modification of protein glycosylation in methylotrophic yeast. Google Patents: 2011.

Chapter 4 Influence of N392 site glycosylation on Fc receptor interactions and physical stability of IgG3 Fc

4.1 Introduction

Fcγ receptors play a central role in linking the humoral and cellular components of an antibody-mediated immune response. The activating and inhibitory Fcγ receptors present on the surface of leukocytes regulate cellular responses by binding to the Fc region of IgG.[1-2] FcγRIIIA is one of the activating Fcγ receptors expressed on the surface of immune cells such as NK cells, macrophages, monocytes, and mast cells. Notably, the NK cells in most people[3] exclusively express FcγRIIIA on their surface and are considered as an important mediator of Antibody Dependent Cellular Cytotoxicity (ADCC). NK cell mediated ADCC activity is believed to be an important mechanism of action for many therapeutic monoclonal antibodies.[4] Two polymorphic variants of FcγRIIIA exist, the high affinity FcγRIIIA-V158 and low affinity FcγRIIIA-F158, which shows marked difference in the their IgG binding capacities.[2] FcγRIIIA polymorphism also affects the clinical outcome of therapeutic antibodies, whose mechanism of action involves binding to FcγRIIIA as patients homozygous for the V158 variant respond better than patients homozygous for the F158 variant.[5]

Not only is glycosylation at the N297 site in IgG necessary for interaction with Fcγ receptors, but the type of glycosylation also influences the strength of the interaction.[6-7] It is now well established that the removal of core fucose at the N297 site in IgG1 significantly increases its affinity to FcγRIIIA and results in an enhanced ADCC activity.[8] This discovery has led to commercialization of afucosylated therapeutic antibodies, which are potent activators of NK-cell mediated ADCC. Examples of glycoengineered antibodies (described in detail in chapter 1, section 1.8) for cancer therapy are Mogamulizumab (approved in Japan in 2012)[9] and Obinutuzumab (approved in US in 2013)[10]. IgG1 subclass has been extensively characterized for its glycosylation-dependent Fcγ receptor binding profile, however there is limited functional

characterization of glycosylation on the other human IgG subclasses. The IgG3 subclass is particularly important since it is known to interact as efficiently as IgG1 with most of the Fcγ receptors, while IgG2 and IgG4 subclasses show reduced affinity to majority of the Fcγ receptors.[11] Most of the previous studies on IgG3-FcγRIIIA binding were performed using a heterogeneous mixture of IgG3 glycoforms.[11-13] Such studies provided little information about any glycosylation-specific Fcγ receptor binding properties of IgG3. Moreover, the influence of N392 site glycosylation on Fc receptor binding remains under-investigated in the literature.

The neonatal Fc receptor, FcRn, is involved in the placental transfer of maternal IgG to fetus and the prolonged half-life of circulating serum IgG and albumin.[14] FcRn is primarily expressed in the vascular endothelial cells where it binds to IgG that are internalized via pinocytosis in the acidic endosomes. The bound IgG are recycled back to circulation by dissociating from the receptor at physiological pH. FcRn-mediated rescue prevents lysosomal degradation of antibodies and thereby maintains their long circulating half-life.[15] FcRn binds to the C_H2-C_H3 domain interface of Fc in a strict pH-dependent manner.[16] The half-lives of the IgG1, IgG2, and IgG4 subclasses are 21 days, while for the IgG3 subclass it is 7 days.[17] The lower half-life of IgG3 has been attributed to a single amino acid difference, R435 in IgG3 vs. H435 in the other IgG subclasses.[18-19] The occupancy of the N297 glycosylation site and type of glycosylation present does not appear to affect FcRn binding and is located away from the FcRn binding site. The N392 glycosylation site in IgG3 is located near the FcRn binding site; however, its influence on FcRn binding remained unknown at the start of these studies. The IgG3 Fc glycovariants produced as described in chapter 3 were used in this chapter to evaluate the influence of N392 glycans on binding to the FcγRIIIA and FcRn.

Antibodies are complex protein molecules whose preservation of higher-order structure is critical for their biological activity. Antibodies, like other proteins, encounter various physical and chemical instabilities during production, storage, shipping, and patient administration that may compromise the efficacy of the drug.[20] Therefore, it is essential to deliver the antibody drug in a stabilized formulation that would minimize the instability risks. Examples of physical instability are aggregation, precipitation, conformational changes, and unfolding.[21] Biophysical techniques are commonly used to monitor conformational stability and colloidal stability of antibodies.[22] The N297 site glycosylation is critical to the conformational stability and structural integrity of IgG.[23-24] Removal of glycans at the N297 site in IgG1 was shown to lower the conformational stability of the C_H2 domain and the aglycosylated IgG1 showed a higher aggregation propensity compared to its glycosylated counterpart.[25] [26] Glycosylation at the N297 site is believed to stabilize the C_H2 domain conformation, which happens to be the least thermally stable domain in the IgG molecule when compared to the Fab and the C_H3 domains.[27] Although the underlying mechanism is not completely understood, it is widely recognized that protein-carbohydrate interactions play an important role in the stabilization of the C_H2 domain.[28] The lower aggregation propensity of the N297 glycosylated IgG1 is believed to be due to shielding of aggregation prone motifs in the C_H2 domain by the glycans.[29] The N392 site in IgG3 is located in the C_H3 domain and its effect on the conformational stability and aggregation propensity of IgG3 Fc remains unknown.

In this chapter, the effect of N392 glycosylation on IgG3 Fc-Fc receptor (FcγRIIIA and FcRn) binding and IgG3 Fc physical stability is evaluated using IgG3 Fc glycovariants (Fig. 4.1). The production of Fc receptors for use in binding assay is also described. It was observed that the N392 site glycans do not affect the ability of IgG3 Fc to bind with Fc receptors but does impact

its physical stability. It was discovered that the N392 site glycans negatively affected the conformational stability but improved the colloidal stability of IgG3 Fc.

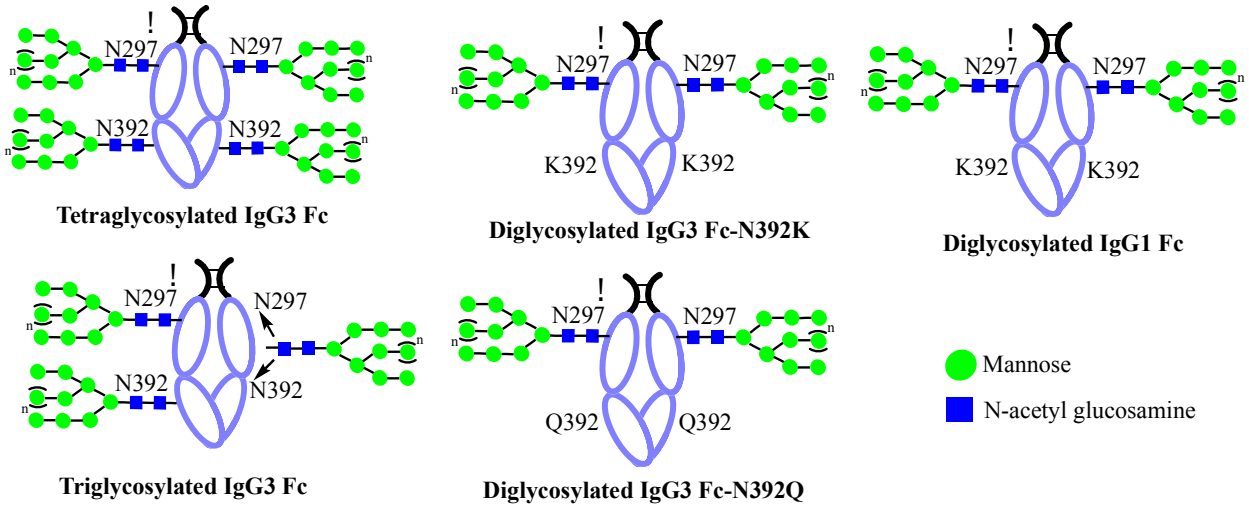

Figure 4.1: Schematic representation of IgG3 Fc glycovariants and IgG1 Fc used for Fc receptor binding and physical stability assessment of IgG3 Fc. High mannose glycans are present on all the Fcs. For triglycosylated IgG3 Fc, the actual attachment site for the third glycan was not determined. It is likely be to present at the N297 site, given the higher site-occupancy at that site.

4.2 Methods

4.2.1 Expression and purification of FcγRIIIA

FcγRIIIA-His_6 (V158 polymorph) was expressed in a glycosylation-deficient strain of the yeast *P. pastoris* (SMD1168) and purified by Ni^{2+}-NTA chromatography, as previously reported by the Tolbert lab.[30] The receptor was further purified using phenyl sepharose chromatography to separate the higher glycosylated forms of the receptor from the partial and non-glycosylated forms, as previously reported by our group.[31]

4.2.2 Cloning of FcRn receptor

FcRn receptor is a heterodimer of two subunits: a transmembrane anchored α-heavy chain and a soluble β2microglobulin (β2m) light chain that are non-covalently associated. FcRn was cloned into *P. pastoris* by two approaches: separate subunits in a dual-vector system and a

single-chain version of the receptor with two subunits linked together in a single vector. For the first approach (Fig. 4.2A), the gene for human α heavy chain (accession # P55899, MGC # 1506, IMAGE # 3163446) was used as a template to amplify the extra-cellular domain (ECD) using primers 5'-GGCGCCCTCGAAGAAAAGAGCAGAAAGCCACCTCTCCCTCC-3' and 5'-CCGCGCGGCGCGGCCGCTTACAGCTCCACCCTGAGGGGCTG-3'. The ECD region of the α chain was identified based on the primers used in a previous study.[32] The gene for β2m (accession # P61769, MGC # 45276, IMAGE #5502428) was amplified using primers 5'-GGCGCCCTCGAGAAAAGAATCCAGCGTACTCCAAAGATT CAGGTTTAC-3' and 5'-GCGCGCGGGGCGGCCGCTTAGTGGTGATGATGGTG ATGCATGTCTCGATCCCACTTAACTATCTT-3'. In the designed primers, a hexahistidine (His_6) tag was fused to the C-terminus of β2m. The amplified DNA from both the genes and *P. pastoris* expression vector pPICZαA were digested with XhoI and NotI and then each gene was separately ligated into pPICZαA using T4 DNA ligase to generate two plasmids, pPICZαA-α and α-β2m. These plasmids were transformed into Top10F' by electroporation and selected on low-salt LB plates with 25 μg/ml zeocin. The colonies were screened by PCR for the presence of the insert and sequenced to ensure no mutation occurred. The confirmed plasmid was purified from the colony and linearized with PmeI for integration into genomic AOX1 gene of a glycosylation-deficient *P. pastoris* yeast strain with the OCH1 deletion (SMD1168). Transformants were selected on YPD pates with 100 μg/ml zeocin. The colonies were named pPICZαA-α and pPICZαA-β2m. The β2m gene was initially cloned in pPICZαA due to the available restriction sites in the multiple cloning region, however it would not be possible to select the β2m gene when transformed into *P. pastoris* that is already transformed with pPICZαA-α (due to the same zeocin selection marker). Therefore, the β2m was transformed into pPIC9K using SacI and NotI

restriction sites to produce pPIC9K-β2m. The construct was linearized with SalI, transformed into *P. pastoris* that was previously transformed with pPICZαA-α and was selected on Minimal Dextrose (MD) plates. The resultant colonies were named pPICZαA-alpha+ pPIC9K-β2m.

For the second approach (Fig. 4.2B), a single-chain FcRn (β2m-linker-α chain) expression plasmid, where both the subunits are linked together by a glycine-serine $(GGGGS)_3$ linker was gifted by the Dimitrov lab.[33] The construct was received in the mammalian expression vector pSecTag2A. To use *Pichia* as an expression host, the single-chain FcRn was shuttled from pSecTag2A to pPICZαA. The insert was PCR amplified using primers 5'-GGCGCCCTCGAGAAAAGAATCCAGCGTACTCCAAAGATTCAGGTTTAC-3' (forward) and 5'- GCCGCGGCGGCCGCTTAATGATGATGGTGGTG GTGTCCACCTCCAGTTTCTGGCAATCCACCTCCACTAGATTTGGCTGGGCTTTCCAG-3' (reverse) that will add a sortase recognition tag (ST) and His_6 tag to the C-terminus of the receptor. The amplified DNA was subcloned into pPICZαA using XhoI and NotI restriction sites. The ligated plasmid was transformed into *P. pastoris* using similar steps as described above. The colonies were named pPICZαA-β2m-L-α-ST-His_6.

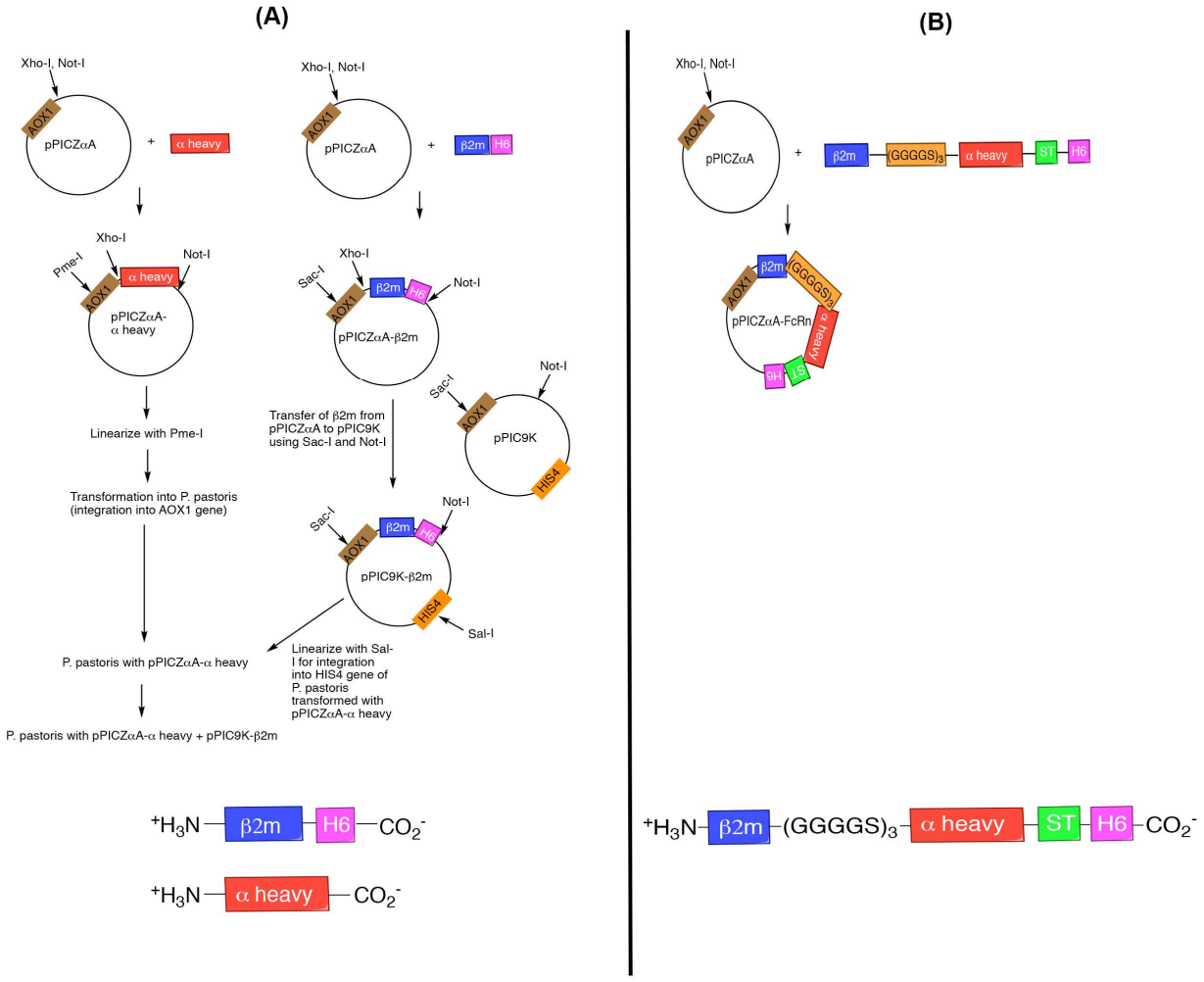

Figure 4.2: Cloning of FcRn into *P. pastoris* expression vector using (A) separate subunits in a dual-vector system and (B) linked subunits in a single vector system. Schematic representation of expressed subunits from both approaches are shown below the cloning strategy.

4.2.3 Expression, purification and biotinylation of FcRn

Single-chain FcRn was expressed in *P. pastoris* in a similar manner as FcγRIIIA and purified using Ni^{2+}-NTA chromatography. The receptor was checked by SDS-PAGE for purity and MS for intact mass. A sortase-mediated ligation was used to attach biotin to the C-terminus of FcRn. For the ligation reaction, the receptor was extensively dialyzed in 50 mM Tris-HCl pH 7.5, 150 mM NaCl. The reaction was carried out using 10 μM FcRn-ST-His_6, 5 mM GGG-EDA (ethylene diamine)-biotin, 2 mM EDTA, 4 mM $CaCl_2$ and 5 μM sortase enzyme at room

temperature for 24 hours. GGG-EDA-biotin was synthesized by Shaofeng Duan (former Tolbert group member).[31] The reaction was quenched by adding an excess of EDTA to chelate the Ca^{2+} required for sortase activity. The biotinylation efficiency was determined by intact protein MS. The excess GGG-EDA-biotin was removed from the sample by extensive dialysis in PBS. The His_6 and ST tags were designed in such a way that His_6 is removed after ligation. The unreacted receptor was removed from the sample by passing the sample through Ni^{2+}-NTA column and collecting the biotinylated FcRn in the flow through.

4.2.4 Kinetic analysis of IgG3 Fc-FcγRIIIA binding

The interactions between different IgG3 Fc glycovariants (tetra-, tri-, and di-glycosylated IgG3 Fc) and FcγRIIIA were measured by BioLayer Interferometry (BLI) using BLItz (ForteBio, Menlo Park, CA). A protein G biosensor tip was hydrated with PBS buffer (50 mM sodium phosphate pH 7.4, 150 mM NaCl) with 1 mg/ml casein as a blocking agent for 15 min. The tip was then dipped in PBS buffer for 15 min. The binding experiment was conducted as follows: an initial baseline was established by dipping the tip in PBS buffer for 30 sec. Next, the tip was loaded with IgG3 Fc glycovariants at a concentration of 0.88 μM for 120 sec to a achieve a response level of 2 nm. A new baseline was established for 30 sec in PBS, then an association and dissociation phase for 180 and 360 sec, respectively was recorded by dipping the tip in FcγRIIIA and PBS, respectively. The FcγRIIIA concentrations used were from 800 nM to 50 nM in two-fold serial dilutions. Between each run, the tip was regenerated using two cycles of 10 mM HCl for 30 sec with one 60 sec cycle of PBS in between. Binding curves were globally fitted to 1:1 binding model and analyzed using BLItz Pro software (ForteBio).

4.2.5 Kinetic analysis of IgG3 Fc-FcRn binding

The interactions between IgG3 glycovariants (tetra- and di-glycosylated IgG3 Fc) and

FcRn were measured by BLI using streptavidin (SA) biosensor tip. The SA tip was first hydrated with PBS pH 6.0 and then with PBS pH 6.0 with 0.05% tween 20 (kinetic buffer) for 15 min each. The tip was loaded with biotinylated FcRn (at 3 μg/ml concentration) in kinetic buffer for 250 sec to a response level of 6 nm. The binding experiment was conducted as follows: a baseline was established by dipping the tip in kinetics buffer for 30 sec. Then, association and dissociation curves recorded by dipping tip in different concentrations of Fc and kinetics buffer, respectively for 60 sec. The Fc concentrations used were from 2727 nM to 170 nM in two-fold serial dilutions. The tip was regenerated between each concentration by two cycles of PBS pH 8.0 for 30 sec with one cycle of PBS pH 6.0 for 60 sec in between. Binding curves were globally fitted to 1:1 binding model and analyzed using BLItz Pro software.

4.2.6 Assessment of physical stability of IgG3 Fc glycovariants

Differential Scanning Calorimetry (DSC) was performed using a MicroCal VP-Auto DSC instrument (MicroCal). IgG3 Fc glycovariants at 0.4 mg/ml in 20 mM citrate-phosphate buffer adjusted to an ionic strength of 0.15 by adding NaCl at pH 6.0 (CP buffer) were prepared. Thermograms were obtained from 10°C to 100°C with a scanning rate of 60°C/hr. Data was analyzed using MicroCal of DSC plug-in for Origin 7.0. The final sample thermogram was obtained from buffer subtraction, baseline fitting, and normalizing concentration. Data was fitted to a non-2-state unfolding model with 2 transitions to calculate heat capacity maximum value (T_m).

Intrinsic (Trp) fluorescence was measured using a PTI Quantum master fluorimeter with 200 μl of 0.2 mg/ml sample in CP buffer. For thermal stability measurements, the temperature was raised in increments of 1.25°C with equilibration time of 120 sec at each temperature. The maximum peak intensity value was calculated using a mean spectral center of mass method

(MSM) and plotted against temperature. Static light scattering intensity was measured simultaneously in the fluorimeter by using a second detector placed at 180° from the fluorescence detector and peak intensity changes at 295 nm were monitored as a function of temperature.

Extrinsic fluorescence measurements (Differential Scanning Fluorimeter) were performed using MX300P QPCR system (Agilent). 100 µl of 0.2 mg/ml sample in CP buffer mixed with 1x of SYPRO^{TM} orange dye (Invitrogen, Carlsbad, CA) were used. Data was collected from 25°C to 90°C using 60°C/hr heating rate. The fluorescence intensity was recorded as a function of temperature.

Turbidity measurements were performed using a Cary 100 UV-Vis spectrophotometer (Varian medical systems). 200 µl of 0.2 mg/ml of sample in CP buffer in a 1 cm path length of quartz cuvette were used. Optical density (OD) at 350 nm was monitored as temperature was raised in increments of 1.25°C from 10-90°C with a heating rate of 60°C/hr.

Far UV Circular Dichroism (CD) was recorded using Chirascan (Applied Photophysics) equipped with a peltier temperature controller. A CD spectra was collected for wavelength range 260 to 200 nm with a resolution of 0.2 nm and a bandwidth of 1 nm. 200 µl of 0.2 mg/ml of sample in CP buffer in a 0.1 cm path length of quartz cuvette were used. The CD signal changes at 228 nm were recorded as temperature was raised from 10°C to 90°C at 2.5°C intervals with a scanning rate of 15°C/hr and 5 min equilibration time at each temperature.

4.3 Results

4.3.1 FcγRIIIA expression/purification/characterization

Human FcγRIIIA receptor bears five N-glycosylation sites: N39, N46, N75, N163, and N170.[34] The yield of the receptor from Ni^{2+}-NTA chromatography was 15-20 mg per liter of

expression. The heavily glycosylated receptor migrates as a smear on SDS-PAGE (Fig. 4.3). The receptor was further purified using phenyl sepharose chromatography as a polishing step and to remove the partially glycosylated forms of the receptor (due to incomplete glycosylation site-occupancy). Based on the elution profile of the WT IgG3 Fc (Chapter 3), it is expected that higher glycosylated forms of the receptor would elute first. As a result, only the first-half of the receptor elution peak was isolated to recover the fully glycosylated form of the receptor. The use of partially glycosylated forms of the receptor in the FcγRIIIA-IgG3 Fc binding assay would be undesirable since the occupancy of N163 glycosylation is known to be important for high affinity interaction of FcγRIIIA with IgG.[34] The purity of the receptor was improved by phenyl sepharose purification and the protein migrated as a consolidated band in SDS-PAGE (Fig. 4.3).

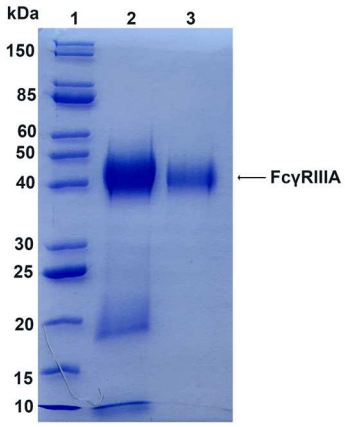

Figure 4.3: Coomassie-stained SDS-PAGE of FcγRIIIA receptor purified from Ni^{2+}-NTA affinity (lane2) and phenyl sepharose (lane3) purification

4.3.2 FcRn expression/purification/characterization

FcRn receptor is a heterodimer of α heavy chain and β2m, which are non-covalently associated in their functional form. An initial attempt was made to express FcRn by cloning the individual subunits into two separate vectors and then sequentially transforming them into *P.*

pastoris. Both the subunits were placed under the control of strong AOX1 promoter (inducible by methanol) and theoretically should be co-expressed and secreted in the media in a heterodimeric form. Unfortunately, no detectable levels of protein expression were observed. For the next attempt, a single-chain version of FcRn receptor was used, where both subunits are covalently connected by a glycine-serine $(GGGGS)_3$ linker. The single-chain FcRn construct was gifted by the Dimitrov lab, which expressed the receptor in 293 FreeStyle cells (mammalian cell line) in a functional form.[33] For expression in *P. pastoris*, the single-chain version of the receptor was shuttled from the existing mammalian expression vector into the *Pichia* expression vector. A sortase recognition tag (ST) consisting of amino acids LPETGGG and a hexahistidine tag (His_6) was added to the C-terminus of the receptor to allow biotinylation and Ni^{2+}-NTA purification of the receptor respectively. About 15-20 mg of the receptor (referred as FcRn-ST) was expressed from 1L spinner flask. The receptor has one N-linked glycosylation site at N102 and migrated as a single band on SDS-PAGE (Fig. 4.4). Digestion of receptor with PNGase F resulted in a gel shift suggesting that the receptor was expressed in a nearly fully glycosylated state. Intact protein MS showed a set of peaks corresponding to the glycosylated receptor and a small peak for the non-glycosylated protein, consistent with the SDS-PAGE results (Fig.4.5).

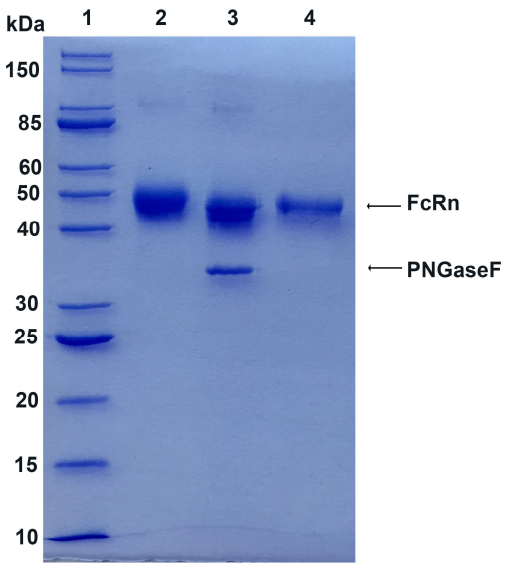

Figure 4.4: Coomassie-stained SDS-PAGE analysis of FcRn-ST receptor. Lanes (1) MW weight marker (2) FcRn-ST (3) PNGase F digested FcRn-ST (4) FcRn-biotin FcRn-biotin was prepared using sortase-mediated ligation.

The distribution of high mannose glycans on the receptor were more skewed toward larger high mannose glycans (>Man10, Fig. 4.5). This is in contrast to IgG3 Fc expressed in the same *P. pastoris* strain, where the most dominant glycoform present was Man8 (Chapter 3). This variation suggests that the glycosylation pattern produced in *P. pastoris* is influenced by the nature of the glycoprotein expressed and/or the location of the glycosylation site in the protein. Intact protein MS of the PNGase F-digested receptor showed a peak corresponding to the expected MW of the protein (Fig. 4.6A). The additional peaks observed in the spectra are likely due to cysteine modifications since these peaks disappeared with reduction of the sample (Fig. 4.6B). The peak with an additional mass of 305 Da could be assigned to glutathionylation of cysteine.[35] The peaks with mass additions of 29 and 48 Da could be possibly assigned to formation of other cysteine adducts (Fig. 4.6A). The receptor has 6 cysteines, out of which two exist as free cysteines (based on X-ray crystal structure) and hence can be potentially modified.[36]

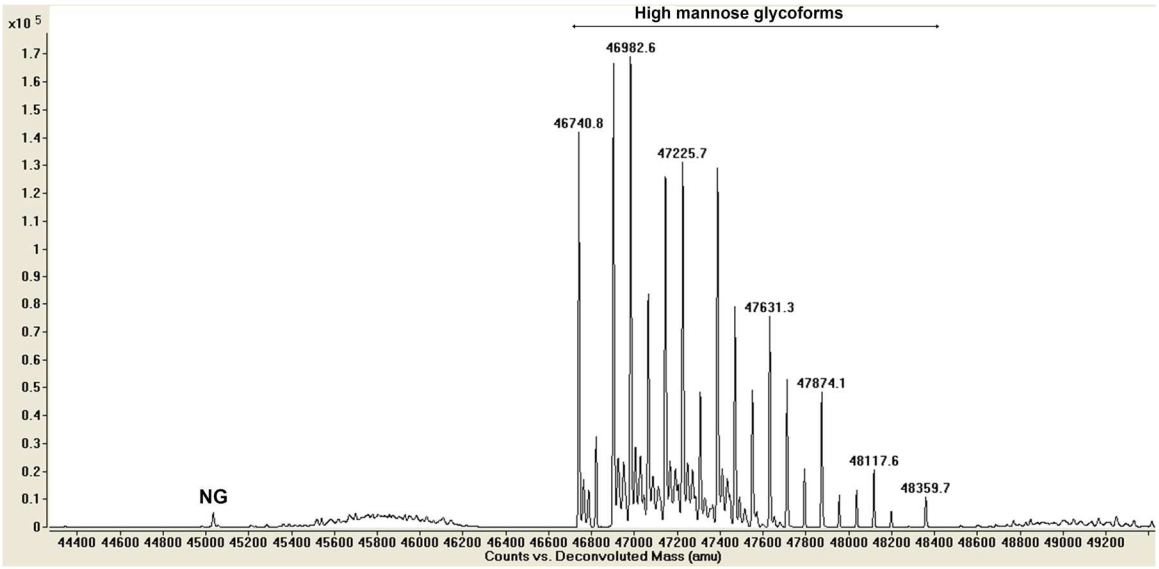

Figure 4.5: Intact protein mass spectra of FcRn-ST under reducing conditions. Multiple peaks correspond to high mannose glycoforms at the N102 glycosylation site. *NG: non-glycosylated.

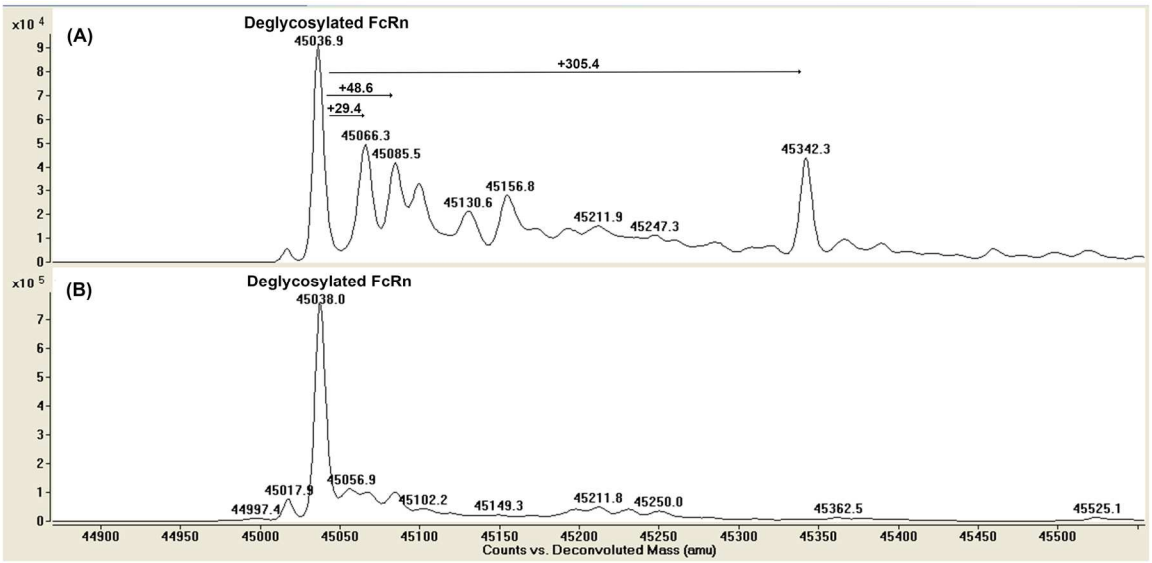

Figure 4.6: Intact protein mass spectra of FcRn-ST under (A) non-reducing conditions and (B) reducing conditions. Expected MW of the deglycosylated FcRn-ST is 45041.2 Da.

4.3.3 Sortase-mediated ligation of FcRn receptor

Sortase, a bacterial enzyme was used to attach biotin to the C-terminus of FcRn for use in

streptavidin based binding assay.[37] The ligation requires an N-terminal glycine-containing peptide and a C-terminal recognition motif LPETG (ST). FcRn-ST-His_6 and an N-terminal polyglycine compound containing biotin separated by a ethylene diamine linker (GGG-EDA-Biotin, Shaofeng Duan from our lab produced this compound) were used in the ligation reaction. The sortase catalyzes cleavage between Thr-Gly and makes a new peptide bond between the N-terminal glycine of GGG-EDA-Biotin and the C-terminus of Thr of FcRn (Fig. 4.7). The His_6 tag was placed downstream of the sortase recognition motif so that it is removed in the ligated product. Such a design allowed separation of any unreacted FcRn-ST-His_6 in the reaction mixture by capturing it on Ni^{2+}-NTA column, while the ligated product remains in the flow through. The EDA linker separates biotin from the C-terminus of FcRn, and thereby may provides some degree of separation between streptavidin and FcRn to prevent potential interference of streptavidin in the FcRn binding assay. The ligation reaction conditions were required to be optimized since the receptor was found to instantly precipitate upon addition of Ca^{2+}. To circumvent this issue, EDTA was added to the reaction prior to addition of Ca^{2+}, which presumably balanced the amount of Ca^{2+} required for sortase activity while preventing protein precipitation.

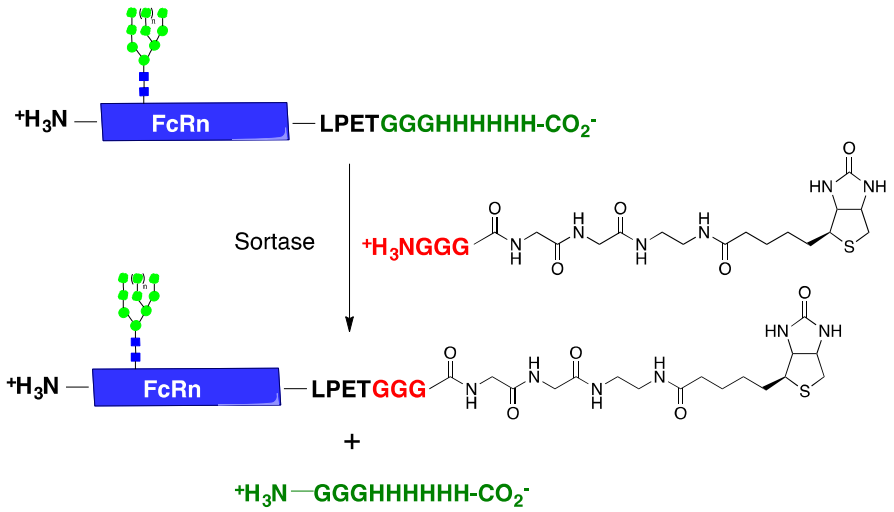

Figure 4.7: Production of biotinylated FcRn using sortase-mediated ligation between FcRn-ST-His_6 and GGG-EDA-Biotin. EDA: ethylene diamine

The reaction progress was monitored by intact protein MS, which showed a peak corresponding to the biotinlylated receptor (Fig. 4.8B). The ligation reaction was shown to be 98% complete based on the peak intensities of the ligated and the unligated receptor. The biotinylated FcRn was used in BioLayer Interferometry (BLI) based FcRn binding assay for immobilizing the receptor on a streptavidin biosensor tip.

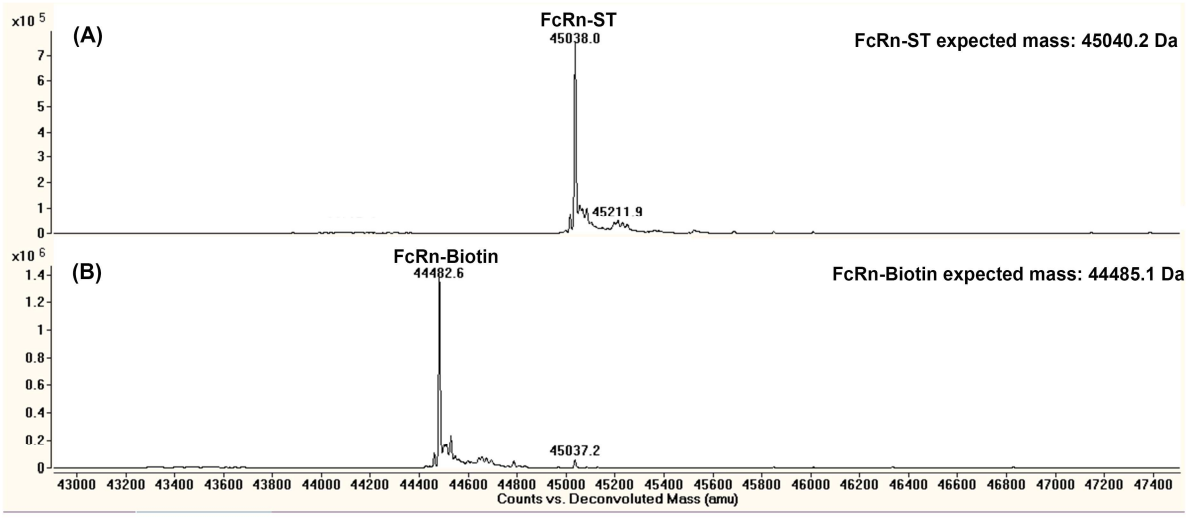

Figure 4.8: Intact protein mass spectra of biotinylated FcRn prepared using sortase-mediated ligation under reducing conditions. The receptor was deglycosylated prior to MS characterization for ease of peak assignment. Panels show peak(s) corresponding to (A) FcRn-ST (B) FcRn-Biotin.

4.3.4 Binding interactions of IgG3 Fc glycovariants with FcγRIIIA

Kinetics of IgG3 Fc-FcγRIIIA binding interactions were assessed by BioLayer Interferometry (BLI) using protein G biosensors. IgG3 Fc glycovariants were first immobilized on a protein G tip, and the receptor was placed in solution (analyte). An immobilization level of 2 nm was achieved using 0.88 μM solution of various IgG3 Fc glycovariants. Then, a baseline was established and association of FcγRIIIA was recorded by dipping the biosensor tip into solution of different concentrations of FcγRIIIA. Once the complex was formed, the dissociation step was recorded by dipping the biosensor in PBS buffer. The kinetic parameters, k_{on} (association rate constant) and k_{off} (dissociation rate constant), were obtained by fitting the curves to 1:1 binding model. Equilibrium dissociation constant (K_D) were calculated from ratio of k_{off} and k_{on}. The applied binding model is consistent with biochemical and structural analysis of this interaction.[12, 38] Fig. 4.9 shows the representative binding curves for the binding of IgG3 Fc glycovariants to FcγRIIIA and Table 4.1 shows the corresponding kinetic parameters.

Tetraglycosylated (N297 and N392 sites occupied) and diglycosylated (only N297 site occupied) IgG3 Fc were compared to check the influence of N392 site glycosylation on receptor binding. Two versions of diglycosylated IgG3 Fc were used, one produced from IgG3 Fc-N392K and the other from the IgG3 Fc-N392Q. Additionally, the diglycosylated IgG1 Fc that naturally has a Lys (K) at the 392 position was also tested for comparison purposes. All the IgG3 Fc glycovariants showed high affinity binding to FcγRIIIA with minor differences. The tetraglycosylated variant showed slightly weaker affinity (56.4 nM) than the diglycosylated N392K variant (41.4 nM) but a comparable affinity to the diglycosylated N392Q variant (50.9 nM). The diglycosylated IgG1 Fc showed the strongest affinity (36.2 nM) compared to all the IgG3 Fc glycovariants. Taken together, these results indicate that IgG3 Fc shows comparable affinity as IgG1 Fc for binding to FcγRIIIA, and the additional presence of N392 glycans in IgG3 Fc does not adversely affect its high affinity binding.

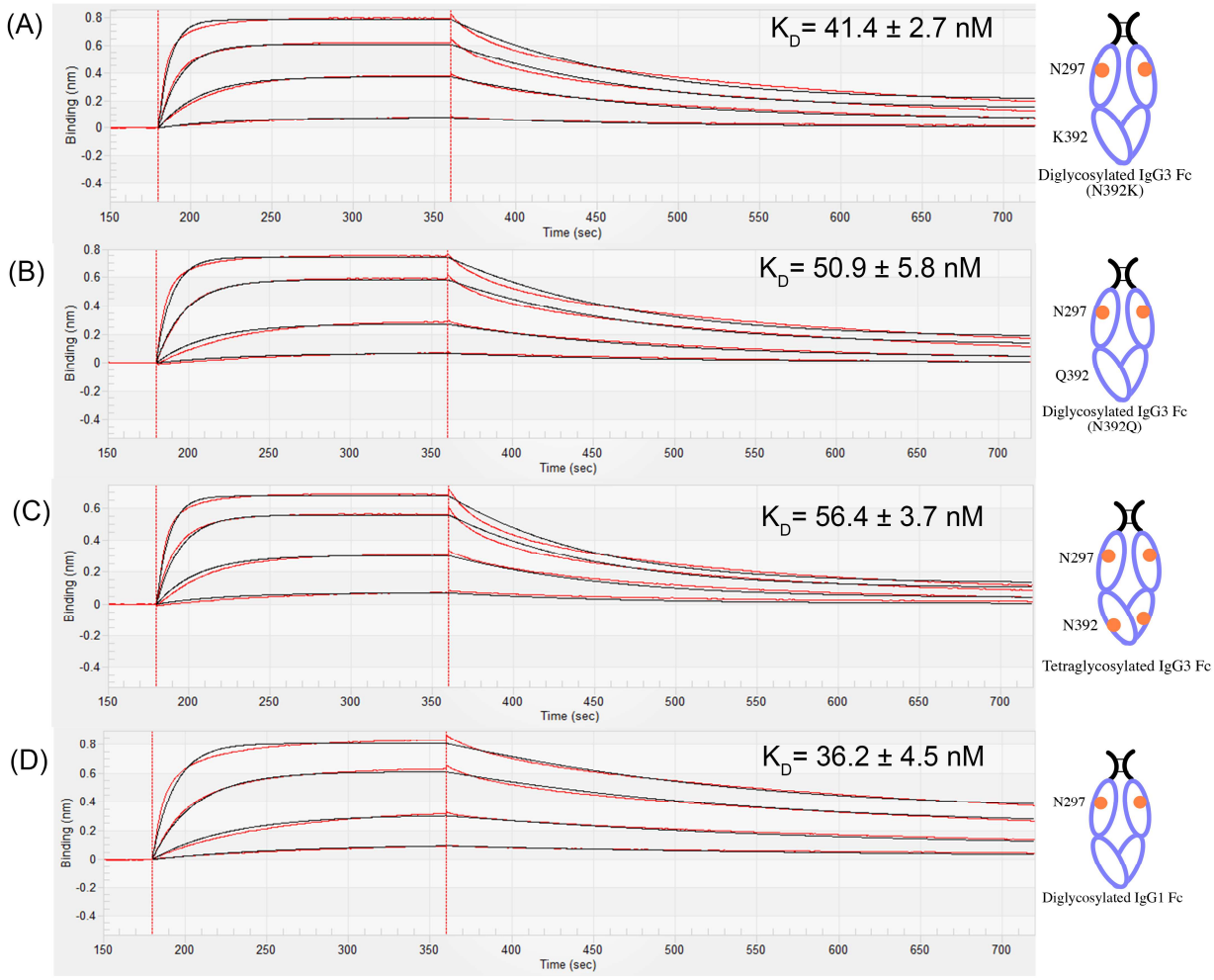

Figure 4.9: Representative BioLayer Interferometry (BLI) binding curves for the interaction of FcγRIIIA with the IgG3 Fc glycovariants. Experimental and fitted data are shown in red and black respectively.

Table 4.1: Kinetic parameters obtained for binding of FcγRIIIA with IgG3 Fc glycovariants. Values are reported as average and standard deviation of triplicate measurements.

Fc Variant	**Average k_{on}*10^5 (1/M.sec)**	**Average k_{off}*10^{-3} (1/sec)**	**Average K_D (nM)**
Diglycosylated IgG3 Fc-N392K	1.6 ± 0.1	6.5 ± 0.2	41.4 ± 2.7
Diglycosylated IgG3 Fc-N392Q	1.21 ± 0.02	6.1 ± 0.7	50.9 ± 5.8
Tetraglycosylated IgG3 Fc	1.6 ± 0.1	9.0 ± 0.2	56.4 ± 3.7
Diglycosylated IgG1Fc	0.93 ± 0.05	3.4 ± 0.4	36.2 ± 4.5

4.3.5 Binding interactions of IgG3 Fc glycovariants with FcRn

Binding kinetics of IgG3 Fc-FcRn interactions were measured by BioLayer Interferometry (BLI) using streptavidin (SA) biosensors. Selectively biotinlylated FcRn (using sortase-mediated ligation) was immobilized on the SA tip, and IgG3 Fc glycovariants (analyte) were placed in solution. FcRn binds to the C_H2-C_H3 domain interface at both the heavy chains of an IgG Fc, thus resulting in a 2:1 binding stoichiometry. Due to the divalent binding nature of the receptor, the FcRn-immobilized assay format is prone to avidity effects that may result in an heterogeneous binding response.[39] However, the FcRn immobilized assay format can also be optimized to minimize the avidity effects and produce a more homogenous binding response that can be fitted to a 1:1 binding model. Several preliminary FcRn binding experiments varying the FcRn loading levels were carried out to find an optimum level. It was observed that having low loading levels of receptor (less than 2.5 nm) produced low analyte signal (less than 0.1 nm). A loading level of 5-6 nm resulted in a reasonable analyte signal with a relatively more homogenous binding response. These binding curves fitted better to a 1:1 binding model and the kinetic parameters of binding were determined (Fig. 4.10, Table 4.2). IgG3 Fc binding to FcRn exhibited fast association and dissociation kinetics, which has been previously reported for IgG1-FcRn interaction.[33, 39] The tetraglycosylated and diglycosylated IgG3 Fc showed similar affinity (K_D~2.5 μM) for the receptor suggesting that the additional presence of N392 glycosylation does not affect IgG3 Fc binding to FcRn. A relatively weaker affinity (K_D ~3 μM) for diglycosylated IgG1 Fc was observed.

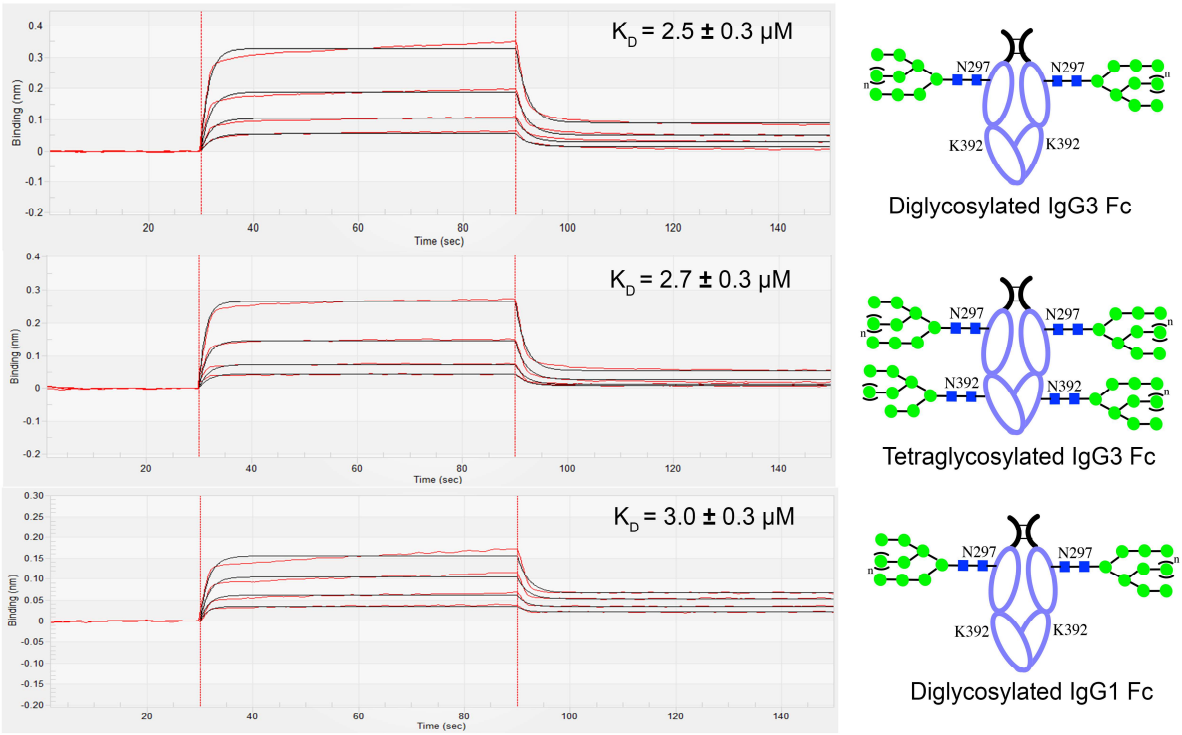

Figure 4.10: Representative BioLayer Interferometry (BLI) binding curves for the interaction of FcRn with the IgG3 Fc glycovariants. Experimental and fitted data are shown in red and black respectively.

Table 4.2: Kinetic parameters obtained for binding of FcRn with IgG3 Fc glycovariants. Values are reported as average and standard deviation of triplicate measurements.

Fc Variant	**Average k_{on}*10^5 (1/M.sec)**	**Average k_{off} (1/sec)**	**Average K_D (µM)**
Diglycosylated IgG3 Fc-N392K	1.5 ± 0.1	0.36 ± 0.03	2.5 ± 0.3
Tetraglycosylated IgG3 Fc	1.4 ± 0.5	0.38 ± 0.05	2.7 ± 0.3
Diglycosylated IgG1Fc	0.96 ± 0.03	0.29 ± 0.02	3.0 ± 0.3

4.3.6 Effect of N392 glycosylation on physical stability of IgG3 Fc

IgG3 Fc glycovariants were analyzed for their biophysical properties and physical stability of IgG3 Fc was assessed as a function of temperature stress. Differences in the stability profile of tetra- and the di-glycosylated IgG3 Fc can be attributed to the presence of N392 glycans. Multiple protein biophysical analysis techniques were employed to probe the physical stability of IgG3 Fc. The parameters obtained from these techniques are listed in Table 4.3. The

overall secondary structure at 10°C was probed by far-UV CD spectroscopy from 260 nm to 200 nm. The CD spectra for all variants showed a clear minimum at 217 nm, consistent with the β-sheet rich structure found in immunoglobulin domains (Fig. 4.11A). The effect of temperature on the secondary structure was probed by CD thermal melting curves. The tetraglycosylated variant showed a lower thermal transition temperature (~60°C) than the diglycosylated variant (~67°C) (Fig. 4.11B).

The overall tertiary structure of the IgG3 Fc glycovariants was evaluated by measuring intrinsic Trp fluorescence at 10°C. The wavelength of maximum intensity (λ_{max}) for all the glycovariants was found to be in the range of 329-334 nm, indicating an overall similarity between them with minor differences (Fig. 4.11C). Structural integrity of the tertiary structure was measured as a function of temperature by monitoring peak intensity changes. A comparable thermal transition temperature (T_m) value for all the IgG3 Fc glycovariants was observed ranging from 54-58°C (Fig. 4.11D), indicating that the presence of N392 glycans do not affect the tertiary structure stability to a notable extent. Static light scattering was measured concomitantly with fluorescence to characterize temperature-induced aggregation. The tetra- and tri-glycovariants showed no detectable change in the intensity of scattered light; however, both the diglycosylated variants showed an increase in intensity of scattered light with T_{onset} of ~66°C and ~64°C for the N392K and N392Q forms respectively (Fig. 4.12B). These results suggest that the presence of the N392 glycans protects IgG3 Fc from temperature-induced aggregation. Extrinsic fluorescence spectroscopy was used to measure conformational stability by monitoring emission from SYPRO^{TM} orange dye. The dye's fluorescence is generally quenched in a protein solution but is increased as more apolar regions are exposed upon protein unfolding. The IgG3 Fc glycovariants did not show any major difference in thermal transition values (58-60°C) (Fig.

4.11E), suggesting no large changes in the tertiary structure stability. Low intensity for the N392Q form was probably due to a bad run or low sample concentration.

The overall conformational stability was evaluated by differential scanning calorimetry (DSC). Typically, DSC thermograms of IgG1 Fc show two major endothermic peaks, corresponding to sequential melting of the C_H2 and C_H3 domains.[24] The diglycosylated variants from IgG3Fc-N392K/Q showed two major endothermic peaks, which could be fitted to two T_m values, T_m1~ 59°C and T_m2~70°C, corresponding to unfolding of the C_H2 and C_H3 domains respectively. Interestingly, the tetraglycosylated variant showed only one major endothermic peak, which could be fitted to T_m1~59°C and T_m2~ 62°C (Fig. 4.13, Table 4.3). The triglycosylated variant also showed one endothermic peak, which was fitted to a single T_m~62°C. An equivalent T_m1 and a reduced T_m2 in the tetraglycosylated IgG3 Fc indicate that the C_H3 domain residing N392 glycans potentially affects the conformational stability of the C_H3 domain. Aggregation propensity was also measured by monitoring OD_{350} as a function of temperature. The IgG3 Fc glycovariants showed a similar trend as seen in the light scattering measurements, where the tetra- and tri- glycosylated variants did not show any detectable change in OD_{350} values and both the di-glycosylated variants (N392K/Q) showed a transition around 83-85°C (Fig. 4.12A).

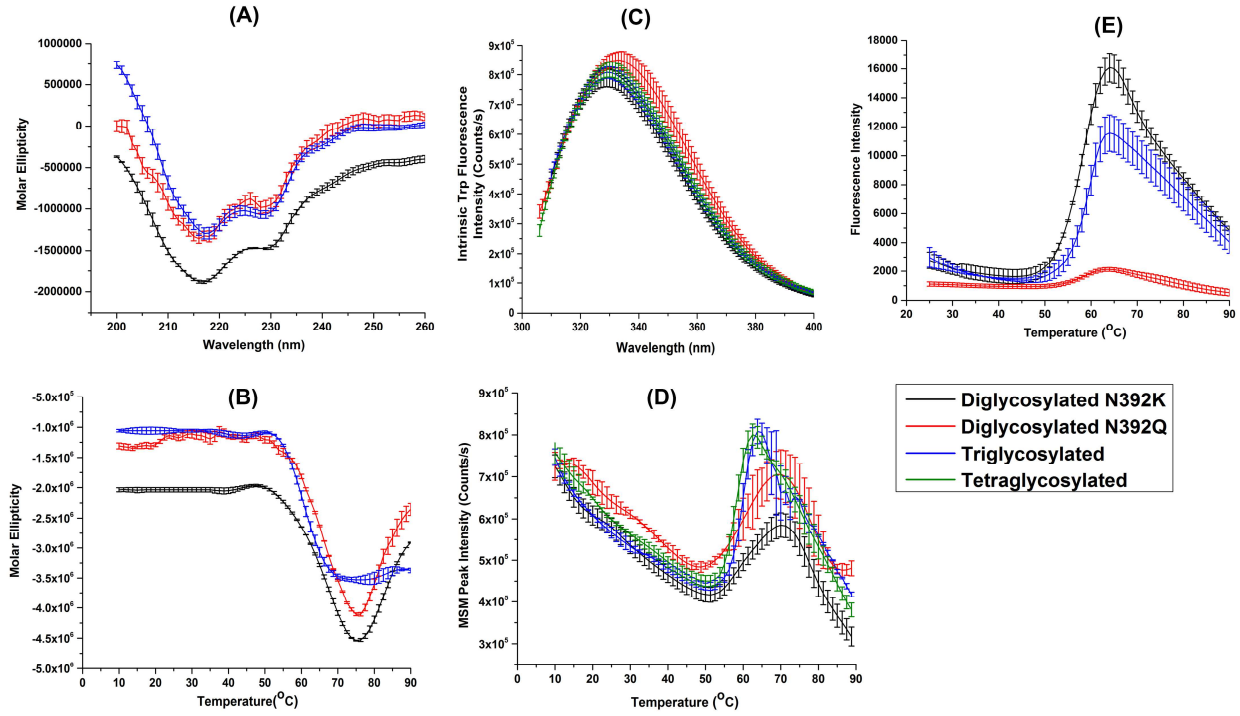

Figure 4.11: Biophysical characterization of IgG3 Fc glycovariants: tetraglycosylated, triglycosylated, diglycosylated (N392K) and diglycosylated (N392Q). Biophysical measurements include (A,B) CD spectroscopy (C,D) Intrinsic Trp fluorescence (E) SYPRO™ extrinsic fluorescence. (A) and (C) are CD and fluorescence spectra measured at 10°C. (B,D,E) show changes in the spectra as a function of temperature.

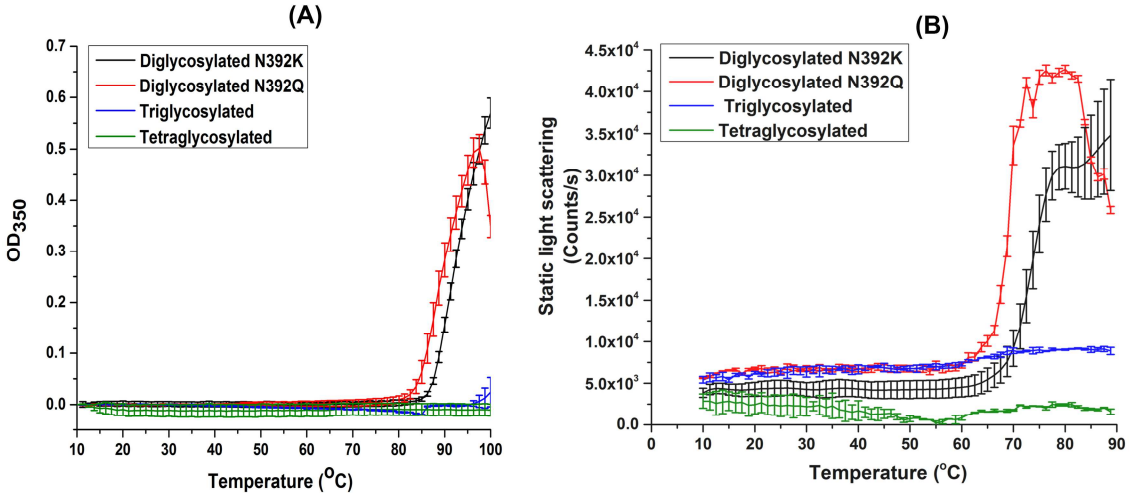

Figure 4.12: Biophysical characterization of IgG3 Fc glycovariants: tetraglycosylated, triglycosylated, diglycosylated-N392K and diglycosylated-N392Q. Biophysical measurements include (A) optical density (OD_{350}) (B) static light scattering as a function of temperature.

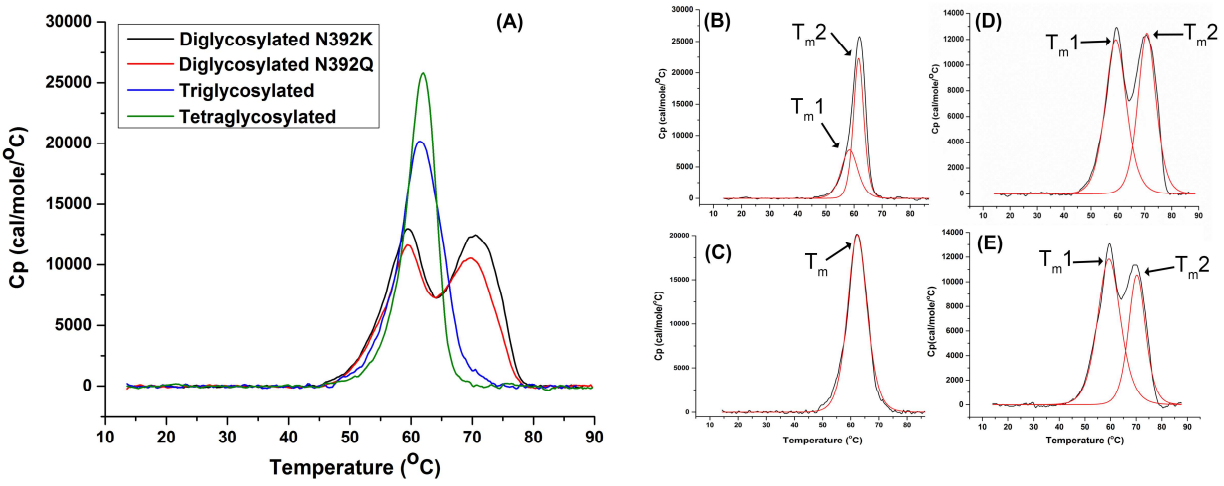

Figure 4.13: Comparison of representative DSC thermograms of IgG3 Fc glycovariants: tetraglycosylated, triglycosylated, diglycosylated (N392K) and diglycosylated (N392Q). Overlay of all DSC curves is shown in (A) and curve fitted thermograms are shown for (B) tetraglycosylated (C) triglycosylated (D) diglycosylated-N392K (E) diglycosylated-N392Q.

Table 4.3: Summary of physical stability parameters obtained by biophysical techniques for characterizing the physical stability of IgG3 Fc glycovariants. Values are reported as average and standard deviation of triplicate measurements

Technique	Parameter	Tetra-	Tri-	Di- (N392K)	Di- (N392Q)
SYPRO orange fluorescence	T_m (°C)	59.8 ± 0.1	*	58.2 ± 0.1	58.5 ± 0.2
	T_{onset} (°C)	49.0 ± 0.2	*	48.9 ± 0.2	49.1 ± 0.2
Intrinsic Fl. melt (peak intensity)	T_m (°C)	56.4 ± 0.1	57.7 ± 0.3	56.4 ± 0.2	54.5 ± 0.6
	T_{onset} (°C)	47.5 ± 0.2	47.3 ± 0.1	47.2 ± 0.1	45.4 ± 0.2
Static light scattering	T_{onset} (°C)	n.d.	n.d.	66.1 ± 0.2	63.5 ± 0.4
CD melt	T_m (°C)	60.5 ± 0.4	*	67.3 ± 0.3	67.3 ± 0.2
OD_{350}	T_{onset} (°C)	n.d.	n.d.	85.0 ± 0.2	83.0 ± 0.4
DSC	T_m1 (°C)	58.6 ± 0.4	62.3 ± 0.2	59.3 ± 0.1	59.4 ± 0.1
	T_m2 (°C)	62.1 ± 0.1		70.6 ± 0.3	70.3 ± 0.1
	T_{onset} (°C)	49.0 ± 0.2	47.8 ± 0.1	47.3 ± 0.1	47.4 ± 0.2
Intrinsic Fl. scan	λ_{max} (nm)	330.0 ± 0.6	329.0 ± 0.0	329.3 ± 0.6	333.5 ± 0.5
CD scan	λ_{max} (nm)	217	*	217	217

n.d. not detected, *expt. not done

4.4 Discussion

4.4.1 Binding interactions of IgG3 Fc glycovariants with Fc receptors

FcγRIIIA is an activating Fcγ receptor that mediates ADCC by binding to the Fc region of IgG in an immune complex. Not only is the presence of N297 glycosylation on the Fc important for binding to FcγRIIIA, but the nature of glycans also influences the strength of the interaction.[40] For example, IgG1 with afucosylated glycoforms at N297 show a higher affinity to FcγRIIIA, whereas truncated glycoforms show lower affinity.[8, 41] IgG3 shows similar affinity and selectivity as IgG1 towards different Fcγ receptors and thus is an attractive IgG subclass to investigate glycosylation-dependent FcγRIIIA binding.[42] There is an emerging interest in correlating Fc effector functions with specific IgG Fc glycoforms since most studies in the past have used IgG Fc with heterogeneous mixture of glycoforms, which is naturally present based on the choice of the expression host. Currently, there are limited reports in the literature characterizing IgG3-FcγRIIIA interactions and none of them mention the N392 glycosylation site.[11-13] IgG3 Fc glycovariants (Chapter 3) are ideally suited for studying the effect of the N392 site glycosylation on Fc receptor binding.

IgG3 Fc with only the N297 site glycosylated exhibited high affinity binding to FcγRIIIA in a low nanomolar range similar to IgG1 Fc since both the Fcs bear high mannose glycoforms (which are devoid of fucose). Removal of fucose from complex glycans at the N297 site has been shown to increase FcγRIIIA binding irrespective of the IgG subclass.[43] Prior studies have reported similar differences in K_D values (less than two fold difference) for IgG1 and IgG3[12-13] with an exception of one study where IgG3 was found to bind with a 5-fold higher affinity than IgG1.[11] The K_D values reported in these studies were in the high nanomolar range since the Fc glycans were mostly fucosylated. IgG1 and IgG3 are generally accepted to have similar

affinities for FcγRIIIA since the contact residues identified on IgG1 for FcγRIIIA binding (based on the IgG1 Fc-FcγRIIIA complex crystal structure) are conserved in IgG3.[44-45] The presence of additional N392 glycans in IgG3 Fc doesn't seem to have a large influence on FcγRIIIA binding. Structurally, the N392 site is located away from the receptor-binding site, and it is possible that the N392 glycans do not induce any long-range conformational changes at the binding site. More details about FcγRIIIA binding site and location of N392 glycans are discussed in chapter 5, section 5.3.10, based on the crystal structure of tetraglycosylated IgG3 Fc.

The FcRn receptor plays a critical role in maintaining long circulating half-lives of IgGs by binding to IgGs at an acidic pH (pH 6.0) in the early endosomes and recycling them back to circulation by releasing IgGs at physiological pH. An increase in IgG binding to FcRn (only at acidic pH with no change at neutral pH) results in an extended half-life, and therefore the IgG-FcRn interaction has received significant attention for improving the pharmacokinetic properties of therapeutic antibodies.[46] Since FcRn binds to IgG in a 2:1 stoichiometry, the nature of the binding response produced from Surface Plasmon Resonance (SPR) or BioLayer Interferometry (BLI) techniques is sensitive to the assay format. Generally, immobilizing the receptor and having IgG in solution results in a more heterogeneous binding response, while the reverse format produces more a homogenous response.[39] However, exceptions to this generalization are also found in the literature.[33, 47] Biotinlylated FcRn was immobilized on streptavidin biosensor in our BLI studies since it is a more convenient assay format to test different IgG glycovariants without requiring biotinylation of each IgG3 Fc glycovariant. Protein G cannot be used to immobilize the Fc for FcRn assay (unlike the FcγRIIIA assay) because it binds to the same region on the Fc where also FcRn binds and thus prevents FcRn from binding. In our studies, site-specific biotinylation was carried out using sortase-mediated ligation to attach biotin to the

C-terminus of FcRn. Generally, the site-specific conjugation techniques are more favorable than random amine coupling for surface immobilization since they are likely to maintain the protein in a particular orientation across the surface and is not likely to impair its functionality.

The FcRn receptor binds to the outer face of the C_H2-C_H3 interface of the Fc, and its binding to the Fc is generally known not to be affected by the N297 site glycosylation due to its distal location. The N392 site in IgG3 is located at the edge of C_H3-C_H3 interface close to the inner face of C_H2-C_H3 interface, and the presence of glycans in this region can be predicted to potentially affect FcRn binding. However, there was no significant difference between IgG1 Fc, tetraglycosylated and diglycosylated IgG3 Fc for binding to FcRn receptor and the K_D value for all the variants ranged between 2-3 μM. A nominal 2-fold higher affinity for IgG1 (K_D~0.63 μM) relative to IgG3 (K_D~1.10 μM) was reported by Stapleton et al.[18] In the same study, it is suggested that IgG3 is cleared faster in serum due to inhibition of IgG3 recycling because of an intracellular competition between IgG1 and IgG3 during the recycling process. Interestingly, if IgG3 is present alone, it is able to recycle as efficiently as IgG1. Based on these findings, it can be hypothesized that IgG1 and IgG3 may have similar *in-vivo* FcRn affinity but due to some unknown process (such as a slightly weaker FcRn binding at acidic pH for IgG3 or increased binding for IgG3 at neutral pH), IgG3 recycling is inhibited in presence of IgG1. Other researchers have also reported similar fold differences between IgG1 and IgG3 for binding to FcRn.[16, 48] A model showing how IgG3 might have an increased binding to FcRn at neutral pH compared to IgG1 is proposed in chapter 5, section 5.3.8, based on the crystal structure of IgG3 Fc. A monovalent Fc-FcRn interaction is generally considered to be a weak affinity interaction with a K_D value between 1-2 μM.[39, 49] There is a large variability in reported K_D values in the literature ranging from 10 nM to 3 μM.[32-33, 39, 46, 50-52] This discrepancy is primarily because of

the assay format used (whether FcRn or IgG is immobilized), quality of the reagents used, analyte concentration and the curve-fitting model used. Based on the crystal structure of the tetra-glycosylated IgG3 Fc (chapter 5), the N392 glycans appear to point away from the site of FcRn binding and this may explain the observed similarities between tetra-and di-glycosylated IgG3 Fc for binding to the FcRn receptor. A more detailed explanation is presented in chapter 5, section 5.3.10.

4.4.2 Effect of N392 glycosylation on physical stability of IgG3 Fc

Antibodies are susceptible to physical degradation and instability issues like aggregation, precipitation, conformational changes and unfolding.[21] Antibody stability is critical from a therapeutic perspective since it can impair its biological activity. The N297 glycosylation is considered critical for the conformational stability and integrity of IgG.[53] Aglycosylated IgG1 Fc exhibits a lower conformational stability for the C_H2 domain and a higher aggregation propensity compared to its glycosylated form.[25-26] Given the high degree of similarity in the primary structure of IgG1 and IgG3, the N297 glycosylation can be assumed to be equally important to IgG3. The effect of N392 glycosylation on the physical stability of IgG3 Fc was studied by comparing the thermal stability of the tetraglycosylated variant with the diglycosylated variant from IgG3 Fc-N392K (only has N297 site glycosylated) to highlight the role of N392 glycosylation. Additionally, to confirm that the results from IgG3 Fc-N392K are due to a lack of glycosylation at position 392 and not due to the presence of Lys at 392, we used the diglycosylated variant from IgG3 Fc-N392Q, since Gln closely resembles Asn if Asn is not glycosylated. Out of the multiple biophysical analysis techniques used in this study, some showed no difference between tetra- and di-glycosylated forms, while other techniques were able to detect significant differences between them. These results affirm the general consensus in the

protein stability community about the value of using multiple biophysical techniques (preferably orthogonal) to probe stability profile of therapeutic protein drugs.

No striking difference in the secondary and tertiary structure among all glycovariants was observed based on CD and fluorescence measurements. There is a possibility of some local conformation change due to the presence of N392 glycosylation that is not detected by the techniques used in this study. The thermal unfolding of IgG3 Fc glycovariants was probed by DSC. In most cases, DSC analysis of IgG Fc is quite useful since it is able to resolve thermal unfolding of the C_H2 and C_H3 domains. A higher T_m for the C_H3 domain relative to the C_H2 domain is attributed to the strong non-covalent interactions between the C_H3-C_H3 domains.[24] Removal of N297 glycans in IgG1 Fc has been shown to reduce thermal stability of the C_H2 domain.[24] In the tetraglycosylated IgG3 Fc, the presence of additional N392 glycans in the C_H3 domain seems to lower the conformational stability of the C_H3 domain. The residue at position 392 in tetraglycosylated IgG3 Fc (chapter 5) structure lies at the edge of C_H3-C_H3 interface and it may be speculated that glycosylation at this position disrupts the C_H3-C_H3 interface and in turn make C_H3 domain less thermally stable. More details about N392 glycans and C_H3-C_H3 interface are presented in chapter 5, section 5.3.10.

Both the techniques analyzing protein aggregation showed a higher aggregation propensity for the diglycosylated IgG3 Fc compared to the tetraglycosylated IgG3 Fc. Exposure of hydrophobic residues upon thermal unfolding is suggested to be one of the mechanisms for protein aggregation.[54] Glycosylation at the N297 site in IgG1 is suggested to shield the aggregation prone motifs in the C_H2 domain and thereby make it less aggregation prone compared to its aglycosylated counterpart.[28] Chennamsetty et al. identified the aggregation motifs in IgG subclasses, one of which is $P_{395}PML_{398}$ in the C_H3 domain.[29] The N392 site

immediately precedes this motif, and it is possible that the N392 glycans shield this motif and make it less aggregation prone (described in detail in chapter 5, section 5.3.10).

In summary, we have shown that the presence of N392 glycosylation on IgG3 does not adversely affect the binding of IgG3 Fc to FcγRIIIA and FcRn. Physical stability assessment of the N392 site glycosylation showed that the N392 glycans reduces the thermal stability of the IgG3 Fc but protects it from temperature-induced aggregation.

4.5 References:

1. Bournazos, S.; Ravetch, J. V., Fcγ receptor pathways during active and passive immunization. *Immunological reviews* **2015,** *268* (1), 88-103.

2. Nimmerjahn, F.; Ravetch, J. V., Fcγ receptors as regulators of immune responses. *Nature Reviews Immunology* **2008,** *8* (1), 34-47.

3. Bournazos, S.; Wang, T. T.; Ravetch, J. V., The Role and Function of Fcγ Receptors on Myeloid Cells. *Microbiology spectrum* **2016,** *4* (6).

4. Seidel, U. J.; Schlegel, P.; Lang, P., Natural killer cell mediated antibody-dependent cellular cytotoxicity in tumor immunotherapy with therapeutic antibodies. *How to improve immune reconstitution in allogeneic hematopoietic stem cell transplantation?* **2015**, 52.

5. Cooper, N.; Stasi, R.; Cunningham‐Rundles, S.; Cesarman, E.; McFarland, J. G.; Bussel, J. B., Platelet‐associated antibodies, cellular immunity and FCGR3a genotype influence the response to rituximab in immune thrombocytopenia. *British journal of haematology* **2012,** *158* (4), 539-547.

6. Arnold, J. N.; Wormald, M. R.; Sim, R. B.; Rudd, P. M.; Dwek, R. A., The impact of glycosylation on the biological function and structure of human immunoglobulins. *Annu. Rev. Immunol.* **2007,** *25*, 21-50.

7. Abès, R.; Teillaud, J. L., Impact of glycosylation on effector functions of therapeutic IgG. *Pharmaceuticals* **2010,** *3* (1), 146-157.

8. Okazaki, A.; Shoji-Hosaka, E.; Nakamura, K.; Wakitani, M.; Uchida, K.; Kakita, S.; Tsumoto, K.; Kumagai, I.; Shitara, K., Fucose depletion from human IgG1 oligosaccharide enhances binding enthalpy and association rate between IgG1 and FcγRIIIa. *Journal of molecular biology* **2004,** *336* (5), 1239-1249.

9. Beck, A.; Reichert, J. M. In *Marketing approval of mogamulizumab: a triumph for glyco-engineering*, MAbs, Taylor & Francis: 2012; pp 419-425.

10. Ratner, M., Genentech's glyco-engineered antibody to succeed Rituxan. Nature Research: 2014.

11. Bruhns, P.; Iannascoli, B.; England, P.; Mancardi, D. A.; Fernandez, N.; Jorieux, S.; Daëron, M., Specificity and affinity of human Fcγ receptors and their polymorphic variants for human IgG subclasses. *Blood* **2009,** *113* (16), 3716-3725.

12. Li, P.; Jiang, N.; Nagarajan, S.; Wohlhueter, R.; Selvaraj, P.; Zhu, C., Affinity and kinetic analysis of Fcγ receptor IIIa (CD16a) binding to IgG ligands. *Journal of Biological Chemistry* **2007,** *282* (9), 6210-6221.

13. Warncke, M.; Calzascia, T.; Coulot, M.; Balke, N.; Touil, R.; Kolbinger, F.; Heusser, C., Different adaptations of IgG effector function in human and nonhuman primates and implications for therapeutic antibody treatment. *The Journal of Immunology* **2012,** *188* (9), 4405-4411.

14. Ghetie, V.; Ward, E. S., Multiple roles for the major histocompatibility complex class I–related receptor FcRn. *Annual review of immunology* **2000,** *18* (1), 739-766.

15. Roopenian, D. C.; Akilesh, S., FcRn: the neonatal Fc receptor comes of age. *Nature Reviews Immunology* **2007,** *7* (9), 715-725.

16. West, A. P.; Bjorkman, P. J., Crystal structure and immunoglobulin G binding properties of the human major histocompatibility complex-related Fc receptor. *Biochemistry* **2000,** *39* (32), 9698-9708.

17. Morell, A.; Terry, W. D.; Waldmann, T. A., Metabolic properties of IgG subclasses in man. *Journal of Clinical Investigation* **1970,** *49* (4), 673.

18. Stapleton, N. M.; Andersen, J. T.; Stemerding, A. M.; Bjarnarson, S. P.; Verheul, R. C.; Gerritsen, J.; Zhao, Y.; Kleijer, M.; Sandlie, I.; de Haas, M., Competition for FcRn-mediated transport gives rise to short half-life of human IgG3 and offers therapeutic potential. *Nature Communications* **2011,** *2*, 599.

19. Kim, J.-K.; Firan, M.; Radu, C. G.; Kim, C.-H.; Ghetie, V.; Ward, E. S., Mapping the site on human IgG for binding of the MHC class I-related receptor, FcRn. *European journal of immunology* **1999,** *29* (9), 2819-2825.

20. Wang, W.; Singh, S.; Zeng, D. L.; King, K.; Nema, S., Antibody structure, instability, and formulation. *Journal of pharmaceutical sciences* **2007,** *96* (1), 1-26.

21. Solá, R. J.; Griebenow, K., Effects of glycosylation on the stability of protein pharmaceuticals. *Journal of pharmaceutical sciences* **2009,** *98* (4), 1223-1245.

22. Chaudhuri, R.; Cheng, Y.; Middaugh, C. R.; Volkin, D. B., High-throughput biophysical analysis of protein therapeutics to examine interrelationships between aggregate formation and conformational stability. *The AAPS journal* **2014,** *16* (1), 48-64.

23. Zheng, K.; Bantog, C.; Bayer, R. In *The impact of glycosylation on monoclonal antibody conformation and stability*, MAbs, Taylor & Francis: 2011; pp 568-576.

24. Ghirlando, R.; Lund, J.; Goodall, M.; Jefferis, R., Glycosylation of human IgG-Fc: influences on structure revealed by differential scanning micro-calorimetry. *Immunology letters* **1999,** *68* (1), 47-52.

25. Kayser, V.; Chennamsetty, N.; Voynov, V.; Forrer, K.; Helk, B.; Trout, B. L., Glycosylation influences on the aggregation propensity of therapeutic monoclonal antibodies. *Biotechnology Journal* **2011,** *6* (1), 38-44.

26. More, A. S.; Toprani, V. M.; Okbazghi, S. Z.; Kim, J. H.; Joshi, S. B.; Middaugh, C. R.; Tolbert, T. J.; Volkin, D. B., Correlating the impact of well-defined oligosaccharide structures on physical stability profiles of IgG1-Fc glycoforms. *Journal of pharmaceutical sciences* **2016,** *105* (2), 588-601.

27. Temel, D. B.; Landsman, P.; Brader, M. L., Chapter Fourteen-Orthogonal Methods for Characterizing the Unfolding of Therapeutic Monoclonal Antibodies: Differential Scanning Calorimetry, Isothermal Chemical Denaturation, and Intrinsic Fluorescence with Concomitant Static Light Scattering. *Methods in enzymology* **2016,** *567*, 359-389.

28. Voynov, V.; Chennamsetty, N.; Kayser, V.; Helk, B.; Forrer, K.; Zhang, H.; Fritsch, C.; Heine, H.; Trout, B. L., Dynamic fluctuations of protein-carbohydrate interactions promote protein aggregation. *PLoS One* **2009,** *4* (12), e8425.

29. Chennamsetty, N.; Helk, B.; Voynov, V.; Kayser, V.; Trout, B. L., Aggregation-prone motifs in human immunoglobulin G. *Journal of molecular biology* **2009,** *391* (2), 404-413.

30. Xiao, J.; Chen, R.; Pawlicki, M. A.; Tolbert, T. J., Targeting a homogeneously glycosylated antibody Fc to bind cancer cells using a synthetic receptor ligand. *Journal of the American Chemical Society* **2009,** *131* (38), 13616-13618.

31. Okbazghi, S. Z.; More, A. S.; White, D. R.; Duan, S.; Shah, I. S.; Joshi, S. B.; Middaugh, C. R.; Volkin, D. B.; Tolbert, T. J., Production, characterization, and biological evaluation of well-defined IgG1 Fc glycoforms as a model system for biosimilarity analysis. *Journal of pharmaceutical sciences* **2016,** *105* (2), 559-574.

32. Lee, C.-H.; Choi, D.-K.; Choi, H.-J.; Song, M.-Y.; Kim, Y.-S., Expression of soluble and functional human neonatal Fc receptor in Pichia pastoris. *Protein expression and purification* **2010,** *71* (1), 42-48.

33. Feng, Y.; Gong, R.; Dimitrov, D. S., Design, expression and characterization of a soluble single-chain functional human neonatal Fc receptor. *Protein expression and purification* **2011,** *79* (1), 66-71.

34. Ferrara, C.; Stuart, F.; Sondermann, P.; Brünker, P.; Umaña, P., The Carbohydrate at FcγRIIIa Asn-162 an element required for high affinity binding to non-fucosylated IgG glycoforms. *Journal of Biological Chemistry* **2006,** *281* (8), 5032-5036.

35. Noubhani, A.; Bégu, D.; Chaignepain, S.; ou Maati, H. M.; Borsotto, M.; Dupuy, J.; d'Estaintot, B. L.; Santarelli, X.; Heurteaux, C.; Gallois, B., Production, in Pichia pastoris, of a recombinant monomeric mapacalcine, a protein with anti-ischemic properties. *Biochemistry and Biophysics Reports* **2015,** *4*, 299-305.

36. Ng, W. K.; Lim, T. S.; Lai, N. S., Expression of soluble human Neonatal Fc-receptor (FcRn) in Escherichia coli through modification of growth environment. *Protein Expression and Purification* **2016,** *127*, 73-80.

37. Mao, H.; Hart, S. A.; Schink, A.; Pollok, B. A., Sortase-mediated protein ligation: a new method for protein engineering. *Journal of the American Chemical Society* **2004,** *126* (9), 2670-2671.

38. Sondermann, P.; Huber, R.; Oosthuizen, V.; Jacob, U., The 3.2-Å crystal structure of the human IgG1 Fc fragment–FcγRIII complex. *Nature* **2000,** *406* (6793), 267-273.

39. Wang, X.; McKay, P.; Yee, L.; Dutina, G.; Hass, P. E.; Nijem, I.; Allison, D.; Cowan, K. J.; Lin, K.; Quarmby, V. In *Impact of SPR biosensor assay configuration on antibody: Neonatal Fc receptor binding data*, mAbs, Taylor & Francis: 2016; pp 00-00.

40. Lux, A.; Nimmerjahn, F., Impact of differential glycosylation on IgG activity. *Crossroads between Innate and Adaptive Immunity III* **2011**, 113-124.

41. Mimura, Y.; Church, S.; Ghirlando, R.; Ashton, P.; Dong, S.; Goodall, M.; Lund, J.; Jefferis, R., The influence of glycosylation on the thermal stability and effector function expression of human IgG1-Fc: properties of a series of truncated glycoforms. *Molecular immunology* **2000,** *37* (12), 697-706.

42. Jefferis, R., Isotype and glycoform selection for antibody therapeutics. *Archives of Biochemistry and Biophysics* **2012**.

43. Niwa, R.; Natsume, A.; Uehara, A.; Wakitani, M.; Iida, S.; Uchida, K.; Satoh, M.; Shitara, K., IgG subclass-independent improvement of antibody-dependent cellular cytotoxicity by fucose removal from Asn< sup> 297</sup>-linked oligosaccharides. *Journal of immunological methods* **2005,** *306* (1), 151-160.

44. Vidarsson, G.; Dekkers, G.; Rispens, T., IgG subclasses and allotypes: from structure to effector functions. *Frontiers in immunology* **2014,** *5*, 520.

45. Sondermann, P.; Huber, R.; Oosthuizen, V.; Jacob, U., The 3.2-Å crystal structure of the human IgG1 Fc fragment–FcγRIII complex. *Nature* **2000,** *406* (6793), 267-273.

46. Dall'Acqua, W. F.; Woods, R. M.; Ward, E. S.; Palaszynski, S. R.; Patel, N. K.; Brewah, Y. A.; Wu, H.; Kiener, P. A.; Langermann, S., Increasing the affinity of a human IgG1 for the neonatal Fc receptor: biological consequences. *The Journal of Immunology* **2002,** *169* (9), 5171-5180.

47. Datta-Mannan, A.; Chow, C.-K.; Dickinson, C.; Driver, D.; Lu, J.; Witcher, D. R.; Wroblewski, V. J., FcRn affinity-pharmacokinetic relationship of five human IgG4 antibodies engineered for improved in vitro FcRn binding properties in cynomolgus monkeys. *Drug Metabolism and Disposition* **2012,** *40* (8), 1545-1555.

48. Firan, M.; Bawdon, R.; Radu, C.; Ober, R. J.; Eaken, D.; Antohe, F.; Ghetie, V.; Ward, E. S., The MHC class I-related receptor, FcRn, plays an essential role in the maternofetal transfer of γ-globulin in humans. *International immunology* **2001,** *13* (8), 993-1002.

49. Yeung, Y. A.; Leabman, M. K.; Marvin, J. S.; Qiu, J.; Adams, C. W.; Lien, S.; Starovasnik, M. A.; Lowman, H. B., Engineering human IgG1 affinity to human neonatal Fc receptor: impact of affinity improvement on pharmacokinetics in primates. *The Journal of Immunology* **2009,** *182* (12), 7663-7671.

50. Neuber, T.; Frese, K.; Jaehrling, J.; Jäger, S.; Daubert, D.; Felderer, K.; Linnemann, M.; Höhne, A.; Kaden, S.; Kölln, J. In *Characterization and screening of IgG binding to the neonatal Fc receptor*, MAbs, Taylor & Francis: 2014; pp 928-942.

51. Magistrelli, G.; Malinge, P.; Anceriz, N.; Desmurs, M.; Venet, S.; Calloud, S.; Daubeuf, B.; Kosco-Vilbois, M.; Fischer, N., Robust recombinant FcRn production in mammalian cells enabling oriented immobilization for IgG binding studies. *Journal of immunological methods* **2012,** *375* (1), 20-29.

52. Abdiche, Y. N.; Yeung, Y. A.; Chaparro-Riggers, J.; Barman, I.; Strop, P.; Chin, S. M.; Pham, A.; Bolton, G.; McDonough, D.; Lindquist, K. In *The neonatal Fc receptor (FcRn) binds independently to both sites of the IgG homodimer with identical affinity*, MAbs, Taylor & Francis: 2015; pp 331-343.

53. Krapp, S.; Mimura, Y.; Jefferis, R.; Huber, R.; Sondermann, P., Structural analysis of human IgG-Fc glycoforms reveals a correlation between glycosylation and structural integrity. *Journal of molecular biology* **2003,** *325* (5), 979-989.

54. Wu, H.; Kroe-Barrett, R.; Singh, S.; Robinson, A. S.; Roberts, C. J., Competing aggregation pathways for monoclonal antibodies. *FEBS letters* **2014,** *588* (6), 936-941.

Chapter 5 Structural characterization of human IgG3 Fc

5.1 Introduction

The Fc region of IgG is generally known to readily crystallize under various conditions and hence is named as fragment crystallizable (Fc). The IgG Fc structures deposited in the protein databank predominantly belong to IgG1 subclass, either present as free Fc or in complex with Fc receptors and other Fc-binding proteins. A list of available IgG1 Fc structure can be found elsewhere.[1] The first human IgG1 Fc structure was solved by Deisenhofer in 1981[2] and since then multiple IgG1 Fc structures have been published, which either differ in the type of glycosylation present or the mutations made to the WT sequence. In recent years, the structures of IgG2 Fc[3] and IgG4 Fc[4] have been reported and were found to be highly similar to the IgG1 Fc structure, owing to 95% sequence homology in the Fc region of the IgG subclasses (Fig. 5.3). The IgG2 Fc and IgG4 Fc structures provides a structural basis for understanding IgG subclass-specific properties, such as Fab arm exchange in IgG4.[4]

The structure of IgG Fc resembles a horse-shoe shape dimer comprising of C_H2 and C_H3 domains. The C_H3 domains in the dimer maintain extensive protein-protein contacts to keep the IgG structure together in conjunction with the hinge disulfide bonds. Generally, no interpretable electron density for the hinge region is observed in the Fc structures due to its flexible and mobile nature. The C_H2 and C_H3 domains display an immunoglobulin (Ig) fold that is stabilized by a conserved disulfide bond. In all the IgG Fc structures, the C_H2 domains do not make any direct contact with each other and the N297 glycans occupy the space between the two C_H2 domains. Interpretable electron density for oligosaccharides is generally observed in Fc structures, which enables determination of the glycan conformation. The N297 glycans lie in close apposition to the inner face of the C_H2 domain and make extensive non-covalent interactions with the protein.[1] The glycans on protein are generally known to be very mobile, and

therefore considered as a hindrance to glycoprotein crystallization. However, in case of IgG Fc, the N297-glycan structure can be reasonably defined primarily due to its unique orientation within the Fc structure that allows multiple points of contact with the protein. The N297 site glycans in IgG Fc are considered important in maintaining the optimal 'open' conformation of the C_H2 domains[5] and removal of glycans has been shown to result in a 'closed' conformation due to mutual collapse of the C_H2 domains.[6] The 'open' conformation of the C_H2 domains is believed to be critical for recognition by Fcγ receptors and C1q complement protein, since the aglycosylated IgG Fc loses its ability to bind with these ligands.[7-8]

In this chapter, we report high-resolution x-ray crystal structures of two variants of human IgG3 Fc fragment. The first variant is IgG3 Fc-N392K that is homogeneously glycosylated with high mannose, $GlcNAc_2Man_5$ (Man5) glycoform at the N297 glycosylation site. The second variant is IgG3 Fc that is glycosylated with high mannose glycoforms, $GlcNAc_2Man_{8-12}$ (Man8-Man12) at the N297 and N392 glycosylation sites (referred as tetraglycosylated IgG3 Fc). To our knowledge, this is the first human IgG3 Fc structure reported and also the first Fc structure from any IgG subclass containing the Man5 glycoform. The analysis of the Man5-IgG3 Fc structure provides insight into structural basis for some of the unusual properties of IgG3 subclass, especially related to binding to protein A, protein G and the neonatal Fc receptor (FcRn). Analysis of the tetraglycosylated IgG3 Fc structure provides information about the location and orientation of the lesser known N392 site glycans and its influence on the IgG3 Fc structure and function.

5.2 Methods

5.2.1 Production and characterization of Man5-IgG3 Fc and tetraglycosylated IgG3 Fc

WT IgG3 Fc and IgG3 Fc-N392K were expressed in the quadruple KO strain of the yeast *P. pastoris* as described in chapter 3, sections 3.2.1-3.2.2. The tetraglycosylated IgG3 Fc and diglycosylated IgG3 Fc-N392K were purified from the protein G-purified WT IgG3 Fc and IgG3 Fc-N392K, respectively by phenyl sepharose chromatography (chapter 3, section 3.2.5). The high mannose (HM) glycoforms on IgG3 Fc-N392K were converted to the Man5 glycoform by digestion with α-1,2 mannosidase and endomannosidase enzymes (chapter 3, section 3.2.6). The prepared Man5-IgG3 Fc and tetraglycosylated IgG3 Fc proteins were characterized by intact protein mass spectrometry and SDS-PAGE.

5.2.2 Crystallization and Data Collection

Man5-IgG3 Fc was concentrated to 10.8 mg/mL in 150 mM NaCl, 10 mM MES, pH 6.6 for crystallization screening. All crystallization experiments were conducted Compact Jr. (Rigaku Reagents) sitting drop vapor diffusion plates at 20 ºC using equal volumes of protein and crystallization solution (0.7 uL) equilibrated against 75 uL of the latter. Crystals that displayed a prismatic morphology were obtained approximately 1 week from the Wizard 3-4 screen (Rigaku Reagents) condition B5 (20% (w/v) PEG 4000, 100 mM sodium citrate/citric acid pH 5.5, 10% (v/v) 2-propanol). The crystals tended to form contact twins but could be readily separated to obtain single crystals for data collection. Samples were transferred to a fresh drop composed of 80% crystallization solution and 20% ethylene glycol and stored in liquid nitrogen.

Tetraglycosylated IgG3 Fc was concentrated to 9.0 mg/mL in 150 mM NaCl, 10 mM MES, pH 6.6 for crystallization screening. All crystallization experiments were conducted Compact Jr. (Rigaku Reagents) sitting drop vapor diffusion plates at 20 ºC using equal volumes (0.7 μL) of protein and crystallization solution equilibrated against 75 μL of the latter. Crystals

that displayed a prismatic morphology were obtained approximately 1 week from the JCSG+ screen (Molecular Dimensions) condition A8 (20% (w/v) PEG 3350, 200 mM ammonium formate). Cryoprotection was carried out by adding 1μL of a 7 M sodium formate solution was added directly to the drop of the initial crystallization screen and samples were then harvested and transferred to a vial containing liquid nitrogen. For both IgG3 Fc crystals, X-ray diffraction data was collected at the Advanced Photon Source IMCA-CAT beamline 17-ID using a Dectris Pilatus 6M pixel array detector.

5.2.3 Structure Solution and Refinement

For **Man5-IgG3 Fc**, intensities were integrated using XDS[9-10] via Autoproc[11] and the Laue class analysis and data scaling were performed with Aimless[12] which indicated that the highest probability was 2/*m* (*P*2 or *P*2$_1$). Structure solution was conducted by molecular replacement with Phaser[13] using a single subunit form previously determined structure of IgG1 Fc (PDB: 4DZ8)[14] as the search model.[15] The top solution was obtained in the space group *P*2$_1$ that contained two molecules in the asymmetric unit. Coordinate and structure factors were deposited to the Wordwide Protein Databank with the accession code 5W38.

For **Tetraglycosylated IgG3 Fc**, intensities were integrated using XDS[9-10] via Autoproc[11] and the Laue class analysis and data scaling were performed with Aimless[12] which indicated that the highest probability was 6/*m*. Structure solution was conducted by molecular replacement with Phaser[13] using a single subunit form previously determined structure of IgG3-N392K as the search model. The top solution was obtained in the space group *P*6$_1$ that contained two molecules in the asymmetric unit. For both the solutions, the model was further improved by automated model building with ARP/wARP.[16] Structure refinement and manual model building were conducted with Phenix[17] and Coot[18] respectively. Disordered side chains were truncated to

the point for which electron density could be observed. Structure validation was conducted with Molprobity[17] and figures were prepared using the CCP4MG package[19] and PyMOL. Full data processing and refinement statistics are provided in Table 5.1. Man8 glycoform was in-silico modeled at the N392 site using GlyProt program.[20] Torsional angles between Asn392-GlcNAc1 as observed in the determined structure were used in the program to model the complete Man8 structure.

Table 5.1: Crystallographic data and refinement statistics for Man5-IgG3 Fc and Tetraglycosylated IgG3 Fc.

Data Collection	Man5-IgG3 Fc	Tetraglycosylated IgG3 Fc
Unit-cell parameters (Å,°)	*a*=64.43, *b*=60.44, *c*=71.40, *β*=109.2	*a*=*b*=97.38, *c*=96.85
Space group	$P2_1$	$P6_1$
Resolution (Å)[1]	45.00-1.80(1.84-1.80)	48.69-2.00(2.05-2.00)
Wavelength (Å)	1.0000	1.0000
Temperature (K)	100	100
Observed reflections	156,654	364,213
Unique reflections	47,374	35,292
$\langle I/\sigma(I)\rangle$[1]	12.7 (2.1)	13.4 (1.7)
Completeness (%)[1]	98.4 (97.7)	100 (100)
Multiplicity[1]	3.3 (3.2)	10.3 (10.6)
R_{merge} (%)[1, 2]	5.5 (57.5)	9.8 (132.1)
R_{meas} (%)[1, 4]	6.6 (69.0)	10.4 (138.7)
R_{pim} (%)[1, 4]	3.6 (37.8)	3.2 (42.1)
$CC_{1/2}$ [1, 5]	0.998 (0.734)	0.998 (0.754)
Refinement		
Resolution (Å) [1]	34.73-1.80	34.33-2.00
Reflections (working/test)[1]	44,926/2,427	33,477/1,764
R_{factor} / R_{free} (%)[1,3]	18.4/22.3	20.5/25.3
No. of atoms (Protein/Water)	3,378/351	3,277/177
Model Quality		
R.m.s deviations		
Bond lengths (Å)	0.009	0.007
Bond angles (°)	1.020	0.906
Average *B*-factor (Å^2)		
All Atoms	28.1	47.6
Protein	27.6	47.9

Water	33.4	42.5
Coordinate error (maximum likelihood) (Å)	0.23	0.27
Ramachandran Plot		
Most favored (%)	98.6	96.7
Additionally allowed (%)	1.4	3.0

1) Values in parenthesis are for the highest resolution shell.
2) $R_{merge} = \Sigma_{hkl}\Sigma_i |I_i(hkl) - \langle I(hkl)\rangle| / \Sigma_{hkl}\Sigma_i I_i(hkl)$, where $I_i(hkl)$ is the intensity measured for the ith reflection and $\langle I(hkl)\rangle$ is the average intensity of all reflections with indices hkl.
3) $R_{factor} = \Sigma_{hkl} ||F_{obs}(hkl)| - |F_{calc}(hkl)|| / \Sigma_{hkl} |F_{obs}(hkl)|$; Rfree is calculated in an identical manner using 5% of randomly selected reflections that were not included in the refinement.
4) R_{meas} = redundancy-independent (multiplicity-weighted) R_{merge}[12, 21]. R_{pim} = precision-indicating (multiplicity-weighted) R_{merge}[22-23].
5) $CC_{1/2}$ is the correlation coefficient of the mean intensities between two random half-sets of data [24-25].

5.2.4 Binding analysis of IgG3 Fc glycoforms with FcγRIIIA

Four different glycoforms at the N297 site of IgG3 Fc were used to evaluate the effect of truncation of high mannose glycoforms on binding to FcγRIIIA receptor. These glycoforms were (i) high mannose (HM) glycoforms (Man8-Man12), obtained directly out of yeast expression, (ii) Man5 glycoform, prepared by digestion of HM glycoforms with α-1,2 mannosidase and endomannosidase enzymes (iii) Fc-GlcNAc, prepared by digestion of HM glycoforms with EndoH enzyme (iv) Deglycosylated Fc, prepared by digestion of HM glycoforms with PNGase F. A BioLayer Interferometry (BLI) based binding assay was used to determine binding affinity, as previously described in chapter 4, section 4.1.4.

5.3 Results and Discussion

5.3.1 Characterization of Man5-IgG3 Fc and tetraglycosylated IgG3 Fc

Both the proteins were characterized by intact protein mass spectrometry and SDS-PAGE. A gel-shift for Man5-IgG3 Fc was observed relative to HM-IgG3 Fc due to removal of mannose residues (Fig. 5.1A). Intact protein MS for Man5-IgG3 Fc showed a peak corresponding to the Man5 glycoform on IgG3 Fc (Fig. 5.1B). The abundance of Man5 glycoform was estimated to be 96% based on MS peak heights. The tetraglycosylated IgG3 Fc showed presence of high mannose glycoforms at the N297 and N392 sites in IgG3 Fc (Fig.

5.1C). SDS-PAGE for the tetraglycosylated IgG3 Fc is shown in chapter 3, Fig. 3.7. The produced proteins were sufficiently pure and homogenously glycosylated, and hence suitable for crystallization trials.

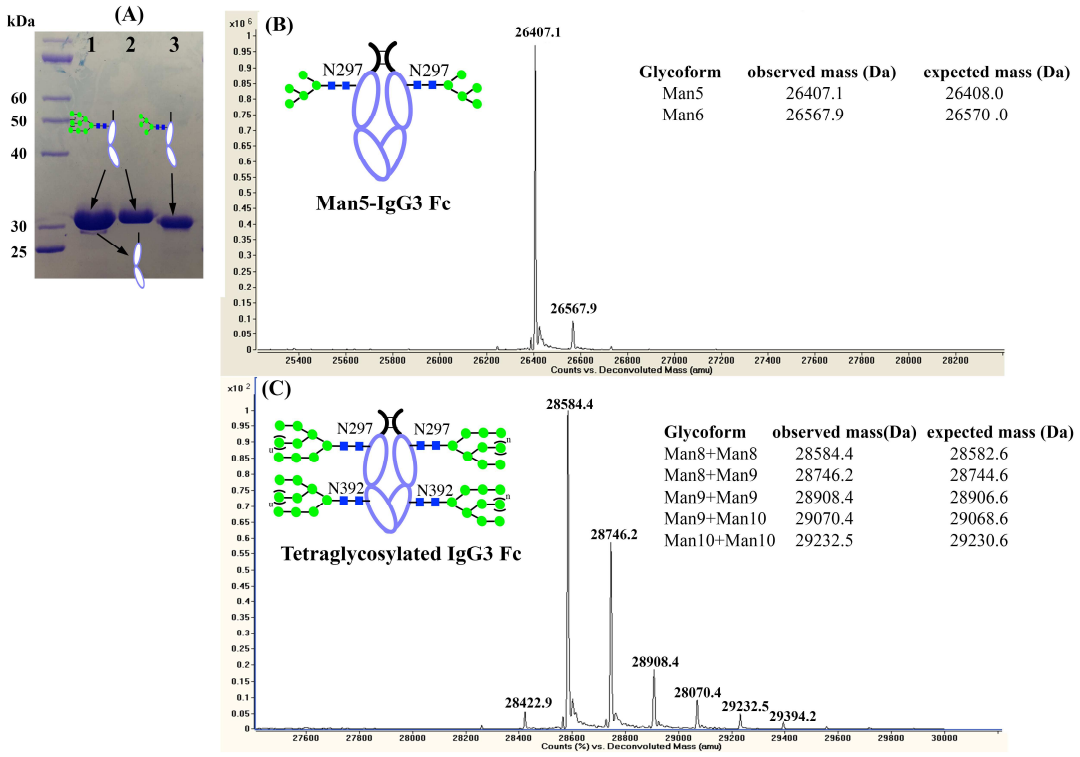

Figure 5.1: Characterization of Man5-IgG3 Fc and tetraglycosylated IgG3 Fc. (A) Coomassie stained SDS-PAGE of IgG3 Fc (N392K) under reducing conditions. Lane 1: protein G purified IgG3 Fc (N392K), lane 2: phenyl sepharose purified diglycosylated HM-IgG3 Fc (N392K), lane3: Man5-IgG3 Fc (N392K) (B) intact protein MS spectra of Man5-IgG3 Fc under reducing conditions (C) intact protein MS spectra of tetraglycosylated IgG3 Fc under reducing conditions. Observed and expected masses for the different high mannose glycoforms are shown in the spectra.

5.3.2 Structural analysis of the two IgG3 Fc variants

Sections 5.3.2 to 5.3.8 describes structural analysis of the Man5-IgG3 Fc variant. We have examined structural features of IgG3 Fc and compared it with other IgG subclasses. A comparison of key amino acid difference between IgG3 and the other subclasses provides an insight into some of the unusual properties of IgG3, especially those related to differential

binding to protein A and the FcRn receptor. The importance of glycosylation at N297 site for binding to FcγRIIIA is demonstrated from a structural perspective. Sections 5.3.9 and 5.3.10 describes structural analysis of the tetraglycosylated IgG3 Fc. Analysis of the location and orientation of the N392 site glycans in this structure helps to explain the results from the biochemical and biophysical studies described in the previous chapter.

5.3.3 Overall IgG3 Fc structure

IgG3 Fc crystallized in the space group $P2_1$, with one homodimer in the asymmetric unit. Ordered electron density was visible for residues L235-L443 and G237-P445 in chain A and B respectively. No interpretable electron density was observed for hinge disulfide bonds and for residues A231-L234 following the hinge. Both the C_H2 and C_H3 domains display an immunoglobulin fold, which is stabilized by intra-chain disulfide bonds (C261-C321 in the C_H2 and C367-C425 in the C_H3). The glycans occupy the space between the C_H2 domains, while extensive non-covalent contact exists between the two C_H3 domains (Fig. 5.2). There is a high degree of sequence homology (over 90%) in the Fc region of the IgG subclasses (Fig. 5.3). Most of the amino acid differences occur on the surface of the Fc, as illustrated for IgG1 and IgG3 (Figures 5.2). The following sections describe the influence of key amino acid differences and glycosylation on the structural features of IgG3 Fc as well as on some of the unusual properties of IgG3, especially its interaction with protein A, protein G and FcRn receptor.

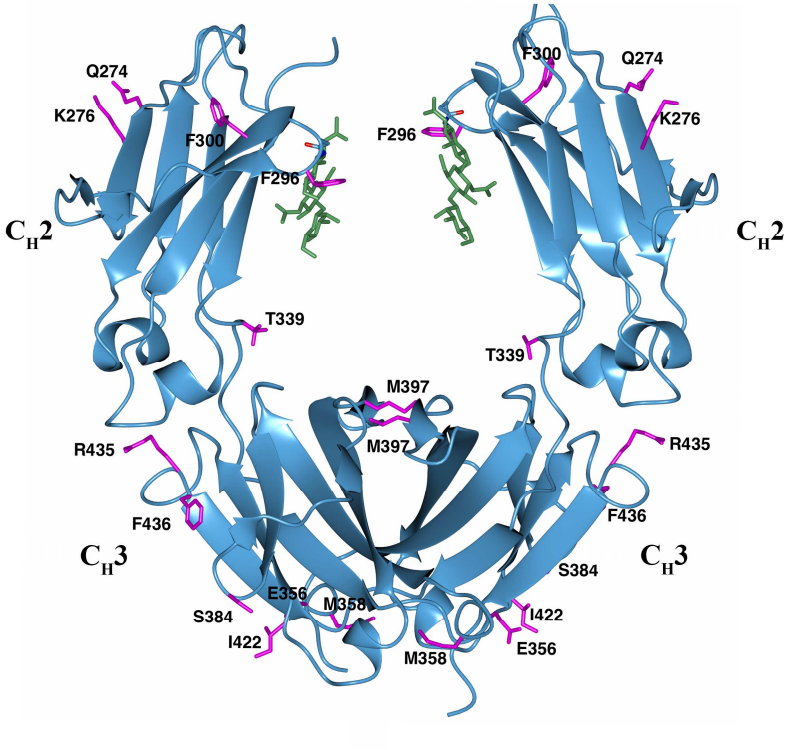

Figure 5.2: The IgG3 Fc structure. Side chains of IgG3 Fc (magenta) that is different in IgG1 Fc (using PDB id 3AVE as reference) are shown in stick representation. The N297 and N-glycans (green) are shown in stick representation.

```
          230        240        250        260        270        280        290
           |          |          |          |          |          |          |
IgG1  TCPPCPAPELLGGPSVFLFPPKPKDTLMISRTPEVTCVVVDVSHEDPEVKFNWYVDGVEVHNAKTKPREEQYNST
IgG2  ECPPCPAP-PVAGPSVFLFPPKPKDTLMISRTPEVTCVVVDVSHEDPEVQFNWYVDGVEVHNAKTKPREEQFNST
IgG3  -CPRCPAPELLGGPSVFLFPPKPKDTLMISRTPEVTCVVVDVSHEDPEVQFKWYVDGVEVHNAKTKPREEQFNST
IgG4  -CPSCPAPEFLGGPSVFLFPPKPKDTLMISRTPEVTCVVVDVSQEDPEVQFNWYVDGVEVHNAKTKPREEQFNST
       Hinge[-------------------------------------------------------------------

     300        310        320        330        340        350        360        370
      |          |          |          |          |          |          |          |
IgG1  YRVVSVLTVLHQDWLNGKEYKCKVSNKALPAPIEKTISKAKGQPREPQVYTLPPSRDELTKNQVSLTCLVKGFYP
IgG2  FRVVSVLTVVHQDWLNGKEYKCKVSNKGLPAPIEKTISKTKGQPREPQVYTLPPSREEMTKNQVSLTCLVKGFYP
IgG3  FRVVSVLTVLHQDWLNGKEYKCKVSNKALPAPIEKTISKTKGQPREPQVYTLPPSREEMTKNQVSLTCLVKGFYP
IgG4  YRVVSVLTVLHQDWLNGKEYKCKVSNKGLPSSIEKTISKAKGQPREPQVYTLPPSQEEMTKNQVSLTCLVKGFYP
      ----------C$_H$2-------------------------][----------------------------------

          380        390        400        410        420        430        440
           |          |          |          |          |          |          |
IgG1  SDIAVEWESNGQPENNYKTTPPVLDSDGSFFLYSKLTVDKSRWQQGNVFSCSVMHEALHNHYTQKSLSLSPGK
IgG2  SDIAVEWESNGQPENNYKTTPPMLDSDGSFFLYSKLTVDKSRWQQGNVFSCSVMHEALHNHYTQKSLSLSPGK
IgG3  SDIAVEWESSGQPENNYNTTPPMLDSDGSFFLYSKLTVDKSRWQQGNIFSCSVMHEALHNRFTQKSLSLSPGK
IgG4  SDIAVEWESNGQPENNYKTTPPVLDSDGSFFLYSRLTVDKSRWQEGNVFSCSVMHEALHNHYTQKSLSLSLGK
      ----------C$_H$3-----------------------------------------------------------]
```

Figure 5.3: Sequence alignment of IgG1 (3AVE), IgG2 (4HAF), IgG3, and IgG4 (4C54) for the hinge and the Fc region. The IgG3 sequence shown here and used for this study is based on

IGHG3*11, *12 allele. The amino acid differences between IgG1 and the other IgG subclasses are shown in red. Amino acid differences unique to IgG3 are highlighted in blue.

5.3.4 C_H2 domain conformation

The C_H2 domain conformation in IgG3 Fc was compared with representative IgG1, IgG2 and IgG4 structures. Independent alignment of the C_H2 and C_H3 domains of different IgG subclasses using IgG3 Fc as a reference showed lower RMS (root-mean-square deviation of atomic positions) values for the C_H3 domain relative to the C_H2 domain. The RMS values for the C_H2 domain superposition using GESAMT[26] for IgG1 Fc (3AVE)[27], IgG2 Fc (4HAF)[3] and IgG4 Fc (4C54)[4] were 1.11 Å/106 Cα, 1.08 Å/105 Cα and 1.14Å/100 Cα respectively, while those for the C_H3 domains showed 0.29 Å/104 Cα, 0.29 Å/104 Cα and 0.39Å/104 Cα respectively. These results suggest that C_H3 domain conformation across IgG subclasses remain relatively constant, while the C_H2 domain shows variability, as previously reported for IgG2 and IgG4 structures. The overall C_H2 domain conformation can be assessed by measuring the distances between Cα atoms of the P238, F241, R301, and P329 residues on both the Fc chains.[3] The C_H2-C_H3 joint provides angular freedom to the C_H2 domain and orients it relative to the C_H3 domain. Moreover, amino acid variations between IgG subclasses, crystal packing and crystal conditions can also influence C_H2-C_H2 domain separation.[3, 28] IgG3 Fc was crystallized in the $P2_1$ space group, whereas a majority of the published IgG1 Fc structures belong to the $P2_12_12_1$ group. The distance between pairs of P238, F241, R301 and P329 residues in the Man5-IgG3 Fc structure is 23.5 Å, 26.3 Å, 35.5 Å and 29.9 Å respectively, which is about 3-4 Å greater than the range (18.6-20.2 Å for P238, 21.5-23.9 Å for F241, 31.9-35.2 Å for R301, 22.6-26.9 Å for P329) of distances reported in multiple IgG1 Fc structures that bear complex-type glycans (Table 5.2). A pronounced correlation between the C_H2 separation and type of glycosylation is generally observed. For example, the C_H2 domains are more spread apart in Man9-IgG1 Fc than for IgG1

Fc with a complex-type glycan.[29] Moreover, a progressive decrease in the C_H2 separation was shown in IgG1 Fc structures when the complex glycans were serially truncated.[5] The smallest separation was reported in the aglycosylated IgG1 Fc structure (3S7G).[6] The Man5 glycoform in IgG3 Fc is a truncated form of a Man9 glycan having similar branch points but lacking the additional α-1,2 mannose residues (Fig. 5.5A). The C_H2 distances in the Man5-IgG3 Fc structure were between those found in the Man9-IgG1 Fc structure and the IgG1 Fc with a complex glycan structure (Fig 5.4, Table 5.2). Based on these results, it is not possible to tell whether the C_H2 separation in IgG3 Fc was due to amino acid differences in IgG3 and IgG1 and/or the Man5 glycoform on IgG3 Fc. The IgG3 subclass exhibits the strongest complement dependent cytotoxicity (CDC), a process initiated by binding of C1q complement to IgG Fc. The core of the C1q complement binding site on IgG1 has been mapped to four spatially close residues in the C_H2 domain, Asp270, Lys322, Pro329, and Pro331.[30] Although these four residues are conserved in IgG3, there are other polymorphic differences between IgG1 and IgG3 around the C1q binding site. These differences are believed to result in subclass-dependent variations in complement activation at the level of C1q binding or the antibody-dependent steps of complement cascade. Mutation of one such polymorphic residue, Lys276 in IgG3 to IgG1-like Asn276 was shown to reduce complement activation.[31] Lys 276 in our Man5-IgG3 Fc structure appears to lie close to Lys322, which has been previously determined to be important for IgG3 driven complement activation.[32]

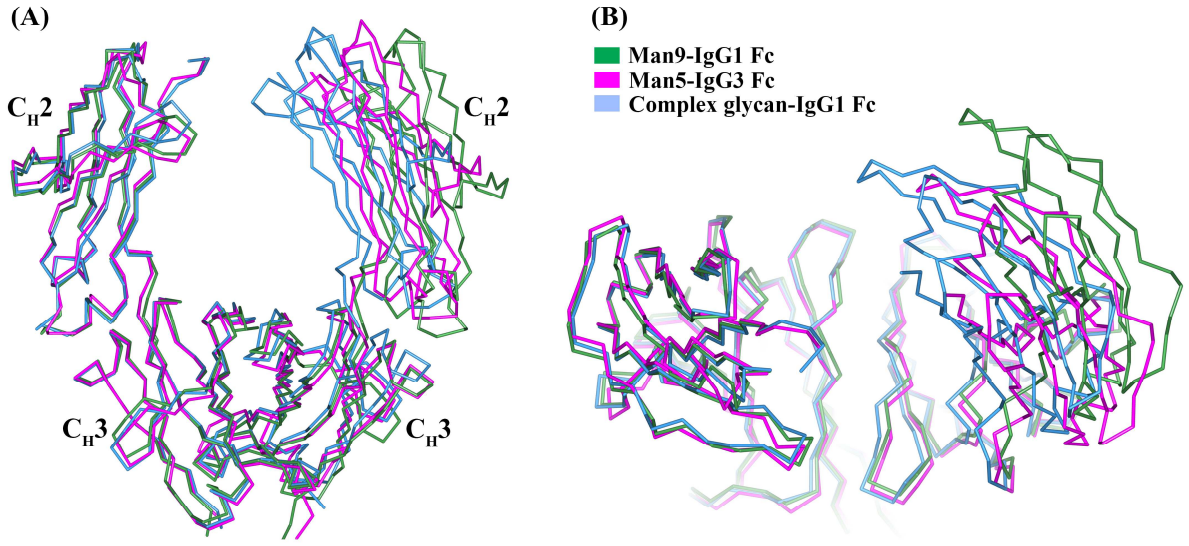

Figure 5.4: The orientation of the C_H2 domain relative to the C_H3 domain shown by superposition of Fc structures aligned using only one Fc chain. The compared Fc structures with different glycan types are Man5-IgG3 Fc (magenta), complex glycan-IgG1 Fc (3AVE) (light blue) and Man9-IgG1 Fc (2WAH) (green). The orientation of the Fc is shown in a (A) side view and (B) side view rotated by 90° about x-axis.

Table 5.2: Separation between C_H2 domain in IgG3 Fc and reported IgG Fc structures

PBD	Fc (glycan)	Space group	Resolu-tion (Å)	P238 (Å)	F241 (Å)	R301 (Å)	P329 (Å)
5W38	IgG3 Fc (Man5)[b]	$P2_1$	1.8	23.5	26.3	35.5	29.9
1FC1	IgG1 Fc (complex)[a]	$P2_12_12_1$	2.9	19.6	23.5	35.2	26.8
1H3T	IgG1 Fc (MN2F)[b]	$P2_12_12_1$	2.4	18.3	21.4	32.8	22.0
1H3U	IgG1 Fc (M3N2F)[b]	$P2_12_12_1$	2.4	19.2	22.0	32.7	24.2
1H3X	IgG1 Fc (G0F)[b]	$P2_12_12_1$	2.4	19.7	21.9	33.9	22.6
1H3V	IgG1 Fc (G2F)[b]	$P2_12_12_1$	3.1	19.4	23.2	32.9	26.9
3AVE	IgG1 Fc (complex)[a]	$P2_12_12_1$	2.0	19.3	21.8	32.7	25.1
2DTS	IgG1Fc (complex-afucosyl)	$P2_12_12_1$	2.2	18.6	21.5	32.2	24.2
3DO3	IgG1 Fc (complex)[a]	$P2_12_12_1$	2.5	20.1	22.4	32.8	23.5
2WAH	IgG1 Fc (Man9)[b]	$P2_12_12_1$	2.5	30.2	29.8	42.8	36.4
4Q6Y	IgG1 Fc closed (S2G2F)[b]	$P2_1$	3.0	13.0	18.5	26.7	21.1
4Q6Y	IgG1 Fc open (S2G2F)[b]	$P2_1$	3.0	20.2	23.9	31.9	NA
4HAF	IgG2 Fc (complex)[a]	$P2_12_12_1$	2.0	NA	27.8	39.5	NA
4C54	IgG4 Fc (complex)[a]	$P2_12_12_1$	1.9	19.7	22.1	33.7	36.1

[a]denotes heterogeneously glycosylated Fc with complex-type biantennary N-glycans
[b]denotes homogenously glycosylated Fc with the indicated glycoform

5.3.5 N-glycosylation

The Man5 glycoform reported in this structure is an intermediate in the biosynthesis of N-linked glycoproteins that is formed just prior to the conversion of high mannose type glycoforms into hybrid and complex glycoforms.[33] Although, the level of the Man5 glycoform found in the normal serum IgG is less than 1%[34], it is present at significantly higher levels (up to 20%) in recombinant mAbs produced in CHO cells.[35] Man5-IgG1 is reported to have higher binding affinity to FcγRIIIA and higher Antibody Dependent Cellular Cytotoxicity (ADCC) when compared to IgG1 bearing complex-type glycoforms.[36] Additionally, Man5-IgG1 exhibits more rapid clearance than other glycoforms due to uptake by mannose receptors and mannose binding proteins.[37] Because of these properties, the level of high mannose glycoforms in mAb therapeutics is considered as a critical quality attribute (CQA) and demonstrating its effect on Fc conformation is important from a Fc glycoengineering perspective.[38]

The conserved N297 glycan in IgG1 Fc structures maintains extensive contacts with protein.[1] The core pentasaccharide ($Man_3GlcNAc_2$) common to high mannose and complex-type glycoforms in IgG1 Fc structures has been shown to maintain identical protein contacts. However in previous IgG1 Fc structures, monosaccharide residues outside of the core pentasaccharide maintained different protein contacts depending on whether they were high mannose or complex type glycans.[2, 29] In both IgG3 Fc chains, ordered electron density for only the first three reducing terminal monosaccharide residues was detected, corresponding to Manβ1-4 GlcNAcβ1-4GlcNAc linked to N297 (Fig. 5.5A,C). No interpretable electron density for the terminal mannose residues was detected, presumably due to its higher dynamic nature or disordered state. In contrast, ordered electron density for nine and three sugars out of eleven were observed for chain A and B, respectively in the Man9-IgG1 Fc structure (Fig. 5.5A)

reported by Crispin et al.[29] In an another related IgG1 Fc structure with hybrid glycoforms (Fig. 5.5A) reported by Bowden et al., electron density was visible for all sugars except the ones beyond the Man4 on the α-1,3 arm of one chain and completely invisible on the other chain.[28] The protein-carbohydrate contacts for the three visible sugars on both the chains of IgG3 Fc were identical to those previously reported in IgG1 Fc structures.[1-2] The contacts found within hydrogen-bonding distance are between: the carbonyl oxygen of the D265 side chain and amide nitrogen of the N-acetyl group on GlcNAc1, and the Nε atom of the R301 side chain and the amide oxygen of the N-acetyl group on GlcNAc2. Also, π-CH type of interactions are possible between phenyl ring of F241 and CH moieties from GlcNAc2 and Man3. (Fig. 5.5B)

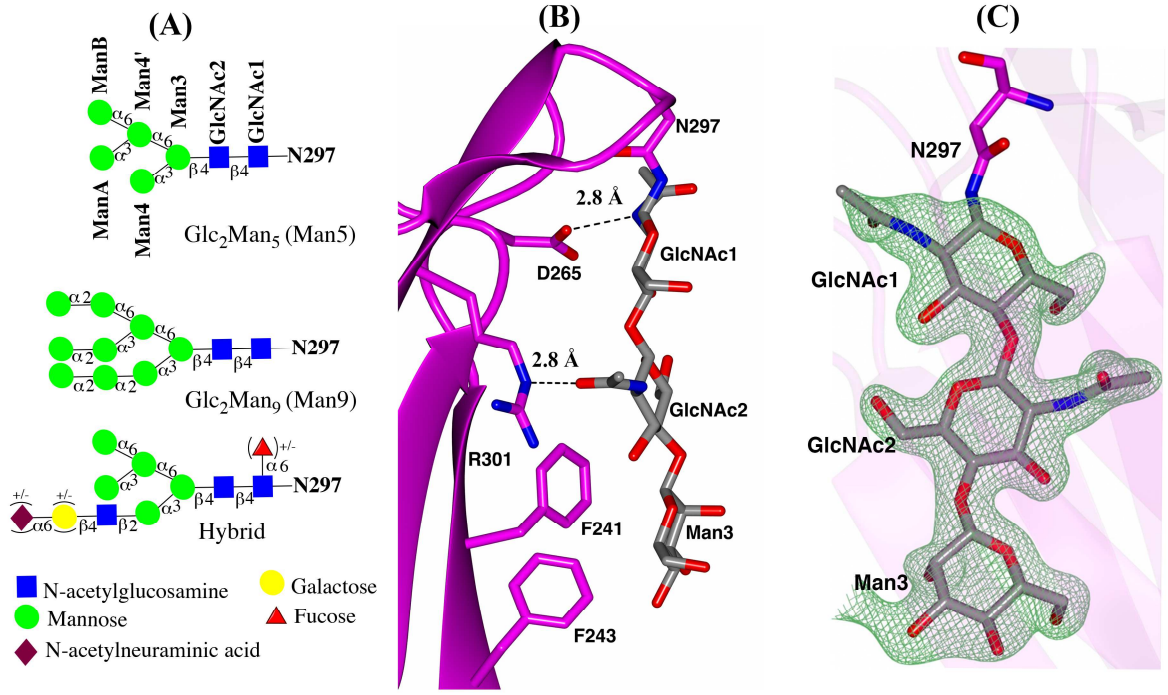

Figure 5.5: N-glycans in IgG3 Fc structure (A) schematic representation of $Man_5GlcNAc_2$ (Man5), $Man_9GlcNAc_2$ (Man9) and hybrid glycoform based on the Essentials system of glycan nomenclature (B) close-up view of N297 attached glycans and protein contacts. H-bonds between protein and carbohydrate are shown as black dotted lines. (C) ordered glycans from chain A in stick representation, shown with the F_o-Fc electron density difference map contoured at 3σ.

We examined the effect of removal of these interactions on binding of IgG3 Fc to FcγRIIIA, a key receptor involved in ADCC activity using a series of sequentially truncated IgG3 Fc glycoforms. These glycoforms included high mannose (Man8-Man12 glycoforms, potentially having additional protein contacts when compared to Man5), Man5, a single GlcNAc monosaccharide residue (disrupting contacts with Man3 and GlcNAc2) and D297 (deglycosylated by PNGase F treatment, also disrupting contacts with GlcNAc1). Representative binding curves for biolayer interferometry (BLI) based Fc-FcγRIIIA binding assay are shown in Fig. 5.6 and the results for these binding experiments are given in Table 5.3. The binding assay showed similar affinity for the high mannose (Man8-Man12) and Man5 glycoforms. However, a 10-fold reduction in affinity was observed for GlcNAc-IgG3 Fc glycoform and no detectable binding was recorded for the deglycosylated IgG3 Fc using highest receptor concentration of 15 μM. The weaker affinity of the GlcNAc-IgG3 Fc was driven by a faster dissociation rate, with the association rate remaining largely unaffected. A similar trend in FcγRIIIA binding was also seen in IgG1 Fc, as previously reported by our group[39] and others.[40] These results indicate that protein-glycan interactions of the core pentasaccharide ($GlcNAc_2Man_3$) were necessary in maintaining high affinity FcγRIIIA binding, and that the IgG3 Fc interactions with GlcNAc1 are essential for FcγRIIIA binding. The functional relevance of protein-glycan contacts observed in Fc structures was first demonstrated by Lund et al. using site-specific mutagenesis to disrupt important contacts.[41-42] In their study, individual mutations of D265, R301, F241 and F243 residues on a mouse-human chimeric IgG3 caused a reduction in complement activity and binding to the receptor FcγRI. The observed protein-glycan contacts mediated by the first two GlcNAc's in our IgG3 Fc structure and the effect of the disruption of these contacts on binding

to FcγRIIIA provides a structural basis for the importance of these sugar residues in IgG3-Fcγ receptor interactions.

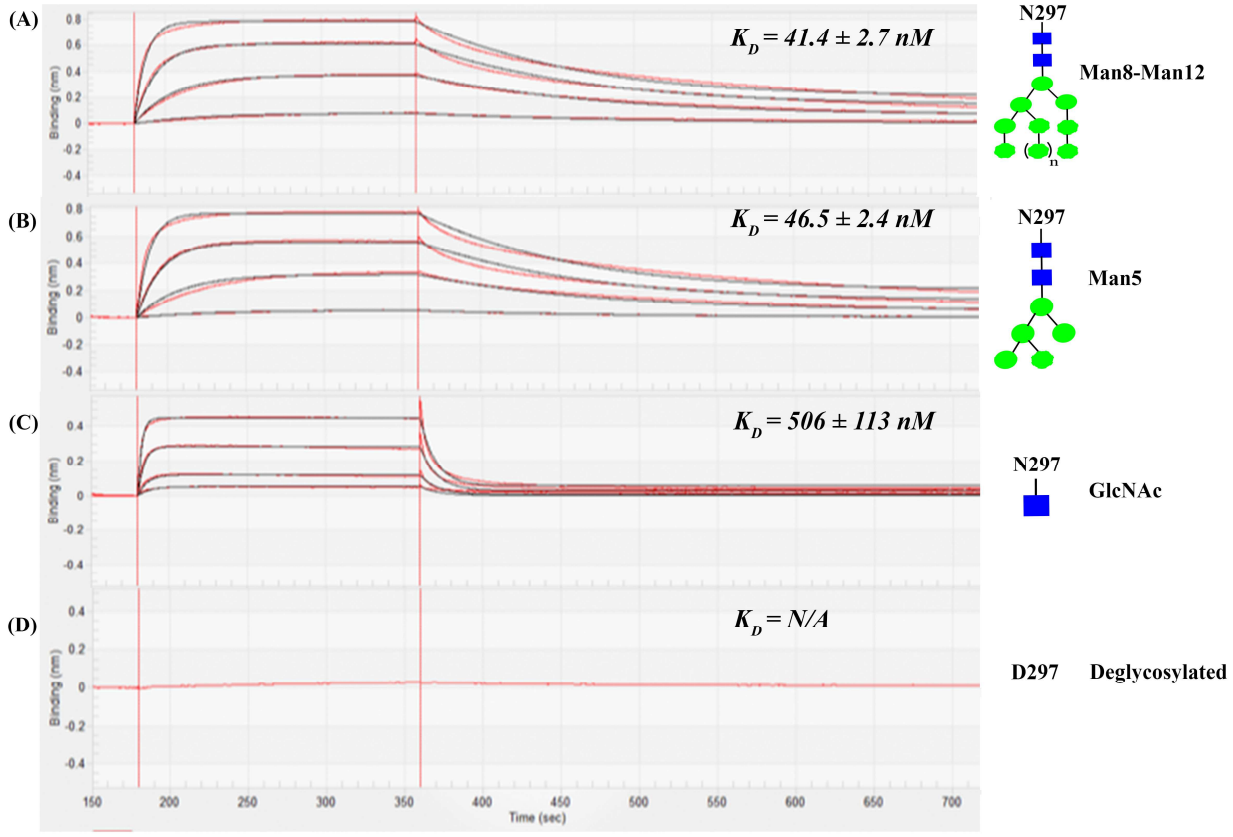

Figure 5.6: Binding analysis of IgG3 Fc glycoforms-FcγRIIIA. Binding curves (BLI curve, red; fitted curve, black) with corresponding glycoform structure are shown in panels for following glycoforms: (A) Man8-Man12 (B) Man5 (C) Fc-GlcNAc and (D) D297 (deglycosylated). The data is shown for FcγRIIIA at concentrations of 800, 400, 200, and 100 nM, which correspond with curves from top to bottom. For Fc-GlcNAc, curves for FcγRIIIA at concentrations of 1600, 800, 400, 200 nM are shown.

Table 5.3: Kinetic parameters obtained for binding of FcγRIIIA with the IgG3 Fc glycoforms

IgG3 Fc glycoform	**Average k_{on}*10^5 (1/M.sec)**	**Average k_{off}*10^{-3} (1/sec)**	**Average K_D (nM)**
Man8-Man12	1.6 ± 0.1	6.5 ± 0.2	41.4 ± 2.7
Man5	1.5 ± 0.1	6.8 ± 0.2	46.5 ± 2.4
Fc-GlcNAc	1.7 ± 0.4	85.8 ± 7.7	506 ± 113
D297	nd*	nd*	nd*

*not detected at highest receptor concentration of 15 µM.

5.3.6 C_H2-C_H3 domain interface

The C_H2-C_H3 interface in IgG class antibodies maintains the orientation of the C_H2 domain relative to the C_H3 domain. Moreover, the outer face of the C_H2-C_H3 domain interface is a binding site for multiple Fc binding proteins like FcRn, protein A, protein G, HSV-1 (herpes simplex virus 1) Fc receptor, rheumatoid factor and TRIM21 (tripartitie motif 21).[43] Any structural change at the interface can potentially alter the conformation of the binding site or the C_H2 domain orientation. The amino acids at the interface are highly conserved among IgG subclasses with a few exceptions. In IgG1, IgG2 and IgG4 Fc structures, the core of the interface is formed by four stabilizing interactions: two salt bridges between K248-E380 and K338-E430 through side chains and two hydrogen bonds between L251-H435 and K340-Y373 through main chains of L251, K340 and side chains of H435, Y373. All these residues are conserved across IgG subclasses except at position 435, where an arginine is present (R435) in IgG3 rather than histidine (H435) as in the other subclasses (Fig. 5.3). It must be noted here that only two IgG3 allotypes (G3m (s,t)/G3m15,16) from the thirteen allotypes contain H435 and these are commonly found in Mongoloid population but rare in Caucasoids.[44]

Both the IgG3 Fc chains showed similar contacts as seen in IgG1 Fc (3AVE), IgG2 Fc (4HAF) and IgG4 Fc (4C54) except for the K248-E380 salt bridge (Fig. 5.7A). The side chain of E380 on both IgG3 Fc chains adopted a different rotameric conformation that was away from side chain of K248 (Fig. 5.7B). Interestingly, despite having arginine at position 435, both the IgG3 Fc chains still maintained a H-bond between residues 251 and 435 (through the main chain carbonyl oxygen of L251 and Nε of R435 side chain in place of Nδ1 from H435 side chain) (Fig. 5.7A). The longer arginine 435 side chain in IgG3 Fc is close to the isoleucine 253 side chain

(less than 4 Å distance), whereas histidine 435 is located away from isoleucine 253 in the IgG1, 2 or 4 subclasses. The conformation of I253 shows variability in the representative IgG1 Fc structures but the H435 conformation remains consistent. In comparing these structures to IgG3 Fc, the I253 and R435 residues in IgG3 Fc are found to be closer than the I253-H435 pair in any IgG1 Fc structures (Fig. 5.8A). A water mediated H-bond between Nη2 of R435 side chain and the main chain amide nitrogen of I253 appears to be present in the chain A of IgG3 Fc but not in chain B (data not shown). Arginine (pKa~12.5), unlike histidine (pKa~6.0) remains positively charged at physiological pH and thereby can potentially alter the side chain conformation of I253 or its local conformation. Isoleucine 253 is a critical residue in the region of IgG Fc where protein A, protein G and FcRn bind.[2, 45] T339 is another residue at the interface that differs across the IgG subclasses. IgG2 and IgG3 contain threonine, while IgG1 and IgG4 have alanine at position 339. In the IgG2 Fc structure, T339 has been shown to maintain contact with D376 either directly or through water mediated H bonds.[3] In the IgG3 Fc structure, the side chains of T339 and D376 on chain A exists in two conformations, while both residues on chain B adopt a single conformation with no contacts between them in either of the chains (Fig. 5.7C). Teplyakov et al. have suggested a ball-and-socket joint in the IgG2 Fc structure between a C_H2 residue forming the ball and C_H3 residues forming the socket that mediate the pivot of the C_H2 domain relative to the C_H3 domain. L251 in the C_H2 domain was shown to fit into a socket formed by residues M428, H429, E430 and H435.[3] These residues are conserved in all IgG subclasses except IgG3 where arginine is present at position 435 (Fig. 5.3). In the IgG3 Fc structure, R453 does not seem to disrupt the socket and L251 in IgG3 Fc was still able to form a similar type of ball-and-socket joint. The longer side chain of R435 can be speculated to extend

the socket closer to the C_H2 domain owing to the proximity of the R435 and I253 residues and thereby may influence the C_H2 domain pivot (Fig. 5.8B).

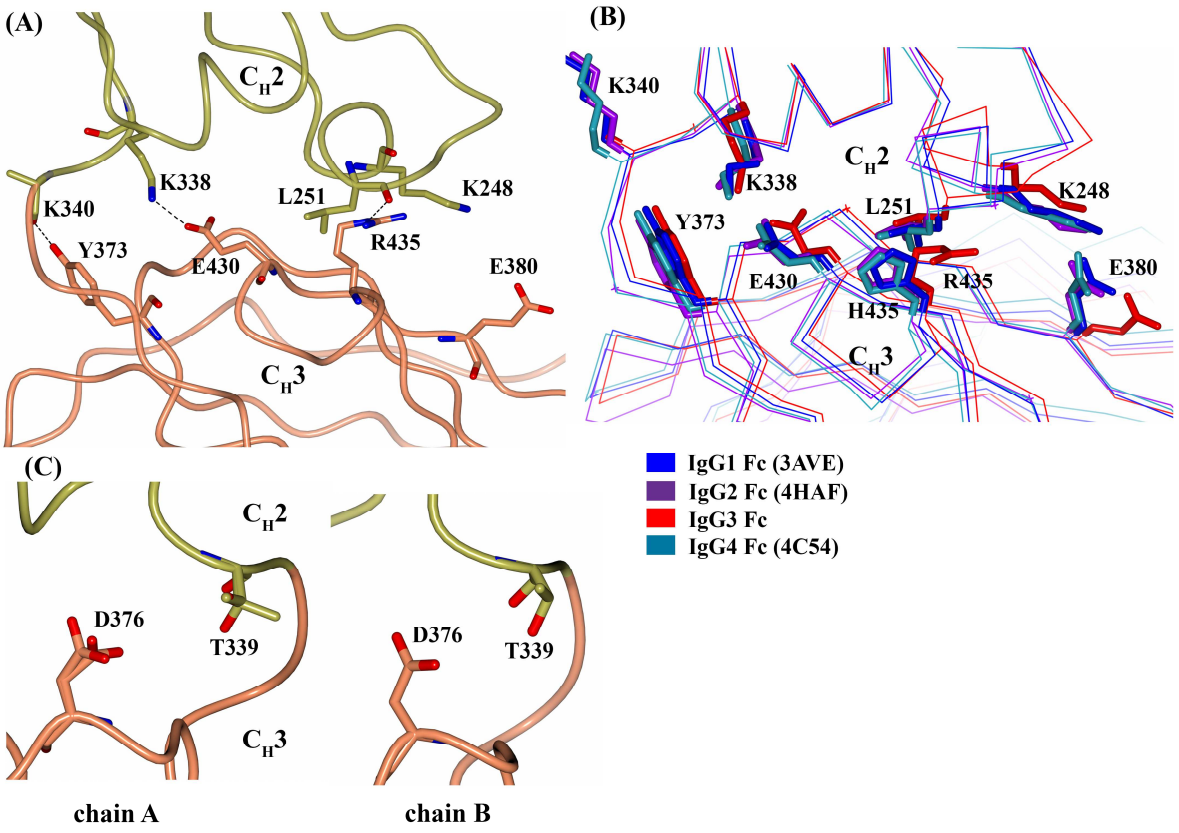

Figure 5.7: C_H2-C_H3 interface of IgG3 Fc. (A) H-bonds and salt-bridge present between C_H2 (gold) and C_H3 (coral) in chain A (B) comparison of C_H2-C_H3 interface across IgG subclasses. The representative Fc structure include IgG1 Fc (3AVE) (blue), IgG2 Fc (4HAF) (purple), IgG3 Fc (red) and IgG4 Fc (4C54) (cyan). Protein backbone is represented by Cα trace and side chains are shown in stick representation. (C) Conformation of T339 and D376 in chains A and B of IgG3 Fc

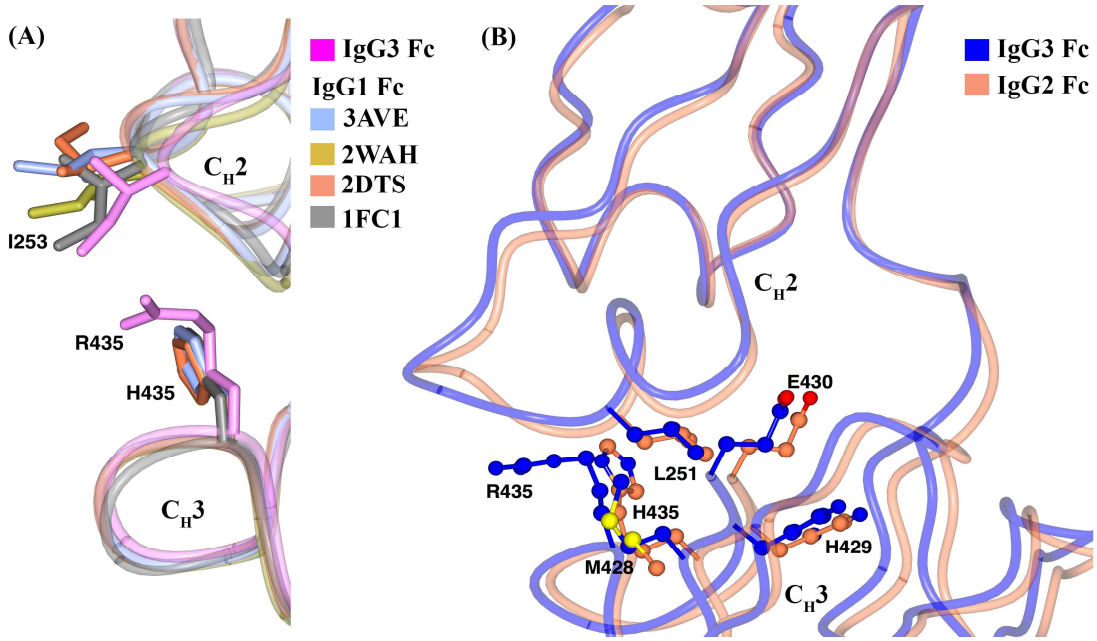

Figure 5.8: Comparison of IgG3 Fc with other Fc structures. (A) conformation of I253 and R435/H435 across multiple IgG Fc structures, as shown in the key. (B) ball-and-socket joint in IgG3 and IgG2 Fc structure. Side chains are represented by stick in (A) and by ball-and-stick in (B).

A functional significance of the C_H2-C_H3 interface with respect to Fc receptor binding was demonstrated in an IgG1 mutagenesis study.[46] In the study, IgG1 with a H435A mutation showed 25% lower binding to FcγRIIA, FcγRIIB and FcγRIIIA, while the mutation increased binding to FcγRI by same amount. An A339T mutation increased FcγRIIIA binding by 34%. Given the distal location of the H435 and A339 from the FcγR binding site, an indirect role of the C_H2-C_H3 interface in FcγR binding through maintenance of C_H2 conformation can be postulated. In the same study, an E380A mutation resulted in an 119% increase in FcRn affinity. E380 doesn't interact directly with FcRn but is a neighboring residue at the binding interface. In summary, the C_H2-C_H3 interface of IgG3 Fc exhibited minor differences compared to that of IgG1 Fc, which may be responsible for subtle differences in its Fc receptor interaction pattern.[47] In one particular case, the C_H2-C_H3 domain interface was shown to generate an Fc-Fc mediated hexameric ring structure in the crystal packing of a full-length IgG1 antibody (1HZH).[48]

Functionally, such hexameric structures resulting from antigen bound antibodies on cells is shown to be effective activators of CDC by binding strongly to the C1q complement protein which also has a hexameric structure.[49] The residues involved in the Fc-Fc interface in the crystal packing of these structures were located at the C_H2-C_H3 interface and overlapped with known sites for Fc-binding proteins. The CDC activity of IgG1 was shown to be affected by disruption of some of the Fc-Fc contacts that were involved in hexamer formation.[49] Although, the C_H2-C_H3 interface in our IgG3 Fc crystal packing do not generate hexameric ring by symmetry operation, the role of interface residues of IgG3 that can potentially mediate Fc-Fc interaction warrants further investigation, especially since IgG3 is known to elicit the strongest CDC among the IgG subclass.

5.3.7 IgG3-protein A and protein G interactions

IgG3 is the only IgG subclass that does not bind to protein A, whereas all IgG subclasses bind to protein G. Both, protein A and protein G bind to the outer face of the C_H2-C_H3 interface, where residues from both domains are involved in binding. Protein A and G have overlapping but non-identical binding sites on IgG Fc's. All the residues involved in protein A and/or protein G binding are conserved across the IgG subclass except for IgG3-R435.[50] H435 in the other IgG subclasses maintains a hydrophobic contact with Y133 and L136 of protein A.[2] When the H435R mutation of IgG1 Fc was modeled on the IgG1 Fc structure in the first published protein A-IgG1 Fc complex (1FC2), R435 was unable to be accommodated in the complex.[2] Although an IgG3 Fc structure alone does not provide direct information on the lack of an IgG3-protein A binding interaction, IgG3 can be reasonably compared with IgG1 in complex with protein A, given the highly conserved nature of the binding interface, and some conclusions can be drawn. We used the 1FC2 complex and a more recently reported Rituximab Fc-protein A (1L6X) complex to

compare IgG3's structure to IgG1's structure in the complex. In both the complexes, the R435 side chain appears to sterically clash with the phenylalanine (Y133/Y15 in 1FC2/1L6X) and glutamine (Q129/Q11 in 1FC2/1L6X) residues of protein A and appear to be more conformationally restricted than H435 (Fig. 5.9A-B). Our analysis is backed by the work of Stapleton et al., who showed that protein A binding ability of IgG3 is restored when Arg is mutated to His.[51] In contrast to protein A, H435 was shown to not make any contact with protein G in the protein G-IgG1 Fc complex.[50] When we compare IgG3 Fc to IgG1 Fc in the complex with protein G, the R435 in IgG3 does not appear to sterically clash with protein G and appears to be accommodated at the binding interface (Fig. 5.9C). Additionally, R435 in IgG3 can be predicted to interact with E27 in protein G through a salt bridge, as the distance between the Nη2 atom of R435 and Oε2 atom of E27 is 3.5 Å. A study investigating binding affinity differences between the IgG subclasses for binding to protein G showed a 3-fold higher affinity for IgG3 compared to IgG1.[52] Based on this information, it could be suggested that the longer R435 side chain in IgG3 can potentially form extra contacts with protein G and thereby result in tighter binding. Our IgG3 Fc structure provides some insight on the likely role of the arginine residue at the 435 position in differential protein A and protein G binding property of IgG3.

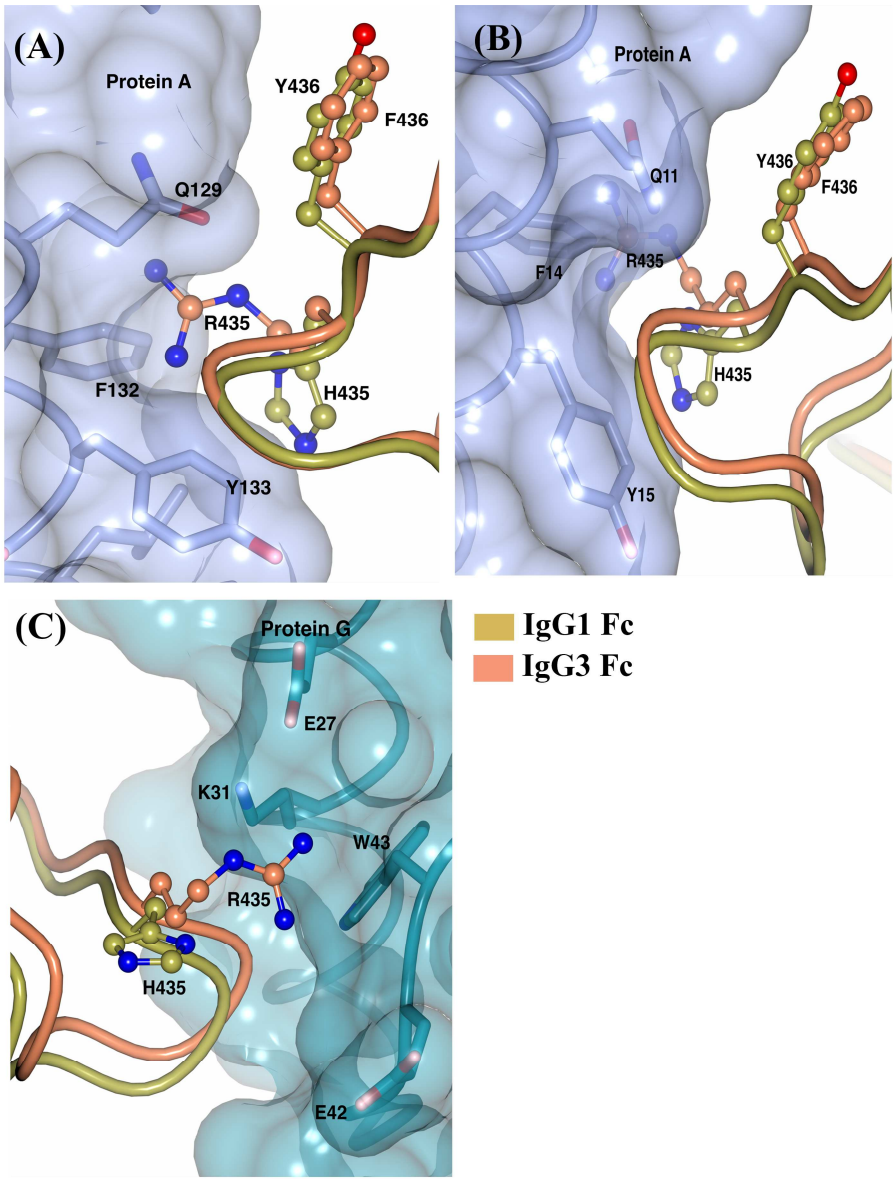

Figure 5.9: IgG3 Fc at Fc-protein A/G binding interface. IgG3 Fc is superposed on IgG1 Fc in the IgG1 Fc-protein A complexes from (A) 1FC2 and (B) 1L6X. (C) IgG3 Fc is superposed on IgG1 Fc in the IgG1 Fc-protein G complex (1FCC). Side chains of Fc and protein A/G are represented by ball-and-stick and stick respectively. The transparent surface of protein A and G are shown in light purple and dark cyan respectively.

5.3.8 IgG3-FcRn interactions

The neonatal Fc receptor (FcRn) is responsible for the long half-life of IgG class antibodies by rescuing IgG from endosomal degradation. It binds to IgG at acidic pH in the endosomes of vascular endothelial cells and recycles it back to circulation by dissociating at pH

7.4.[53] FcRn binds to the outer face of the C_H2-C_H3 domain interface overlapping the protein A and protein G binding sites. Analysis of the FcRn-IgG binding interface based on the Fc-FcRn crystal structure and molecular dynamics simulation revealed three contacts to be most stabilizing.[45, 54-55] These include a Fc-I253 interaction with a pocket formed by hydrophobic residues on FcRn, and salt bridges involving H310 and H435 of the Fc with corresponding E115 and D130 residues of FcRn which maintain the pH dependence of the interaction. The lower half-life of IgG3 (~7 days) has been suggested to be due to an intracellular competition between IgG1 (half-life of ~21 days) and IgG3 during the FcRn recycling process. Interestingly, FcRn-mediated transport models showed that IgG3 was transported as efficiently as IgG1 if present alone but only affected in presence of IgG1.[51] IgG3 showed a slightly 2-fold weaker affinity at pH 6.0 when compared to IgG1 and an increased binding at pH 7.4 relative to IgG1.[51] These differences were suggested to play a role in less efficient IgG3 recycling also. Interestingly, an IgG3 allotype with H435 shows IgG1 like half-life, implying a role for the amino acid at position 435 in FcRn affinity. Moreover, a H435A mutation in IgG1 was shown to reduce FcRn binding by more than 10-fold.[46] We modeled the probable IgG3-FcRn binding interface by superposing the IgG3 Fc structure on the available IgG1 Fc (YTE)-FcRn complex[45], and analyzed various scenarios in which R435 can influence FcRn binding. The R435 residue appears to be accommodated at the binding interface with some rearrangement (Fig. 5.10). Moreover, R435 in IgG3 can be predicted to interact with E133 in FcRn through a salt bridge, as the distance between the Nη2 atom of R435 and Oε2 atom of E133 is 3.0 Å. The arginine side chain (free amino acid pKa~12.5) remains positively charged at pH 7.4 and can still maintain ionic interactions with FcRn, unlike the histidine side chain (free amino acid pKa~6.0) which is likely to be less than 10% protonated at pH 7.4. This can contribute to increased binding of IgG3 at

physiological pH relative to the other IgG subclasses. Moreover, R435 can indirectly influence FcRn binding through I253, given their proximity in the structure (Fig. 5.7A) and the importance of I253 at the binding interface (a I253A mutation in IgG1 was shown to result in more than 10-fold weaker FcRn binding[46]). Although, the IgG3 Fc structure alone does not provide conclusive evidence pertaining to IgG3-FcRn interaction, it helps to shed light on the possible role of arginine at position 435 at the binding site.

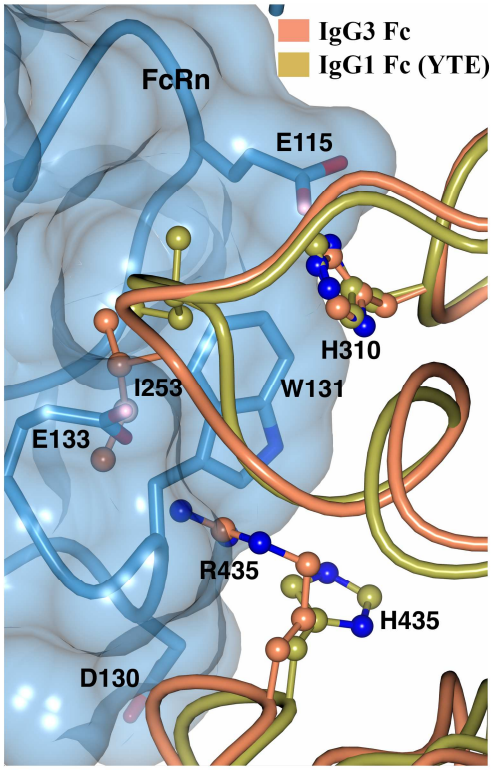

Figure 5.10: IgG3 Fc at the Fc-FcRn binding interface. IgG3 is superposed on IgG1 Fc (YTE) in the Fc (YTE)-FcRn complex (4N0U). Fc and FcRn residues are shown in ball-and-stick and stick representation respectively. Transparent surface of FcRn is shown in blue.

5.3.9 Crystal structure of tetraglycosylated IgG3 Fc

The tetraglycosylated IgG3 Fc (contains high mannose glycans at both the N297 and N392 sites) crystallized in a hitherto unreported $P6_1$ space group for IgG Fc with a complete dimer in the asymmetric unit, and its structure was solved at 2.0 Å resolution (Fig. 5.11A, Table

5.1). The Man5-IgG3 Fc (which contains the Man5 glycoform only at the N297 site) crystallized in a different space group $P2_1$. Most of the published IgG Fc structure belong to a related $P2_12_12_1$ space group with a few in *P1*, *C2*, $C222_1$, $P6_122$ and *P622* space groups. The six-fold crystallographic axis in the tetraglycosylated IgG3 Fc structures generates a hexameric assembly of Fc molecules in a helical arrangement (Fig. 5.11C). The C_H2 domains of the symmetry related Fc structures are oriented inwards facing the axis of the helix, and the Fc-Fc interface is formed by contacts between the C_H2 domain in chain A of one molecule and C_H2 domain in chain B of another. Interpretable electron density was observed for residues Pro238 to Leu443 and Gly237 to Pro445 for chains A and B respectively. Residues Pro291 to Phe296 and Ser298 to Phe301, which flank the N297 glycosylation site on chain B were disordered and could not be modeled. The overall structure of tetraglycosylated IgG3 Fc is similar to Man5-IgG3 Fc; superposition of the two structures using GESAMT[26] yields a RMSD deviation of 2.10 Å for C_α of 383 residues. For the tetraglycosylated IgG3 Fc structure, interpretable electron density was only visible for the first three and four sugars out of ten ($GlcNAc_2Man_8$) for chains A and B respectively at the N297 site, and for the first two and one sugar out of ten for chains A and B respectively at the N392 site (Fig. 5.11B). A similar number of sugars residues (first three out of seven on both chains) were visible in the Man5-IgG3 Fc structure. The conformation of N297 glycans and their contacts with the C_H2 domain were similar in both the IgG3 Fc structures. Based on the orientation of the first two GlcNAc residues at the N392 site in the tetraglycosylated IgG3 Fc structure, it appears that the glycans at the N392 point towards the N-terminus of Fc and run anti-parallel to the N297 glycans (Fig. 5.11A).

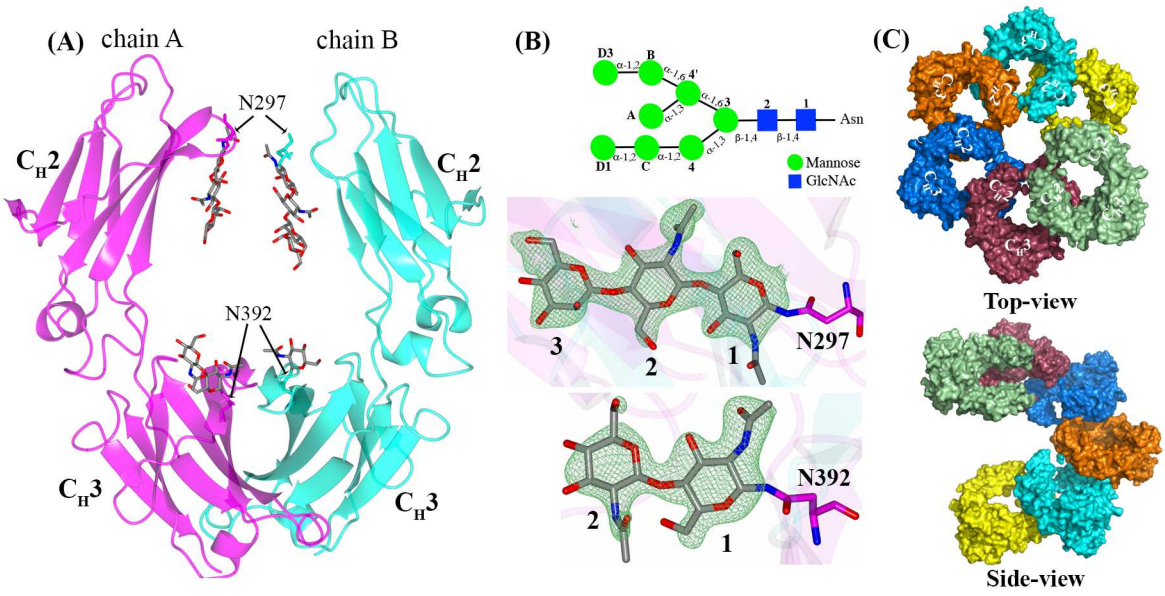

Figure 5.11: Crystal structure of the tetraglycosylated IgG3 Fc. (A) overall structure of IgG3 Fc with interpretable glycan structures at the N297 and N392 sites. Chains A and B of Fc are shown in magenta and cyan, respectively and glycans are shown in stick representation (B) Schematic representation of the Man8 glycoform and electron density difference omit map (Fo-Fc, green mesh) contoured at 3σ showing the glycans at the N297 and N392 sites (C) Top and side-views of the symmetry related Fc molecules organized in a helical arrangement.

Since only a small part of the Man8 structure at the N392 site was visible in the crystal structure, the full structure was in-silico modeled using GLYPROT[20] to visualize the entire oligosaccharide. The modeled Man8 glycan appear to point away from the protein surface and remain largely solvent exposed (Fig. 5.12A). Crystal packing analysis revealed presence of a cavity large enough to fit Man8 glycan in the vicinity of N392 site between the two Fc molecules related to one another by two-fold rotation. The modeled Man8 glycan was found to fit reasonably well in this cavity and a possible glycan-glycan interface was revealed between the two Fc molecules related by two-fold rotation (Fig. 5.12B).

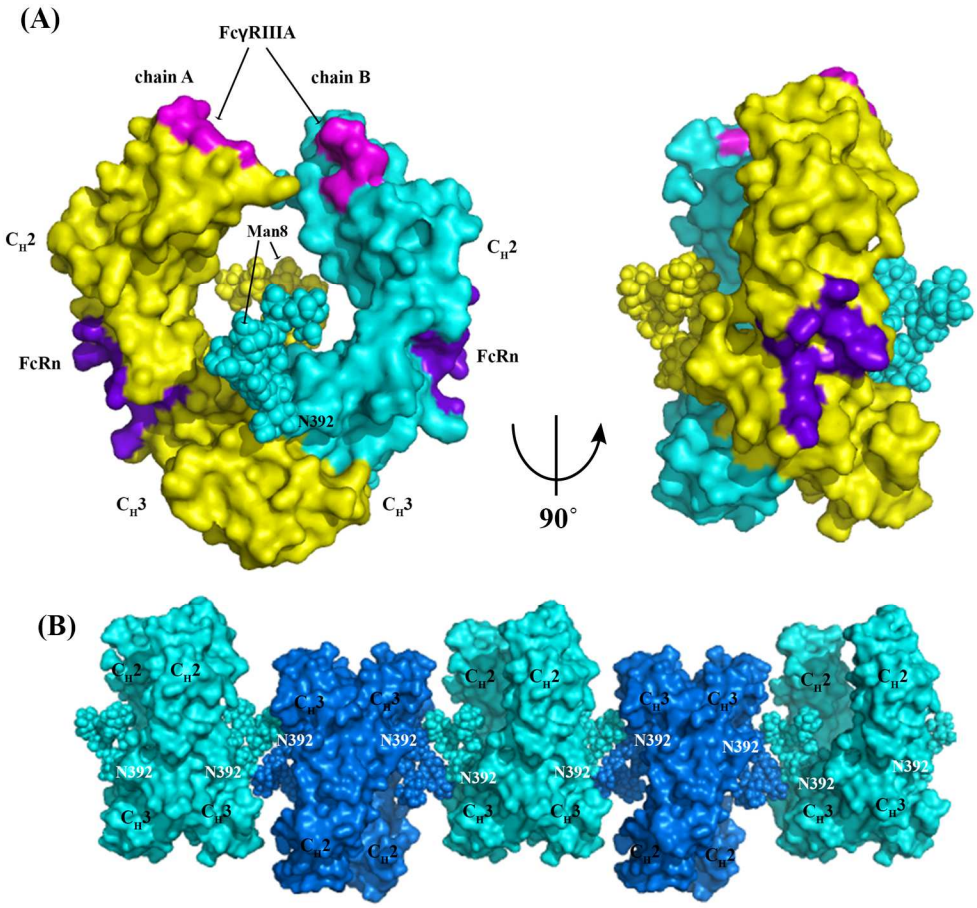

Figure 5.12: Conformation of the in-silico modeled Man8 glycan at the N392 site and its orientation in the Fc structure and crystal packing. (A) Tetraglycosylated IgG3 Fc structure with modeled Man8 glycan at the N392 site. Chain A and B of Fc are shown in yellow and cyan, respectively and glycans are represented by spheres and color matched to their respective chain. The FcγRIIIA and FcRn binding sites on Fc are shown in magenta and purple, respectively. (B) Organization of modeled N392-Man8 glycan between two Fc molecules (related by two-fold rotation) in the crystal packing. Fc is colored by symmetry and glycans are represented by spheres and color matched to its respective Fc. The N297 glycans are not shown in this figure for the sake of simplicity.

The N392 glycans are cleaved at much slower rate under native conditions by the PNGase F enzyme, which cleaves between the first GlcNAc of N-glycan and the Asn side chain (chapter 3, section 3.3.1, Fig. 3.19). Crystallographic analysis of PNGase F with the N, N'-diacetylchitobiose core showed that the N-acetyl group of first GlcNAc formed one of the site for glycan recognition by the enzyme.[56] In the tetraglycosylated IgG3 Fc structure, the N-acetyl

group of the first GlcNAc at the N392 site is largely buried by the C_H3-C_H3 domain interface, which may explain the inability of PNGase F to cleave glycans at this site. A dramatic difference in the levels of fucosylated glycoforms was detected between the two glycosylation sites, as about 90% of glycoforms at the N297 site were fucosylated, while no fucosylated glycans were detected at the N392 site (chapter 2, section 2.3.3). A fucose residue is added to the first GlcNAc of glycan close to the protein surface by α-1,6 fucosyltransferase. Structural analysis of several glycoproteins by Thaysen-Anderson *et al.* suggested that lower levels of fucosylation and higher levels of high mannose glycans are associated with the glycosylation sites that have low site accessibility.[57] In the tetraglycosylated IgG3 Fc structure, the accessible surface area (ASA) for the N297 site is 101.2 Å, while ASA for the N392 site is 60.9 Å. About 50% of ASA of the N392 site (if exists as Fc monomer) is buried due to formation of C_H3-C_H3 dimer interface. The relatively more shielded N392 site may explain the inaccessibility of α-1,6 fucosyltransferase close to the glycoprotein surface.

5.3.10 Influence of N392 glycans on Fc receptor binding and physical stability of IgG3 Fc

The *in-vitro* binding studies of IgG3 Fc with FcγRIIIA and FcRn receptors suggest that the additional presence of the N392 site glycans on IgG3 Fc does not have a large impact on receptor binding (chapter 4, section 4.2.4). We examined the orientation of the N392 glycans in the tetraglycosylated IgG3 Fc structure to help explain our binding results. Structurally, the N392 glycosylation site is located distal to the FcγRIIIA binding site. The in-silico modeled Man8 glycan in the tetraglycosylated IgG3 Fc structure show that the glycans from the N392 site are oriented away from the receptor binding site and hence may not have a direct influence on binding (Fig. 5.12A). Moreover, it could also be proposed that the presence of N392 glycans does not induce any long-range conformational changes at the receptor binding site. This is an

important observation since prior studies have shown that binding to FcγRIIIA can be affected by changes made distal to the binding site, such as amino acid mutations at the C_H2-C_H3 domain interface.[58-59] Such effects have been attributed to long-range forces existing in the Fc molecule owing to its dynamic and flexible nature.[60] The neonatal Fc receptor (FcRn) binds to the outer face of C_H2-C_H3 interface on both the heavy chains of Fc. The N392 site in IgG3 Fc is located at the edge of C_H3-C_H3 interface close to the inner face of C_H2-C_H3 interface and the presence of glycans in this region can be predicted to potentially affect the FcRn binding (Fig. 5.12A). However, our binding results suggest that the presence of additional glycans at the N392 site in IgG3 Fc does not impact its ability to bind with FcRn. It is possible that the N392 glycans are accommodated in the Fc structure such that FcRn binding remains unaffected. In the in-silico modeled Man8 glycan in the tetraglycosylated IgG3 Fc structure, the entire glycan is located away from the FcRn binding site (Fig. 5.12A).

The residue at 392 position lies at the edge of the C_H3-C_H3 interface of Fc. Both Lys (in diglycosylated variant, PDB: 5W38) and Asn (in tetraglycosylated variant) at the 392 position point away from the interface and their side chains show no contact with the other C_H3 domain residues (Fig. 5.13A). The C_α- C_α distances between residues at the C_H3-C_H3 interface in the vicinity of Asn/Lys392 residues in both the IgG3 Fc variants were compared to detect changes in the inter-C_H3 domain separation. The C_α- C_α distances between N/K 392 of one C_H3 domain and S400', D399', and L398' of the second C_H3 domain (prime denotes residue on second C_H3 domain) were increased from 8.26 to 9.08 Å, 7.12 to 7.72 Å, and 8.67 to 8.80 Å in the tetraglycosylated IgG3 Fc (N392) structure compared to the diglycosylated IgG3 Fc (K392) structure (Fig. 5.13A). Rispens *et al.* measured differences in the strength of C_H3-C_H3 interface in different IgG3 variants and found that C_H3-C_H3 dissociation rate was ten fold faster in the case

of IgG3 with Asn392 rather than Lys392 (it is not known if the Asn392 was glycosylated in this study).[61] Taken together, it can be proposed that the N392 glycans may disrupt the interactions at the edge of C_H3-C_H3 interface and thereby can potentially reduce the C_H3 domain conformational stability. An example of extreme manifestation of glycans disrupting the C_H3-C_H3 interface was demonstrated by Ishino *et al*. by adding glycosylation sites at the core of IgG1 C_H3-C_H3 interface to generate the Fc in a completely monomeric state.[62] Chennamsetty *et al.* identified aggregation motifs in IgG subclasses, one of which is $P_{395}PML_{398}$ in the C_H3 domain.[63] This motif succeeds the N392 glycosylation site in IgG3 and is enclosed between the pair of N392 glycans in the tetraglycosylated IgG3 Fc structure (Fig. 5.13B). It is possible that the N392 glycans in IgG3 Fc protects it from aggregation by shielding this aggregation hot-spot. A similar effect was demonstrated by introducing an additional glycosylation site in the Fab domain of Bevacizumab to shield a potential aggregation hot-spot.[64] It was suggested that the extra glycosylation protected the antibody against aggregation by increasing the solubility of unfolded protein intermediates.

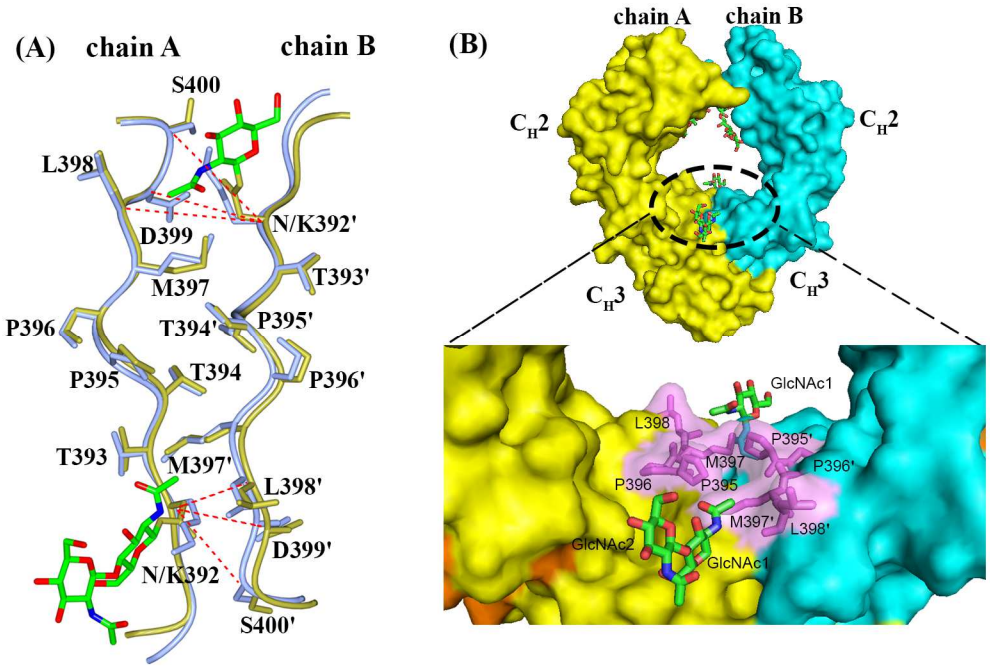

Figure 5.13: Effect of N392 glycans on the C_H3-C_H3 interface of IgG3 Fc. (A) comparison of C_H3-C_H3 interface in the tetraglycosylated (gold) and diglycosylated (PDB: 5W38, blue) IgG3 Fc structures in the vicinity of residue 392, which is glycosylated Asn in the former and Lys in the latter structure. Cα- Cα distances between residue 392 and each of L398, D399, and S400 for both the Fc chains are shown by red dash lines. (B) location and orientation of N392 glycans with respect to the aggregation motif $P_{392}PML_{398}$ at the C_H3-C_H3 interface. Prime symbol denotes residue from the second C_H3 domain.

5.4 References

1. Nagae, M.; Yamaguchi, Y., Function and 3D structure of the N-glycans on glycoproteins. *International journal of molecular sciences* **2012,** *13* (7), 8398-8429.

2. Deisenhofer, J., Crystallographic refinement and atomic models of a human Fc fragment and its complex with fragment B of protein A from Staphylococcus aureus at 2.9-and 2.8-. ANG. resolution. *Biochemistry* **1981,** *20* (9), 2361-2370.

3. Teplyakov, A.; Zhao, Y.; Malia, T. J.; Obmolova, G.; Gilliland, G. L., IgG2 Fc structure and the dynamic features of the IgG CH 2–CH 3 interface. *Molecular immunology* **2013,** *56* (1), 131-139.

4. Davies, A. M.; Rispens, T.; Ooijevaar-de Heer, P.; Gould, H. J.; Jefferis, R.; Aalberse, R. C.; Sutton, B. J., Structural determinants of unique properties of human IgG4-Fc. *Journal of molecular biology* **2014,** *426* (3), 630-644.

5. Krapp, S.; Mimura, Y.; Jefferis, R.; Huber, R.; Sondermann, P., Structural analysis of human IgG-Fc glycoforms reveals a correlation between glycosylation and structural integrity. *Journal of molecular biology* **2003,** *325* (5), 979-989.

6. Borrok, M. J.; Jung, S. T.; Kang, T. H.; Monzingo, A. F.; Georgiou, G., Revisiting the role of glycosylation in the structure of human IgG Fc. *ACS chemical biology* **2012,** *7* (9), 1596-1602.

7. Walker, M. R.; Lund, J.; Thompson, K. M.; Jefferis, R., Aglycosylation of human IgG1 and IgG3 monoclonal antibodies can eliminate recognition by human cells expressing Fc gamma RI and/or Fc gamma RII receptors. *Biochemical Journal* **1989,** *259* (2), 347.

8. Tao, M. H.; Morrison, S. L., Studies of aglycosylated chimeric mouse-human IgG. Role of carbohydrate in the structure and effector functions mediated by the human IgG constant region. *The Journal of Immunology* **1989,** *143* (8), 2595-2601.

9. Kabsch, W., Automatic indexing of rotation diffraction patterns. *Journal of Applied Crystallography* **1988,** *21* (1), 67-72.

10. Kabsch, W., Xds. *Acta Crystallographica Section D: Biological Crystallography* **2010,** *66* (2), 125-132.

11. Vonrhein, C.; Flensburg, C.; Keller, P.; Sharff, A.; Smart, O.; Paciorek, W.; Womack, T.; Bricogne, G., Data processing and analysis with the autoPROC toolbox. *Acta Crystallographica Section D: Biological Crystallography* **2011,** *67* (4), 293-302.

12. Evans, P. R., An introduction to data reduction: space-group determination, scaling and intensity statistics. *Acta Crystallographica Section D: Biological Crystallography* **2011,** *67* (4), 282-292.

13. McCoy, A. J.; Grosse-Kunstleve, R. W.; Adams, P. D.; Winn, M. D.; Storoni, L. C.; Read, R. J., Phaser crystallographic software. *Journal of applied crystallography* **2007,** *40* (4), 658-674.

14. Strop, P.; Ho, W.-H.; Boustany, L. M.; Abdiche, Y. N.; Lindquist, K. C.; Farias, S. E.; Rickert, M.; Appah, C. T.; Pascua, E.; Radcliffe, T., Generating bispecific human IgG1 and IgG2 antibodies from any antibody pair. *Journal of molecular biology* **2012,** *420* (3), 204-219.

15. Weerawarna, P. M.; Kim, Y.; Kankanamalage, A. C. G.; Damalanka, V. C.; Lushington, G. H.; Alliston, K. R.; Mehzabeen, N.; Battaile, K. P.; Lovell, S.; Chang, K.-O., Structure-based design and synthesis of triazole-based macrocyclic inhibitors of norovirus protease: Structural, biochemical, spectroscopic, and antiviral studies. *European journal of medicinal chemistry* **2016,** *119*, 300-318.

16. Langer, G.; Cohen, S. X.; Lamzin, V. S.; Perrakis, A., Automated macromolecular model building for X-ray crystallography using ARP/wARP version 7. *Nature protocols* **2008,** *3* (7), 1171-1179.

17. Adams, P. D.; Afonine, P. V.; Bunkóczi, G.; Chen, V. B.; Davis, I. W.; Echols, N.; Headd, J. J.; Hung, L.-W.; Kapral, G. J.; Grosse-Kunstleve, R. W., PHENIX: a comprehensive Python-based system for macromolecular structure solution. *Acta Crystallographica Section D: Biological Crystallography* **2010,** *66* (2), 213-221.

18. Emsley, P.; Lohkamp, B.; Scott, W. G.; Cowtan, K., Features and development of Coot. *Acta Crystallographica Section D: Biological Crystallography* **2010,** *66* (4), 486-501.

19. Potterton, L.; McNicholas, S.; Krissinel, E.; Gruber, J.; Cowtan, K.; Emsley, P.; Murshudov, G. N.; Cohen, S.; Perrakis, A.; Noble, M., Developments in the CCP4 molecular-graphics project. *Acta Crystallographica Section D: Biological Crystallography* **2004,** *60* (12), 2288-2294.

20. Bohne-Lang, A.; von der Lieth, C.-W., GlyProt: in silico glycosylation of proteins. *Nucleic acids research* **2005,** *33* (suppl 2), W214-W219.

21. Evans, P., Scaling and assessment of data quality. *Acta Crystallographica Section D: Biological Crystallography* **2006,** *62* (1), 72-82.

22. Diederichs, K.; Karplus, P. A., Improved R-factors for diffraction data analysis in macromolecular crystallography. *Nature structural biology* **1997,** *4* (4), 269-275.

23. Weiss, M. S., Global indicators of X-ray data quality. *Journal of Applied Crystallography* **2001,** *34* (2), 130-135.

24. Karplus, P. A.; Diederichs, K., Linking crystallographic model and data quality. *Science* **2012,** *336* (6084), 1030-1033.

25. Evans, P., Resolving some old problems in protein crystallography. *Science* **2012,** *336* (6084), 986-987.

26. Krissinel, E., Enhanced fold recognition using efficient short fragment clustering. *Journal of molecular biochemistry* **2012,** *1* (2), 76.

27. Matsumiya, S.; Yamaguchi, Y.; Saito, J.-i.; Nagano, M.; Sasakawa, H.; Otaki, S.; Satoh, M.; Shitara, K.; Kato, K., Structural comparison of fucosylated and nonfucosylated Fc fragments of human immunoglobulin G1. *Journal of molecular biology* **2007,** *368* (3), 767-779.

28. Bowden, T. A.; Baruah, K.; Coles, C. H.; Harvey, D. J.; Yu, X.; Song, B.-D.; Stuart, D. I.; Aricescu, A. R.; Scanlan, C. N.; Jones, E. Y., Chemical and structural analysis of an antibody folding intermediate trapped during glycan biosynthesis. *Journal of the American Chemical Society* **2012,** *134* (42), 17554-17563.

29. Crispin, M.; Bowden, T. A.; Coles, C. H.; Harlos, K.; Aricescu, A. R.; Harvey, D. J.; Stuart, D. I.; Jones, E. Y., Carbohydrate and domain architecture of an immature antibody glycoform exhibiting enhanced effector functions. *Journal of molecular biology* **2009,** *387* (5), 1061-1066.

30. Idusogie, E. E.; Presta, L. G.; Gazzano-Santoro, H.; Totpal, K.; Wong, P. Y.; Ultsch, M.; Meng, Y. G.; Mulkerrin, M. G., Mapping of the C1q binding site on rituxan, a chimeric antibody with a human IgG1 Fc. *The Journal of Immunology* **2000,** *164* (8), 4178-4184.

31. Tao, M.-H.; Smith, R.; Morrison, S., Structural features of human immunoglobulin G that determine isotype-specific differences in complement activation. *The Journal of experimental medicine* **1993,** *178* (2), 661-667.

32. Thommesen, J. E.; Michaelsen, T. E.; Løset, G. Å.; Sandlie, I.; Brekke, O. H., Lysine 322 in the human IgG3 C H 2 domain is crucial for antibody dependent complement activation. *Molecular immunology* **2000,** *37* (16), 995-1004.

33. Brooks, S. A., Protein Glycosylation. *Encyclopedia of Industrial Biotechnology* **2010**.

34. Flynn, G. C.; Chen, X.; Liu, Y. D.; Shah, B.; Zhang, Z., Naturally occurring glycan forms of human immunoglobulins G1 and G2. *Molecular immunology* **2010,** *47* (11), 2074-2082.

35. Alessandri, L.; Ouellette, D.; Acquah, A.; Rieser, M.; LeBlond, D.; Saltarelli, M.; Radziejewski, C.; Fujimori, T.; Correia, I. In *Increased serum clearance of oligomannose species present on a human IgG1 molecule*, MAbs, Taylor & Francis: 2012; pp 509-520.

36. Yu, M.; Brown, D.; Reed, C.; Chung, S.; Lutman, J.; Stefanich, E.; Wong, A.; Stephan, J.-P.; Bayer, R. In *Production, characterization and pharmacokinetic properties of antibodies with N-linked mannose-5 glycans*, MAbs, Taylor & Francis: 2012; pp 475-487.

37. Goetze, A. M.; Liu, Y. D.; Zhang, Z.; Shah, B.; Lee, E.; Bondarenko, P. V.; Flynn, G. C., High-mannose glycans on the Fc region of therapeutic IgG antibodies increase serum clearance in humans. *Glycobiology* **2011,** *21* (7), 949-959.

38. Reusch, D.; Tejada, M. L., Fc glycans of therapeutic antibodies as critical quality attributes. *Glycobiology* **2015,** *25* (12), 1325-1334.

39. Okbazghi, S. Z.; More, A. S.; White, D. R.; Duan, S.; Shah, I. S.; Joshi, S. B.; Middaugh, C. R.; Volkin, D. B.; Tolbert, T. J., Production, characterization, and biological evaluation of well-defined IgG1 Fc glycoforms as a model system for biosimilarity analysis. *Journal of pharmaceutical sciences* **2016,** *105* (2), 559-574.

40. Subedi, G. P.; Hanson, Q. M.; Barb, A. W., Restricted motion of the conserved immunoglobulin G1 N-glycan is essential for efficient FcγRIIIa binding. *Structure* **2014,** *22* (10), 1478-1488.

41. Lund, J.; Takahashi, N.; Pound, J.; Goodall, M.; Nakagawa, H.; Jefferis, R., Oligosaccharide-protein interactions in IgG can modulate recognition by Fc gamma receptors. *The FASEB journal* **1995,** *9* (1), 115-119.

42. Lund, J.; Takahashi, N.; Pound, J. D.; Goodall, M.; Jefferis, R., Multiple interactions of IgG with its core oligosaccharide can modulate recognition by complement and human Fc gamma receptor I and influence the synthesis of its oligosaccharide chains. *The Journal of Immunology* **1996,** *157* (11), 4963-4969.

43. Vidarsson, G.; Dekkers, G.; Rispens, T., IgG subclasses and allotypes: from structure to effector functions. *Frontiers in immunology* **2014,** *5*, 520.

44. Lefranc, M.-P.; Lefranc, G., Human Gm, Km, and Am allotypes and their molecular characterization: a remarkable demonstration of polymorphism. *Immunogenetics: Methods and Applications in Clinical Practice* **2012**, 635-680.

45. Oganesyan, V.; Damschroder, M. M.; Cook, K. E.; Li, Q.; Gao, C.; Wu, H.; Dall'Acqua, W. F., Structural insights into neonatal Fc receptor-based recycling mechanisms. *Journal of Biological Chemistry* **2014,** *289* (11), 7812-7824.

46. Shields, R. L.; Namenuk, A. K.; Hong, K.; Meng, Y. G.; Rae, J.; Briggs, J.; Xie, D.; Lai, J.; Stadlen, A.; Li, B., High resolution mapping of the binding site on human IgG1 for FcγRI, FcγRII, FcγRIII, and FcRn and design of IgG1 variants with improved binding to the FcγR. *Journal of Biological Chemistry* **2001,** *276* (9), 6591-6604.

47. Bruhns, P.; Iannascoli, B.; England, P.; Mancardi, D. A.; Fernandez, N.; Jorieux, S.; Daëron, M., Specificity and affinity of human Fcγ receptors and their polymorphic variants for human IgG subclasses. *Blood* **2009,** *113* (16), 3716-3725.

48. Saphire, E. O.; Parren, P. W.; Pantophlet, R.; Zwick, M. B.; Morris, G. M.; Rudd, P. M.; Dwek, R. A.; Stanfield, R. L.; Burton, D. R.; Wilson, I. A., Crystal structure of a neutralizing human IGG against HIV-1: a template for vaccine design. *Science* **2001,** *293* (5532), 1155-1159.

49. Diebolder, C. A.; Beurskens, F. J.; de Jong, R. N.; Koning, R. I.; Strumane, K.; Lindorfer, M. A.; Voorhorst, M.; Ugurlar, D.; Rosati, S.; Heck, A. J., Complement is activated by IgG hexamers assembled at the cell surface. *Science* **2014,** *343* (6176), 1260-1263.

50. Sauer-Eriksson, A. E.; Kleywegt, G. J.; Uhlén, M.; Jones, T. A., Crystal structure of the C2 fragment of streptococcal protein G in complex with the Fc domain of human IgG. *Structure* **1995,** *3* (3), 265-278.

51. Stapleton, N. M.; Andersen, J. T.; Stemerding, A. M.; Bjarnarson, S. P.; Verheul, R. C.; Gerritsen, J.; Zhao, Y.; Kleijer, M.; Sandlie, I.; de Haas, M., Competition for FcRn-mediated transport gives rise to short half-life of human IgG3 and offers therapeutic potential. *Nature Communications* **2011,** *2*, 599.

52. Akerström, B.; Björck, L., A physicochemical study of protein G, a molecule with unique immunoglobulin G-binding properties. *Journal of Biological Chemistry* **1986,** *261* (22), 10240-10247.

53. Roopenian, D. C.; Akilesh, S., FcRn: the neonatal Fc receptor comes of age. *Nature Reviews Immunology* **2007,** *7* (9), 715-725.

54. Martin, W. L.; West Jr, A. P.; Gan, L.; Bjorkman, P. J., Crystal structure at 2.8 Å of an FcRn/heterodimeric Fc complex: mechanism of pH-dependent binding. *Molecular cell* **2001,** *7* (4), 867-877.

55. Huang, X.; Zheng, F.; Zhan, C.-G., Binding structures and energies of the human neonatal Fc receptor with human Fc and its mutants by molecular modeling and dynamics simulations. *Molecular BioSystems* **2013,** *9* (12), 3047-3058.

56. Kuhn, P.; Guan, C.; Cui, T.; Tarentino, A. L.; Plummer, T. H.; Van Roey, P., Active site and oligosaccharide recognition residues of peptide-N4-(N-acetyl-β-d-glucosaminyl) asparagine amidase F. *Journal of Biological Chemistry* **1995,** *270* (49), 29493-29497.

57. Thaysen-Andersen, M.; Packer, N. H., Site-specific glycoproteomics confirms that protein structure dictates formation of N-glycan type, core fucosylation and branching. *Glycobiology* **2012,** *22* (11), 1440-1452.

58. Grevys, A.; Bern, M.; Foss, S.; Bratlie, D. B.; Moen, A.; Gunnarsen, K. S.; Aase, A.; Michaelsen, T. E.; Sandlie, I.; Andersen, J. T., Fc engineering of human IgG1 for altered binding to the neonatal Fc receptor affects Fc effector functions. *The Journal of Immunology* **2015,** *194* (11), 5497-5508.

59. Monnet, C.; Jorieux, S.; Urbain, R.; Fournier, N.; Bouayadi, K.; De Romeuf, C.; Behrens, C. K.; Fontayne, A.; Mondon, P., Selection of IgG Variants with Increased FcRn Binding Using

Random and Directed Mutagenesis: Impact on Effector Functions. *Frontiers in immunology* **2014,** *6*, 39-39.

60. Frank, M.; Walker, R. C.; Lanzilotta, W. N.; Prestegard, J. H.; Barb, A. W., Immunoglobulin G1 Fc domain motions: implications for Fc engineering. *Journal of molecular biology* **2014,** *426* (8), 1799-1811.

61. Rispens, T.; Davies, A. M.; Ooijevaar-de Heer, P.; Absalah, S.; Bende, O.; Sutton, B. J.; Vidarsson, G.; Aalberse, R. C., Dynamics of inter-heavy chain interactions in human immunoglobulin G (IgG) subclasses studied by kinetic Fab arm exchange. *Journal of Biological Chemistry* **2014,** *289* (9), 6098-6109.

62. Ishino, T.; Wang, M.; Mosyak, L.; Tam, A.; Duan, W.; Svenson, K.; Joyce, A.; O'Hara, D. M.; Lin, L.; Somers, W. S., Engineering a monomeric Fc domain modality by N-glycosylation for the half-life extension of biotherapeutics. *Journal of Biological Chemistry* **2013,** *288* (23), 16529-16537.

63. Chennamsetty, N.; Helk, B.; Voynov, V.; Kayser, V.; Trout, B. L., Aggregation-prone motifs in human immunoglobulin G. *Journal of molecular biology* **2009,** *391* (2), 404-413.

64. Courtois, F.; Agrawal, N. J.; Lauer, T. M.; Trout, B. L. In *Rational design of therapeutic mAbs against aggregation through protein engineering and incorporation of glycosylation motifs applied to bevacizumab*, MAbs, Taylor & Francis: 2016; pp 99-112.

Chapter 6 Summary, Conclusions and Future directions

6.1 Summary

All four IgG subclasses carry a consensus N-glycosylation site at N297 in the C_H2 domain of the Fc region. The presence of glycosylation at the N297 site is critical for antibody-mediated effector functions as well as the conformational stability of IgG. Only in case of IgG3, there is an additional glycosylation site at N392 in the C_H3 domain of the Fc region. This site has nearly gone unmentioned in the literature and was only recently found to be glycosylated in human serum IgG3.[1] However, the biological role of the N392 glycans and its effect on IgG3 structure and function remains under investigated. The focus of this dissertation work is to investigate the influence of N-linked glycosylation on the Fc receptor binding interactions and physical stability of IgG3 Fc. Site-specific glycosylation analysis was carried out to characterize the glycosylation pattern at the N297 and N392 glycosylation sites on IgG3 isolated from human serum. Additionally, we have determined the crystal structure of the Fc fragment of IgG3, whose structural features could explain some of the IgG3-specific properties and also our results from the biochemical and biophysical studies on IgG3 Fc. The following is a summary of contents presented in each chapter of this dissertation work.

Chapter 2: This chapter presents the results for site-occupancy and site-specific glycosylation analysis of the N297 and N392 sites in human serum IgG3. The glycosylation site-occupancy was determined to be roughly 100% and 10% for the N297 and N392 sites, respectively. The two sites showed differences in their glycosylation patterns, characterized by significant variations in the levels of core fucose, bisecting GlcNAc and high mannose glycans. These results demonstrate that glycan processing is not uniform across the two glycosylation sites in IgG3 and factors such as protein primary structure and local conformation around the glycosylation site

can influence the site-occupancy and the composition of the oligosaccharide structure. Moreover, the detection of N392 glycans in endogenous human IgG3 establishes a biological relevance to the lesser known N392 glycosylation site and thereby make a case for its further biological and biophysical evaluation.

Chapter 3: This chapter presents the results for recombinant expression and characterization of IgG3 Fc in yeast *P. pastoris*. Two site-specific glycovariants of IgG3 Fc were prepared, one with two sites glycosylated (tetraglycosylated) and another with only the N297 site glycosylated (diglycosylated) to evaluate the influence of N392 site glycosylation on IgG3 structure and function. Both the IgG3 Fc variants showed presence of high mannose glycans at the occupied glycosylation sites. The high mannose glycans can be converted to Man5 glycoform by cleavage of α-1,2 mannose residues. The mannose trimming reaction was found to be incomplete (only 78% conversion to Man5) due to presence of modified high mannose glycans (non-cleavable α-1,2 mannose linkages). To counter this, members of the Tolbert lab deleted few genes in the yeast *P. pastoris* to reduce the levels of these modified glycans. This chapter presents results for the susceptibility of high mannose glycans produced in different yeast strains to produce Man5 glycoform using *in-vitro* α-1,2 mannosidase digestion. A significant improvement in Man5 conversion was observed (~95%) with additional knock-outs of PNO1, BMT1 and BMT2 genes.

Chapter 4: This chapter presents the results for the influence of the N392 site glycans on the binding of IgG3 Fc with Fc receptors and the physical stability of IgG3 Fc. An activating Fcγ receptor, FcγRIIIA, and the neonatal Fc receptor (FcRn) were recombinantly produced in *P. pastoris,* and an *in-vitro* kinetic binding assay was developed to determine the binding affinity.

The binding results revealed that the binding of IgG3 Fc to both of the receptors is not largely influenced by the additional presence of N392 site glycans. Assessment of the impact of the N392 site glycans on physical stability of IgG3 Fc revealed that the presence of N392 site glycans reduced the conformational stability of IgG3 Fc but improved the colloidal stability of IgG3 Fc.

Chapter 5: This chapter presents high-resolution x-ray crystal structures of tetraglycosylated and diglycosylated IgG3 Fc. General structural features of IgG3 Fc are described and compared to the available Fc structures from the other IgG subclasses. The important amino acid differences between IgG3 and the other subclasses that have been implicated in IgG3-specific properties, related to binding to protein A, protein G and FcRn, are discussed from a structural perspective. The observed protein-glycan (from the N297 site) contacts in the IgG3 Fc structure, supported by the results that show reduced binding to FcγRIIIA upon glycan truncation (and hence the loss of protein-glycan contacts), provides a structural basis for the importance of N297 glycosylation in receptor binding. The location and orientation of the N392 site glycans in the tetraglycosylated IgG3 Fc structure helps to provide an explanation for the non-effect of the N392 glycans on the receptor binding interactions of IgG3 Fc and the observed effects on the physical stability of IgG3 Fc.

6.2 Conclusions

This dissertation work explored the influence of the N297 and N392 site glycosylation on the structure, Fc-receptor interaction, and physical stability of human IgG3 Fc. The differences in the glycosylation pattern between the N297 and N392 sites on human serum IgG3 indicate site-

specific variations in glycan processing. These variations are likely due to the relatively buried nature of the N392 glycosylation site within the Fc structure, which potentially limits the accessibility of the glycan modifying enzymes. The yeast *P. pastoris* served as a suitable expression host to produce IgG3 Fc that is glycosylated at the N392 site, which enabled biochemical and biophysical characterization of the N392 site glycans. No large change in the binding affinity of IgG3 Fc for FcγRIIIA and FcRn was detected due the additional presence of N392 site glycans. The structural location and orientation of the N392 glycans could explain the non-effect of the N392 glycans on the Fc receptor binding interactions of IgG3 Fc. The impact of the N392 glycans on the physical stability of IgG3 Fc can be explained by the position of these glycans at the C_H3-C_H3 interface. Amino acid differences between IgG3 and the other IgG subclasses, which have been attributed to result in IgG3-specific properties were mapped in the structure and a structural basis for differential binding of IgG3 to protein A and FcRn is proposed. The functional significance of the observed protein-glycan (from the N297 site) contacts in the structure is demonstrated by reduced binding affinity to FcγRIIIA upon glycan truncation.

6.3 Future directions

This dissertation work provides preliminary information about the immunological role of N392 site glycosylation in human IgG3. The presence of additional N392 glycans on IgG3 Fc was shown to have no effect on binding to FcγRIIIA and FcRn; however, the possibility of its influence on binding to other types of Fcγ receptors cannot be ruled out. Generally, assessment of IgG binding affinity to FcγRIIIA is a good surrogate for prediction of IgG-mediated ADCC activity, but, in this case, an ADCC assay would be useful to check if the N392 glycans play any

role that is not directly related to binding with FcγRIIIA, such as formation of an immune complex. Based on the crystal packing around the N392 glycosylation and the accessible nature of N392 glycans, it could be suggested that the N392 glycans may influence Fc-Fc interactions. IgG-IgG interactions through the Fc region have been implicated in the formation of immune precipitates and reaction of rheumatoid factor (autoantibody) with the Fc of IgG.[2] Further studies will be required to test this hypothesis. There is another immunologically relevant Fc receptor, TRIM21, that bind to the C_H2-C_H3 interface.[3] It remains to be investigated if the N392 glycans have any effect on binding to this receptor.

Mannose-Binding Lectins (MBL) and Ficolins are lectins (carbohydrate binding proteins) that play an important role in the innate immune system by recognizing sugars on the surface of invading pathogens. These pathogen-bound lectins bind to natural IgG (polyreactive IgG secreted by B cells in absence of infection) and form an immune complex, which can be cleared by antibody effector functions.[4] It will be interesting to see if the N392 glycans on IgG3 are recognized by these lectins and thereby have a potential role in the innate immune system. This is an attractive hypothesis on two counts. First, natural IgG predominantly belong to IgG3 subclass[5] and second, due to the accessible nature of terminal mannose and GlcNAc sugars present at the N392 site, which are recognition motifs for the MBL and Ficolins. Lastly, molecular dynamic simulations of IgG3 Fc might be useful to better understand the effect of N392 glycans on the conformational stability of IgG3 Fc. Such studies will now be possible with the available crystal structure of IgG3 Fc.

6.4 References:

1. Stavenhagen, K.; Plomp, R.; Wuhrer, M., Site-Specific Protein N-and O-Glycosylation Analysis by a C18-Porous Graphitized Carbon–Liquid Chromatography-Electrospray Ionization Mass Spectrometry Approach Using Pronase Treated Glycopeptides. *Analytical chemistry* **2015,** *87* (23), 11691-11699.

2. Nezlin, R., Interactions between immunoglobulin G molecules. *Immunology letters* **2010,** *132* (1), 1-5.

3. Keeble, A. H.; Khan, Z.; Forster, A.; James, L. C., TRIM21 is an IgG receptor that is structurally, thermodynamically, and kinetically conserved. *Proceedings of the National Academy of Sciences* **2008,** *105* (16), 6045-6050.

4. Puga, I.; Cerutti, A., Protection by natural IgG: a sweet partnership with soluble lectins does the trick! *The EMBO journal* **2013,** *32* (22), 2897-2899.

5. Panda, S.; Zhang, J.; Yang, L.; Anand, G. S.; Ding, J. L., Molecular interaction between natural IgG and ficolin–mechanistic insights on adaptive-innate immune crosstalk. *Scientific reports* **2014,** *4*, 3675.